UNIVERSITY OF SOUTHAMPTON

FACULTY OF NATURAL AND ENVIRONMENTAL SCIENCES

Centre for Biological Sciences

Investigating the role of pectin methylesterases in regulating root development in *Arabidopsis thaliana*

by

Przemysław Michał Ociepa

Thesis for the degree of Doctor of Philosophy in Biological Sciences

January 2017

Abstract

The growth, development, and the final shape of plants depend on modifications to the structure and elasticity of the primary cell wall which consists of cellulose, hemicellulose and pectin. The level of methylesterification of homogalacturonan (HG) component of pectin in the cell wall is one of the major factors that could determine cell wall rigidity, cell expansion, root bending, and other plant developmental processes. Demethylesterified HG backbones have the ability to crosslink via calcium making the cell wall more rigid or to be hydrolysed and make it weaker. However, it is still poor understanding of how pectin methylesterification could affect developmental processes like root growth. The methylesterification state of pectin is controlled by pectin methylesterases (PMEs) and their inhibitors (PMEIs). *Arabidopsis thaliana* genome contains a large number of PME and PMEI isoforms making gene knockout approaches difficult due to potential redundancy. Therefore, an alternative approach is needed that provides the means to simultaneously affect the activity of multiple PMEs. Polyphenon-60 (PP60) was used as the main tool in this study to investigate PMEs and PMEIs activity on *Arabidopsis* root development. PP60 is a green tea catechin extract believed to act in a similar way as PMEI by binding to the active site of PME as shown by *in vitro* analysis. Here it has been discovered that PP60 caused overexpression of some PME genes and enhanced PME activity *in vivo,* contrary to what has been speculated in previous studies. The addition of PP60 to the growing media caused inhibition of primary root elongation and reduced the number of lateral roots and root hairs probably due to increased PME activity. Phytohormones, auxin and brassinosteroids are involved in root development and it has been shown that the manipulation of phytohormone levels together with PME activity influenced primary root growth. Finally, border-like cells contain a high amount of HG and experiments showed that addition of PP60 made the cells dispersed in a slightly acidic environment. The activity of cell wall modifying enzymes and PMEs can change under different pH regimes. More basic pH 8 caused cells to cluster together but they were surrounded by a vast amount of mucilage rich in de-esterified homogalacturonan. Together, these results suggest different actions of PMEs and PP60 depending on the media pH. Moreover, pectins are involved in cell wall integrity maintenance mechanism and are overproduced when the cell wall is subjected to damage by cellulose biosynthesis inhibition. The inhibition of cellulose biosynthesis by isoxaben caused changes in metabolism and increased production of nucleotides suggesting monosaccharides being incorporated to compensate lack of cellulose microfibrils. In summary, the results showed that disruption in either pectin or cellulose components of the primary cell wall caused by chemical treatment trigger mechanisms responsible for maintenance of cell wall integrity and therefore plant growth and development.

Table of Contents

List of Tables

List of Figures

1. General Introduction

2. Materials and methods

3. Bioinformatic analysis of pectin methylesterases in *Arabidopsis thaliana* root

4. Pharmacological approaches to study the function of pectin methylesterases during root development

5. Auxin and brassinosteroid regulation of PME activity

6. The organisation of border-like cells in the Arabidopsis root tip is affected by methylesterification state of homogalacturonan

7. Metabolomics of *Arabidopsis* seedlings in response to cellulose biosynthesis inhibition

Acknowledgements

The project was funded by INTERREG IV European Cross Channel Programme “England – France”, The Kerkut Charitable Trust and The European Molecular Biology Organisation.

I would like to thank my supervisor, Alan Marchant for all the time and work he put to teach me how to be a good researcher.

I would like to thank Jérôme Pelloux, Patrice Lerouge, Azeddine Driouich, Maïté Vicre-Gibouin and Laurent Gutierrez for hosting me at their laboratories at the University of Picardie Jules Verne and the University of Rouen. Many thanks to Marie Dumont, Romain Castilleux, and Abdoul Koroney for helping me with immunolabelling and confocal microscopy experiment; Ludivine Hocq, Sylvain Lecomte, Oliver Habryło, Fabien Sénéchal, Fabien Miart, and Florian Philippe for very warm welcoming and help in settling in new places. Merci beaucoup!

Thank you also to Thorsten Hamann for the agreement to continue and help with the metabolomics project partially in Norway. I would also like to thank Javad Najafi for taking care of me during my visit in NTNU; Manikandan Veerabagu and Timo Engelsdorf for helping me with the experimental work, Per Bruheim and Jens Rohloff for explaining how to analyse the data on mass spectrometer.

Many thanks to David Johnston from the Biomediacal Imaging Unit at Southampton General Hospital for training in microscopy methods and Siobhan Braybrook from the Sainsbury Laboratory Cambridge University for hosting me at her laboratory and training in Atomic Force Microscopy.

I would like to thank Inka Lusebrink for probing criticism of my work and helping with the statistical analysis.

I would like to thank community of Biological Sciences Postgraduate Society for providing a vibrant environment in which I could develop my skills and ideas. Additionally, I would like to thank my best lab colleges, Emily Farthing, Ilectra Adam and Tania Garcia who are always there when things are going wrong and taught me how to laugh again and to love science again. Many thanks to Flora O’Brien and Miguel Ramirez for countless coffee breaks which kept me going.

I am very grateful for meeting Maria Guillaume and her family who helped me with my first steps abroad.

Finally, I would like to thank my family for their constant support. Dziękuję bardzo!

In loving memory of my grandma who always took my side and was very proud of my work.

Definitions and Abbreviations

1-NAA	1-N-naphthaleneAcetic Acid
ABA	ABscisic Acid
ABP	Auxin Binding Protein
ACC	1-aminocyclopropane-1-carboxylic acid
ACR	*Arabidopsis* CRinkly
ADPG	Arabidopsis Dehiscence Zone Polygalacturonase
AFM	Atomic Force Microscopy
AGP	ArabinoGalactan Protein
ARAD	ARAbinan Deficient
ARF	Auxin Response Factor
Aux/IAA	Auxin/Indole-3-Acetic Acid
AuxRE	Auxin Responsive Element
BLC	Border-Like Cell
BLR	BeLlRinger
BR	BRassinosteroid
bZIP	basic leucine ZIPper transcription factor
CACS	Clathrin Adaptor Complex Subunit
CG	(-)-Catechin Gallate
CESA	CEllulose SynthAse
CPC	CaPriCe
CSLC	Cellulose Synthase-Like family C
CWD	Cell Wall Damage
CWI	Cell Wall Integrity
DAMP	Damage-Associated Molecular Pattern
dCMP	deoxyCytidine MonoPhosphate
dCDP	2'-deoxyCytidine DiPhosphate
dGDP	2'-deoxyGuanosine 5'-DiPhosphate
Dha	3-deoxy-D-lyxo-heptulosonic acid
DMF	DiMethylFormamide
DP	Degree of Polymerization
dTMP	deoxyThymidine MonoPhosphate
dUDP	2'-deoxyUridine 5'-DiPhosphate
eBL	2,4-epiBrassinoLide
EC	(-)-EpiCatechin
ECG	(-)-EpiCatechin-3-Gallate
ECMs	ExtraCellular Matrices
EGC	(-)-EpiGalloCatechin
EGCG	(-)-EpiGalloCatechin-3-Gallate
ER	Endoplasmic Reticulum
ETC	Enhancer Of Try And CPC
FDA	Fluorescein DiAcetate
FER	FERonia
FITC	Fluorescein IsoThioCyanate
FRET	Fluorescence Resonance Energy Transfer
GA	Gibberellin
GalUA	GalactUronic Acid
GCG	(-)-GalloCatechin Gallate
GL/EGL	GLabra/Enhancer of GLabra
Glc	Glucose
GRP	Glycine-Rich Proteins
GT	GlycosylTransferase
GUI	Graphical User Interface
HG	HomoGalacturonan
HMS	Highly Methyl Esterified Seeds

HRGP	Hydroxyproline-Rich GlycoProtein
IAA	Indole-3-Acetic Acid
IQR	InterQuartile Range
IXR	IsoXaben Resistant
JA	Jasmonic Acid
Kdo	3-deoxy-D-manno-octulosonic acid
LRP	Lateral Root Primordium
mAbs	monoclonal Antibodies
MAMP	Microbe-Associated Molecular Pattern molecule
MAP	Mitogen-Activated Protein
MCA	MID1-Complementing Activity
OGA	OligoGAlacturonide
ORF	Open Reading Frame
PAD	PhytoAlexin Deficient
PBS	Phosphate-Buffered Saline
PCA	Principal Component Analysis
PCD	Programmed Cell Death
Pcz	Propiconazole
PG	PolyGalacturonase
PGA	PolyGalacturonic Acid
PL	Pectate Lysase
PLL	Pectate Lyase-Like
PLS-DA	Partial Least Squares Discriminant Analysis
PLT	PLeThora
PME	Pectin MethylEsterase
PMEI	Pectin MethylEsterase Inhibitor
PP60	PolyPhenon-60
PRP	Proline-Rich Protein
QC	Quiescent Center/Quality Control
QRT	QuaRteT
QUA	QUAsimodo
RALF	Rapid ALkalization Factor
RG	RhamnoGalacturonan
RHD	Root Hair Defective
RLK	Receptor-Like Kinase
ROP	RhO-related Protein
ROS	Reactive Oxygen Species
SSNMR	multidimensional Solid-State NMR
TAE	Tris-Acetate-EDTA
THE	THEseus
TIP	Tonoplast Intrinsic Protein
TRY	TRiptYchon
TTG	Transparent Testa Glabra
UPLC-MS	Ultra-Performance Liquid Chromatography-Mass Spectrometry
UTP	Uridine 5'-TriPhosphate
VIP	Variable Importance in Projection
WAK	Wall-Associated Kinase
WER	R2R3 WEREWOLF
WOX	WUSCHEL-related homeobOX
XG	XyloGlucan
XGA	XyloGAlacturonan
XTH	endoTransglucosylase/Hydrolases
XXT	Xylosyl Transefase

1. General introduction

The cell wall is one of the main features of plant cells. For a long time, the cell wall was considered as a simple physical barrier between the cell and the external environment. However now the major cell wall function is to form a strong network that gives shape and protects cells from external stress such as pathogen attack. Additionally, it provides essential roles in intercellular signalling responses to a variety of stimuli and the regulation of the transport of molecules to the cell. Plants produce two types of cell wall: primary in young and growing cells, and secondary cell wall, a strong, lignin-impregnated structure (**Fig. 1.1 A**). The primary cell wall is typically a thin, flexible layer consisting of cellulose, hemicellulose, pectin and glycoproteins (**Fig. 1.1 B**). The secondary cell wall is deposited after cell enlargement and often has a distinctive composition and organization. The cell wall can undergo set of changes to adapt to the needs of the plant involving many signalling pathways. These changes can be qualitative (lignification, cutinisation) and/or quantitative (accumulation of cellulose).

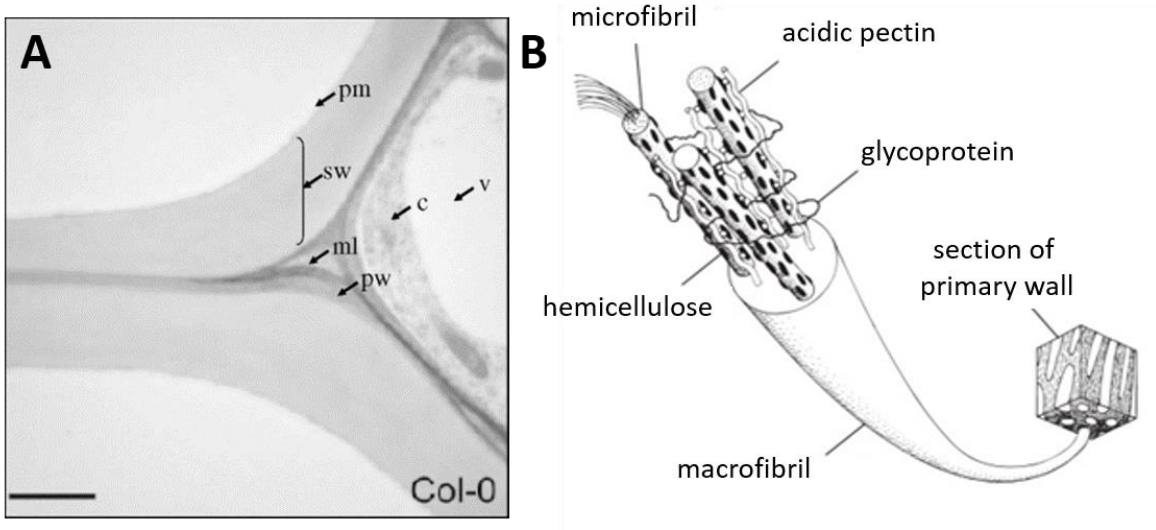

Figure 1.1. The cell wall of *Arabidopsis thaliana*. (A) Transmission electron micrograph of WT *A. thaliana* Columbia-0 transverse root section showing middle lamella (ml), primary wall (pw), and secondary wall (sw) of the metaxylem. Also labelled are the plasma membrane (pm), cytosol (c) and vacuole (v). Bar = 2 lM. (B) Structure of primary cell wall. Adapted from Gibson, 2012.

1.1 Plant cell wall

1.1.1 Primary cell wall

Extracellular matrices (ECMs) are built by complex polymer mixtures produced by cells and deposited outside the cell membrane. One common feature of ECM in diverse

organisms is the presence of polysaccharides as main structural components. Examples include chitin found in fungi and molluscs, chondroitin and hyaluronan produced by vertebrates, and peptidoglycan of bacterial cell walls. The plant's primary cell wall is composed of three closely associated polysaccharides including cellulose, hemicellulose, pectins and additionally a number of glycoproteins. There are several models describing the organisation of cell wall components within the primary cell wall (Carpita and Gibeaut, 1993). Cellulose microfibrils may form a primary network with hemicellulose which tether adjacent microfibrils together. Hemicellulose might be covalently attached to pectic polysaccharides anchoring cellulose microfibrils (**Fig. 1.2**; Cosgrove, 2005).

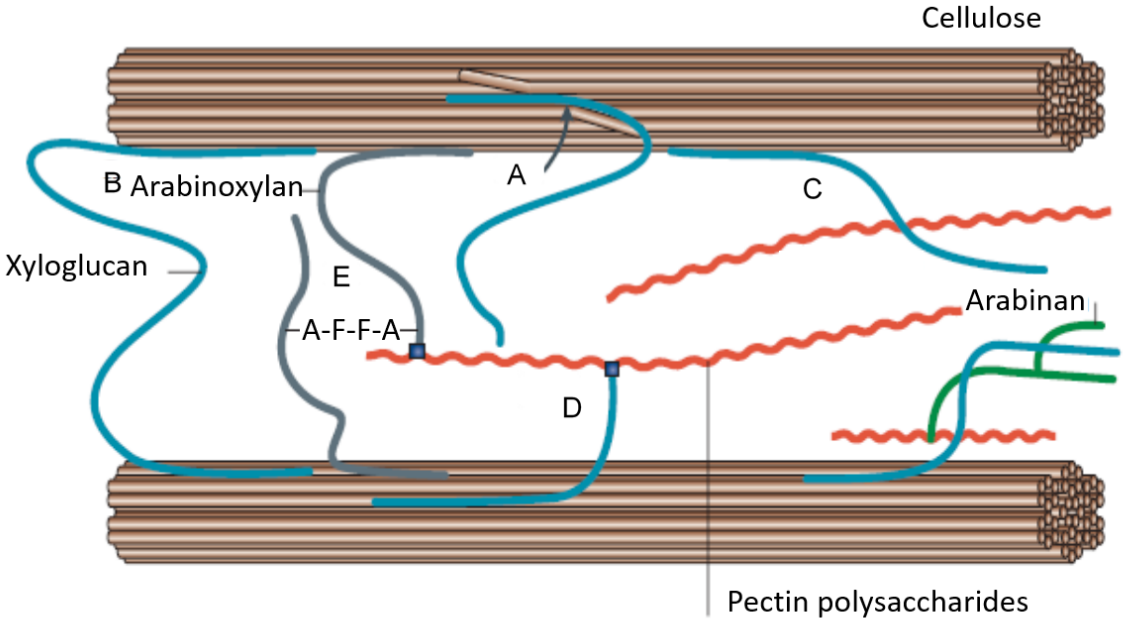

Figure 1.2. The primary cell wall network. It is suggested that xyloglucan (blue lines) might be entrapped in the microfibril (A); spontaneously bind to the cellulose surfaces (B); adhere the microfibril to other matrix polysaccharides (C); might be covalently attached to pectin polysaccharides (red lines) (D). Arabinoxylans (grey lines) might be cross-linked by ferulic acid esters (A-F-F-A) and bind cellulose and pectin (E). Adapted from Cosgrove, 2005.

1.1.2 Cellulose

Cellulose (polymers of β-1,4-linked glucose) represents the main load bearing element of plant cell walls and thus inhibition of cellulose biosynthesis leads to dramatic weakening of the cell wall. Isoxaben has been used as a tool to inhibit cellulose biosynthesis by binding to cellulose synthase subunit, and examine cell wall maintenance mechanism (more in **chapter 1.7.2**; Hamann, 2015a). Cellulose microfibrils are typically composed of approximately 36 hydrogen-bonded chains and organized into a thin (3 to 5 nm in diameter) polymer (Somerville, 2006). Each chain contains between 8000 and 15000 glucose residues and it is the largest biopolymer known in nature (Mutwil et al., 2008).

1.1.3 Hemicelluloses

The second major group of polysaccharides involved in the primary cell wall composition are hemicelluloses. They contribute to the rigidity of the primary wall, interacting with the cellulose microfibrils via formation of non-covalent bonds. They are grouped into xyloglucan, xylans, mannans and glucomannans (Scheller and Ulvskov, 2010).

Xyloglucan (XG) is the most abundant hemicellulose in primary cell walls believed to be involved in direct or indirect crosslinking of microfibrils (Talbott and Ray, 1992). XGs are made of repetitive units with a special code used to denote the different side chains. Glucose (Glc) residue is designated G, while X denotes α-D-Xyl-(1,6)-Glc, L for β-Gal, S for α-L-Araf and a Gal residue substituted with α-L-Fuc is designated F (**Fig. 1.3**; Fry et al., 1993). Recently, it has been shown that root tissue contains two types of xyloglucan: a fucogalactoxyloglucan composed of neutral subunits and a previously unidentified xyloglucan composed of neutral and acidic subunits (Pena et al., 2012). The biological significance of XG was confirmed by the observation that expansins (see **Chapter 1.3**) induce creep more effectively in long artificial cellulose/XG composites (Whitney et al., 2000; Ryden et al., 2003).

Xylans are a diverse group of hemicellulose polysaccharides with the familiar feature of a backbone of β-(1,4)-linked xylose residues (Scheller and Ulvskov, 2010). Xylans are the major non-cellulosic polysaccharide in primary walls, constituting about 20% of the wall (Scheller and Ulvskov, 2010). A common modification of xylans is substitution with α-(1,2)-linked glucuronosyl and 4-O-methyl glucuronosyl residues. Arabinose residues are the most common substitutes attached to the xylan backbone and are known as arabinoxylans and glucuronoarabinoxylans (**Fig. 1.3**) (Zablackis et al., 1995). Moreover, most xylans are acetylated to various degrees in secondary walls (Scheller and Ulvskov, 2010).

In some hemicelluloses the backbones may consist entirely of mannose, as in mannans and galactomannans, or with mannose and glucose in a non-repeating pattern as in glucomannans and galactoglucomannans (**Fig. 1.3**). The *Arabidopsis* mutant *Atcsla7* lacking the major (gluco)mannan synthase in seeds has been shown to have an embryo lethal phenotype, which confirms essential roles of mannans (Goubet et al., 2003).

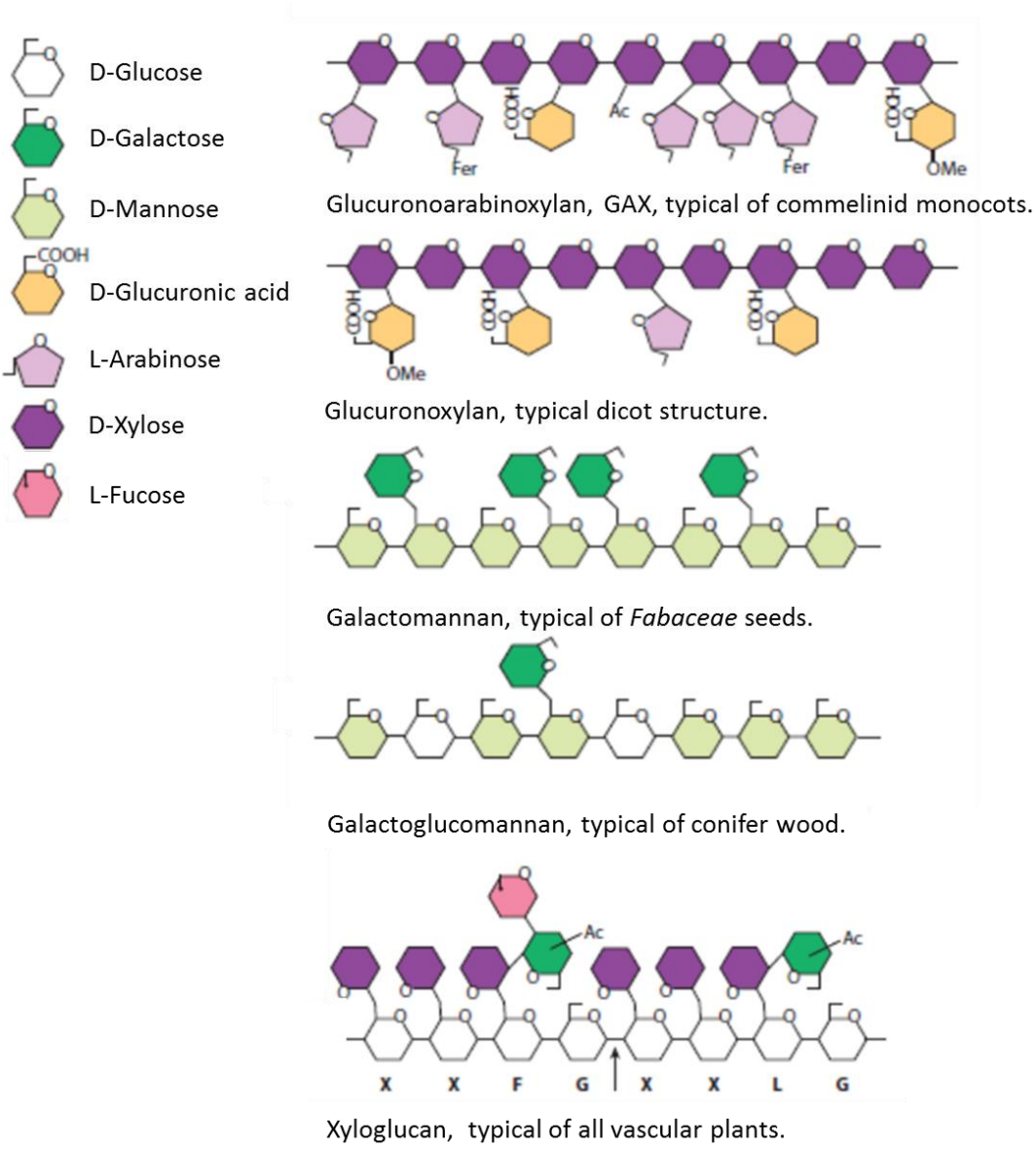

Figure 1.3. Schematic illustrations of the types of hemicelluloses found in plant cell walls. "Fer" denotes addition of ferulic acid (3-methoxy-4-hydroxycinnamic acid), which is characteristic of xylans in monocots. Xyloglucan [β-D-Glucose-(1,4)]$_n$ backbone substituted with side chains as seen in pea and *Arabidopsis*. The arrow indicates the typical β-glucanase cleavage site. The letters under the xyloglucan (XG) molecule illustrate the symbols used for the most common side chains. Adapted from Scheller and Ulvskov, 2010.

1.1.4 Pectins

Pectins are the most complex polysaccharides found in plants and have several functions. The cell wall contains approximately 50% (w/w) pectin with the content varying depending on environment, tissue and species (Zablackis et al., 1995). Several pectic polysaccharides can be detected in the cell wall, including homogalacturonan (HG), xylogalacturonan (XGA), apiogalacturonan, rhamnogalacturonan I (RGI), and rhamnogalacturonan II (RGII) (**Fig. 1.4**; Ridley et al., 2001).

Pectins are important determinants of wall thickness and they glue the cells together in an adhesive layer, called middle lamella that is deposited during cell division (Iwai et al.,

2002). Calcium crosslinking of pectin contributes to wall strength by bringing blocks of homogalacturonan chains into a tightly packed conformation. Rhamnogalacturonan II-borate complexes contribute to wall expansibility and cell adhesion (**Fig. 1.8**).

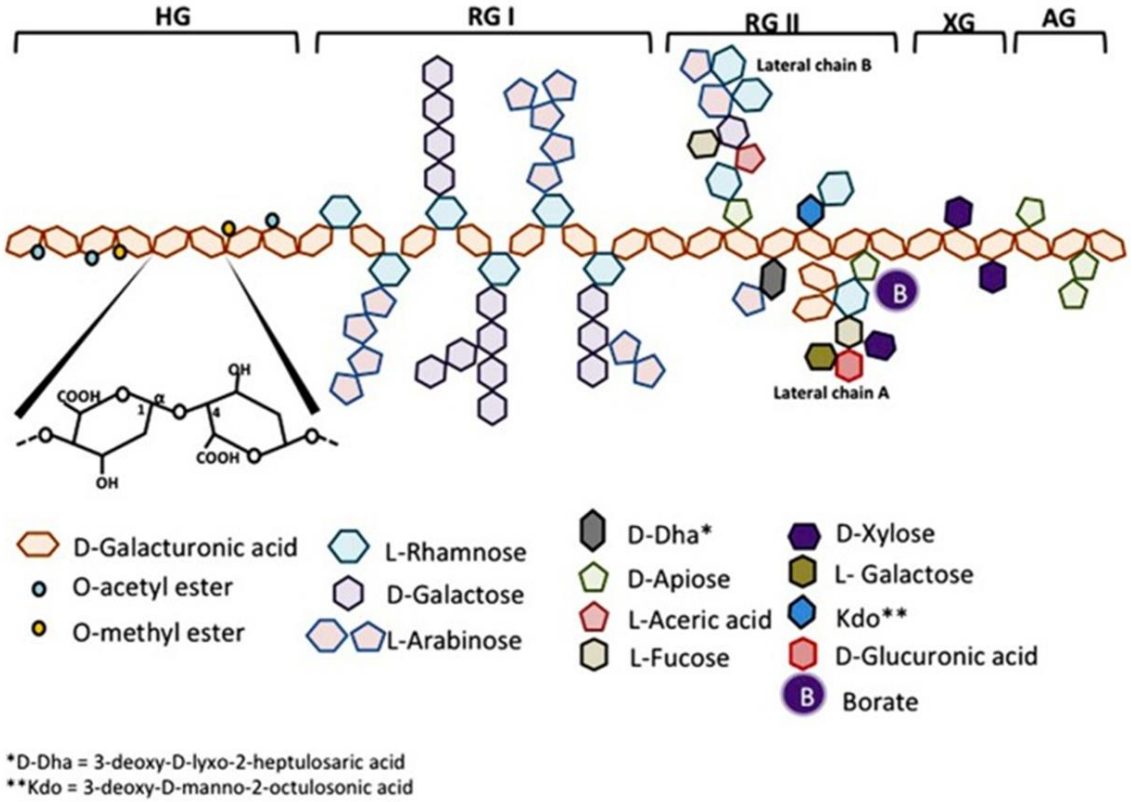

Figure 1.4. Schematic representation of pectin structure. Schematic showing the five pectic polysaccharides: homogalacturonan (HG), xylogalacturonan (XG), apiogalacturonan (AG), rhamnogalacturonan I (RG-I) and rhamnogalacturonan II (RG-II) linked to each other. Adapted from Leclere et al., 2013.

Cell adhesion is reduced in mutants that have insufficient homogalacturonan-calcium complexes (*Arabidopsis pme3* mutant which displays an increased efficiency in protoplast isolation from leaf tissue (Lionetti et al.), branched rhamnogalacturonan I, or rhamnogalacturonan II dimerization via boron (tobacco *nolac-H18* mutant in glucuronyltransferase 1 (Iwai et al., 2002). It has been shown using multidimensional solid-state NMR (SSNMR) spectroscopy that the primary wall of higher plants consists of a polysaccharide network, in which cellulose interacts with both hemicellulose and pectins on the nanometre scale (Wang and Hong, 2016). The breakdown products of pectins, oligogalacturonides (OGAs) (i.e. α-1,4-linked oligomers of galacturonic acid (GalUA)), function as potent signal molecules of plant-defence responses during pathogen attack (Ridley et al., 2001).

1.1.4.1 Homogalacturonan

Homogalaturonan (HG) is the most abundant pectin which can account for greater than 60% of pectins in the cell wall. It constitutes at least 23% of *Arabidopsis* leaf walls, up to 35% in tomato fruit and around 52% in mango (Caffall and Mohnen, 2009). HG molecule is a homopolymer chain of approximately 100 to 200 α-1,4-linked GalUA residues which can be substituted at various positions with other sugar residues, including xylose and apiofuranose (**Fig. 1.4**; Caffall and Mohnen, 2009). HG is present in the middle lamella which is the interspace between two neighbouring cells. The backbone of HG might be covalently linked to RGI and RGII, and is also hypothesized to be covalently crosslinked to XG. HG can undergo many modifications when incorporated into cell wall. It is synthesised in the Golgi apparatus by glycosyltransferases, substituted with methyl groups at the C6 position and acetylated in O2 and O3 position before finally being secreted to the cell wall in a highly methylesterified state (**Fig 1.5**). HG may be substituted by one or more β-1,3-xylose forming xylogalacturonan, or by one or two β-1,3-apiose residues forming apiogalacturonan (**Fig. 1.4**) (Sterling et al., 2006). The areas and degree of methylesterification and acetylation of HG can vary depending on tissue and developmental stage of the cell. Demethylesterification of HG is catalysed by pectin methylesterases (PMEs; see **chapter 1.5.1.1**) which have different modes of action (Micheli, 2001). When PMEs act randomly (non-blockwise), the demethylesterification process releases protons and promotes hydration which may contribute to cell wall loosening. The blockwise acting of PMEs give rise to blocks of free carboxyl groups which could interact to create a pectate gel (Wolf and Greiner, 2012). This is possible due to the property of demethylesterified HG chains to connect via Ca^{2+}-mediated cross-linking. Additionally, this interaction prevents embedded cellulose microfibrils from sliding and maintains the cell wall plasticity (Pelloux et al., 2007).

1.1.1.1 Rhamnogalacturonan I

Rhamnogalaturonan I (RGI) is the only type of pectin not built of a galacturonic acid backbone. It is a branched polymer with a backbone of disaccharide (α-1,4-D-GalA-α-1,2-L-Rha) repeats (**Fig. 1.6**). The α-1,5-linked-L-Ara*f* and β-1,4-linked-D-Gal*p* side chains are 4-linked to approximately half of the rhamnose residues of the RGI backbone (Caffall and Mohnen, 2009). Two putative arabinosyltransferases in *Arabidopsis* named ARABINAN DEFICIENT1 (ARAD1) and ARAD2 are known to be involved in the biosynthesis of arabian side chains in RGI (Harholt et al., 2012).

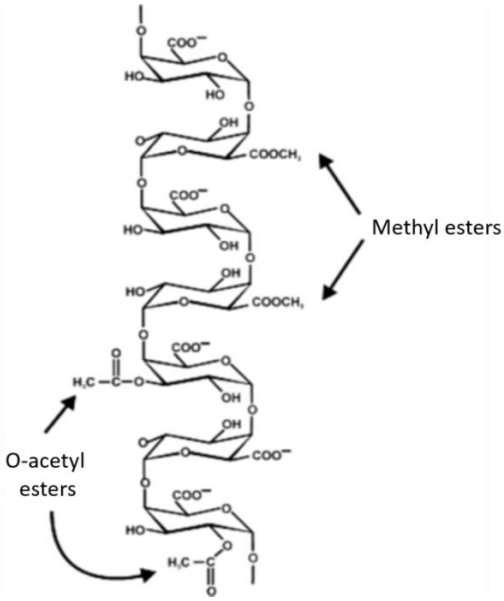

Figure 1.5. Homogalacturonan structure and modification. There are shown representative sites of methylesterification at the C-6 and O-acetylation at the O-2 or O-3 of the carbohydrate ring. Adapted from Caffall and Mohnen, 2009.

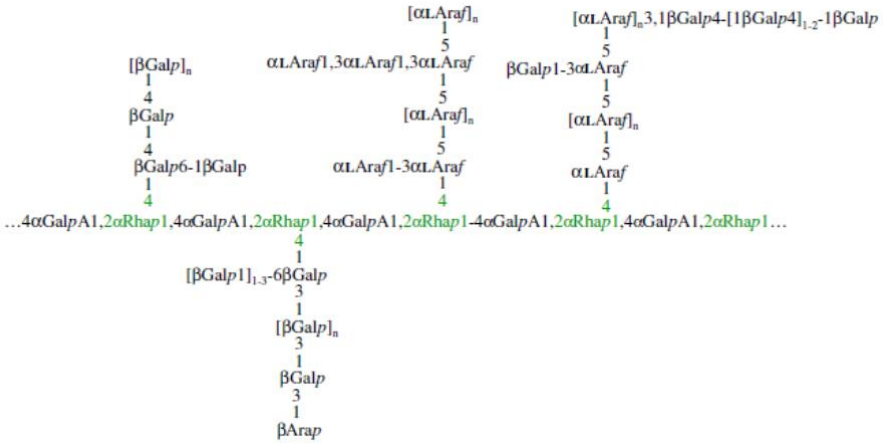

Figure 1.6. The structure of RG-I. The structure of RG-I with sidechains of α-(1,5)-L-arabinan, β-(1,4)-galactan, and arabinogalactan. Additionally, the α-1,5-L-arabinan chains may be branched with long chains of 3-linked branches of mono- or dimeric L-arabinan or mono-, di-, or oligomeric branches of β-(1,3)-linked Gal. Adapted from Caffall and Mohnen, 2009.

1.1.1.2 Rhamnogalacturonan II

Rhamnogalacturonan II (RGII) was first isolated from the cell wall of cultured sycamore cells as a fragment of pectic polysaccharide which is resistant to endopolygalacturonase hydrolysis (Darvill et al., 1978). RGII is a structurally complex pectic polysaccharide present in the primary cell wall and despite the high degree of complexity, the structure of RGII is highly conserved across all plant species studied to date (Bar-Peled et al., 2012a). RGII consists of an α-1,4-linked homogalacturonan backbone that is substituted with four different oligosaccharide side chains named A, B, C, and D (**Fig. 1.7**;

Pérez et al., 2003). It is built by at least 12 different glycosyl residues and 22 glycosidic linkages. Among the characteristic residues are: aceric acid, apiose, 3-deoxy-D-lyxo-heptulosonic acid (Dha) and 3-deoxy-D-manno-octulosonic acid (Kdo) present only in RGII (Bar-Peled et al., 2012a). Two apiosyl residues of sidechain A from separate RGII molecules are covalently cross-linked by boric acid and form a RGII diester (**Fig. 1.8**; O'Neill et al., 2001). It has been suggested that RGII cross-linking via boron increases the strength of the wall and affects the size of molecules that can diffuse through the wall. Such results confirm the hypothesis that cross-linking of RGII results in the formation of a pectin network within the primary cell wall (Chormova et al., 2014).

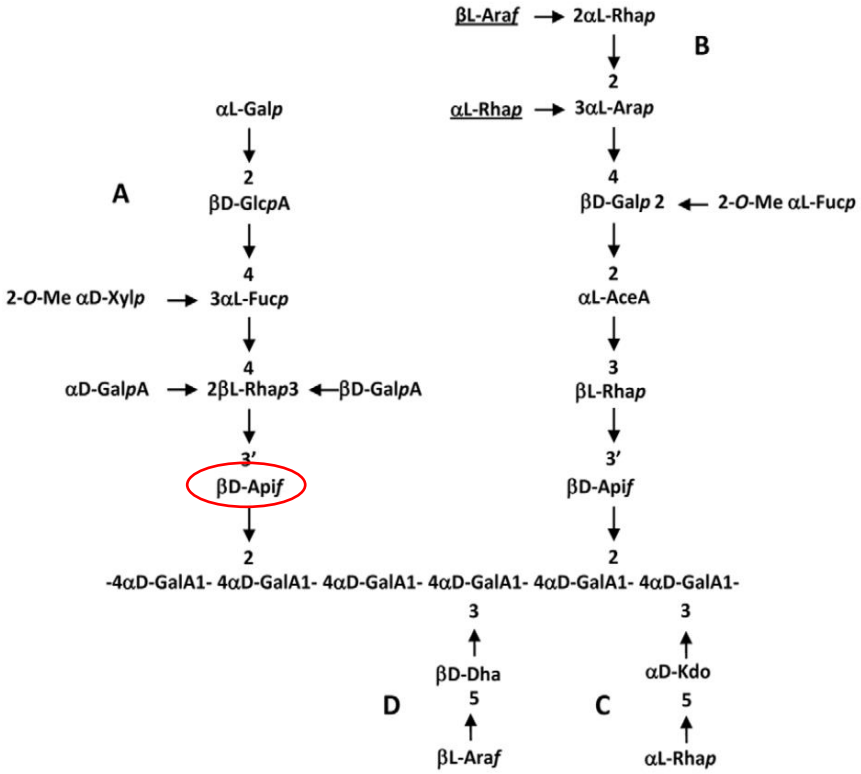

Figure 1.7. The structure of RG-II. RG-II is composed of an a-1,4-linked homogalacturonan backbone that is substituted with four side chains A to D. The underlined sugars are absent in *Arabidopsis* but present in the walls of pteridophytes and lycophytes. Adapted from O'Neill et al., 2004. Only the apiosyl residue of side chain A (red circle) is involved in the borate-diester cross-linking of RG-II.

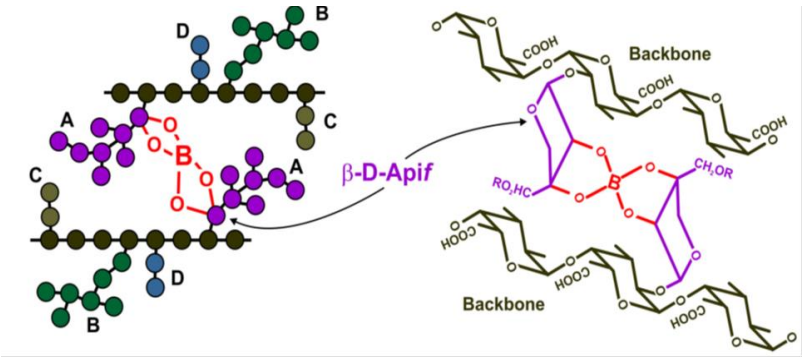

Figure 1.8. Cartoons showing the borate cross-linking of two RGII molecules. Adapted from Bar-Peled et al., 2012b.

1.2 Cell wall synthesis

1.2.1 Cellulose

Cellulose is synthesized by membrane complexes which extend a microfibril from the plasma membrane (**Fig. 1.9**). The plant cellulose synthase (CESA) family of genes comprises ten members in *Arabidopsis thaliana* from which three are required to make a functional cellulose-synthesizing complex (Taylor et al., 2003; Endler and Persson, 2011). Different sets of genes are involved in the formation of primary and secondary wall: *CESA1*, *CESA3* and *CESA6* are required to form the primary wall Arioli, 1998, whereas *CESA4*, *CESA7* and *CESA8* are associated with secondary walls (Taylor et al., 2003). 12 CESA proteins of each three types form a hexameric rosette composed of total 36 CESA proteins although there is no direct experimental evidence confirming a 1:1:1 stoichiometry of the three CESA types (Kumar and Turner, 2015). The stacking of cellulose microfibrils into crystalline cellulose is promoted by hydrogen bonds between hydroxyl groups and oxygen atoms within a single glucose chain and between neighbouring chains as well as van der Waals forces (McFarlane et al., 2014). All these forces aggregate glucan chains together side by side. The cellulose synthases are closely associated with each other and tightly connected to the plasma membrane which minimizes sliding as the enzyme moves through the plasma membrane in response to elongation of the growing glucan chains. It is suggested that cellulose synthase is attached to microtubules and the movement of it is controlled by a close association between microtubules and the plasma membrane as the result of correlations between microtubule and microfibril organization (Somerville, 2006; Guerriero et al., 2010). Within the wall of young cells, the microfibrils are arranged parallel with each other and laid down in layers which are oriented differentially leading to the strengthening of mechanical properties. It is generally accepted that the energy of polymerization provides the motive force that moves the cellulose synthase complex through the membrane (Somerville, 2006; Guerriero et al., 2010).

1.2.2 Hemicellulose

XG constitutes up to 20-30% of cell wall hemicelluloses and consists of a β-1,4-linked glucan backbone. There is a great structural diversity in XG with regards to substitution patterns. The glucan backbone of XG is believed to be synthesized by members of the cellulose synthase-like family C (CSLC) genes (Davis et al., 2010), whereas the mechanism responsible for patterning of xylosyl substitutions remains unclear. Several xylosyl transefases (XXTs) have been identified in *Arabidopsis* and a mutant analysis for

xxt1, *xxt2*, and *xxt5* demonstrated that all three of these genes are involved in XG biosynthesis (Zabotina et al., 2012).

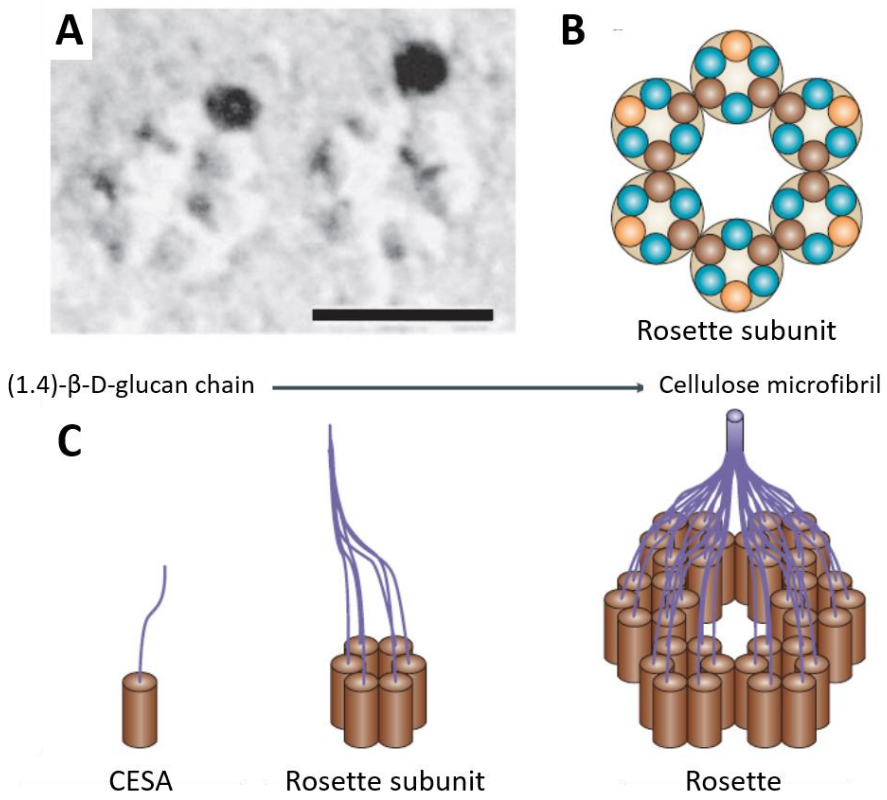

Figure 1.9. The cellulose synthase complex. (A) Immunogold labelling of CESA complex in the plasma membrane. Bar = 30 nm. (B) Model of hexameric particle rosette with three different CESA proteins (α, orange; β, brown; γ, green). (C) Model of CESA complexes synthesizing a cellulose microfibril. Each CESA protein synthesizes a single β-1,4-linked glucan chain. 36 β-D-glucan chains are produced by a particle rosette, which comprising of a hexamer of CESA hexamers. Adapted from Cosgrove, 2005.

The xylosyl substituents of XG can be further substituted. The galactosyltranserase was one of the first identified enzymes involved in XG biosynthesis (Perrin, 1999) and the analysis of *mur2* and *mur3 Arabidopsis* mutants revealed that they are affected in the same gene encoding a XG β-1,2-galactosyltransferase (Vanzin et al., 2002; Madson, 2003). The enzyme has been shown to be highly specific for the addition of the third galactose in the repeating XXXG unit of xyloglucan. XLT2, a galactosyltransferase was identified for its specificity for the second xylosyl residue (Jensen et al., 2012). *Arabidopsis* plants with mutations in both *MUR3* and *XLT2* showed XG nearly devoid of galactosylation. Moreover, a single XG α-1,2-fucosyltransferase, FUT1, was shown to add a terminal fucosyl group to a galactosyl or galacturonosyl residue of XG (Pena et al., 2012).

Recently it has been shown that glycosyl hydrolases are involved in the maturation and incorporation of XG into the wall and have a major impact on XG substitution pattering. The XG modifying enzymes including endotransglucosylase/hydrolases (XTH) are required

for altering the length of the polysaccharide, incorporating it into the wall structure, and/or remodelling the network during cell elongation (Rose et al., 2002).

1.2.3 Pectins

The conventional pathway for secretion of a eukaryotic protein involves an N-terminal region, termed the signal peptide or leader sequence, which directs the premature protein to the endoplasmic reticulum (ER), at which the remainder of the protein is cotranslationally translocated through the Sec61 complex into the ER lumen (Rapoport, 2007; Rose and Lee, 2010). It then passes through the endomembrane system, or secretory pathway, comprising the Golgi apparatus and trans-Golgi network, where it is packaged into vesicles that migrate to, and fuse with, the plasma membrane, releasing the protein cargo into the cell wall (Rose and Lee, 2010).

The Golgi apparatus is the site of synthesis of all non-cellulosic cell wall polysaccharides other than callose (Driouich et al., 2012). The synthesis of pectic polysaccharides occurs in the Golgi apparatus where they are packaged into vesicles that fuse with the plasma membrane delivering their cargo to the wall (Nunan and Scheller, 2003; Geshi et al., 2004; Harholt et al., 2010; Driouich et al., 2012). A Golgi stack has four defined regions: the cis and medial, where enzymes involved in addition of xylosyl and galactosyl residues are localized; trans-Golgi, and the trans-Golgi network (Staehelin et al., 1990). Cargo intended for secretion is transported through the endoplasmic reticulum (ER) to the cis face of the Golgi body. Wall polysaccharides are continually synthesized and moved through Golgi stacks from the cis face to the trans face of the Golgi (Zhang and Staehelin, 1992). The side chain branches of pectin are added in different cisternae by different families of glycosyltransferases (GT) (**Fig. 1.10**). The specific compartmentalization of pectin synthesis has been detected where the RGI and HG backbone synthesis and the methylesterification of galacturonic acid residues occur in the cis-medial Golgi, whereas the arabinose-containing side chains of RGI are detected only in the trans-Golgi network (Driouich et al., 2012). Pectic polysaccharides then are integrated into the wall network (**Fig. 1.11**) by crosslinking reactions via boron in adjacent RGII chains and via Ca2+ in adjacent HG chains and physical interactions with cellulose and hemicellulose (Harholt et al., 2010), though the exact mechanisms remain largely unknown.

A few pectic biosynthetic enzymes have been identified and shown to be localized in the Golgi apparatus. The complexity and diversity of pectin structures confirm the large number of enzymes required for its biosynthesis. Mohnen, 2008 have predicted 67 different glycosyltransferases, methyltransferases, and acetyltransferases participating in pectin biosynthetic pathways, and so far only one has been completely identified, namely, the

homogalacturonan galacturonosyltransferase GAUT1 from *Arabidopsis thaliana* (Sterling et al., 2006). Recently, Liwanag et al., 2012 reported the identification of β-1,4-galactan synthase, which was designed, GALS1. The enzyme belongs to glycosyltransferase family GT92, which has three members in *Arabidopsis*. Loss-of-function mutants in all three genes are galactan deficient, and the isolated GALS1 protein catalyses β-1,4-galactan synthesis *in vitro*.

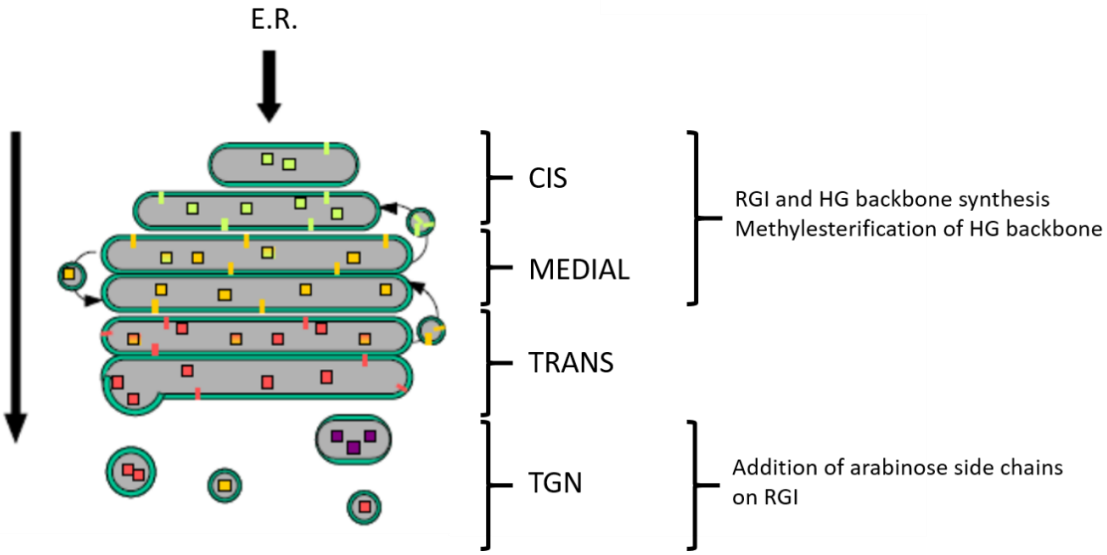

Figure 1.10. The plant Golgi apparatus. Glycoproteins and wall polysaccharides (coloured squares) are synthesized largely by membrane bound glycosyltransferases (coloured sticks) in the flattered vesicles of the Golgi apparatus. The direction of cargo flow is showed by the large black arrows. Adapted from Caffall and Mohnen, 2009.

1.3 Cell wall proteome

The arabinogalactan proteins (AGPs), proline-rich proteins (PRPs), glycine-rich proteins (GRPs), and wall-associated kinases (WAKs) are wall-associated proteins and are hypothesized to assist in structural reinforcement of the wall and regulatory pathways. AGPs are a family of non-enzymatic cell surface hydroxyproline-rich glycoproteins (HRGPs). AGPs include a large group of cell-wall proteins which share common features, including their ability to bind to β-D-glucosyl Yariv reagent (Yariv et al., 1967). AGPs are characterized by the extensive O-glycosylation of the protein backbone which takes place post-translationally in the Golgi apparatus (Nguema-Ona et al., 2012). Typically, the carbohydrate component accounts for more than 90% w/w of the mass of the glycoprotein and consists mainly of arabinose and galactose residues; although other minor sugars including rhamnose, fucose, glucuronic acid and xylose are also present (Showalter, 2001). AGPs have been implicated to be involved in a variety of functions including cell expansion (Willats and Knox, 1996) and pollen tube growth (Coimbra et al., 2010; Nguema-Ona et al., 2012). The PRPs are wall-associated proteins that are secreted into wall matrix where they

eventually become cross-linked, giving strength to the wall (Kieliszewski et al., 1995). The expression of GRPs is induced by stress and they are hypothesized to interact with components of signalling pathways, and thus, may be regulators of wall structure. WAKs have been implicated in cell elongation, morphogenesis, and defence against pathogens (Jamet et al., 2008).

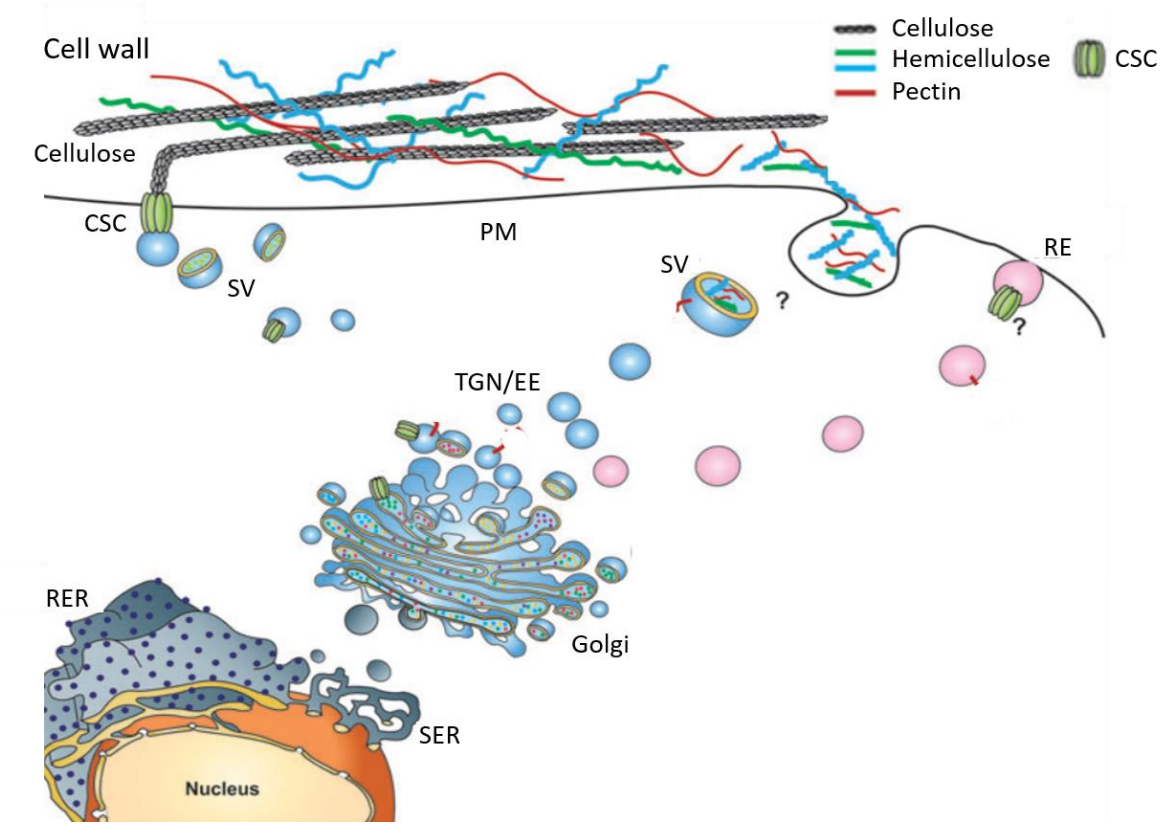

Figure 1.11. Post-Golgi trafficking and polysaccharide deposition in a plant cell. Many of proteins involved in the cell wall biosynthesis and polysaccharides are synthesized in the Golgi apparatus and transported to the plasma membrane (PM) via the trans-Golgi Network (TGN) (light blue vesicles). Cellulose synthase complexes (CSC; green barrels) are grouped in the Golgi and secreted to the PM, where cellulose biosynthesis takes place. Hemicellulose and pectins are synthesized in the Golgi, secreted to the apoplast and incorporated into the cell wall. It is suggested that CSCs can recycle through the TGN/Early endosome (EE) (pink vesicles). Dotted interior of Golgi represents cargo. RER, rough endoplasmic reticulum; SER, smooth endoplasmic reticulum; TGN/EE, trans-Golgi Network/Early endosome; SV, secretory vesicles; PM, plasma membrane; CSC, cellulose synthase complex. Adapted from Worden et al., 2012.

1.4 Growth of primary cell wall

New cells are formed by cell division in the meristems. Cells need to undergo expansion, often this is anisotropic expansion (i.e. in one direction). The wall expansion must be matched by the synthesis and integration of new wall materials to prevent thinning to the point of mechanical instability. Changes in cell turgor pressure provide the mechanical

energy that is used for the cell wall extension and result in the stretching of wall polymers in a mechanism called wall stress relaxation (Cosgrove, 1997). It allows the cells to absorb water and physically expand. The growing plant cells characteristically exhibit acid growth, which results from the action of pH-dependent wall-loosening proteins named expansins (Cosgrove, 1989; McQueen-Mason et al., 1992; Cosgrove, 2000). Expansins are a group of non-enzymatic wall proteins that induce wall stress relaxation by disrupting the hydrogen bonds between hemicellulose and microfibrils (**Fig. 1.12**; Link and Cosgrove, 1998). Addition of exogenous expansin can stimulate cell enlargement, whereas endogenous expansins are at least partially limiting for cell growth. The current model of the cell wall network stated that the main load-bearing network consists of cellulose-xyloglucan connections, which is controlled by expansins and perhaps wall-bound xyloglucan endotransglycoslase activity (Fry et al., 1992; Cosgrove, 2000). Additionally, it has been proposed that hydroxyl radicals (•OH) are supplied by the growing cell to loosen their cell walls and stimulate cell enlargement. There have been two hypotheses proposed to explain the source of •OH production in the cell wall: natural reactions dependent on reductant (i.e. acorbate), transition metal ions (i.e. copper), and a source of H_2O_2 (i.e. O_2) in the cell wall; and peroxidase-mediated reactions (Müller et al., 2009). •OH can cleave wall polysaccharides by non-enzymatically removing a hydrogen atom from polysaccharides (Liszkay et al., 2003).

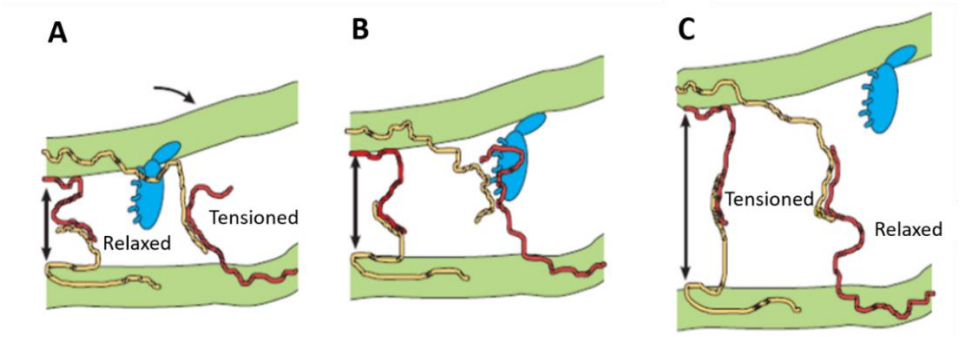

Figure 1.12. A model of expansin's wall-loosening action. Cellulose microfibrils are connected to each other by hemicelluloses and pectins (thin yellow and red lines) that can be attached to the microfibril surface and to each other. The expansin protein (blue) is suggested to disrupt the bonding of the glycans to the microfibril surface (a) or to each other (b). Turgor providing the mechanical stress makes the expansin to act which results in a displacement of the wall polymers (c) and slippage in the points of polymer adhesion (compare b and c) Adapted from Cosgrove, 2000.

1.5 Enzymes involved in modifications of pectin

Pectinases are classified by substrate specificity or mode of action into various classes, such as pectin methylesterases, polygalacturonases, pectate lyases and pectin lyases.

1.5.1.1 Pectin methylesterases

Pectins are synthesized and methylesterified in the Golgi and afterwards secreted into the wall in a highly methylesterified state. A de-esterification of pectins is provided by wall-associated pectin methylesterases (PMEs) which convert the methoxyl groups into carboxyl groups on the homogalaturonan backbone and release both methanol and protons. There are 66 *PME* genes in *Arabidopsis* and they can be separated into two groups (Louvet et al., 2006). Type I genes contain two or three introns and encode a long targeting sequence, whereas type II genes contain five or six introns and encode either a short or no targeting sequence (Micheli, 2001). The activity of PME can be regulated by their proteinaceous inhibitors (PMEIs; see the next subchapter) or by the pro-region. PME protein sequence analysis revealed that they can be classified into two groups (1 and 2). Group 1 PMEs do not contain the Pro region, whereas PME genes of group 2 encode proteins with pre-pro-regions which are considered as PME's signature. The pre-region was defined as signal peptide required for protein targeting to the endoplasmic reticulum. The pro-region remains attached to the mature protein through the *cis*, medial and *trans* Golgi secretion. Only the mature part of the PME is found in the cell wall (**Fig. 1.13**). The cleavage of the pro region from the mature PME might occur after the secretion of the mature PME into the cell wall. This process involves subtilases (SBTs), a family of serine proteases. It has been shown that PME17 from *Arabidopsis* is strongly co-expressed with SBT3.5 and SBT3.5 has the ability to release processed PME17 to the apoplasm (Sénéchal et al., 2014). Due to its similarity to the PME inhibitor domain, it is believed that the role of the pro-region is to inhibit the mature part during its secretion to the cytoplasm to prevent premature demethylesterification of pectin before their placement in the cell wall (Micheli, 2001, Pelloux et al., 2007).

Using the set of more than 100 available PME protein sequences from plants, fungi and bacteria it has been shown that PMEs contain six strictly conserved residues, where three of them (aspartic acid, arginine and tryptophan are involved in the active site (**Fig. 1.14**; Markovič and Janeček, 2004). The fourth region contains the strictly conserved aspartic acid residue which plays a role in the PME active site together with arginine and tryptophan in the fifth segment.

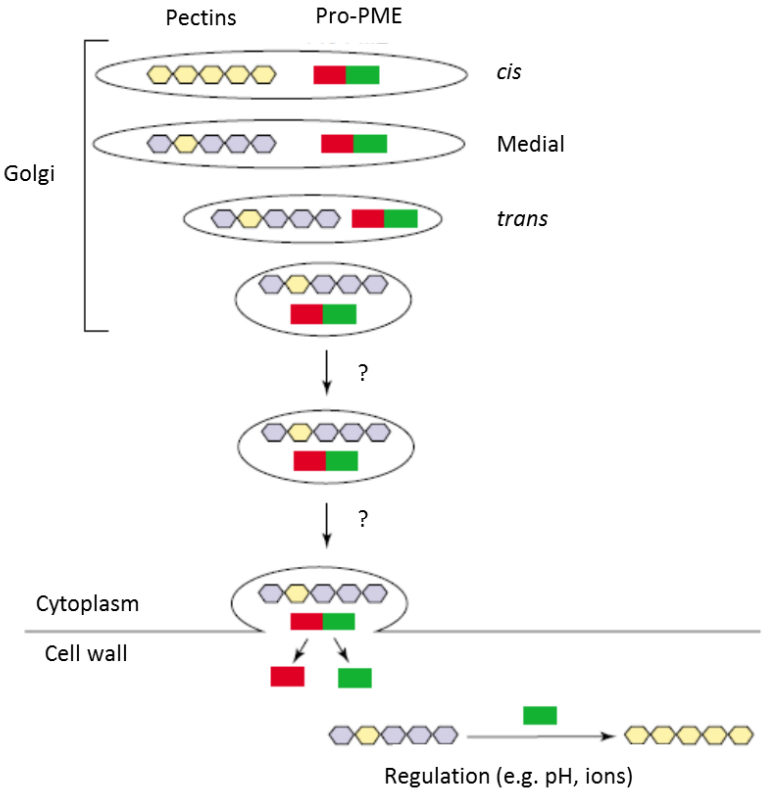

Figure 1.13. Co-secretion of pectin and pectin methylesterase (PME) into the cytoplasm. The pro-region (red) probably inhibits the mature part of the protein (green) during its secretion to prevent premature demethylesterification of pectins. Demethylesterifed pectin is shown in yellow and methylesterified in violet. Adapted from Micheli, 2001.

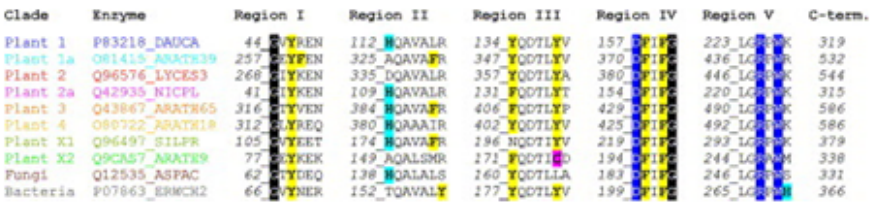

Abbreviation	Source
P83218_DAUCA	*D. carota*, cv. TipTop
O81415_ARATH39	*A. thaliana*, ch. 4, gn. T2H3.6
Q96576_LYCES3	*L. esculentum*, str. VFNT Cherry, fruit, gn. PME3
Q42935_NICPL	*Nicotiana plumbaginifolia*, somatic embryos
Q43867_ARATH65	*A. thaliana*, ch. 1, gn. T18A20.7, AtPME1
Q9TOP8_ARATH18	*A. thaliana*, ch. 2, gn. AtPME4
Q96497_SILPR	*S. pratensis*, flower bud, cl. lambda GEM2
Q9CAS7_ARATH9	*A. thaliana*, ch. 1, gn. T17F3.3
Q12535_ASPAC	*Aspergillus aculeatus*, str. KSM510, gn. PME1
P07863_ERWCH2	*E. chrysanthemi*, str. B374, (str. 3937), PemA

Figure 1.14. Amino acid sequence alignment of conserved segments of selected PMEs. Conserved glycines (Gly) are showed in black. The three catalytic residues are highlighted in blue. Cysteine (Cys), histidine (His) and tyrosine (Tyr) amino acids are highlighted in pink, turquoise, and yellow, respectively. Adapted from Markowic and Janecek, 2004.

The demethylesterification of pectins by PME can have opposite consequences for the plasticity of the cell wall depending on the mode of action (**Fig. 1.15**). It is proposed that PMEs deesterification of pectins via blockwise activity along the chain favours pectin gelation and cell wall stiffening due to the formation of Ca^{2+} bridges between free carboxyl groups of adjacent pectin chains. Moreover, blockwise PME activity promotes degradation of HG by activating pectin hydrolases like polygalacturonases (Ralet et al., 2012, Williams and Benen, 2002). Alternatively, the localized reduction in pH, due to the non-blockwise de-esterification process, could promote acidic growth of cell wall and extension by stimulating the activity of several cell wall-loosening expansins which have important consequences for cell adhesion (Wolf and Greiner, 2012). It is suggested that these opposite effects, cell wall loosening and stiffening are associated with different PMEs isoforms or are regulated by different microenvironment conditions as apoplastic pH and the availability of cations (Louvet et al., 2006). Some studies showed the PMEs play an important role in pollen tube walls (Wolf et al., 2012). The pollen tube tip region is composed of a pectin layer, where neither cellulose nor callose has been detected. The application of an exogenous PME from orange (*Citrus sinensis*) peel induces thickening of the cell wall at the tip inhibiting the pollen tube growth (Röckel et al., 2008). It can be explained by enhanced extracellular enzyme activity which generates extra carboxyl groups on the pectin residues cross-linked by calcium (Bosch et al., 2005). After demethylesterification, pectins form Ca^{2+} cross-linked complexes which together with RGII diester bonds are thought to affect the cellulose-xyloglucan network by influencing the wall porosity and the accessibility of primary cell wall relaxation proteins to their substrates (Pelloux et al., 2007).

1.5.1.2 Pectin methylesterases inhibitor

There have been several compounds reported, both proteinaceous and non-proteinaceous which have inhibitory effects on PMEs. The proteinaceous PME inhibitor (PMEI) has been found in kiwi fruit and the related PMEIs genes were discovered in *Arabidopsis* (Balestrieri et al., 1990; Wolf et al., 2003). Inhibition of PME by PMEI occurs through the formation of an inactive complex between enzyme and inhibitor (Jolie et al., 2010). PME and PMEI form a complex in which the inhibitor covers the place where active site is located (**Fig. 1.16**). The physiological function of PMEI lies in the modulation of the endogenous PME activity during plant growth and development Peaucelle et al., 2008a. Additionally, PMEI might indirectly play a role in plant defence against pathogen attack by limiting the action of microbial pectin-degrading enzymes. Moreover, PME activity can be inhibited by a green tea catechin extract (see **chapter 1.5.1**).

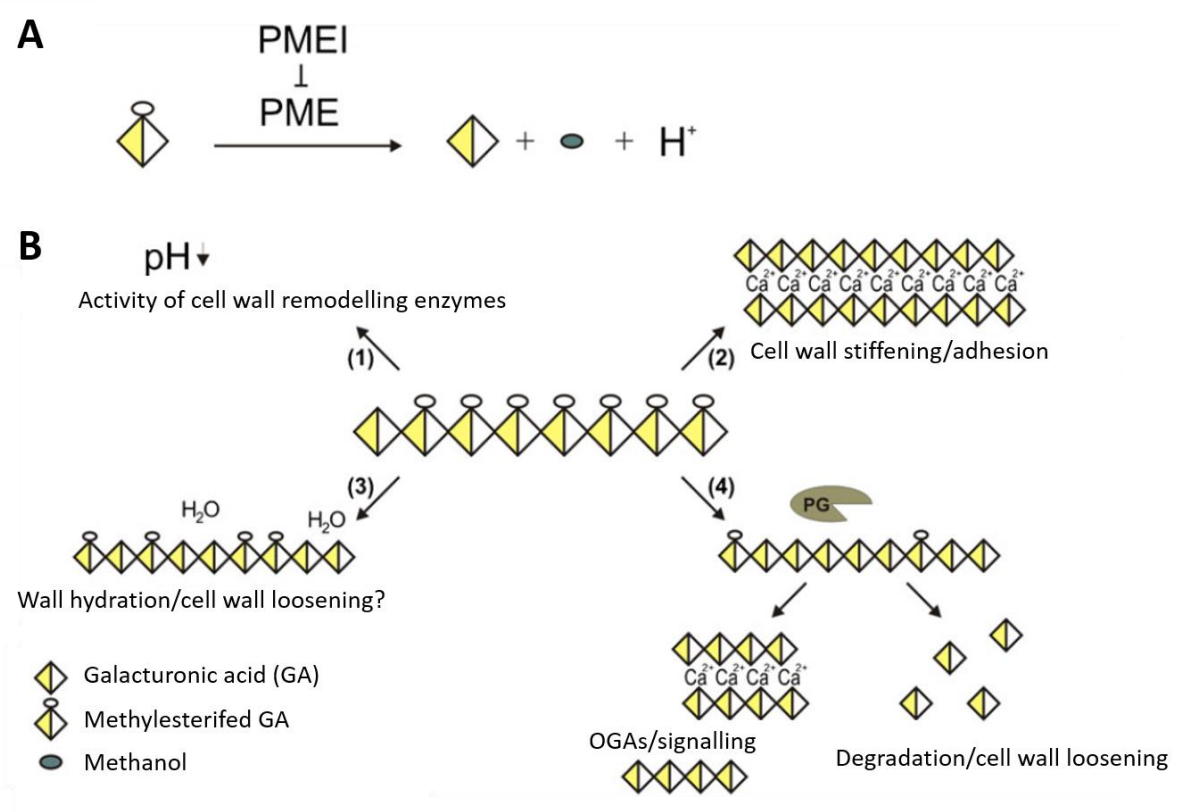

Figure 1.15. Schematic representation of homogalacturonian demethylesterification. (A) The pectin methylestease (PME) catalyses the reaction which leads to release of a free carboxyl group, methanol and protons, respectively. Pectin methylesterase inhibitor (PMEI) can prevent the reaction through interaction with PME. (B) Possible consequences of PME activity. 1 Reaction outlined in A can cause a reduction in pH which may alter cell wall properties by changing the activity of cell wall remodelling enzymes. 2 Blockwise demethylesterification of more than nine galacturonic acid residues can cross-link the adjacent HG backbones via Ca^{2+} which leads to gelation and stiffening of the pectin. 3 Non-blockwise demethylesterification might promote hydration, which in turn can reduce the wall stiffness. 4 The degradation of HG by polygalacturonase (PG) requires PME activity. In addition to the wall loosening effect of pectin removal, PG activity can result in the production of oligogalacturonides (OGAs), which can act as signalling molecules during pathogen attack and normal development. Adapted from Wolf and Greiner, 2012.

Food technologists are trying to strengthen cell-cell adhesion to stop tissue softening of heat-treated fruits and vegetables. It can be achieved by lowering the degree of esterification of pectin, whether or not in combination with addition of Ca^{2+} ions (Van Buggenhout et al., 2009). A commonly used pre-processing technique which lowers esterification of pectin is low-temperature blanching (Ni et al., 2005; Sila et al., 2005). During blanching, the catalytic activity of endogenous PME is enhanced, which leads to an increase in free pectic carboxyl groups providing a greater opportunity for the pectic polymers to be ionically cross-linked with divalent ions like Ca^{2+} (Canet et al., 2004; Sila et al., 2004).

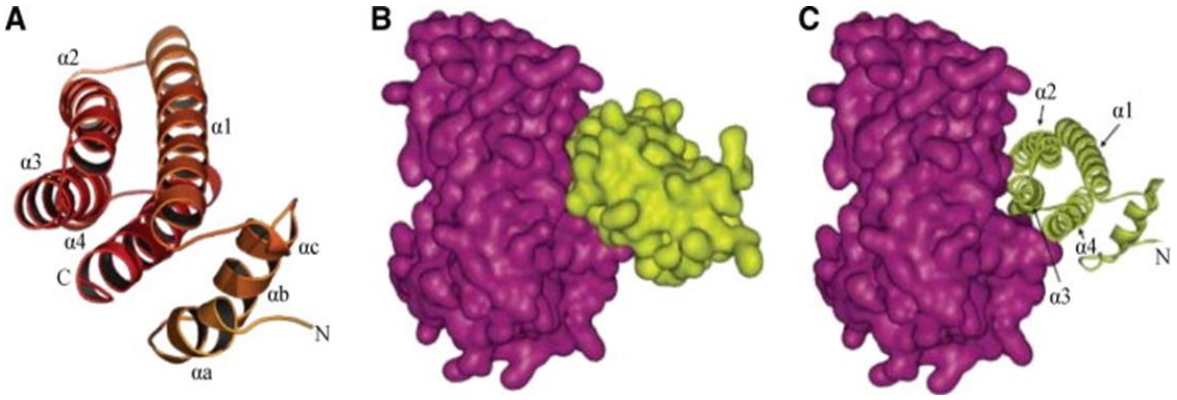

Figure 1.16. Three-dimensional model of the PMEI action. A. Three-dimensional structure of kiwi PMEI. B, C. The complex between tomato PME (violet) and kiwi PMEI (green). The α-helices α2, α3 and α4 of the inhibitor fit into the substrate binding cleft of the enzyme. Adapted from Jolie et al., 2010.

1.5.1.3 Pectin lyases and pectate lyases

Pectate lysases (PLs) are a family of endo-acting depolymerizing enzymes which cleave pectate (demethylesterified pectin) thereby yielding oligosaccharides with 4-deoxy-a-D-mann-4-enuronosyl groups at their non-reducing ends (Solbak et al., 2005). Plant pectate lyase-like (PLL) genes encode proteins with strong amino acid sequence homology with an isoform of bacterial pectate lyases (Wing et al., 1990) and exist as large families in plants. Although there are 26 PLL genes in *Arabidopsis*, the activity of the proteins encoded by these genes is poorly reported in the literature. Analysis of the expression profiles of all PLL genes showed their expression in flowers suggesting all PLL genes have some role in either flower development and/or flower-associated functions. It is believed that PLLs function in pollen germination by loosening the cell wall to allow pollen tube emergence (Palusa et al., 2007). PLLs can act as extracellular virulence agents, and their role in the production and release of cell wall oligogalacturonides is important for activation of plant defence mechanisms (De Lorenzo et al., 1991). The function of only one of the PLL genes (*powdery mildew resistance 6*; *PMR6*) is known (Vogel et al., 2002). Recessive mutations in the *PMR6* exhibited strong resistance to *Erysiphe cichoracearum*, suggesting the gene is a determinant of powdery mildew sensitivity. However, *pmr6* mutant was susceptible to other bacterial and fungal pathogens, *Pseudomonas syringae* and *Peronospora parasitica* respectively (Vogel et al., 2002). Additionally, *pmr6* plants were smaller due to decreased cell expansion, suggesting a role for PMR6 in plant growth and development.

Pectin lyases are the enzymes capable of degrading pectin polymers directly via a β-elimination mechanism that results in the formation of unsaturated oligogalacturonides without methanol production (Yadav et al., 2009). Phylogenetic analysis revealed 67 pectin lyase genes in *Arabidopsis* clustered into five well-supported groups. The exon/intron structure of the pectin lyase genes were highly conserved in each of the groups, indicative

of their functional conservation. The pectin lyase genes were non-randomly distributed across the *Arabidopsis* chromosomes, and a high proportion of the pectin lyase genes might be derived from tandem duplications (Cao, 2012). Most pectin lyases are produced by microorganisms and pectin lyase gene expression is generally induced by neutral pH, carbon sources and pectin, and is repressed by glucose (Trigui-Lahiani and Gargouri, 2007).

1.5.1.4 Polygalacturonases

Polygalacturonases (PGs) are key homogalacturonan (HG) hydrolysing enzymes that contribute to pectin disassembly during many stages of plant development, such as organ abscission and microspore release that require cell separation as well as fruit ripening and pollen tube growth (Hadfield and Bennett, 1998). Depending on their mode of action, endo- and exo-PGs can be distinguished. Endo-PGs require at least four consecutive demethylesterified GalA residues of the HG chain to hydrolyse the HG polymer at random sites (Protsenko et al., 2008). Therefore, the methylation state of the HG chains directly influences possible endo-PG-mediated HG cleavage. Endo-PGs activity might lead to complete hydrolysis of pectin polymers and has the potential to cause rapid cell elongation or cell separation (Senechal et al., 2014). Exo-PGs attack the free ends of demethylesterified HG chains and therefore reduce the overall polymer length. It is believed that the resulting modification might have less influence on the HG properties than the random cleavage by endo-PGs and therefore can be used to fine-tune the extensibility of the primary cell wall (Abbott and Boraston, 2007).

The *Arabidopsis* genome contains 69 PG genes and their expansion can be attributed to whole genome and segmental duplications (González-Carranza et al., 2007). The well characterised PGs in *Arabidopsis* are involved in cell separation. Endo-Pg encoded by *QUARTET2* (*QRT2*) is essential for pollen grain separation and is part of a small family of three closely related endo-PGs, including ARABIDOPSIS DEHISCENCE ZONE POLYGALACTURONASE1 (ADPG1) and ADPG2. Genetic analysis showed that ADPG1 and ADPG2 are essential for silique opening. Moreover, ADPG2 and QRT2 assist in floral organ abscission, while all three genes contribute to anther dehiscence (Ogawa et al., 2009). The degree of methylesterification is one important aspect that seems to be tightly regulated, but recent data emphasizes the importance of pectin-hydrolysing PGs in cell elongation processes. It has been found that the *nimna* (*nma*) *Arabidopsis* mutant has cell elongation defects in embryos. *NMA* encodes an exo-PG and is preferentially expressed in reproductive tissue (Babu et al., 2013).

1.6 The function of oligogalacturonides

1.6.1 Oligogalacturonides as damage-associated molecular patterns

Plant immunity responses are activated by microbe-associated molecular pattern molecules (MAMPs) like bacterial flagellin or fungal chitin (Jones and Dangl, 2006). Pathogens can also be sensed indirectly by the release of endogenous molecules like oligosaccharides upon tissue injury and these molecules are referred to as damage-associated molecular patterns (DAMPs; Trouvelot et al., 2014). The eliciting oligosaccharides were identified as oligogalacturonides (OGAs), oligomers of α-1,4-linked galacturonic acid released from HG after hydrolysis by PGs. *In vitro*, the active OGAs are generated by plant-encoded PG-inhibiting proteins (PGIPs) which block the complete hydrolysis of HG to galacturonic acid (Kalunke et al., 2015).

The biological active OGAs have a degree of polymerization (DP) between 10 and 15 which is optimal for the formation of Ca^{2+}-mediated crosslinks resulting in structures called “egg boxes” (Cabrera et al., 2008). Exogenously applied OGAs activate a range of defence responses, including the expression of defence-related genes and the production of reactive oxygen species (**Fig. 1.17**; Galletti et al., 2008). This happens through binding of OGAs to the extracellular domain of the *Arabidopsis* wall-associated receptor kinase 1 (WAK1) indicating that WAK1 acts as a receptor for OGAs (Brutus et al., 2010). The signal transduction pathway starts with the activation of the phosphorylation of the *Arabidopsis* mitogen-activated protein (MAP) kinases MPK3 and MPK6 which triggers a robust oxidative burst required for the accumulation of callose in the cell wall (Galletti et al., 2011). Recently it has been proven that endogenously generated OGAs accumulate to significant concentrations and function as signalling molecules similar to that when OGAs are exogenously applied. It was achieved using a chimeric protein consisting of a PG and a specific PGIP. Expression of the PGIP-PG chimeric (called “OG machine”) protein in *Arabidopsis* under the control of a pathogen-induced promoter resulted in increased resistance to pathogen infection (Benedetti et al., 2015).

Plants are able to sense mechanically damaged tissues and respond to it similarly as to pathogen infection. Resistance induced by both OGAs and wounding is independent of SA-, JA-, and ethylene-mediated signalling pathways and requires PHYTOALEXIN DEFICIENT3 (PAD3), a cytochrome P450 that catalyses the last step of camalexin biosynthesis (Chassot et al., 2008). Camalexin is an indole alkaloid known to inhibit the growth of virulent strains of *Pseudomonas syringae*. The accumulation of camalexin is not observed after wounding nor after OGAs treatment, although it is induced after inoculation

with *Botrytis cinerea* in wounded leaves (Ferrari et al., 2013). This data suggest that wound-induced resistance to *Botrytis* is mediated by OGAs.

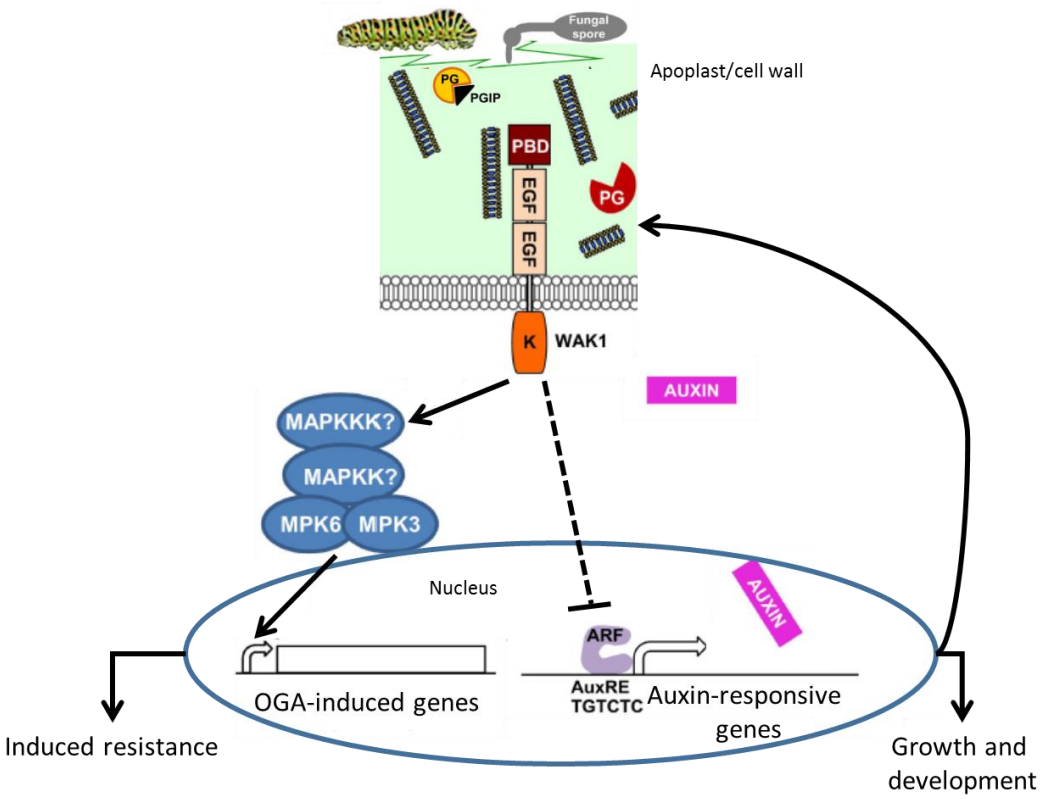

Figure 1.17. A schematic of the activation of *Arabidopsis thaliana* defence and developmental responses triggered by oligogalacturonides (OGAs). The release of OGAs from the cell wall is mediated by degradation of homogalacturonan by mechanical damage or by the action of PGs secreted by pathogens. During the pathogen attack, PGIPs in the apoplast influence PG activity, favouring the accumulation of active OGAs. OGAs are then perceived by WAK1 and trigger MAPK-mediated activation of OGA-mediated genes like *PAD3*. It has been shown that auxin also induces the expression of plant PGs and other pectin-degrading enzymes Laskowski et al., 2006. The action of these enzymes may release OGAs in the apoplast that can inhibit auxin-related responses, creating a negative feedback loop. A dashed line indicates a hypothetical cascade. EGF – epidermal growth factor domain; PBD – pectin binding domain. Adapted from Ferrari, et al. 2013.

1.6.2 Oligogalacturonides as regulators of plant development

OGAs may be important not only in defence against pathogens, but also in regulatory mechanisms of growth and development. OGAs have been shown to inhibit auxin-induced adventitious root formation in *Arabidopsis* leaf explants (Savatin et al., 2011). Inhibition of root formation was observed when OGAs were supplied together with IAA and it was overcome by higher amounts of auxin. Additionally, IAA was capable of counteracting defence responses triggered by OGAs (Savatin et al., 2011). The activity of OGAs affected early responses too, such as inhibition of auxin-induced gene expression (**Fig. 1.17**). This was confirmed by the ability of OGAs to prevent IAA-induced expression of GUS driven by the auxin-inducible promoter DR5 (Savatin et al., 2011). Moreover, OG-auxin antagonism

also occurs when the auxin-regulated genes are induced by the translation inhibitor cycloheximide, suggesting that OGAs may act downstream of Aux/IAA repressors, possibly at the level of the promoter regions of auxin-responsive genes. Furthermore, OGAs inhibited the induction of the late auxin-responsive genes like *Nt114*, encoding a glutathione *S*-transferase in tobacco (Mauro et al., 2002). The role of OGAs as regulators of growth and development is still to be proven with more experiments involving endogenous OGAs signalling.

1.7 A brief introduction to chemical biology

Using the application of small chemical compounds, new phenotypes can be described through the perturbation of cellular functions that can be linked to growth and development. The introduction of chemical biology as a tool for basic research has advanced significantly and demonstrates the potential of this approach in plant cell wall biology. The use of isoxaben and polyphenon 60 as a tool in chemical biology are described below.

1.7.1 Polyphenon-60

Polyphenols are secondary metabolites of plants and are involved in defence against ultraviolet radiation and pathogen attack. All plant phenolic compounds arise from a common intermediate, phenylalanine, or a close precursor, shikimic acid (Quideau et al., 2011). The main classes of polyphenols include phenolic acids, flavonoids, stilbenes and lignans. Polyphenols may have therapeutic health effects for a variety of chronic pathological conditions. Tea is the second most frequently consumed beverage worldwide and tea polyphenols have received public attention due to the positive association between tea consumption and beneficial health effects (Kuriyama et al., 2006). Antioxidant effects of polyphenols may be protective against cardiovascular diseases, development of cancer or carcinogenesis (Pandey and Rizvi, 2009). It has been proposed that the gallolyl moiety of tea catechins play the critical roles in specific activities of catechins (Ikeda et al., 2005).

Polyphenon-60 (PP60), also known as green tea catechin extract, is a mix of catechins composed of (-)-epigallocatechin-3-gallate (EGCG), (-)-epicatechin-3-gallate (ECG), (-)-epigallocatechin (EGC), (-)-epicatechin (EC), (-)-gallocatechin gallate (GCG), and (-)-catechin gallate (CG). It has been shown to act as PME inhibitor *in vitro* and has the potential use in the examination of the role of PMEs and PMEI in plant growth and development (Lewis et al., 2008a). Enzymatic activity of PME with PP60 was tested using

ruthenium red staining of esterified pectin-infused plates of agarose medium. Demethylesterifed pectin is the cause for a stained zone after PME incubation. A serial dilution of PME was incubated in agarose plates with or without PP60. The inhibition of citrus and tomato PME by PP60 has been demonstrated by the change of the staining diameter upon addition of increasing PP60 concentrations (**Fig. 1.18**) (Lewis, et al., 2008). These results have shown that green tea catechins can be used to inhibit PME activity *in vitro* and have a potential to be useful as a PME inhibitor *in vivo* to understand the role of PME in cell wall modulation of adhesion and rigidity.

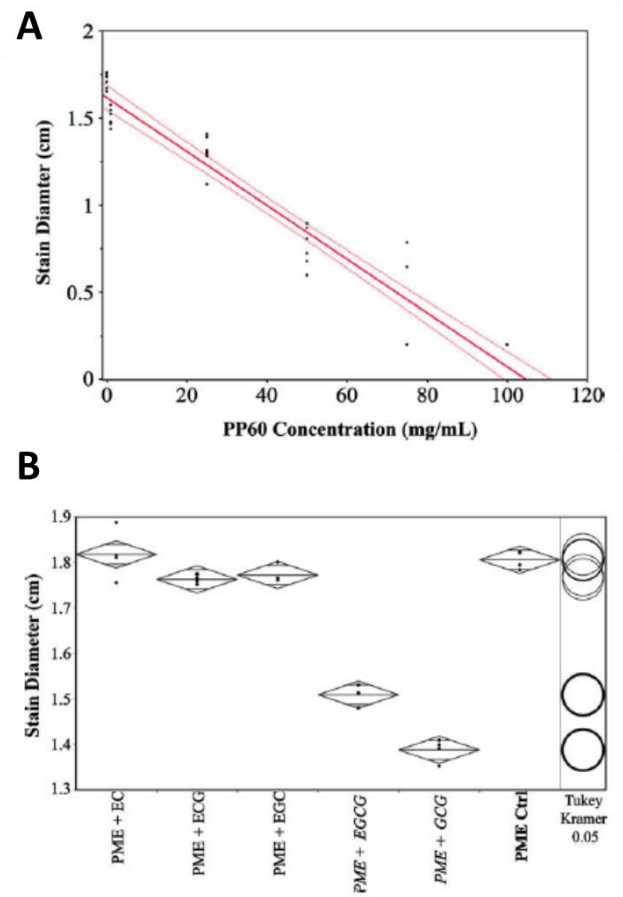

Figure 1.18. The *in vitro* inhibition of PME activity by PP60 and its components. (A) The relationship of diameter of staining of a consistent citrus PME solution with a treatment of varied PP60 concentrations. (B) Individual catechin effects on PME. Diamonds are 95% confidence intervals and non-overlapping circles in the Tukey's test show significant differences. Adapted from Lewis et al., 2008.

The green tea extract contains the number of different catechins from which EGCG is the most abundant (Adachi et al., 2002; **Fig. 1.19**). EGCG has been extensively examined for its beneficial effects in clinical and animal studies. It has been shown it can exert pro-oxidant actions and promote cytotoxicity in anti-tumour activity (Nakagawa et al., 2004). It has been shown that EGCG could increase the percentage of cells in the G1 phase, which may partially contribute to cell growth inhibition. Moreover, it was observed that EGCG induced significant cell apoptosis in human colorectal cancer cells, suggesting that the

EGCG antiproliferative effects are in part through the apoptosis pathway (Du et al., 2012). EGCG was found to directly interact with membrane components, including proteins and lipids regulating activities of cell surface growth factor receptors (Rodriguez et al., 2006). EGCG has been shown to have a protective role against the neurotoxin MPTP, an inducer of a Parkinson's-like disease, by competitively inhibiting the uptake of the drug due to molecular similarity (Aquilano et al., 2008).

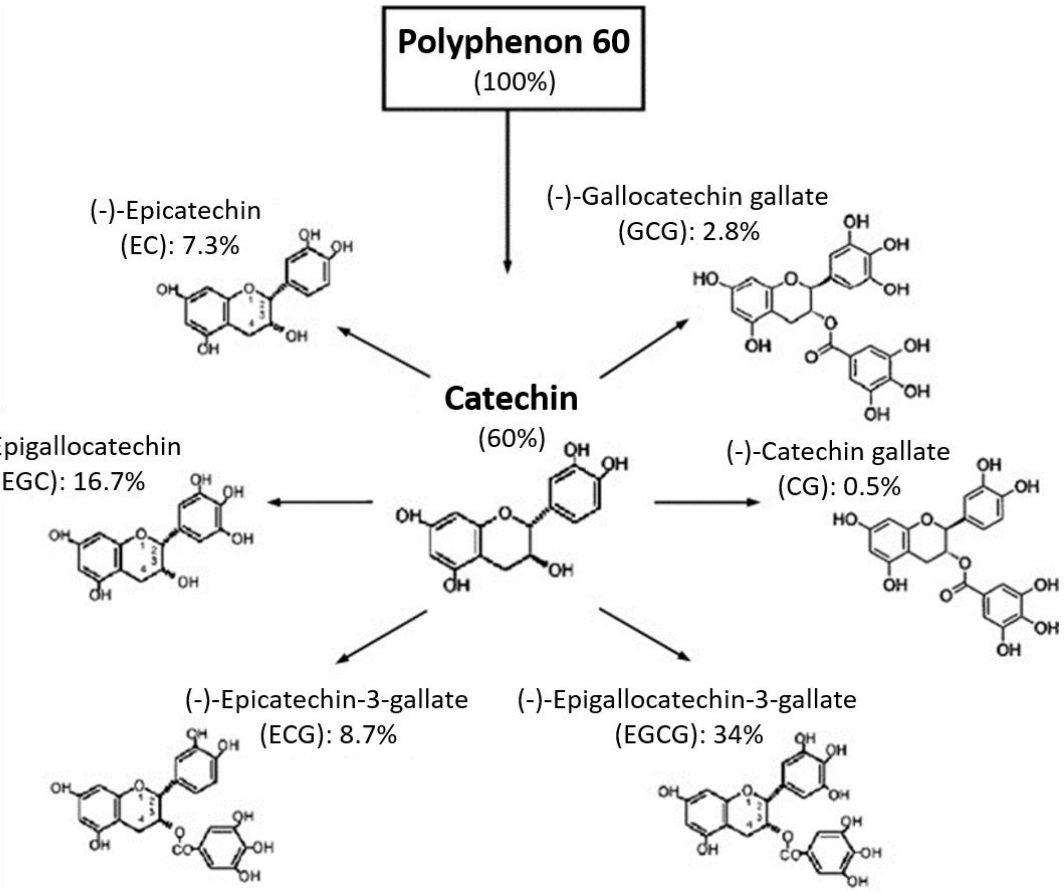

Figure 1.19. Catechins present in Polyphenon-60. EGCG is the most abundant catechin which consists nearly half of the catechins content and it is the most active PME inhibitor. Adapted from Lim et al., 2013.

In a recent study it has been shown that PP60 and EGCG had different inhibitory capacities toward plant and fungal PMEs. EGCG induced a 40% inhibition of AtPME31 and *Citrus sinensis* PME activities. In contrast, the measured activity of *Botrytis cinerea* PME1 was weakly inhibited (20%) at higher concentrations of EGCG (L'Enfant et al., 2015). It shows that plant PMEs were more sensitive to EGCG compared to fungal enzymes. It is hypothesized that the gallate group could be responsible for this inhibition (L'Enfant et al., 2015). It has been shown that EGCG interacts with the catalytic site of PME. The extended docking model of the EGCG molecule to large surface area of the PME revealed that this ligand prefers clustering at the enzyme active site (**Fig. 1.20**). The fluorescence resonance energy transfer (FRET) method was used to investigate the site of EGCG binding to PME and it was found that the PME tryptophans from the binding site interact with the EGCG

(Lewis et al., 2008b). The EGCG binding site is relatively small compared to the PMEI from kiwi fruit where PMEI has a direct contact with wide active binding site cleft of PME, covering the binding site access point (Di Matteo et al., 2005). EGCG have influence on root development showing decrease in primary root length and root waving (Wolf et al., 2012). These results show that catechins like PP60 mix can be a useful tool for plant developmental studies.

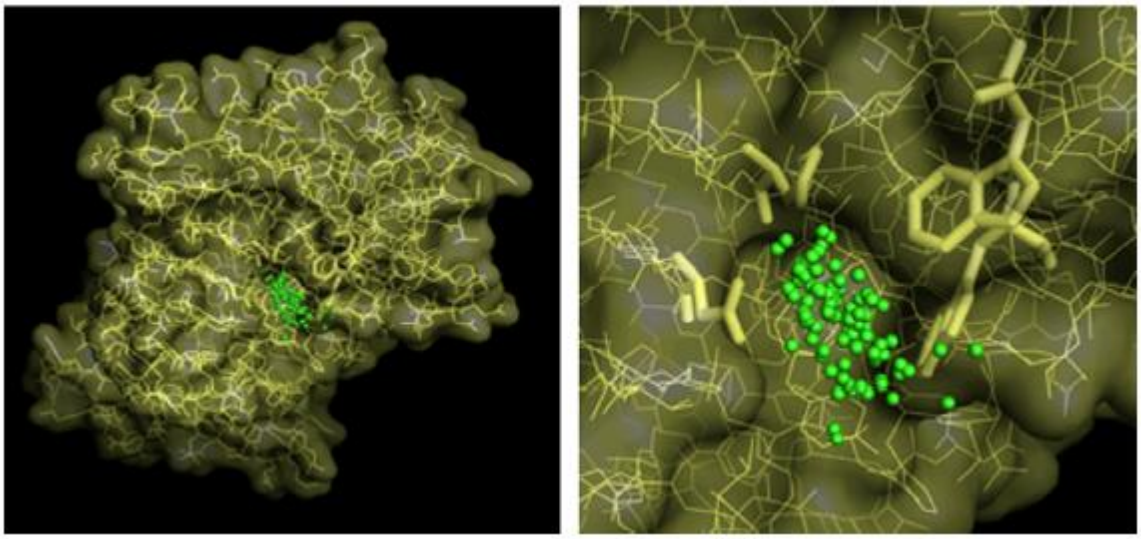

Figure 1.20. Docking model showing the interaction of EGCG with the catalytic site of PME. Green dots represent the ligands around the binding site area. The number of dots corresponds to the number of the random docking runs. Adapted from Lewis et al., 2008.

1.7.2 Isoxaben

The inhibitor used frequently to inhibit cellulose production during primary cell wall formation is isoxaben (Heim et al., 1990). The inhibitor became an excellent tool for studying cell wall integrity (CWI) mechanisms after the phenotypic effects observed could be easily validated using a resistant mutant like *isoxaben resistant 1-1* (*ixr1-1*; Scheible et al., 2001). The resistance to isoxaben is caused by an amino acid change in the CESA3 cellulose synthase. This change is located at a site quite distant from the highly conserved residues that have been proposed to be a component of the active site. One of the possible explanations is that the mode of action of the herbicide involves these regions in binding of regulatory molecules and that the *ixr1* mutation may alter these sites instead of affecting the catalytic site (Scheible et al., 2001). The effects of isoxaben start to appear early and it has been observed that labelled cellulose synthase proteins disappeared from the plasma membrane within five minutes after start of treatment in *Arabidopsis* seedlings (Paredez et al., 2006). After approximately one hour of isoxaben treatment, elongation of root epidermal cells was significantly reduced compared to controls (Tsang et al., 2011). A further 3-4 h of isoxaben treatment caused increased reactive oxygen species (ROS) and jasmonic acid

(JA) production in seedlings (Denness et al., 2011). Deposition of lignin and callose was detected in the elongation zones of isoxaben treated roots after 5-6 h (Hamann et al., 2009). Moreover, during the same period, effects on carbohydrate metabolism (transcriptional and metabolic) were observed, highlighting that effects of cellulose biosynthesis inhibition are not restricted to signalling cascades and cell walls (Wormit et al., 2012).

1.8 Plant cell wall integrity mechanisms

The plant cell wall is an interface between plant cell and surrounding environment. To perceive stimuli from the environment and derived from the plant itself, plants must produce different types of sensors. The stimuli can have two properties: chemical (ligands, small fragments) or physical (displacement of plasma membrane). Plant-derived chemical stimuli can take a form of cell wall fragments (oligogalacturonides), metabolites or peptides. Non-plant-derived stimuli represent sources extracted from invading pathogens (like FLG22; Ferrari et al., 2013). The current knowledge of the molecular basis responsible for the detection of stimuli and the mode of action in plants is limited, whereas more is known about mechanisms in *Saccharomyces cerevisiae*. The mechanism which monitors the functional integrity of the cell wall and triggers adaptive changes in cell wall and cellular metabolism is called the cell wall integrity (CWI) maintenance mechanism. Its role is to maintain wall integrity in response to developmental (i.e. cell division) or environmental (i.e. osmotic shock) stresses (Levin, 2011).

1.8.1 Signalling molecules implicated in cell wall integrity monitoring and signal translation

CWI disruption is caused by cell wall damage that changes the physical structure of the wall and/or disrupts the surface tension of the wall. Cell wall damage is caused by physical forces appearing during cell morphogenesis, abiotic stress or enzymatic digestion of cell walls during pathogen infection. A popular strategy to investigate CWI maintenance is manipulation of cellulose production to cause physical cell wall damage in a highly controlled and specific manner. Tools to generate CWD include genetic (mutations in cellulose synthase genes) and chemical inhibition (isoxaben as the most popular inhibitor; de Castro et al., 2014, Scheible et al., 2001).

Several studies have identified different signalling components and compounds required for CWI maintenance (**Fig. 1.21**). Recent findings indicate a large number of different receptor-like kinases (RLKs) to be involved in cell wall damage perception

(Engelsdorf and Hamann, 2014). FERONIA (FER) and THESEUS1 (THE1) are the most informative candidates amongst the different RLK candidates. FER is a receptor for the RAPID ALKALINIZATION FACTOR1 (RALF1) peptide and RALF1-FER interaction has an influence on calcium based signalling processes between the ovule and the pollen tube (Haruta et al., 2014). Additionally, FER regulates ROS based signalling and possibly cell wall modifications during root hair and pollen tube growth by controlling RHO GTPase activity (Duan et al., 2010). These results may suggest the possibility of particular RALF-like peptides and FER-like RLKs combinations that coordinate cell elongation processes between adjacent and in individual cells via calcium/ROS-based signalling processes (Hamann, 2015a). THE1 is another RLKs family member that also has been implicated in regulation of cell elongation. *the1 Arabidopsis* mutant seedlings have reduced cell elongation due to cellulose deficiency, ectopic lignin deposition and reduced ROS production. Overexpression of THE1 causes increased lignin deposition (Denness et al., 2011). Finally, MID1-COMPLEMENTING ACTIVITY1 (MCA1) is the third protein of particular interest. It has been shown that it can function as plasma membrane localized calcium channel in *Arabidopsis* and yeast (Shigematsu et al., 2014). Moreover, MCA1 is involved in mechano-perception dependent growth processes and short-term responses to isoxaben (Denness et al., 2011). Wall-associated kinases (WAKs) are also discussed as signalling components since they have been shown to bind pectin and pectin-derived epitopes, oligogalacturonides (OGs). A recent study has provided evidence that pectin together with brassinosteroid (BR)-based signalling processes is an important regulator of cell wall integrity during growth and development (Wolf et al., 2012).

ROS, calcium, jasmonic acid (JA) and 1-aminocyclopropane-1-carboxylic acid (ACC)-based signalling processes are required for signal translation and regulation of responses to cellulose biosynthesis inhibition (Denness et al., 2011). The available data on the CWI maintenance mechanism is still limited and mostly indirect. It is suggested that initial stimulus perception leads to release of a peptide like RALF1, which activates a FER-like RLK. FER in turn activates NADPHoxidases via a RHO GTPase and calcium dependent process. NADPHoxidases derived ROS is required to modulate JA production, while JA in turn represses ROS production. However, it remains to be determined what is the primary stimulus responsible for peptide release (Hamann, 2015a).

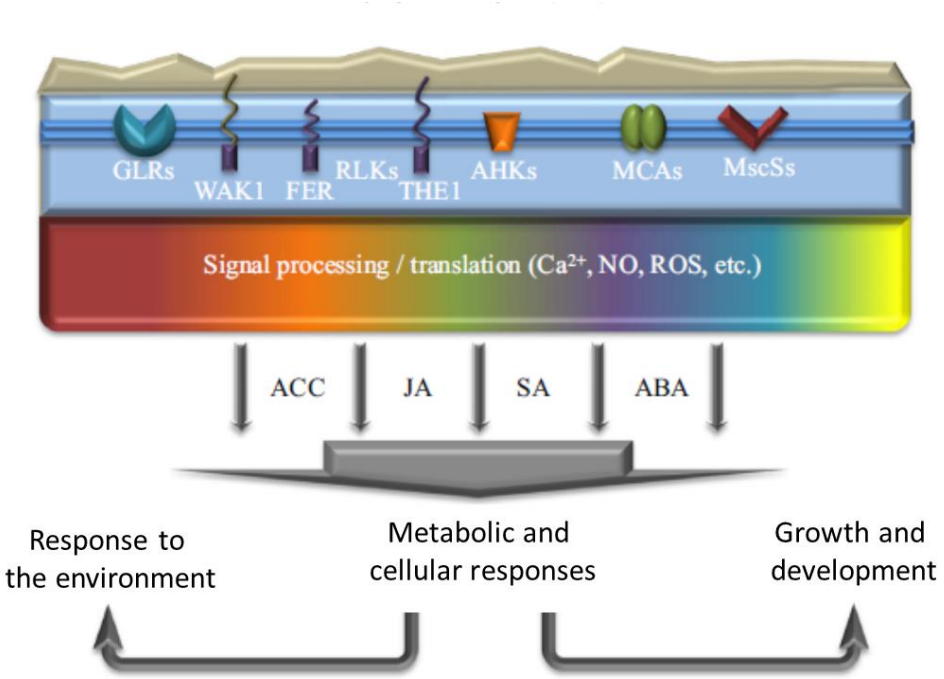

Figure 1.21. Different gene families and signalling components involved in cell wall integrity maintenance. GLRs – glutamate-like receptors; WAK – wall-associated kinase; FER – FERONIA; RLKs – receptor-like kinases; THE – THESEUS; AHKs – ARABIDOPSIS HISTIDINE KINASEs; MCAs – MID1-COMPLEMENTING ACTIVITY; MscSs – mechanosensitive channel of small conductance; ACC - 1-aminocyclopropane-1-carboxylic acid; JA – jasmonic acid; SA – salicylic acid; ABA – abscisic acid. Beige colour indicates cell wall, dark blue – plasma membrane, light blue – the plasma membrane-cell wall space containing sensors and signalling components. Adapted from Hamann, 2015b.

1.9 Plant phytohormones

Hormones are chemical messengers produced in the cell which modulate cellular processes by interacting with specific receptors linked to cellular transduction pathways. Most plant hormones are synthesized in one tissue and act on specific target sites in another tissue at low concentrations. Plant development is regulated by six major types of hormones (excellent reviews about functions in plants of each hormone are in brackets): auxin (Zhao, 2010), cytokinins (O'Brien and Benkova, 2013, Keshishian and Rashotte, 2015), gibberellins (Davière and Achard, 2013), ethylene (Schaller, 2012), abscisic acid (Gomez-Cadenas et al., 2015), and brassinosteroids (Fridman and Savaldi-Goldstein, 2013). Auxin and brassionosteroid biosynthesis pathways are described in this section together with their function in root development. For the rest of hormones only their functions in root development are described.

1.9.1 Auxin and its function

Auxin was discovered as a plant growth hormone due to its ability to stimulate differential growth in response to light stimuli. The *in vitro* bioassay in which blocks placed on cut hypocotyls and containing auxin stimulated growth of oat coleoptile segments led to the identification of indole-3-acetic acid (IAA) as the main naturally occurring auxin in plants (**Fig. 1.22**). Auxin biosynthesis is very complex with tryptophan-dependent and –independent pathways contributing to *de novo* auxin production. Moreover, IAA can be released from IAA conjugates by hydrolytic cleavage of IAA-amino acids. IAA-methyl ester, and IAA-sugar (Woodward and Bartel, 2005).

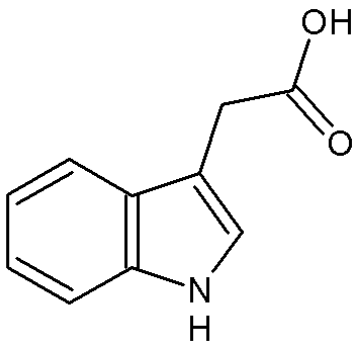

Figure 1.22. Chemical structure of indole-3-acetic acid (IAA).

De novo auxin production is highly localized and local biosynthesis plays a key role in determining local auxin gradients. The dominant view in the auxin field postulates that polar auxin transport is responsible for generating auxin gradients and auxin maxima which are essential for plant development. It was believed for a long that the shoot was the only source of auxin biosynthesis and that other parts of a plant were dependent on polar auxin transport to supply auxin. It is now clear that both shoot and root can produce auxin (Petersson et al., 2009). Auxin control of root elongation has shown that low concentrations (10^{-10} to 10^{-9} M) of auxin promote the growth of intact roots, while higher concentrations (10^{-6} M) inhibit growth. Therefore, roots may require a minimum concentration of auxin to grow, but auxin concentrations that promote elongation in stems strongly inhibit root growth (Overvoorde et al., 2010). Although elongation of the primary root is inhibited, initiation of lateral roots is stimulated by higher auxin levels (Fukaki et al., 2007). Bending of a plant in response to gravity results from the lateral redistribution of auxin. According to the current model of gravitropism, auxin transport in a vertically oriented root is equal on all sides. However, when root is oriented horizontally, the cap redirects most of the auxin the lower side inhibiting the growth of that lower side (Band et al., 2012).

1.9.2 Brassinosteroid and its function

Brassinosteroids (BRs) are steroid hormones that regulate various aspects of plant growth and development, such as cell division and elongation and sex determination. Mutants defective in BR biosynthesis or signalling are dwarfed with short hypocotyls, dark green leaves, and delayed senescence (Choe et al., 2002). Brassinolide (BL) is the final product of brassinosteroids biosynthesis which involves multiple intermediates (**Fig. 1.23**)

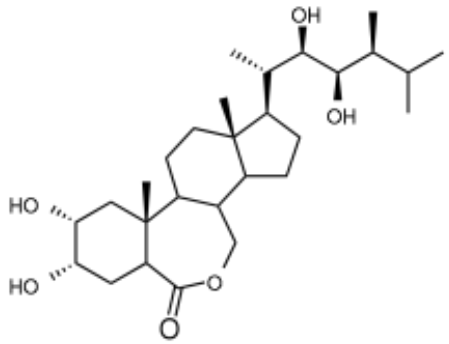

Figure 1.23. Chemical structure of brassinolide.

BRs are a group of hormones that play pivotal roles in a wide range of developmental processes in plants, including cell division and elongation in stems and roots, reproductive development, leaf senescence, and stress responses (Haubrick and Assmann, 2006). The phenotypes of BR-deficient mutants, which typically have reduced root growth, suggest that BRs are required for normal root elongation. However, similar to auxin, exogenously applied BRs promote root growth at low concentrations and inhibit root growth at high concentrations (Wei and Li, 2015). Moreover, BR promotes gravitropic responses, and this effect is associated with enhanced expression of the auxin efflux transporter PIN2 in the root elongation zone (Li et al., 2005). BRs and auxin can act synergistically on primary and lateral root development and more on this can be found in **chapter 5.1.3**.

1.9.3 Other hormones

Gibberellins (GAs) are the best known for their promotion of stem elongation and seed germination. The GAs are diterpenoids that are formed from four isoterpenoid units (**Fig. 1.24**). Extreme dwarf mutants of *Arabidopsis*, in which biosynthesis of GA is blocked, have shorter roots than control plant, and application of GA to the shoot promotes both shoot and root elongation (Ubeda-Tomas et al., 2008).

Cytokinins have been shown to have effects on many physiological and developmental processes including leaf senescence, vascular development, nutrient mobilization, and apical dominance. Naturally occurring cytokinins are synthesized from isoprene and are chemically related to carotenoid pigments and the plant hormones gibberellin and abscisic acid (**Fig.1.24**). Cytokinins negatively regulate the root apical meristem and the mechanism by which it is controlled has been discovered. Cytokinins accelerate the process of vascular differentiation at the root tip decreasing the size of the root apical meristem. Therefore, increased cytokinin function enhances cell differentiation into vascular tissue which results in fewer meristematic cells and less root growth (Dello Ioio et al., 2007).

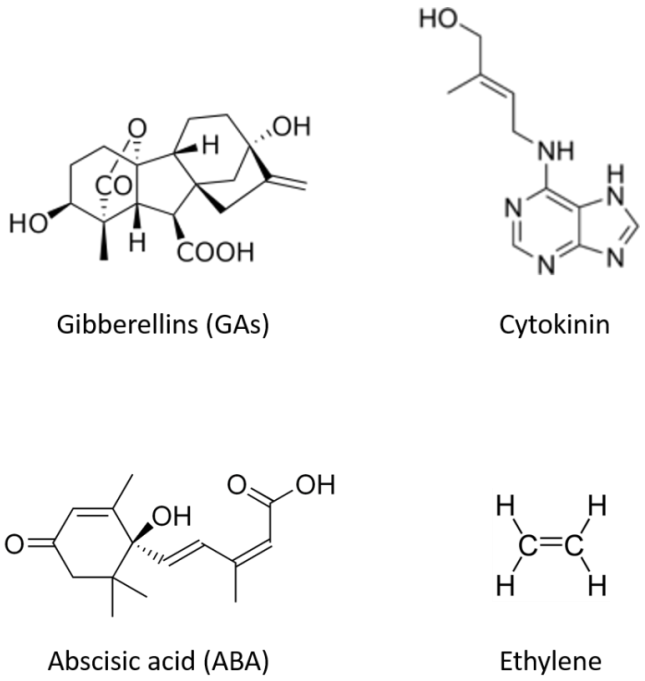

Figure 1.24. Structural diversity of plant hormones.

Ethylene (C_2H_4) is the simplest olefin and a gaseous hormone (**Fig. 1.24**). It has been shown to regulate a wide range of responses in plants like seed germination, cell expansion and differentiation, flowering, and abscission. Ethylene is capable of inducing adventitious formation in leaves, stems, and even other roots. It has also been shown to act as a positive regulator of root hair formation. In ethylene-treated *Arabidopsis* roots, non-hair cells differentiate into hair cells producing root hairs in abnormal locations (Rahman et al., 2002).

Abscisic acid (ABA) is an important plant hormone that regulates growth and stomatal closure, particularly when the plant is under environmental stress, seed maturation and dormancy. ABA is a 15-carbon compound similar to some of carotenoid molecules (**Fig. 1.24**). It has been shown that root growth of well-watered plants is slightly greater in the wild type than in the ABA-deficient mutant (Xu et al., 2013). ABA also affects the degree of root

branching in response to auxin. ABA response mutants show reduced sensitivity to auxin for initiation of lateral roots, implying that ABA signalling is part of this response (Xu et al., 2013).

1.10 The organization of *Arabidopsis* root

Roots are the organs which grow under the soil where they respond to a variety of environmental stimuli. The main functions of roots are to provide structural support to the aerial part of a plant and acquire water and nutrients crucial for plant growth and development. The study of plant roots has been greatly advanced through the use of the model plant *Arabidopsis thaliana* whose roots have a simple cellular organisation and can be easily grown on non-soil media. In *Arabidopsis*, a region of the root with a tip consisting of undifferentiated cells is called the root apical meristem (**Fig. 1.25 C**). These cells give rise to the different cells of the root through three distinct developmental phases on their way to maturity. In the meristematic zone cells divide to generate a pool that will elongate and differentiate. Following division, they undergo anisotropic elongation and increase in length by many times their width. Finally, in the differentiation zone once cell expansion has ceased, cells acquire their final shape, form and functions (**Fig. 1.25 A**). When the pattern of the primary root has been established, further growth results in branching of the primary root to produce an efficient and dynamic root system (Dolan et al., 1993). The production of lateral roots occurs in the differentiation zone from the cells adjacent to the xylem poles, called the xylem pole pericycle cells (**Fig. 1.25 B**). A subset of these cells is stimulated to divide creating a lateral root primodium which undergo seven stages of development. The lateral root emergence from the parent root epidermis occurs through cell expansion (Casimiro et al., 2003).

1.10.1 Primary root growth

The apical-basal polarity of the embryo is established early during embryogenesis where a shoot meristem is positioned between cotyledons at the apical (top) and a root meristem at the basal (bottom) end (Mansfield and Briarty, 1991). The first step in *Arabidopsis* embryogenesis include the asymmetric zygote division to produce a small apical cell that divides producing the proembryo, and a larger basal cell that divides to produce the suspensor connecting the embryo to maternal tissue (**Fig. 1.26**). Next, one of suspensor cells is specified to become the founder cell of the root meristem, called the hypophysis. The asymmetrical hypophysis division generates a cell that subsequently becomes the quiescent centre (QC) and a lower basal cell from which the columella stem

cells and columella are derived (Petricka et al., 2012). A few transcriptional factors have been implicated in the making of an embryonic root. WUSCHEL-related homeobox (WOX) genes are expressed in dynamic and partially overlapping patterns during embryogenesis (Haecker et al., 2004). Recently it has been shown that WOX5 is essential for QC maintenance by suppressing stem cell division (Forzani et al., 2014). Further, the cells are specified through activity of plant hormones in which auxin plays the major role (**Fig. 1.26 A).** The hypophysis is not specified and roots are not formed in mutants lacking AUXIN RESPONSE FACTOR5 (ARF5), which is one of the 23 ARF genes in *Arabidopsis* (Hardtke and Berleth, 1998; see **chapter 5.1.1**). Repression of ARF5 causes upregulation of PIN1, an auxin transporter which directs auxin flow basally into the hypophysis. PIN1-mediated accumulation of auxin is proposed to affect hypophysis specification through the action of additional auxin-responsive Aux/IAA and ARF pairs expressed in the hypophysis (Weijers et al., 2006).

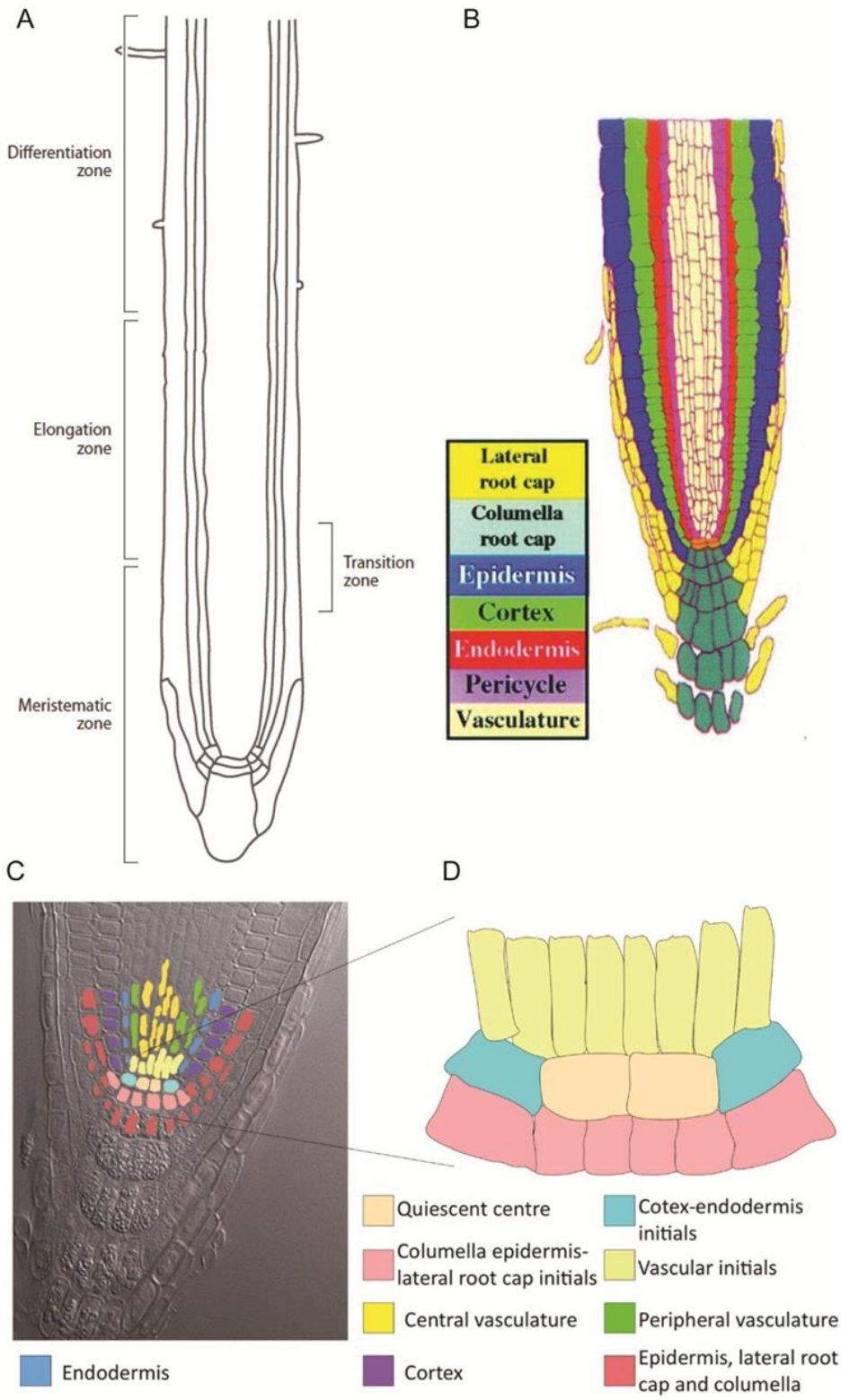

Figure 1.25. The organization of *Arabidopsis thaliana* root. (A) Developmental zones shown through a longitudinal section of the primary root. Cell division occurs in the meristematic zone, cell expansion in the elongation zone, and cell differentiation, where root hairs start to appearing, occurs in the differentiation zone. (B) Distinct tissue types in a longitudinal section. Adapted from Marchant et al., 1999. (C) Cleared root tip of *Arabidopsis* with various cell types distinguished with different colours. (D) Magnification of root stem cell niche. Adapted from Azpeitia et al., 2013.

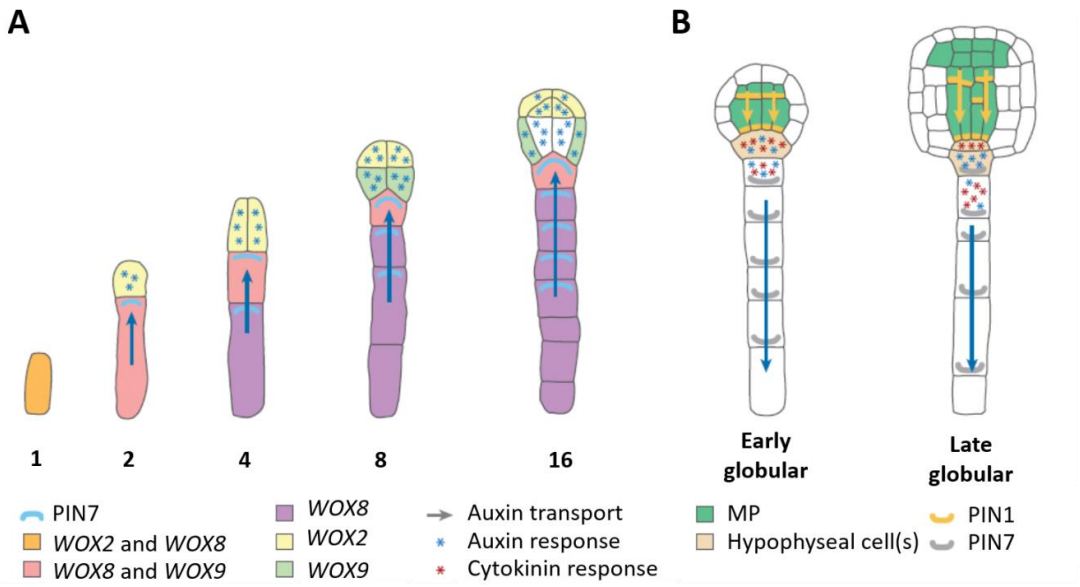

Figure 1.26. Control of embryonic root development in *Arabidopsis*. (A) The early stages of embryogenesis. *WOX* genes are expressed in different and overlapping patterns that regulate cell fate decisions, including that of apical-basal polarity at the 2-cell stage by WOX2 in the apical cell (yellow) and by WOX8 and 9 in the basal cell (pink). Auxin transport is also involved in this process via PIN7 transporter (light blue) which directs auxin from basal cells to the apical part of the embryo. The blue arrow shows the auxin transport direction and blue stars indicate cells with auxin response maxima. (B) The early and late globular stages. During these stages the hypophyseal cell (peach) is specified and divides asymmetrically to produce different cell lineages. Expression of transcription factor MP (dark green) allows the hypophyseal cells to specify. The role of auxin has also been characterized and it is transported into the hypophyseal cell by PIN1 (yellow) and out of this cell by basally localized PIN7 (grey) in suspensor cells. As a result, the maximum auxin response can be observed in the hypophyseal cell and in the upper suspensor cell of the early globular stage (blue stars). Cytokinin response is seen in the same cells at this stage (red stars). However, after hypophyseal cell division auxin responses are found in basal daughter cell and cytokinin in the apical cell during late globular stage. Yellow and blue arrows indicate the direction of auxin transport. Adapted from Petricka, et al., 2012.

When auxin transport is chemically inhibited it interferes with hypophysis specification and root formation, which confirms an important role for PIN transporters in root formation (Friml et al., 2003, Hadfi et al., 1998). Taken together with the localization of PINs, this observation led to a model in which auxin transport and accumulation establish the apical-basal axis and the hypophysis (Friml et al., 2003). Starting from the two-cell stage, PIN7 in the basal cells facilitates auxin transport towards the apical cell to generate an auxin response. PIN7 is localized apically until the globular stage of embryogenesis to maintain the auxin maximum in the proembryo (**Fig. 1.26 B**). During the early globular stage, localization of PIN1 to the basal membranes of the inner cells of the proembryo and redistribution of PIN7 to the basal membrane of suspensor cells causes an auxin response maximum in the hypophysis (Friml et al., 2003). Therefore, localization of PIN1 and changes in polarity of PIN7 might specify the hypophysis during embryogenesis and lead to root formation. In addition to auxin, cytokinin is detected in the hypophysis and its apical cell during the globular stage (Wang and Chong, 2015, Muller and Sheen, 2008).

The tip of every growing root consists of several cell layers called the root cap which play a major role in root tip protection and interaction with rhizosphere (Barlow, 2002). In dicot plants the root cap is divided into columella and lateral root cap cells (**Fig. 1.27 A**). The columella cells are derived from their own independent set of initials, and the surrounding lateral root cap cells originate from a ring of lateral root cap and protoderm initials (Wenzel and Rost, 2001). These tissues along with the epidermis create the exterior surface of the root. The main role of columella cells is gravity sensing whereas the epidermis plays an important role in water and nutrient uptake (Blancaflor et al., 1998). The columella is derived from the division of the columella initials located below the QC, whereas the epidermis and the root cap are derived from the epidermal/lateral root cap initials located next to the QC. The epidermal/root cap initials divide periclinally to produce a daughter cell that will become a new layer of root cap and anticlinally to produce cells that will differentiate into epidermal tissue (**Fig. 1.27 C**; van den Berg et al., 1997).

The root apical meristem established during embryogenesis provides new cells for the growing root. It contains stem cells which give rise to new cells with a very low mitotic activity, the QC. The QC is essential for specification of the stem cell niche and maintenance of the undifferentiated state of stem cells initials (van den Berg et al., 1997). Dividing and specialisation of cells creates the plant vasculature which includes xylem and phloem vessels that transport water and nutrients (xylem) and products of photosynthesis (phloem) to and from the shoot. In *Arabidopsis* roots, the vasculature is organized into a stele, which contains xylem and phloem surrounded with pericycle layer. These tissues are derived from the set of pericycle initials proximal to the QC (Dolan et al., 1993). The phloem consists of sieve elements and companion cells that are derived from asymmetric divisions of procambial initial cells (Bonke et al., 2003). The two types of xylem, protoxylem and metaxylem have different functions and structures. Protoxylem cells have characteristic, spiral cell wall thickenings, are smaller, differentiate early and usually mature when the plant matures. Metaxylem cells have pitted cell wall thickenings, differentiate later, are larger and form the water-conducting vessels (Baum et al., 2002). Cortical and endodermal cell layers are derived from the cortex/endodermal initial cells which regenerate themselves through anticlinal division and produce the cortex initial daughter cells (**Fig. 1.27 B**). Next, these cells divide periclinally to produce the endodermal and cortex precursors (Cui and Benfey, 2009, Miyashima and Nakajima, 2011).

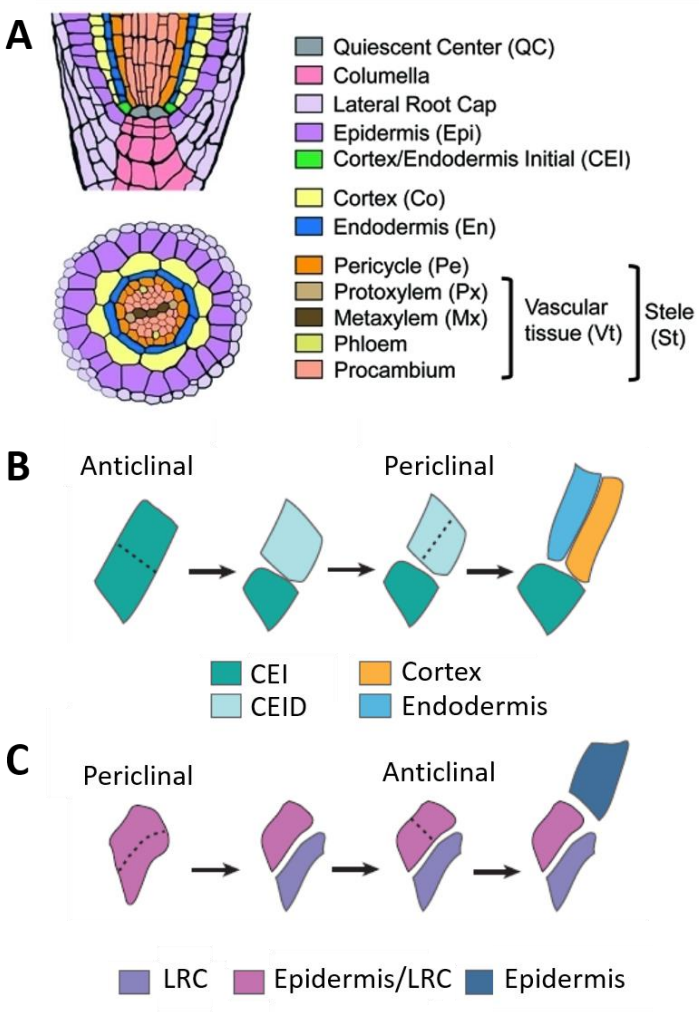

Figure 1.27. Organisation of cell types in *Arabidopsis* root. (A) Schematic representation of different cell and tissue types in Arabidopsis root. Cell types are shown in different colours. (B) Divisions of cortex/endodermis initial (CEI) cells. First CEI cell divides anticlinally to produce two daughter cells then one divides periclinally to give rise to the cortex and endodermis lineages. (C) Divisions of the epidermal/lateral root cap (LRC) initials. The LRC initial cell divides periclinally to produce the LRC cell and then anticlinally to give rise to epidermal cells. Adapted from Miyashima and Nakajima, 2011 (A, B) and Petricka, et al., 2012 (C).

1.10.2 Root hair development

Root hairs are long tubular-shaped outgrowths from root epidermal cells. In *Arabidopsis*, root hairs can grow to 1 mm or more in length and are approximately 10 µm in diameter. Because they increase the root surface area and root diameter, root hairs are generally thought to be involved in nutrient and water acquisition, anchorage, and microbe interactions (Grierson et al., 2014). The first step in root hair development is the specification of an epidermal cell to differentiate as a root hair cell. The root epidermis has a distinct position-dependent pattern of root hair cells and non-hair cells (Duckett et al., 1994, Galway et al., 1994). Trichoblasts (root hair cells) are positioned outside the intercellular space between two cortical cells (called the “H” position), whereas atrichoblasts (non-hair cells)

are located over a single cortical cell (called the “N” position; **Fig. 1.28 A**). The *Arabidopsis* primary root possesses eight files of cortical cells, therefore there are eight root hair cells files and approximately 10 to 14 non-hair cell files (Duckett et al., 1994). This correlation between cell position and cell differentiation implies that cell-cell communication is critical for the establishment of cell type in the root epidermis. The root hair and non-hair cell fate is proposed to rely on the activity of two competing sets of transcription factors, the R2R3 WEREWOLF (WER) and MYB23 proteins versus the one-repeat Mybs CAPRICE (CPC), TRIPTYCHON (TRY), and ENHANCER OF TRY AND CPC 1 (ETC1). They are able to form an active or inactive complex, respectively, with the TRANSPARENT TESTA GLABRA (TTG) and GLABRA3/ENHANCER of GLABRA3 (GL3/EGL3) proteins. It is proposed that a relatively high level of WER is present in epidermal cells in the N position which leads to formation of the active complex, expression of GLABRA2 (GL2), and non-hair cell differentiation (Bruex et al., 2012).

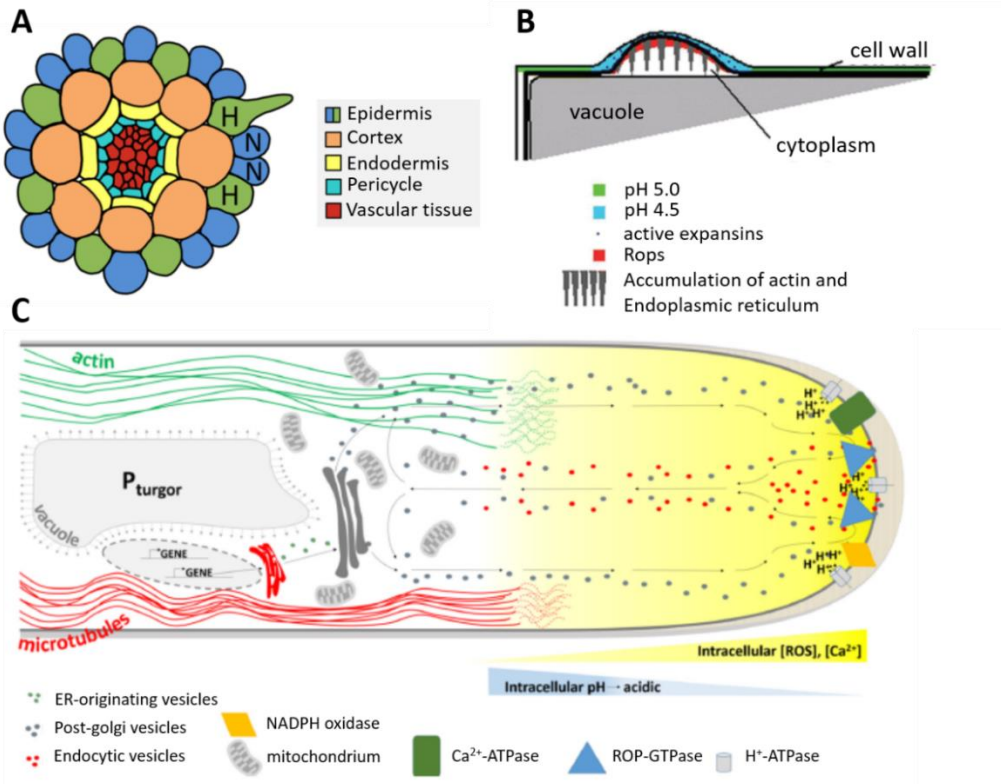

Figure 1.28. Schematic representation of root hair and non-hair cell, root hair initiation and growth. (A) The cellular organisation through the *Arabidopsis* root depicting the position of root hair (H) and non-hair (N) cells (B) Diagram showing the initiation process where Rop proteins localize to the initiation site and the pH of the cell wall drops. The local pH change activates expansins which loosen the cell wall. Large amounts of endoplasmatic reticulum (ER) and actin accumulates at the bulge site. (C) Growth of the root hair tip. The tip is full of vesicles derived from the ER and Golgi delivering the new wall material. Together with endocytotic vesicles formed at the very tip they display a reverse streaming. ROP proteins are localized to the tip together with Ca^{2+}-ATPases and NADPH oxidases. NADPH oxidases are responsible for the formation of ROS and Ca^{2+} gradient (yellow colour). A tip focused pH gradient is also present. Microtubules (red lines) are believed to be responsible for root tip growth direction and actin filaments (green lines) allow the polar vesicle transport. Adapted from Balcerowicz et al., 2015 and Grierson, et al., 2014.

Before the root hair begins to grow, the Rop family, small GTP-binding proteins, appear at the growth site (Molendijk et al., 2001; **Fig. 1.28 B**). Shortly after Rop localization, the root hair cell starts to bulge out and the pH of the cell wall falls. This pH drop may activate expansin proteins that cause wall loosening. The mechanism responsible for the pH change is unclear. It may be due to local changes in the cell wall structure, ion exchange, or local activation of proton ATPases or other proton transport activity (Bibikova et al., 1998). During the bulge enlargement, the endoplasmatic reticulum within it condensates and actin accumulates (Baluška et al., 2000, Vazquez et al., 2014). The tip growth progresses through exocytosis of vesicles in the root hair apex (**Fig. 1.28 C**). These vesicles are produced by smooth and rough endoplasmatic reticulum and Golgi complexes. They contain cell wall polysaccharides and proteins, which will be incorporated into the newly forming cell walls. Additionally, membrane proteins like cell wall synthases and membrane transporters are carried to the plasma membrane where they take part in tip growth expansion. During tip growth, the cytoplasm accumulates in apical parts of the cell and the nucleus is typically located at the base of the cytoplasmic dense area tracking the tip until root hair growth stops (Ketelaar et al., 2002). When *Arabidopsis* root hairs are 5-10 µm long the Ca^{2+} concentration at the tip increases significantly and remains very high throughout tip growth (Bibikova et al., 1999, Wang et al., 2015). The calcium gradient is maintained by RHO-RELATED PROTEIN FROM PLANTS2 (ROP2) activity which initiates the generation of reactive oxygen species (ROS) by the NADPH oxidase, ROOT HAIR DEFECTIVE2 (RHD2) (Jones et al., 2007). ROP GTPase-stimulated ROS accumulation activates calcium channels in these cells. The calcium gradient at the tip of the hair is believed to be a part of the mechanism that controls the direction of growth, by facilitating fusion of exocytotic vesicles with the apical plasma membrane (Pei et al., 2012).

1.10.3 Lateral root development

After the pattern of the primary root has been established and the individual cell types have begun to differentiate, further growth of the root results from branching to produce the most efficient and dynamic root system. The root system is composed of lateral roots and the primary root. Lateral roots are important to optimize the ability of the root system to acquire nutrients and water. Lateral roots in *Arabidopsis* are formed in the differentiation zone of the primary root from pericycle cells positioned next to the xylem poles called the xylem pole pericycle. A subset of these cells, the founder cells, are stimulated to divide to form a lateral root primordium (LRP). The LRPs usually do not form adjacent or opposite to each other (Dubrovsky et al., 2006, Dastidar et al., 2012). The founder cells undergo anticlinal cell divisions during the first stage of LRP development.

However, not all the founder cells develop into LRP or lateral roots and the mechanisms pattering the local spacing of LRP remain poorly understand.

The stage I of lateral root development is accomplished when pairs of the pericycle founder cells undergo several rounds of asymmetric division to create a new LRP composed of up to 10 cells of equal length (**Fig. 1.29 A**; Malamy and Benfey, 1997). Next, in the stage II, these cells divide periclinally to give rise to an inner and outer layer. Further, both anticlinal and periclinal divisions create a dome-shaped primordium (stages III-VI) which emerges (stage VII-VIII) form the primary root (Malamy and Benfey, 1997, Peret et al., 2009). The emergence of lateral root through the primary root epidermis is believed to occur primarily via cell expansion. After emergence, activation of the apical meristem of the lateral root begins its growth.

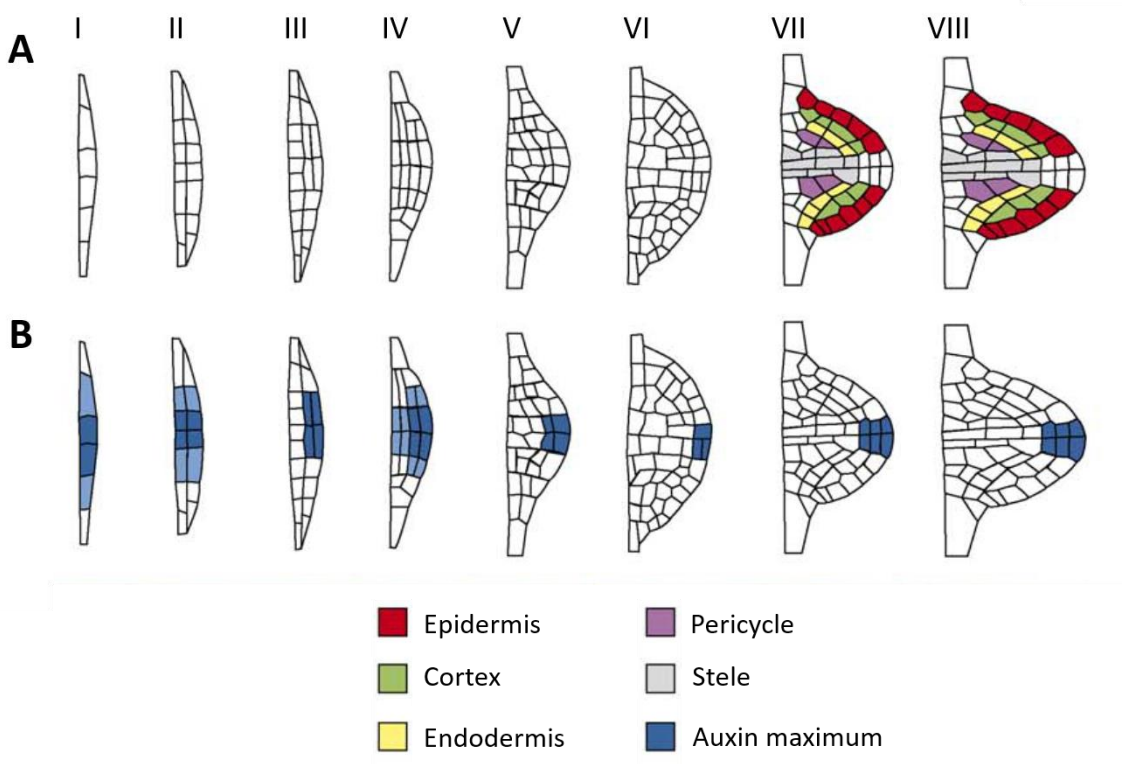

Figure 1.29. First stages of *Arabidopsis* lateral root development. (A) Schematic representation of the eight stages of lateral primordium development. (B) Auxin signalling maximum is demonstrated with the *DR5::GUS* reporter (blue gradient). Adapted from Péret, et al., 2009.

The lateral root development is largely controlled by auxin through multiple auxin-signalling modules (Lavenus et al., 2013). It has been shown that auxin has a role in regulating the distance between two LRP through the BDL/IAA12-MP/ARF5 signalling module (De Smet et al., 2010b) and transcriptional regulators PLETHORA3 (PLT3), PLT5, and PLT7 (Hofhuis et al., 2013). Furthermore, the work with an *Arabidopsis* line expressing a reporter gene for auxin-dependent gene activation (pDR5: GLUCURONIDASE) has shown that the founder cell initiation process occurs together with the activation of auxin

response genes in the regions where lateral root development takes place (Laskowski, 2013, Dubrovsky et al., 2008). Additionally, the positioning of lateral roots is determined by primary root bending. It has been shown that bending has an effect on longitudinal lateral root positioning by directing LRP initiation towards the outer face of bends (Kircher and Schopfer, 2016). This process could involve the receptor-like kinase *Arabidopsis* CRINKLY4 (ACR4) which prevents cell division in the surroundings of induced founder cells (De Smet et al., 2008).

The emergence of a lateral root requires cell elongation which is facilitated through deposition of new cell wall elements and inflow of water. A recent study has shown that knockout mutations in the tonoplast intrinsic protein (AtTIP) aquaporins delay lateral root emergence, resulting in a strong reduction of lateral root number (Reinhardt et al., 2016). These results showed that regulation of the tonoplast water permeability plays, together with the plasma membrane permeability, an important role in early lateral root growth and development. Moreover, it has been observed that auxin regulates the expression of plasma membrane aquaporins by repressing their expression, and therefore decreasing tissue hydraulic properties, which facilitates LRP emergence (Péret et al., 2012). These data fit the model where auxin maxima are at the lateral root meristem but not in the lateral tissues allowing them to uptake water and elongate (**Fig. 1.29 B**).

1.10.4 Border cells and root cap

Plant roots are constantly exposed to a variety of natural enemies like pathogenic fungi and bacteria. These organisms inhabit the soil around the root system and considering the fact that roots are essential for plant survival, they must be defended efficiently. To counteract infection, plants release a variety of biologically active compounds into the soil. These molecules are called root exudates and are known to have a multitude of functions in interactions with the microbial communities acting as signalling molecules, attractants, stimulants, inhibitions or repellents (Baetz and Martinoia, 2014). By definition, low molecular weight antimicrobial chemicals that are present in the plant before infection are called phytoanticipins, whereas inducible compounds that are not detectable in healthy plants are named phytoalexins (VanEtten et al., 1994). Highly potent antifungal or antimicrobial root exudates are tryptophan-derived secondary metabolites, such as glucosinolates or the indole derivative camalexin, which is the only well characterized phytoalexin in *Arabidopsis* (Iven et al., 2012, Schlaeppi et al., 2010).

Root tips of many plants are programmed to produce a number of cells released into the external environment. These living cells are defined as border cells (Hawes et al., 2002). The release of root exudates is correlated with the highly controlled, inducible formation and

release of metabolically active border cells. This is happening due to the activity of cell wall degrading enzymes which separate cells from the root and from each other. Release of border cells is regulated by mechanical effects and water from the soil. It is believed, the cap and border cells assist the growing root during the mechanical penetration of the soil by reducing friction at the root-soil interface (Driouich et al., 2007). Border cells were also shown to be involved in the response to abiotic stress. It has been shown that exposure of border cells to aluminium induces secretion of a layer of mucilage that chelates aluminium and prevents it from penetrating the root tip (Miyasaka and Hawes, 2001). Besides environmental signals, border cell production is initiated during the invasion of pathogenic microorganisms as a plant defence mechanism (Cannesan et al., 2011). It was shown that the formation of root border cells and exudation of the phytoalexin pisatin is stimulated in pea when root tips are incubated with a plant pathogen (Cannesan et al., 2011).

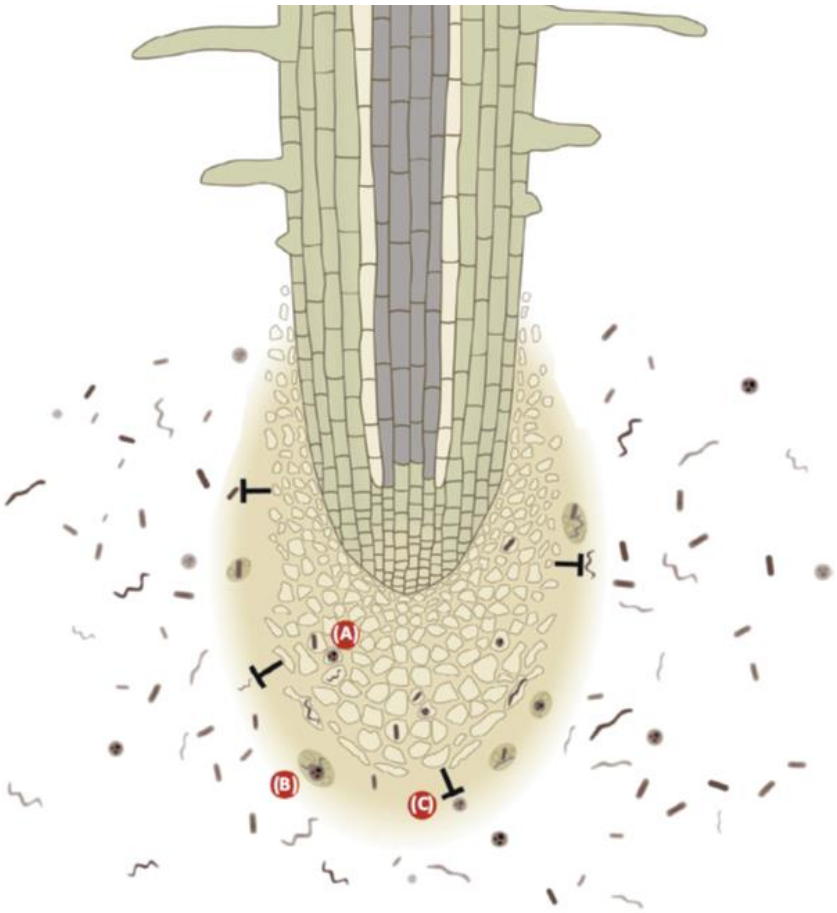

Figure 1.30. Action of border cells and their exudates against pathogens. Depicted microorganisms represent pathogenic fungi, bacteria, viruses, and nematodes. (A) Border cells attract pathogens which penetrate them to prevent the root tip infection. (B) The mucilage layer containing mainly polysaccharides and proteins but also extracellular DNA is secreted by border cells and represents a matrix that traps pathogens. (C) The inhibition or killing of pathogens through high and low molecular weight compounds released by border cells. Adapted from Baetz and Martinoia, 2014.

Border cells together with their exudates can account for root tip resistance via at least three mechanisms that act to cope with pathogens. First, border cells located at the

peripheral cap can attract pathogens to get infected, a strategy that gives temporary protection to the root tip (**Fig. 1.30 A**). After the removal of the border cell layer, the root tip remains uninfected, defence gene expression is not triggered, and root growth proceeds normally (Gunawardena and Hawes, 2002). Secondly, border cells can act as chemical and physical barriers towards pathogens by secreting a mucilaginous matrix composed of up to 95% polysaccharides and 5% extracellular proteins (Wen et al., 2007; **Fig. 1.30 B**). Finally, the analysis of protein exudates derived from root cap and border cells in pea confirmed that the complex mixture of approximately 100 proteins contains mostly stress and defence-related proteins (De-la-Peña et al., 2010, Liao et al., 2012; **Fig. 1.30 C**).

It is commonly known that the root architecture and development are controlled by phytohormones like auxin. The role of auxin in root cap shaping and differentiation has been studied in maize. It has been shown that the border cell release is significantly increased after the incubation of roots with auxin or the auxin transport inhibitor NPA. Thus, it seems like border cells detachment is regulated by auxin polar transport (Ponce et al., 2005). The possible role of border and border-like cells is to protect the root meristem from pathogenic infection. They seem to do so by removing of infected cells from the cap and remaining the root tip free of infection (Gunawardena and Hawes, 2002).

1.11 Aims

Plant cell walls are very important and highly complex cellular structures, since they are required for cell shape maintenance, defence against environmental change and form a major sink for carbohydrates produced during photosynthesis. Wall composition and structure determine biomass quality, thus influencing the efficiency with which bioenergy can be produced from ligno-cellulosic biomass. In parallel they also influence the ability of food crops to resist altered environmental conditions, such as increased drought occurrence and pathogen infection. Plant cell wall composition and structure are determined both by polysaccharides and proteins residing in the wall and their crosslinking in the wall. While knowledge of cell wall components has dramatically increased in the last few years, our understanding of the processes regulating the structure and composition of the cell wall in growing cells is still limited.

The project aims to advance the understanding of the involvement of pectin in plant root development. Roots are a popular and attractive system to work with as they undergo cell division at the primary root tip, post-embryonic organogenesis to make lateral roots, cell expansion in the elongation zone of the primary and lateral roots and tip growth elongation in root hairs. Pectin methylesterases (PMEs) enzymes from the model plant *Arabidopsis thaliana*, are known to be involved in the demethylesterification of homogalacturonan (HG), and were used as targets to affect the modification of pectin. As the *Arabidopsis* genome contains 66 PME isoforms, possible redundancy masks the phenotypes of single or double mutants. To circumvent this potential redundancy, Polyphenon-60 (PP60) is used as a pharmacological tool to alter PME activity in roots of wild-type plants. PP60 is a mixture of catechins isolated from green tea acting in a similar way as pectin methylesterases inhibitors (PMEIs) to inhibit PME activity *in vitro*. Furthermore, we aim to explore the involvement of HG in cell adhesion and approaches focus on border-like cells (BLCs) organisation. BLCs organization is believed to be controlled by HG content and status. Finally, we aim to understand changes in cell wall and carbohydrate metabolism after cell wall damage. We use isoxaben as a tool to inhibit cellulose biosynthesis in wild type *Arabidopsis* plants and the *isoxaben resistance 1-1 (ixr1-1)* mutant which is resistant to the inhibitor.

2. Material and methods

2.1 Plant material and growth conditions

Seeds of *Arabidopsis thaliana* ecotype Col-0 were surfaced-sterilized before being plated on agar-solidified media. For seed sterilisation, 500 µL of 70% (v/v) ethanol (EtOH) was added to the desired number of seeds, mixed by shaking for 30 seconds and incubated for 5 min at room temperature. EtOH was removed after brief centrifugation at 13,000 rpm (Peqlab, PerfectSpin 24; used in all cases unless otherwise stated). After EtOH removal, 500 µL seed sterilisation solution (10% (v/v) bleach (Domestos, UK), 0.05% (v/v) Triton X-100 (Fisher Scientific, UK)) was added to the seeds, which were incubated for 15 min at room temperature with occasionally mixing. Seed sterilisation fluid was removed following brief centrifugation. Seeds were washed 3 times with 500 µL sterile DI H_2O, and resuspended in 500 µL sterile DI H_2O. Seeds were sown onto standard medium (0.5 MS (Duchefa Biochemie), 1% (w/v) sucrose (Fisher Scientific, UK), and 0.8-1% (w/v) agar) in 120 mm^2 square petri dishes (Greiner, Germany). For experiments with pharmacological treatment medium contained addition of chemicals depending on treatment (see below). To achieve pH 8.0 of media, NaOH was added in drops to a liquid media until required pH was obtained. In case of pH 4.5 HCl was added. Then 0.5 M MES salt was added before autoclaving to keep pH at a stable level. After autoclaving media was poured onto petri dishes. Dishes were sealed with micropore tape (the 3M) in order to maintain a sterile environment. Seeds were stratified for 2 days at 4°C in the dark before being grown at 80 µmol/m^2/s irradiance, 23°C, 16 hours light/8 hours dark, with dishes in a vertical orientation. All the chemicals were obtained from Sigma-Aldrich unless stated otherwise.

For polyphenon-60 (PP60) treatment, fresh PP60 stock solution was prepared by dissolving 50 mg of PP60 in 1 mL of DI H_2O and filtered using a syringe filter 0.2 µm. Appropriate aliquots of PP60 stock solution were added to media after autoclaving to obtain final concentrations stated in each result chapter. For PP60 treatment in time-series PME activity assay, Col-0 seedlings were grown in a liquid media on a horizontal shaker at 130 rpm.

iPMEIox seeds were obtained from Sebastian Wolf (University of Heidelberg, Germany). The inducible iPMEIox construct was generated by using the PMEI5 entry clone to transfer the coding sequence to the β-estradiol-inducible vector. For iPMEIox experiment,

agar plate-grown seedlings were incubated in 0.5 liquid MS medium supplemented with PP60 and/or 6 µM β-estradiol (both obtained from Sigma-Aldrich) for the indicated time. Control seedlings were incubated in medium supplemented with appropriate amounts of water (for PP60 control) or DMSO (for β-estradiol control) for the same time.

2.2 Morphometric analysis

Media plates were placed vertically causing the roots to grow on the agar surface and each plate contained more than 15 seedlings. For primary root measurements, root tips were marked on the plate using a razor blade each day starting from 4th day after germination. Images were taken at the last day. Measurements of root hairs were taken from 7 day old seedlings. Photographs were taken using Leica D-LUX 3 camera and root hair length was measured on 20 seedlings with 20 root hairs for each in one biological replicate. Root hair density was measured as a number of root hairs between 12 – 15 mm from the root tip. For lateral root measurements, each plate from one biological replicate contained around 10 seedlings. Images were taken after 12 days of growth and the number of all lateral roots and length of the three longest ones in close proximity to hypocotyl were quantified. Pictures for primary root and lateral roots measurements were taken using Nikon D50 camera. All the growth parameters were analysed using ImageJ software and NeuronJ plug in.

2.3 Molecular biology methods

2.3.1 RNA extraction

For plant RNA extraction, root tissue from different treatments was frozen in liquid nitrogen and ground to a fine powder using a mortar and pestle. 100 mg of grinded root tissue was transferred to a 15 mL polypropylene tube containing 2 mL of TLES buffer (100 mM Tris-HCl pH8, 100 mM LiCl, 10 mM EDTA pH8, 5% SDS) and mixed by vortexing. Next, 2% PEG8000 (200 µL) was added to the tube and vortexed. It was then incubated for 10 min. at room temperature (RT) and centrifuged for 10 min. at 12000 g at RT. The supernatant (2 mL) was transferred to a new tube (15 mL). To each tube, 2 mL of phenol (heated to 80°C) was added and vortexed for 30 sec., then 2 mL of chloroform:isoamyl alcohol (24:1) was added and again vortexed for 20 sec. The tubes were centrifuged at 4°C for 10 min. at 12000 g. The supernatant (2 mL) from the upper phase was transferred to a new tube (15 mL) and 2 mL of 4 M LiCl was added and vortexed. All tubes were incubated

overnight at 4°C. After incubation, the tubes were centrifuged at 4°C for 30 min at 12000 g and the supernatant was removed carefully. The remaining pellet was dissolved in 125 µL of H_2O and transferred to an Eppendorf tube and kept on ice. Next, 12.5 µL of 3 M sodium acetate pH 5.2 and 250 µL of absolute ethanol was added, vortexed and left at -80°C for 1-3 hours. The tubes were centrifuged at 4°C for 20 min at 12000 g (or at the full speed in a microcentrifuge). The supernatant was removed and the pellet washed with 500 µL of 80% ethanol by mixing. The tubes were centrifuged for 5-10 min. at 12000 g, ethanol removed and the pellet was left to dry.

2.3.2 DNase treatment of RNA

The issue of genomic DNA contamination in RNA samples was solved by using the Ambion (Applied Biosystems) TURBO DNase Kit according to manufacturer's instructions. 0.1 volume 10x DNase I Buffer and 1 µL rDNase I were added to the RNA and mixed gently. The reaction tubes were incubated at 37°C for 20-30 min. After incubation 0.1 volume DNase Inactivation Reagent was added and mixed well. The tubes were left for 2 min at room temperature, mixed occasionally. The last step included centrifugation at 10.000g for 1.5 min and the RNA was transferred to a fresh tube. Finally, the pellet was dissolved in 22 µL of H2O and 1 µL of dissolved RNA was run on an electrophoresis gel and 1 µL used for quantification with a NanoDrop1000.

2.3.3 cDNA synthesis

For cDNA synthesis 4 µg of RNA extract was converted to cDNA using Transcriptor High Fidelity Kit version 08 (Roche) according to manufacturer's instructions. Briefly, an anchored-oligo$(dT)_{15}$ and RNA were mixed and thermally denatured at 65°C for 10 minutes and chilled on ice. Next, 4 µL of reaction buffer, 0.5 µL RNase inhibitor, 2 µL 10 mM deoxynucleotide mix and 1.1 µL reverse transcriptase were added giving the final volume of 20 µL. The reaction was incubated for 30 min. at 45°C followed by 5 min. at 85°C. cDNA was stored at 4°C and used directly for qPCR amplifications.

2.3.4 DNA and RNA gel electrophoresis

For RNA gel electrophoresis 1 µL of 5x loading buffer, 4 µL of water and 1 µl of a sample were mixed and then run on 1% agarose (1% agarose in Tris-acetate-EDTA (TAE) buffer, SYBR safe) using a PeqLab (model: 40-1214) electrophoresis tank.

2.3.5 Real-time PCR conditions and data analysis

Real-time PCR was performed on a Roche LightCycler 480 using SYBR Green Kit (Roche) according to the manufacturer's protocol. First, a master mix was prepared by mixing 1.15 mL of SYBR Green, 10 µl cDNA and 640 µl of sterilized water. Each 9.2 µl reaction contained 7.2 µl of the master mix and 2 µl of primers mix (final concentration of each primer 2.5 µM). Priming efficiency was measured by the host laboratory before by performing a standard curve. Samples were subjected to thermal-cycling conditions of 95 °C for 10min, and 45 cycles of 10 s at 95 °C and 15 s at 60 °C for annealing and extension. Samples were normalised to reference genes. The most stably expressed reference genes (here: *TIP41* and *CACS*) were selected using geNorm. The melting curve was designed to increase from 55 to 95 °C, and melting temperatures for each amplicon and primer efficiencies were estimated using a calibration dilution curve and slope calculation. Expression levels were determined as the number of cycles needed for the amplification to reach a cycle threshold fixed in the exponential phase of the PCR.

2.4 Biochemical methods

2.4.1 Protein extraction at pH 7.0

For protein extraction 50 mg of frozen material was transferred to a tube, 200 µL of phosphate (50 mM Na_2HPO_4; 2 mM citric acid; 1M NaCl; 0.01% [v/v] Tween 20) buffer was added and vortexed. The mixture was incubated for one hour in 4°C on a shaker with a speed of 225 rpm. Next the tubes were centrifuged at 4°C for 30 min at 14000 rpm. After centrifugation 180 µL of the supernatant was transferred to a new tube and stored at 4°C.

2.4.2 Protein extraction at pH 5.0

For time-series PME activity assay, seedlings were harvested on the 6 days of growing at 0, 3, 6, 9, 12, and 24-hour time points. Seedlings were placed in an aluminium bag and immediately frozen in liquid nitrogen. Then the plant material was ground to a fine powder using a mortar and pestle. For protein extraction 50 mg of frozen tissue was transferred to a tube, 100 µL of sodium acetate (50 mM sodium acetate; 1M LiCl; pH 5.0) buffer was added and vortexed. The mixture was incubated for one hour at 4°C on a shaker with a speed of 225 rpm. Next the tubes were centrifuged at 4°C for 30 min at 14000 rpm. After centrifugation 100 µL of the supernatant was transferred to a new tube. In the next step the extract was filtrated using column tubes (Amicon Ultra – 0.5 mL Centrifugal Filters).

The columns were washed with 500 µL of phosphate buffer (pH 7.5) and centrifuged at room temperature (RT) for 5 min at 13000 g. Then 100 µL of extracts was added to columns and centrifuged at RT for 15 min at 13000 g. Each column was rinsed with 200 µL of phosphate buffer (pH 7.5) and centrifuged at RT for 10 min at 13000 g followed by a rinse with 100 µL of phosphate buffer (pH 7.5). At the end columns were centrifuged at RT for 4 min at 13000 g. The extract was transferred from the column to a new tube and the volume adjusted to 140 µL. The tubes were stored at 4°C.

2.4.3 Protein determination by the Bradford method

The concentration of protein was determined using Bradford reagent. The solution of BSA (1 mg/mL) was diluted 10x by adding 900 µL of phosphate buffer (50 mM; pH 7.5). The assay was performed on 96-well clear plate. The standard curve was prepared from six points with a final concentration of protein: 0, 1, 2, 3, 5, and 10 µg/µL. BSA dilution was made in phosphate buffer and 160 µL of each point was put in wells in duplicates. For a blank control only phosphate buffer was used. For protein extracts 2 µL of each extract was added to a well and adjusted to 160 µL with phosphate buffer. Next, 40 µL of Bradford reagent was added to each well and incubated for 5 min at room temperature. The absorbance was measured at 595 nm using a BioTek PowerWave microplate spectrophotometer.

2.4.4 Pectin methylesterase activity assays

2.4.4.1 Spectrophotometric assay

PME activity can be determined by monitoring the release of methanol produced during pectin hydrolysis by the action of the enzyme. In this method, methanol is oxidized to formaldehyde by the action of alcohol oxidase enzymes. It reacts with acetyl acetone resulting in compounds that absorb in the visible region (Anthon and Barrett, 2004). The reaction mixture consisted of 5 µL enzymatic extract, 5 µL alcohol oxydase solution (0.025 U), 5 µL of pectin solution (20 mg/mL), and 85 µL phosphate pH 7.5 for each well in a clear 96-well plate. The standard curve reaction mixture consisted of 10 µL MeOH (0, 15, 30, 45, 75, and 150 nM), 5 µL alcohol oxydase solution (0.025 U), 5 µL of pectin solution (20 mg/mL), and 80 µL phosphate pH 7.5 for each well. As a blank control phosphate buffer was used instead of the protein extract. All the solutions were prepared in phosphate buffer. After mixing, the reaction was started by incubating the plate for 30 min at 28°C. The OD at 420 nm was measured as the 0-time point. Next, 100 µL of exposing solution (ammonium acetate, 0.2 mM, 0.2% (v/v) acetylpropionyl, and 0.3% (v/v) glacial acetic acid) was added

and incubated for 15 min at 68°C. The final absorbance was read at 420 nm. The activity of PME was calculated basing on total release of methanol.

2.4.4.2 Gel diffusion assay

Ruthenium red binds to pectin when the number of methyl esters attached to the pectin decreases and this was used as the basis for a gel diffusion assay for PME activity (Downie et al., 1998). 1% agarose was dissolved in a buffer containing 0.1 M citric acid and 0.2 M Na_2HPO_4 with pH adjusted to 6.3. The citrus pectin was dissolved in miliQ water by heating at 80°C for 10-15 min. and vortexing occasionally. 0.1% (w/v) of pectin was added to the agarose with buffer. From this mixture, approximately 15 mL was poured into 120 mm square dishes. After cooling, wells with a diameter of 3 mm were punched in the agarose using a plastic Pasteur pipette. 10 µL of freshly extracted protein and buffer only as control were dispensed into each well. This was incubated for 16 h at 37°C, and the gel was washed twice with distilled water. Next, the gel was stained with an aqueous solution of 0.02% (w/v) ruthenium red for 1 h and washed twice with distilled water. The plates were photographed immediately and the area of the halo was measured using ImageJ.

2.4.5 Polygalacturonase activity assay

The polygalacturonase (PG) activity was determined by the amount of hydrolysed polygalacturonic acid (PGA) by measuring the increase in reducing groups during the reaction course using galacturonic acid (GalA) as a standard (Somogyi, 1952). The reaction mixture consisted of 12.5 µL of protein extract (pH 5.0), 12.5 µL of sodium acetate buffer (50 mM; pH 5.0), and 25 µL of substrate (polygalacturonic acid 1%) for each well in a clear 96-well plate. The buffer and substrate were mixed prior to addition to wells. To determine the concentration, range of GalA that would yield a linear standard curve, a plate containing increasing GalA concentrations (0, 10, 15, 25, 50, and 100 nM) was tested. Each concentration was replicated three times. The substrate and enzyme blanks were prepared in the same way as the analysed sample except that the necessary amount of the acetate buffer was added to the substrate (enzyme) solution instead of the enzyme (substrate) solution. The plate with samples and standard curve was incubated at 37°C for 1 h. After incubation, the enzymatic reaction was stopped by adding a copper reagent. The copper reagent consisted of 25 parts of solution A (sodium carbonate, 25 mM; potassium sodium tartrate, 10 mM; sodium bicarbonate, 25 mM; sodium sulfate, 1.5 M) to 1 part of solution B (15% (w/v) of copper sulfate pentahydrate) mixed prior to use. The OD at 620 nm was measured as the 0-time point. Next, 75 µL of reagent arsenomolybdate was added to each well and well mixed. The reagent arsenomolybdate consisted of 10 mM ammonium

molybdate tetrahydrate and 0.5 mM of sodium arsenate added gradually until precipitates stop forming. The solution was placed at 37°C overnight and then stored in an opaque (dark) bottle. The plate was incubated at 80°C for 30 min. and the final absorbance was read at 620 nm.

2.4.6 GUS expression

Whole seedlings were immersed in GUS staining solution and incubated at 37°C overnight. The GUS staining solution was made up of 100 µl of 40 mg/ml X-Gluc (5-bromo-4-chloro-3-indolyl-β-D-glucuronide cyclohexylammonium salt (Thermo Scientific)) in dimethylformamide (DMF) and GUS staining buffer (Sodium phosphate, 100 mM; Disodium ethylenediamine tetraacetate, 10 mM; K ferrocyanide, 0.5 mM; K ferricyanide, 0.5 mM; Triton X-100, 1% [v/v] (pH 7.0)). After GUS staining tissue was cleared using a freshly prepared chloral hydrate solution (25g in 10ml of H_2O) for 2h. To image the GUS staining patterns, the samples were transferred to a microscope slide with a 50% glycerol mounting solution and examined using DotSlide microscope with Olympus BX61 frame.

2.4.7 Chlorophyll content measurements

Chlorophyll was isolated using a protocol developed by Yang and Ohlrogge, 2009. Briefly, rosette tissues from freshly harvested seedlings were weighed, frozen in liquid nitrogen and ground to a fine powder using a pestle and mortar. 1 mL of 80% cold acetone was added and the samples vortexed and incubated for 20 min. in the dark at room temperature. After incubation the samples were vortexed again and centrifuged for 10 min. /5000 rpm. The absorbance was measured at 663 nm for chlorophyll a and 647 nm for chlorophyll b, and 470 nm for carotenoids. The content was calculated from equations:

Chlorophyll a (µg/mg FW) = $12.25(A_{663}) - 2.79(A_{647})$

Chlorophyll b (µg/mg FW) = $21.50(A_{647}) - 5.10(A_{663})$

Total chlorophyll (µg/mg FW) = $7.15(A_{663}) + 18.71(A_{647})$

Carotenoids (µg/mg FW) = $[1000(A_{470}) – 1.82$ (Chl. a) – 85.02 (Chl. b)]/198

2.4.8 Cellulose and pectin histochemistry

Fresh roots were incubated with Calcofluor white M2R (Sigma) 1 mg/L for 10 min. in the dark first. After careful washes with distilled water, roots were then incubated with a solution of 0.05 (v/w) ruthenium red stain (Sigma) in deionized water for 10 min. then washed extensively in deionized water. Roots were mounted in water on glass microscope slides and observed immediately using a microscope equipped with UV fluorescence (excitation filter, 359 nm; barrier filter, 461 nm). Images were acquired with a Leica DFC 300 FX camera. For each treatment, 15 to 20 roots were observed.

2.4.9 Immunofluorescence Labelling

The anti-pectin monoclonal antibodies (mAbs) used in this study are shown in **Table 2.1**. The secondary antibody used was fluorescein isothiocyanate (FITC)-conjugated goat anti-rat (Sigma-Aldrich).

Table 2.1 List of the anti-pectin monoclonal antibodies (mAbs) used in this study.

Antibody	Epitopes
LM19	de-esterified HG
LM20	methyl-esterified HG
JIM13	arabinogalactan protein (β-D-GlcA-(1,3)-α-D-GalA-(1,2)-α-L-Rha)
LM2	arabinogalactan protein (β-linked glucuronic acid)
LM1	extensins
LM8	xylogalacturonan

Roots of 12- to 14-days old seedlings were fixed for 1h in 4% (w/v) paraformaldehyde and 1% (v/v) glutaraldehyde in 50 mM PIPES, pH 7, and 1 mM $CaCl_2$ (adapted from Willats et al., 2001). Roots were washed in 50 mM PIPES, 1 mM $CaCl_2$, pH 7, and incubated for 30 min in a blocking solution of 3% (w/v) bovine serum albumin (Sigma) in phosphate-buffered saline (PBS), pH 7.2. After being carefully rinsed in PBS containing 0.05% (v/v) Tween 20 (PBST), roots were incubated overnight at 4°C with the primary antibody (dilution 1:10 in 0.1% [v/v] PBST). After five washes with 0.05% PBST, roots were incubated with the appropriate secondary antibody (dilution 1:50 in 0.1% PBST) for 2 h at 37°C. Roots were rinsed in 0.05% PBST, mounted in anti-fade solution (Citifluor AF2; Agar

Scientific), and examined using a confocal laser-scanning microscope (Leica TCS SP2 AOBS; excitation filter, 488 nm; barrier filter, 500–600 nm). Control experiments were performed by omission of the primary antibody. An average of 8 to 10 root apices were examined for each antibody.

2.5 Bioinformatic methods

2.5.1 Expression and function analysis

For the coexpression and domain analysis all the genes ID for PMEIs and PMEs were processed using GeneMania application (v. 3.1.1).

For the expression analysis the PMEs and PMEIs genes were analysed using Genevestigator 4.0 and *Arabidopsis* eFP Browser (bar.utoronto.ca).

2.5.2 Phylogenetic analysis

Seventy-one Arabidopsis PMEI protein sequences were selected by alignment of PMEI1 protein sequence using BLAST (blastp; blast.ncbi.nlm.nih.gov) with *Arabidopsis* and reference proteins (refseq_protein) database.

The protein sequences were downloaded from NCBI database and aligned using ClustalX 2.1. Phylogenetic tree was drawn with the neighbour-joining method using MEGA software (5.05) using pairwise deletion; Poisson uniform rates model; 1000 replicates were used for bootstrap analysis.

2.5.3 Chromosomal location of PME genes

The chromosomal locations of the pectin methylesterase genes were determined using the Chromosome Map Tool (http://www.arabidopsis.org/jsp/ChromosomeMap/tool.jsp) on TAIR.

2.6 Atomic Force Microscopy

The Atomic Force Microscopy (AFM; **Fig. 2.1**) images the topography of a sample surface or, if a force is applied, the rigidity of the sample over a region of interest. AFM uses a cantilever with a very sharp tip to scan over a sample surface. As the tip approaches the

surface, the force between the surface and the tip cause the cantilever to deflect towards the surface. However, as the cantilever is brought even closer to the surface, such that the tip makes contact with it, repulsive force takes over and makes the cantilever to deflect away from the surface. Detection of the cantilever deflections towards or away from the force is measured by a laser beam. By reflecting the beam off the flat top of the cantilever, any cantilever deflection will cause slight changes in the direction of the reflected beam (**Fig. 2.1 B**). A photodetector is used to track these changes. Thus, if an AFM tip passes over a soft surface, the resulting cantilever deflection is recorded by the photodetector. The softness and firmness of the sample surface influence the deflection of the cantilever. By using a feedback loop to control the force applied to the surface by the tip, the AFM can generate an accurate map of the surface features.

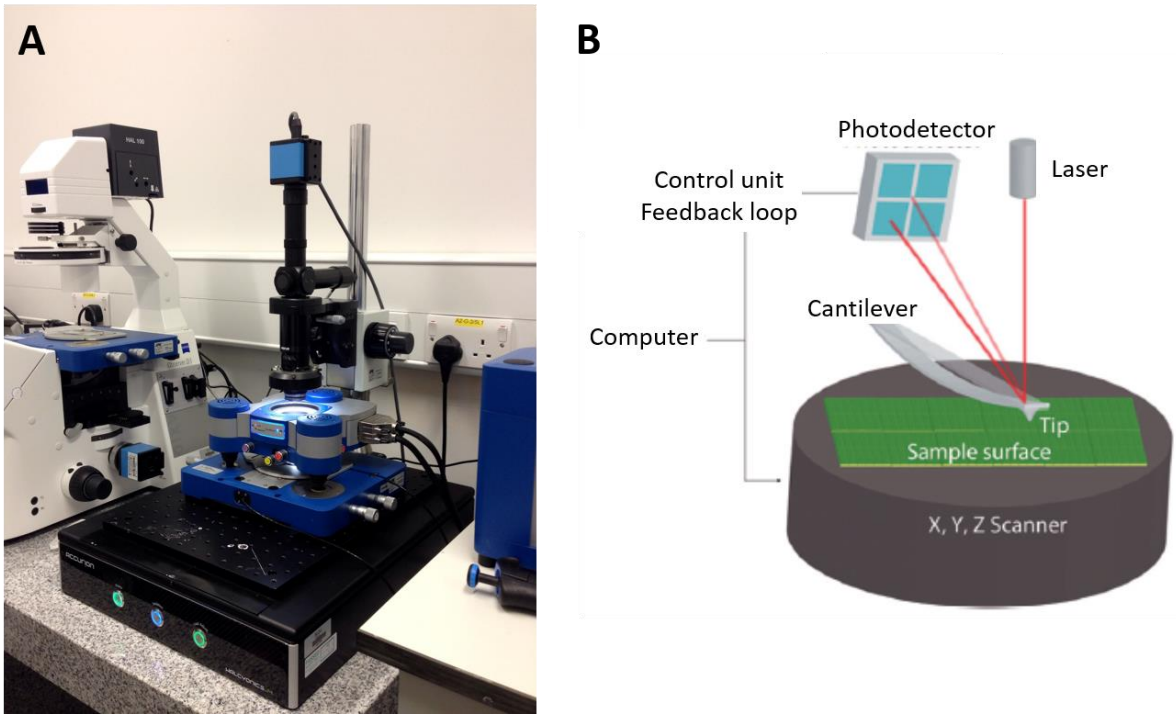

Figure 2.1. Atomic Force Microscopy (AFM). (A) NanoWizard AFM used in experiments. (B) Schematics of the main set-up. A sharp tip is attached to a flexible cantilever and is used to indent the sample surface. A known force is applied on the sample which bends the cantilever. The deformation of cantilever is then monitored via a laser beam reflecting from the top surface of the cantilever into a photodetector. This provides force-displacement curves which are used to extract the mechanical properties of the sample. Adapted from Milani et al., 2013.

AFM data was collected by a stand-alone NanoWizard AFM (**Fig. 2.1 A**) equipped with a CellHesion module allowing greater z-movement (JPK Instruments AG, Germany). Roots were dissected from solid media grown plants and immobilized on glass slides using a stiff 1% agarose or double-sided tape. Measurement of wall properties alone were ensured by suppression of turgor pressure by immersion of all roots in a hypertonic solution 0.5 M mannitol for a minimum of 30 minutes before measurement. The following cantilevers were used: ‘Nano World’ (NanoWorld AG Headquarters, Switzerland) tips with a spring constant (which relates the applied normal force to the normal deflection of the cantilever)

of 45 N/m, with probes of a 10 nm radius (R10). Force maps of samples were determined as follows: an AFM cantilever loaded with a tip was used to indent the sample over a 100x100 µm square area, indentations were kept to around 10% of cell height (250–500 nm), within the area 64x64 pixels or less measurements were made resulting in 4096 or less force indentation measurements.

2.7 Statistical analysis

The GraphPad Prism v.7 was used to obtain all descriptive and comparative statistics. Analyses of variance (ANOVA) for sets of data groups were performed with “Multiple comparisons/Post-hoc” testing. Once a significant difference ($p<0.05$) was detected, “Post-hoc” tests, using the Holm-Sidak or Tukey algorithm, were performed to test which of the possible multiple comparisons between the data groups were significant.

2.8 Metabolomics methods

2.8.1 Plant Growth and Sampling

Surface-sterilized seeds (approx. 30-50 mg) of the *Arabidopsis* ecotype Col-0 and *ixr1-1* mutant were added each to a separate 250 mL Erlenmeyer flask with 125 mL 0.5MS medium and were grown on a shaker at 130 rpm under long day conditions (16 h of light/8 h of dark) with a light intensity of 145 µmol/m^2/s and temperature 22°C. The medium was supplemented or not with 1% sucrose and 0.6 µM isoxaben (dissolved in DMSO) to give four different growth conditions (sucrose+isoxaben - SX; sucrose/non-isoxaben - S; non-sucrose+isoxaben - NSX; non-sucrose/non-isoxaben - NS). Flasks without isoxaben were supplemented with DMSO. Seedlings were grown for 6 days, next transferred to new flasks with respective media conditions, and then material was harvested for metabolomics analysis after 0, 3, 6, 9, and 12 hours for Col-0 (referred in treatments as C) and after 0 and 12 hours for *ixr1-1* (referred in treatments as R) in three replicates. For sucrose starvation stress, plants were grown in flasks supplemented with sucrose and then transferred to a new media without sucrose and/or isoxaben.

2.8.2 Extraction and UPLC-Synapt HDMS QTOF MS analysis of metabolites

To investigate the change in primary and secondary metabolite levels, 6 days old *A. thaliana* seedlings were harvested at different time points (0, 3, 6, 9 and 12 hours) post isoxaben addition for time course analysis. Metabolites were extracted using a previously

described method optimised for liquid culture growth (Forcat et al., 2008). Seedlings were harvested in foil packets and immediately flash frozen in liquid nitrogen. Samples were then freeze-dried using a VIRTIS Bench Top 3.3/ Vacu-freeze freeze dryer for a minimum of 24 hours and homogenised using a Quiagen tissue lyser II at a frequency 25 Hz s^{-1} for 2 min after adding 3 mm tungsten carbide beads. 6.5 mg (± 0.3 mg) of freeze-dried tissue was used with three technical repeats performed per sample. Samples were extracted using 400 µL of extraction buffer (10% methanol, 1% acetic acid) with an internal standard (ribitol, Sigma-Aldrich) for 30 min on ice. The internal standard was used to correct for analyte losses or other unwanted effects during the analytical process. Samples were then centrifuged for 10 min at 4°C, the supernatant removed and re-extraction performed with 400µL of extraction buffer (without the internal standard). Extractions were pooled and centrifuged 3 times and the supernatant removed after each centrifugation in order to ensure all debris was removed. Samples were centrifuged for 10 min at 4°C before pipetting 150 µL of each into 1.5 mL glass autosampler vials (VMR).

Samples, together with blank control, test and quality control samples (QC) were then quantified with UPLC-Synapt HDMS coupled to a Q-TOF MS (Waters) fitted with an electrospray ion source operating in positive mode (**Fig. 2.2**). QC and test samples were used in order to monitor the performance of the system, to correct possible drifts, and also to help fusing data from different analytical batches, in this case, different time period data. QC samples were generated by combining aliquots from all samples analysed thus representing a bulk control sample. Test samples, comprising a limited number of components were prepared from commercially available plant phytohormones: jasmonic acid, salicylic acid and abscisic acid. UPLC-Q-TOF-MS enables MS and MS/MS data acquisition in a single injection strategy. Chromatographic separation of molecules was performed using a Waters Acquity HSS T3 1.8 um, 2.1mm x 100mm column maintained at 40°C with a LC mobile phase containing 0.2% formic acid in water.

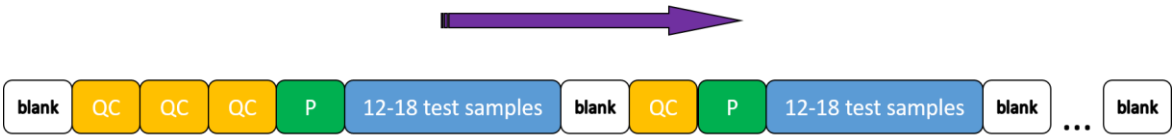

Figure 2.2 UPLC-MS run order. QC and blank samples were analysed repeatedly throughout the sequence. P – test mixtures. An arrow shows the direction of run.

2.8.3 Processing raw data to analyse metabolites content

To facilitate data analysis all chromatograms were converted to mzXML files using ProteoWizard (v3.0.9.134) software. The conversion from .raw files enables the processing

of data files using a software independent from Waters. The data was analysed using XCMS Online. XCMS Online (xcmsonline.scripps.edu) is a cloud-based informatics platform designed to process and visualizes mass-spectrometry-derived, untargeted metabolomic data. This web-based platform is an extension of the original open-source R package XCMS that was released in 2006. The parameters used for all the jobs were based on: UPLC/UHD Q-TOF, optimized for UPLC with ~15 min gradient, high resolution ESI-QTOF-MS. The statistical test performed was Welch t-test (Xi et al., 2014). Detailed XCMS parameters are described in appendix.

Data was processed in pair-wise, multi-group and meta-analysis job mode directly loading .mzXML files into XCMS Online. A pairwise job allows the comparison of two groups whereas multigroup job allows 3 or more groups of samples to be analysed. Meta-analysis is a higher-order analysis that aims to identify shared metabolic patterns among multiple independent two-group comparisons. Any MS data was compared versus the composite database for metabolite identification.

2.8.4 Pair-wise comparison of data files

Converted data files from 12h time points were uploaded to XCMS Online for a pair-wise job. After preliminary analysis, only significantly ($p<0.05$) changing features were used for further analysis. Untargeted metabolomics cannot perform pathway and network analysis without knowing metabolite identity. The conventional work flow is to identify each metabolite experimentally before mapping them onto metabolic pathways/networks. Instead of treating metabolite identification and metabolic pathway/network analysis as two separate steps, one theoretical framework was used. If a list of significant spectral features reflects a biological activity, the true metabolites they represent should show enrichment on a local structure in the metabolic network. The software implementation of this approach is named “mummichog”. Mummichog was used in XCMS Online environment and features were manually matched with potential chemical identifications. Next, the identified metabolites were searched in KEGG Atlas for their ID and metabolic pathways they take part in. Metabolic maps were created using web-based Pathway Projector in Graphical User Interface (GUI).

2.8.5 Multi-group comparison of data files

For multi-group comparison of data, files from 0, 3, 6, 9, and 12h time points were used for Col-0 analysis and 0 and 12h time points for *ixr-1-1* together with QC files. After preliminary analysis in XCMS Online, the identified features were incorporated into Metaboanalyst (v3.0) environment. Metaboanalyst runs on the statistical package R (v3.2.3)

used metabolites peak intensity as representative of concentration (Xia et al., 2015). The data was transformed and saved as comma-separated values (.csv) files. After uploading the files into Metaboanalyst, data integrity was checked and variables with missing values were excluded. Data was filtered using interquartile range (IQR) to remove variables that are unlikely to be of use when modelling the data. Normalization of data was processed in two steps: first, samples were normalised by reference feature (ribitol) and then mean-centred and divided by the standard deviation of each variable. That prepared files were used for further analysis.

2.8.6 Important features analysis

The features which changes were significant (p-value < 0.05) after XCMS Online processing were used for further analysis. These data were first analysed by an unsupervised principal component analysis (PCA), which identified the presence or absence of sugar as the principal source of variance. To sharpen the separation between treatments and genotypes, data were next analysed using a partial least squares discriminant analysis (PLS-DA) to further determine which metabolites were responsible for separating these groups. The specific metabolites contributing most significantly to the differences identified by PLS-DA between treatments and genotypes were determined using the variable importance in projection (VIP) analysis in the Metaboanalyst environment.

2.8.7 Meta-analysis of untargeted metabolomic data

Meta-analysis was performed on pair-wise jobs after 12h of treatment. The pair-wise jobs created in XCMS Online were analysed on the same platform. Features with fold change less than 2 and p values greater than 0.05 were filtered and plotted.

3. Bioinformatics analysis of pectin methylesterases in *Arabidopsis thaliana* root

3.1 Introduction

Pectin is synthesized and transported to the wall in a highly methylesterified state. Plants utilise PMEs to alter the methylesterification status of the HG in the wall and consequently affect the properties of the pectin. Depending on the PME mode of action HG chains may bind together to strengthen cell wall or be degraded for signalling purposes. Plants have evolved to have a large number of genes encoding putative PMEs. In *Arabidopsis*, 66 open reading frames (ORFs) have been annotated as full-length PMEs, in *Populus trichocarpa* 89 ORFs, whereas the numbers appeared to be lower in *Oryza sativa* (35 ORFs). It is believed that the lower number of PME genes in rice reflects a lower abundance of HG in grasses than in dicotyledonous species (Pelloux et al., 2007). The reason for such a large number of genes is currently not understood. Some higher plant PMEs contain the mature, active part of the protein preceded by an N-terminal extension (PRO region) that varies in length and shares similarities with the PME inhibitor domain (Camardella et al., 2000). Based on the presence or absence of the PMEI domain, a classification has been created and two groups distinguished (**Fig. 3.1**). *Arabidopsis* PMEs group 1 lacks a PMEI domain while those of group 2 have between 1-3 PMEI domains. It has been found that group 2 PMEs constitute 65% of total PMEs in *Arabidopsis*, 54% in *Oryza sativa* and 57% in *Populus trichocarpa*.

Various experiments have shown that PMEs are involved in diverse physiological processes associated with both vegetative and reproductive plant development. Some of their roles, based on reverse genetic and biochemical approaches in *Arabidopsis*, are described below.

On the basis of publically available transcriptomic data, seven PME genes are found to be expressed in the *Arabidopsis* seed coat, particularly mucilage secretory cells. One of them, *PME58* presented the highest level of expression in the early stages of seed development (Turbant et al., 2016). The adherent mucilage of *pme58* mutants was less stained by ruthenium red, which binds to pectin, when compared to wild-type seed but only in the presence of EDTA. Moreover, the surface area of mucilage secretory cells was decreased in *pme58*. There results suggest a higher degree of HG methylesterification

resulting from a decrease in PME activity (Turbant et al., 2016). Another PME gene expressed during seed coat development is HIGHLY METHYL ESTERIFIED SEEDS (HMS) which is abundant during mucilage secretion (Levesque-Tremblay et al., 2015). The *hms-1* mutant displays altered embryo morphology and mucilage extrusion. It has been proposed that HMS is required for cell wall loosening in the embryo to ease cell expansion during the accumulation of storage reserves. The role of HMS in the seed coat is likely to be masked by redundancy caused by expression of other PMEs (Levesque-Tremblay et al., 2015).

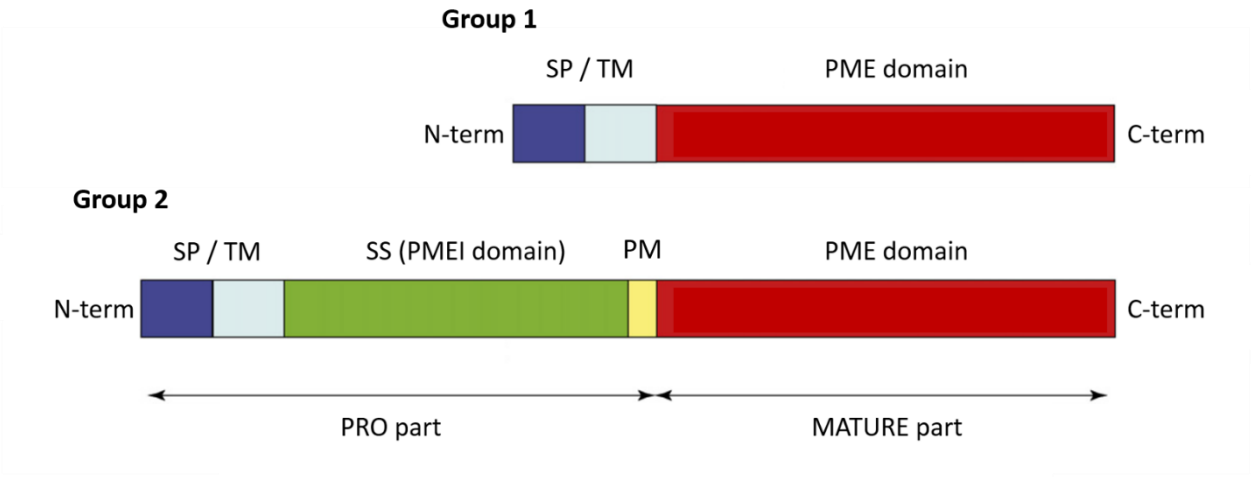

Figure 3.1. Pectin methylesterases structural domains. Group 1 and 2 PMEs possess a conserved PME domain. Group 2 PMEs has an N-terminal extension called PRO region, which shares similarities with the PMEI domain and a processing motif (PM) which may be the target for subtilisin-like proteases. The signal peptide (SP) or transmembrane domain (TM) are responsible for targeting to the endomembrane system leading to the export of PMEs to the cell wall.

It has been reported that a mutation in the BELLRINGER (BLR) transcription factor, caused ectopic primordia formation in the floral meristem as the result of meristem-specific changes in the methylesterification status of HG (Peaucelle et al., 2011b). The ectopic primordia formation was reversed in the *blr pme5* double mutant suggesting the involvement of PME5 in this process. Moreover, it has been shown that *blr* mutant plants have defects in internode elongation due to reduced cell expansion caused by downregulation of *PME5* expression (Peaucelle et al., 2011b). Another PME, *PME35*, is specifically expressed in the basal part of the inflorescence stem. The loss of function mutant *pme35* showed reduced the mechanical strength of the supporting tissue in stem resulting in loss of directional growth (Hongo et al., 2012).

Recently it has been shown that PME48 is involved in the remodelling of pectin in *Arabidopsis* pollen. Pollen grains from *pme48* mutant displayed a significant delay in imbibition and germination *in vitro* and *in vivo*. Additionally, many pollen grains showed two

tips emerging comparing to just one in wild type and the degree of methylesterification of HG was higher in mutant pollen grains (Leroux et al., 2015).

Furthermore, PME activity is important for the virulence of pathogens through the control of the esterification status of pectin. The response of plants to the bacterial hemibiotroph *Pseudomonas syringae* pv *maculicola* ES4326 (*Pma* ES4326) were studied revealing that five PME genes (*PME1*, *PME17*, *PME31*, *PME39*, and *PME44*) contributed to immunity (Bethke et al., 2013). Single mutants in these PME genes showed enhanced susceptibility phenotypes in preliminary bacterial growth assays. Additionally, PME activity increased during pattern-triggered immunity in wild type plants, but did not change in single mutants, suggesting that the determinant of immunity is not total PME activity but instead specific effects on the pattern of pectin methylesterification due to the action of different PMEs (Bethke et al., 2013).

Knowledge about the involvement of PMEs and the cell wall methylesterification state in *Arabidopsis* root development is still limited. The first discovery of PME participation in *Arabidopsis* root development comes from characterization of PME3 (Guenin et al., 2011). The main phenotypic trait correlated with *pme3* mutation was a large increase in the number of adventitious roots emerging on the hypocotyls. This suggests a new pathway regulating adventitious rooting in which changes in methylesterification state of HG and cell wall mechanics control adventitious root initiation. Recently, *PME17* has been discovered to be expressed in roots and processed by a subtilisin-type serine protease (SBT), SBT3.5 (Sénéchal et al., 2014). *PME17* and *SBT3.5* were strongly expressed in the root epidermis and both *pme17* and *sbt3.5* showed similar root phenotypes where the primary root was elongated. The root elongation could be caused by lower PME activity which leads to lower demethylesterification of HG and less Ca^{2+} crosslinks between HG making the cell wall more extensible. Additionally, expression analysis of other PME isoforms revealed that expression of *PME3* was downregulated and *PMEI4* upregulated. Both genes are expressed in the root elongation zone suggesting they could contribute to the overall changes in total PME activity and increased root length in *pme17* mutant (Sénéchal et al., 2014).

Many of the functions and the evolution of the genes responsible for producing pectin methylesterases (PMEs) are incompletely understood. Latest attempts in understanding evolution of pectin modifying enzymes is based on work with the moss *Physcomitrella patens* and other plants (McCarthy et al., 2014). The initial hypothesis stated that a single ancestral gene was present for each pectin-related gene family in the common ancestor of land plants. But the existence of multiple members in the early land plants that gave rise to the mosses and vascular plants was confirmed, contracting this hypothesis (McCarthy et

al., 2014). Limited information is available on the expression of PME genes in the *Arabidopsis* root. Because phylogenetic analyses can be the basis for molecular and biochemical analyses of protein families, genome-wide research on the PME gene family in *Arabidopsis* was performed. Analyses of sequence phylogeny, expression profiling, and functional networks were performed to provide insights into the evolutionary mechanisms of *Arabidopsis*' PME protein family in roots.

3.2 Results

3.2.1 Phylogenetic analysis of the PME and PMEI family

To examine the phylogenetic relationships between *Arabidopsis* PMEs, phylogenetic analyses of the PME protein sequences based on neighbour joining (NJ) method using MEGA 5 was performed. Phylogenetic trees were built to relate sequences to expression profiles (**Fig. 3.2**). Based on their phylogenetic relationships, the *Arabidopsis* PME and PMEI family were divided into 4 groups, designated from Group 1 to Group 4 (**Fig. 3.2**). Group 1 contained 35 and 40 members for PME and PMEI respectively and constituted the largest clade in the PME phylogeny. The PME family tree was built before (Louvet et al., 2006) and showed similarities with the one created below. In both families group 3 comprised with only two members, At5g09760 and At5g64640 for PMEs and At4g02250 and At1g55770 in case of PMEIs. Group 4 of PMEs did not contain a PRO sequence.

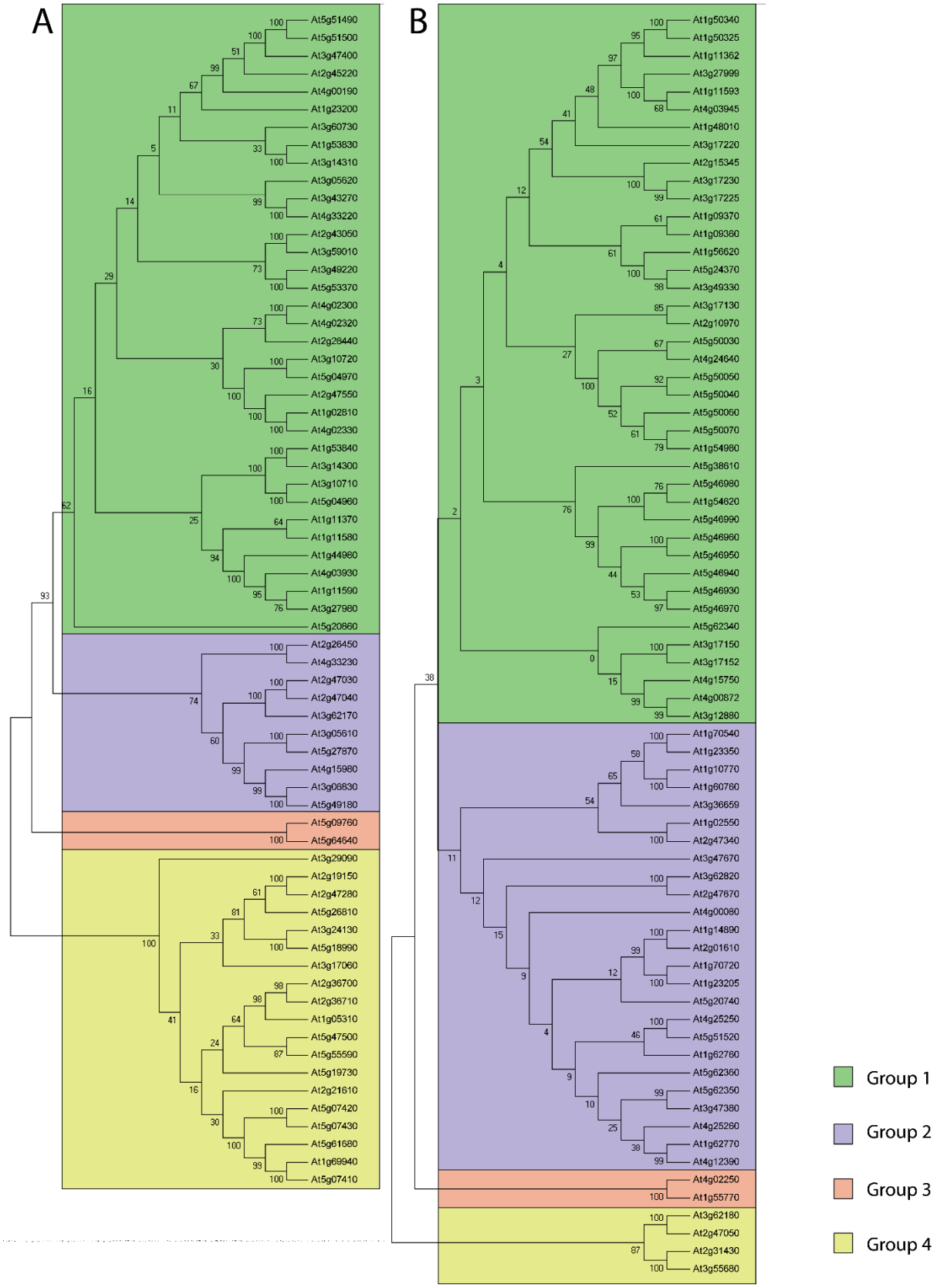

Figure 3.2. Phylogenetic analysis of the PME and PMEI protein sequences. The analysis of PME (A) and PMEI (B) indicates that four subgroups (1, 2, 3, and 4) can be separated on the basis of the robustness of the node. For A, a similar analysis was previously performed (Louvet et al., 2006).

3.2.2 Functional network of *Arabidopsis* PMEs and PMEIs

Availability of the fully sequenced *Arabidopsis thaliana* genome means it provides ease of genes analysis. The high number of knockdown and knockout mutants can be analysed to provide insight into gene function and expression. During evolution many genes are duplicated and transposed to other regions of the genome while maintaining their activity and similar biochemical functions. These genes are clustered into gene families. The *Arabidopsis* genome contains 996 gene families consisting of more than 8000 genes (arabidopsis.org/browse/genefamily). The PME and PMEI gene families in *Arabidopsis* consist of 66 and 69 genes, respectively. Genes involved in the same biological pathways are usually expressed cooperatively, and thus information on their interaction is key to understanding the biological systems at the molecular level. To further explore which genes are possibly regulated by members of the PME and PMEI families, a protein-protein interaction network was assembled. Analysis of those genes showed they indeed group separately according to their activity (**Fig. 3.3**). The PME family which contains a PRO region share protein domains with the PMEI family. Additionally, some of the PMEs are co-expressed with PMEI indicating specific interaction of both proteins. A few PME genes show unknown function/activity according to their protein domains. PMEs and PMEIs are not the only enzymes involved in the modification of pectins. The pectate lyase family is involved in cleavage of demethylesterified HG and requires the presence of calcium ions generating oligosaccharides with unsaturated galacturonosyl residues at their non‐reducing ends Mar ín‐Rodríguez et al., 2002. The analysis showed that many of PME proteins share domains with pectate lyase family (**Fig. 3.3**).

3.2.3 Expression pattern of PME and PMEI genes in roots

Expression profiling is a useful tool for understanding gene function. A comprehensive expression analysis was performed using publicly available microarray data for Genevestigator and eBrowser. The transcriptomic data of PME and PMEI expression in roots suggests a correlation in expression patterns of PMEs and PMEIs in different tissue types and developmental stages. Many developmental processes, such as hypocotyl growth, are regulated by the methylesterification state of homogalacturonan which has been confirmed at the transcriptome and proteome level. It has been shown before that PME and PMEI expression can be clustered into several groups with PMEs and PMEIs co-expressed in the same tissue (Wolf et al., 2009). Cluster analysis of publicly available microarray data of PME and PMEI expressed in root tissues show four distinct expression clusters, each

containing different PME and PMEI isoforms (**Fig. 3.4**). In the first 3 clusters there are a comparable number of PME and PMEI genes expressed in the same tissue type. The last cluster contains PME genes that do not group together with the other ones (*At1g53840* and *At3g49220*). The specific localization of PMEs and PMEIs expression suggests that the both proteins may be required for development of specific tissues. It is possible that particular PMEs are regulated by specific PMEIs and this is indicated by co-expression in various tissues. Thus it seems that both PME and PMEI function is important in regulating HG methylesterification status during root development.

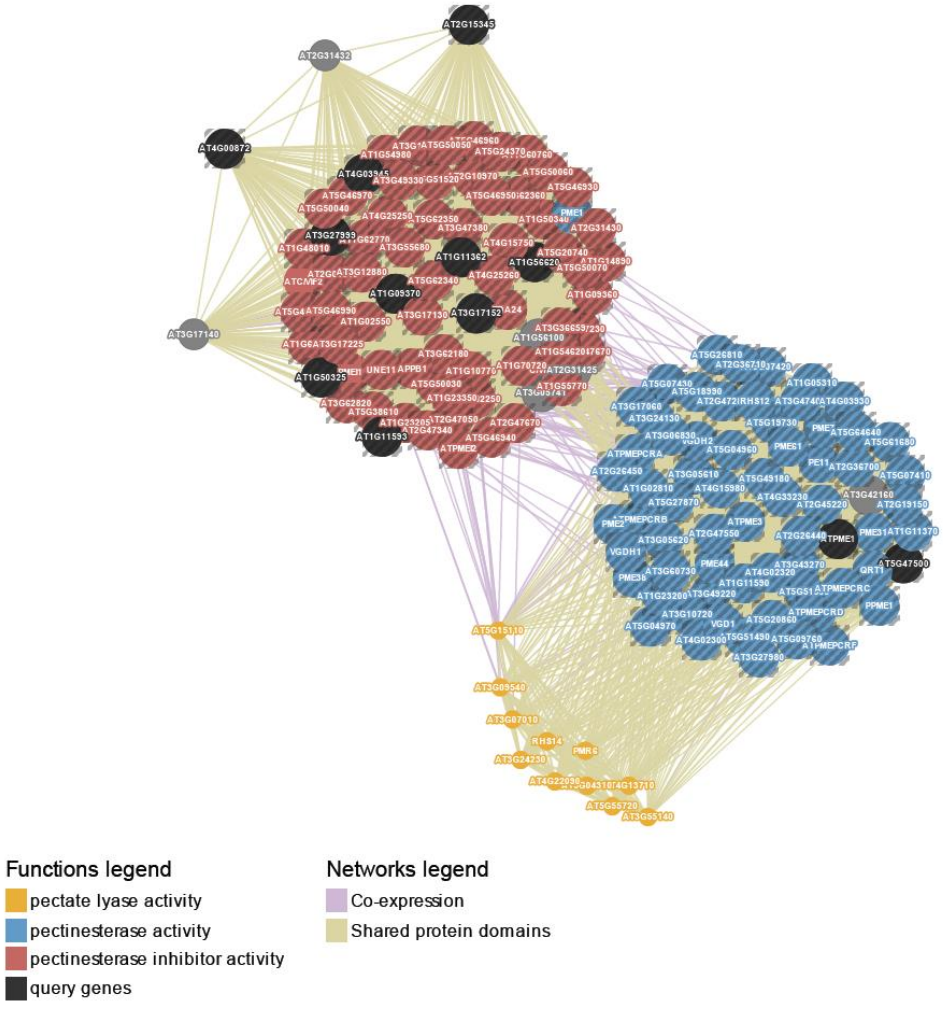

Figure 3.3. A real-time network integration of PME and PMEI genes. All the members of PME and PMEI families are mapped. The gene function was predicted from the composite network using a variation of the Gaussian field label propagation algorithm that was adopted to be more suitable for unbalanced classification problems like gene function prediction. Label propagation algorithms, like most function prediction algorithms, assign a score to each node in the network, called the 'discriminant value', that reflects the computed degree of association that the node has to the seed list defining the given function (Mostafavi et al., 2008). This analysis reveals a total of 11 pectin lyase proteins that showed domain similarity to PMEs.

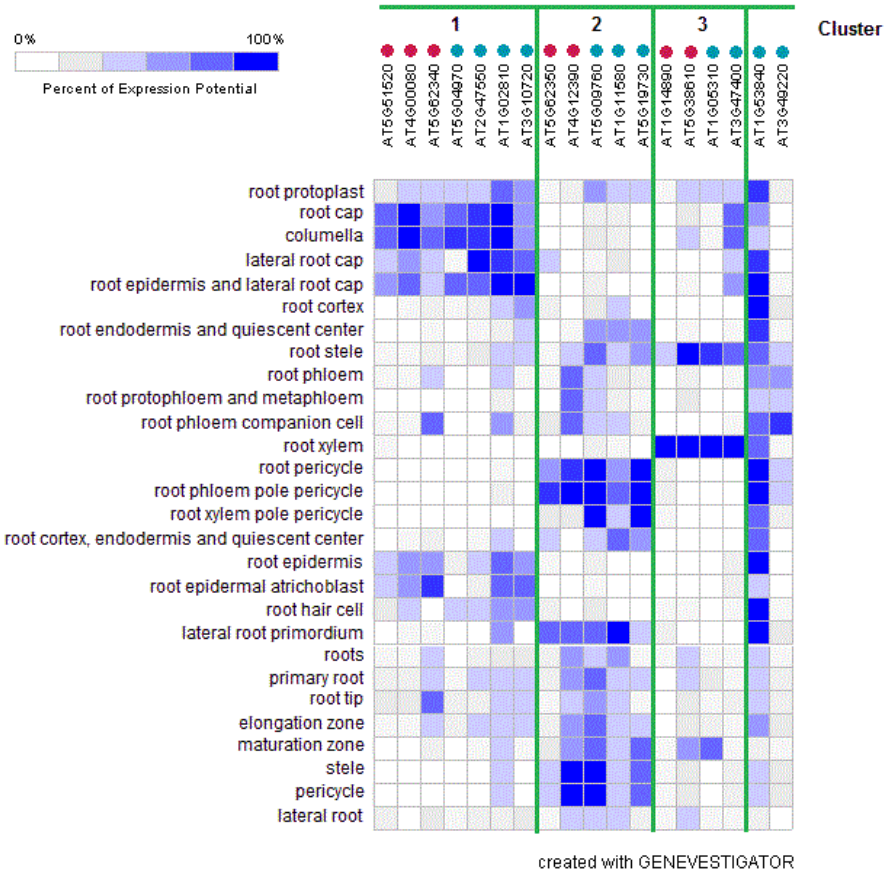

Figure 3.4. Clustering analysis of PME and PMEI expression in *Arabidopsis* root. PMEs are shown in blue circles together with PMEIs (red circles). Cluster analysis was based on microarray data obtained from Genevestigator. The expression potential of a gene is a robust indicator for the maximal expression level of this gene. It represents the top percentile of all expression values for this gene.

Root expression analysis indicated that all of the PME genes expressed in roots belong to either Group 1 or 4 of PMEs (**Table 3.1**). Only five PMEs belong to Group 4 which does not have a PRO region. In the case of PMEI genes, four were classified in Group 2 and only one, *At3g17230*, in Group 1. Isoelectric point (pI) is a pH value at which a protein has no net electrical charge (Sillero and Ribeiro, 1989). All PMEs, with exception of At2g26440, and PMEIs have basic values of pI, which means they function at pHs above 7.

Table 3.1. PME and PMEI genes expressed in roots. Gene annotation, knockout lines, group based on phylogenetic analysis, expression profiling based on Genevestigator and eBrowser data, and pI values are shown for each PME gene. Homozygous knockout lines were selected only. Expression profiles contain 4 *Arabidopsis* organs/tissues with the highest estimated expression.

Gene	Knockout line	Gr.	Expression (Genevesigator; 4 plant tissues with the highest level)	Calculated pI value
Pectin methylesterases				
At2g19150	SM_3_31463	4	Root endodermis, primary root, radicle	8.7
At2g36710	SALK_207148	4	Silique, replum, stem, root xylem	6.6
At2g43050	SAIL_875_H09	1	Sperm cell, stem, testa, root cortex	8.9
At2g45220	SALK_059908	1	Leaf, root cortex, root hair cell, node	9.4
At2g26440	SALK_058895	1	Replum, guard cell, endosperm, leaf	4.9
At4g03930	SALK_064017	1	Testa, general seed coat, giant cell, peripheral endosperm	7.2
At4g33220	SALK_050157	1	Suspensor, shoot apex, replum, guard cell	7.3
At4g02330	SALK_008958	1	Petiole, seedling culture, root hair protoplast, abscission zone	8.6
At5g19730	SALK_136556	4	Ovule, root phloem pole pericycle protoplast, carpel, pericycle	9.4
At5g20860	WiscDsLox421D6	1	Root endodermis, cambium cell, phloem, starch sheath cell	9.7
At5g55590	SALK_024104	4	Chalazal endosperm, root endodermis, cambium cell, internode cell	6.7
At1g53840	SALK_120021	1	Root xylem, root protoplast, lateral root primordium, root hair cell	8.5
At2g47550	SAIL_68_A05	1	Leaf, columella, root, lateral root cap	9.0
At3g47400	SAIL_504_F02	1	Root xylem, root epidermis, columella, lateral root cap	10.3
At3g10720	SALK_122120	1	Root epidermis, columella, lateral root cap, root epidermal atrichoblast	6.5
At2g21610	SALK_004890	4	Columella, root epidermis, leaf, lateral root cap	8.0
At5g04960	SALK_136678	1	Root hair cell, maturation zone, root phloem, lateral root	9.1
At5g04970	SALK_094562	1	Columella, root epidermis, root hair cell, lateral root cap	8.3
At5g51490	SALK_111942	1	Micropylar endosperm, root hair cell, root apical meristem, root epidermal atrichoblast	9.9
At5g51500	SALK_107597	1	Root epidermal atrichoblast, root epidermis, root tip, root phloem	10.0
Pectin methylesterases inhibitor				
At1g10770	SALK_110378	2	Pollen, stamen, petal, sepal	10.1
At1g62770	SALK_024495	2	Abscission zone, suspensor, radicle, primary root	9.9
At3g17230	SALK_043560C	1	Suspensor, ovule, ovary replum	6.7
At3g47380	SALK_015169C	2	Root epidermal atrichoblast, lateral root cap, root epidermis, mesophyll cell	10.7
At5g51520	SALK_046369C	2	Root epidermis, columella, root epidermal atrichoblast, lateral root cap	9.4

3.2.4 Chromosomal location and duplication events of *Arabidopsis* root PMEs

Chromosomal macro- and micro-scale duplication and rearrangement are thought to be the major modes of genome evolution (Blanc and Wolfe, 2004). To investigate the relationship between PME genes and potential gene duplication within the genome, the locations of PME genes from Table 3.1 were compared in duplicated chromosomal blocks that were previously identified in *Arabidopsis* (Blanc et al., 2000). PME genes were unevenly distributed among *Arabidopsis* 5 chromosomes, relative to corresponding duplicated genomic blocks (**Fig. 3.5**). Within identified duplication events, only At3g47380/At3g47400 and At5g51500/At5g51520 are retained as duplicates, whereas all others lack corresponding duplicates. Interestingly, the At3g47380/At3g47400 and At5g51500/At5g51520 members are located in tandem clusters on the chromosomes 3 and 5.

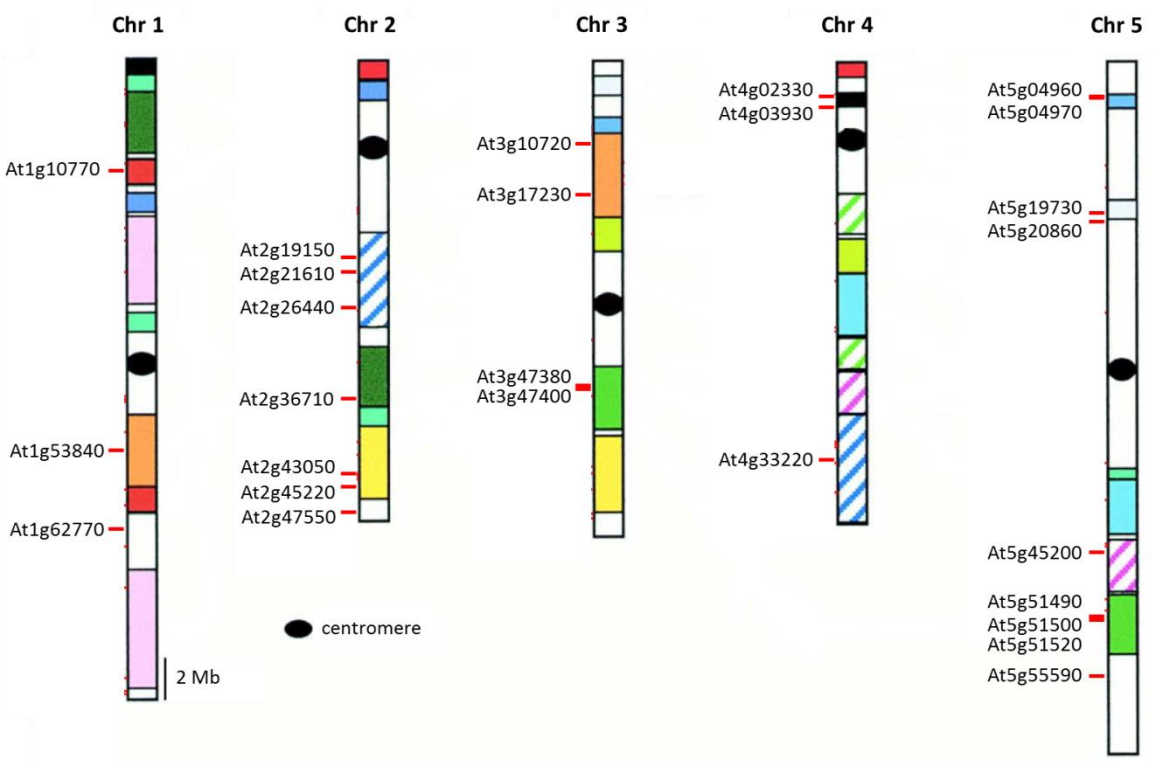

Figure 3.5. Chromosomal locations of the PME genes in *Arabidopsis* root. 26 genes selected from out of 66 PMEs are shown. Paralogous regions in the putative ancestral constituents of the *Arabidopsis* genome are depicted using the same colours according to Blanc et al., 2000.

3.2.5 Cellulose biosynthesis inhibition-mediated changes in PME and PMEI gene expression

Isoxaben has been a valuable tool for the analysis of cell wall synthesis because of its specific interaction with the cellulose synthase complex and mutants which show resistance to isoxaben. Isoxaben is known to inhibit cellulose biosynthesis therefore inducing compensatory effects in cell wall including changes in pectin levels. There is more HG crosslinking and changes in PMEs expression after cellulose biosynthesis inhibition caused by isoxaben treatment in *Arabidopsis* suspension-cultured cells. Moreover, the differential expression of a large number of PME genes indicates that modulation of HG is an aspect of the adaptation to cellulose synthesis disruption (Manfield et al., 2004b). Indeed, selected genes change their expression after isoxaben treatment with PMEs and PMEIs being overexpressed and downregulated, respectively compared to mock treatment in liquid media grown seedlings (**Fig. 3.6**).

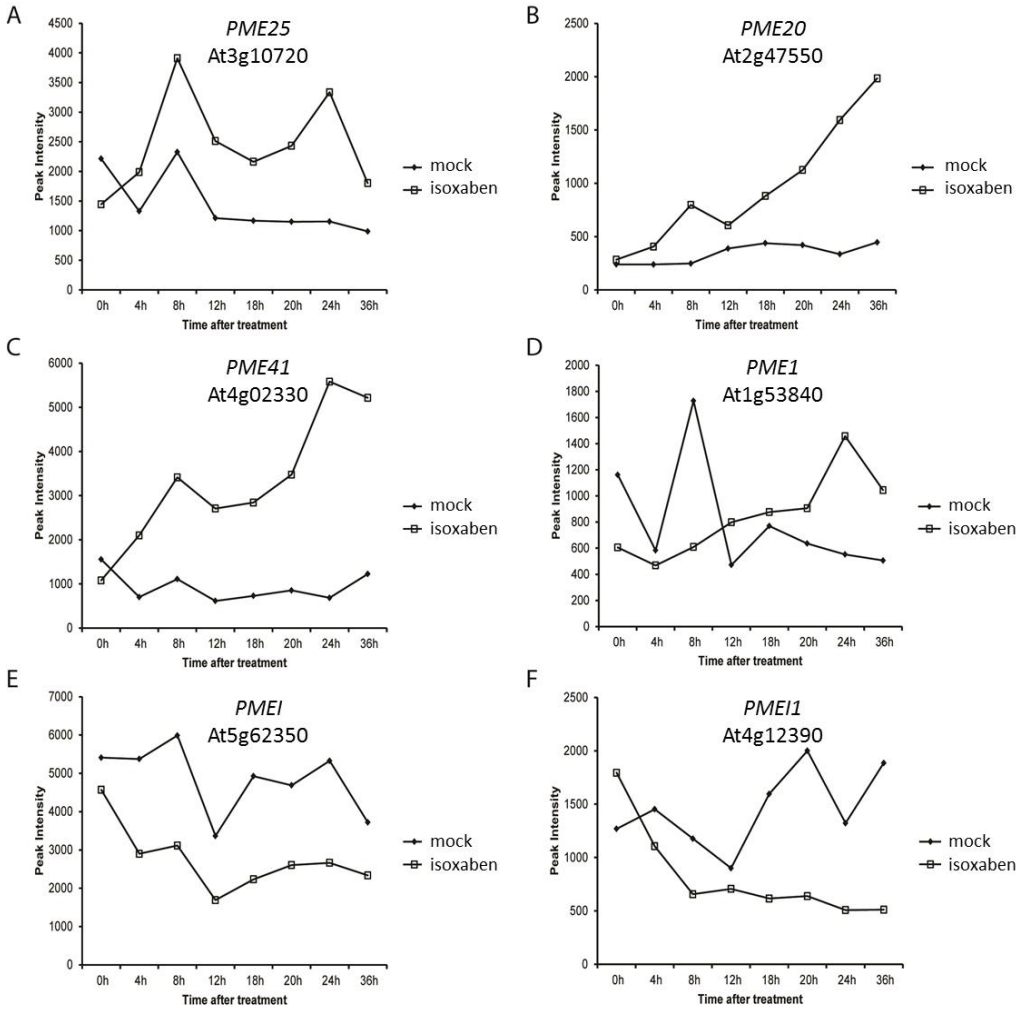

Figure 3.6. Expression levels of PMEs (A-D) and PMEIs (E and F) isoforms after isoxaben treatment from microarray experiment. The experiment was prepared by Hamann et al., 2009.

3.3 Discussion

PME and PMEI proteins share specific domains and expression patterns suggesting that PMEIs may control PMEs activity. This transcriptional and biochemical pathway would allow the fine-tuning of HG structure with consequent effects on cell wall plasticity and root growth. Recently, it has been shown that PME17 is inhibited by PMEI4 in roots (Sénéchal et al., 2015b). Analysis of the *pmei4* mutant revealed that total PME activity was increased and proteomic analyses showed that the level of PME17 was higher compared to wild-type. Here it has been shown that there are potential PME and PMEI pairs according to online databases. It would be interesting to further explore these correlations using protein interaction and enzyme activity analysis and learn if PMEs and PMEIs expressed in the same tissue types indeed interact with each other.

In this result, a correlation was shown between expression profiles and the phylogenetic tree, notably for group 1 and a subset of group 4 for PMEs and group 2 for PMEIs. Such expression-to-sequence relationship was previously shown for some members of the PME family during silique development (Louvet et al., 2006). The lack of corresponding duplicates shown in **Fig. 3.5** suggests that dynamic changes occur following segmental duplication that causes the loss of many genes. Therefore, segmental duplication is not the major factor that contributed to expansion of the pectin methylesterase gene family in *Arabidopsis* root. There was only one cluster which seemed to be segmentally duplicated. Duplicated genes may have different evolutionary fates, as indicated by divergence in their expression patterns. The expression profiles of PME genes in *Arabidopsis* do not share similar expression patterns (Pelloux et al., 2007). This indicates that substantial changes in function may have occurred during the evolution of duplicated genes. During long-term evolution, the expression patterns of the paralogs and duplicated genes have diverged (Blanc and Wolfe, 2004). Such a process may increase the adaptability of duplicated genes to environmental changes, thus conferring a possible evolutionary advantage.

4. Pharmacological approaches to study the function of pectin methylesterases during root development

4.1 Introduction

The pectin methylesterase (PME) protein family contains 66 isoforms that function in regulating cell wall properties in different tissues, developmental stages, and under various stress conditions. The activity of these enzymes must be controlled and plants have evolved a transational mechanism where a group of PMEs have an auto-inhibitory domain and post-transational mechanism which involves pectin methylesterases inhibitors (PMEIs). The PMEI family contains 69 isoforms. The PMEs in *Arabidopsis* are divided into two groups: group I which has an N-terminal extension (PRO region) with significant similarity to PMEI proteins; Group II PMEs is characterized by the absence of this PRO region (Pelloux et al., 2007). The analysis of PMEI from ripe apricot and kiwi showed significant sequence homology to plant invertase inhibitors and to the PRO-region of group I PMEs (Scognamiglio et al., 2003, Camardella et al., 2000). Furthermore, the high DNA sequence similarity of two genes *At1g48020* and *At3g17220* in *Arabidopsis* to kiwi PMEI revealed to be putative PMEIs and were named as *PMEI1* and *PMEI2* respectively (Wolf et al., 2003). *In vitro* analysis of PMEI1 and PMEI2 showed both are able to inhibit the activity of PME from orange and PMEs extracted from the *Arabidopsis* floral tissues. Moreover, qPCR and GUS reporter analysis showed high expression of both isoforms in flowers (Wolf et al., 2003) and the confocal laser scanning microscopy revealed PMEI2 fused to yellow fluorescence protein (YFP) present in the apical wall of growing pollen tubes. In contrast, PMEI1::YFP was found throughout the pollen cell wall (Röckel et al., 2008). Furthermore, PMEI2 has been shown to completely inhibit PME activity in the leaves of *Nicotiana benthamiana*, either when expressed in this tissue or when added to leaf extracts. Finally, PMEI1 and PMEI2 were shown to be regulators of the pollen-expressed PME isoform PME1 from *Arabidopsis* (Röckel et al., 2008). A screening of *Arabidopsis* accessions identified a new accession, Djarly, with altered seed mucilage release. The locus affecting mucilage release was identified and predicted to encode a PMEI, named PMEI6. The expression of protein is specific to the epidermal cells of the seed coat and is secreted to the apoplasm. It has been shown that PMEI6 inhibits PME activity in mature, dry seeds and modulates HG methylesterification in the outer cell wall of seed coat epidermal cells (Saez-Aguayo et al., 2013).

The high number of PME and PMEI isoforms makes the functional studies difficult due to the potential redundancy in knockout mutants of PMEs or PMEIs by other isoforms. Therefore, a chemical biology approach has been used. Previous studies have shown that an extract from green tea containing a range of polyphenolic compounds termed catechins could be potential kiwi's PME inhibitor with one of its components, EGCG (see **chapter 1.7.1**), being the most effective (Lewis et al., 2008b). The study of EGCG on PMEs activity using GUS reporter lines showed that after transferring PME34 and PME3::GUS lines to EGCG-containing media, GUS activity was upregulated in the growing zone of the root and downregulated in the differentiated parts of the root (Wolf et al., 2012). Additionally, when EGCG was administered in liquid medium to wild type plants they showed cell swelling in the transition/elongation zone of the root tip.

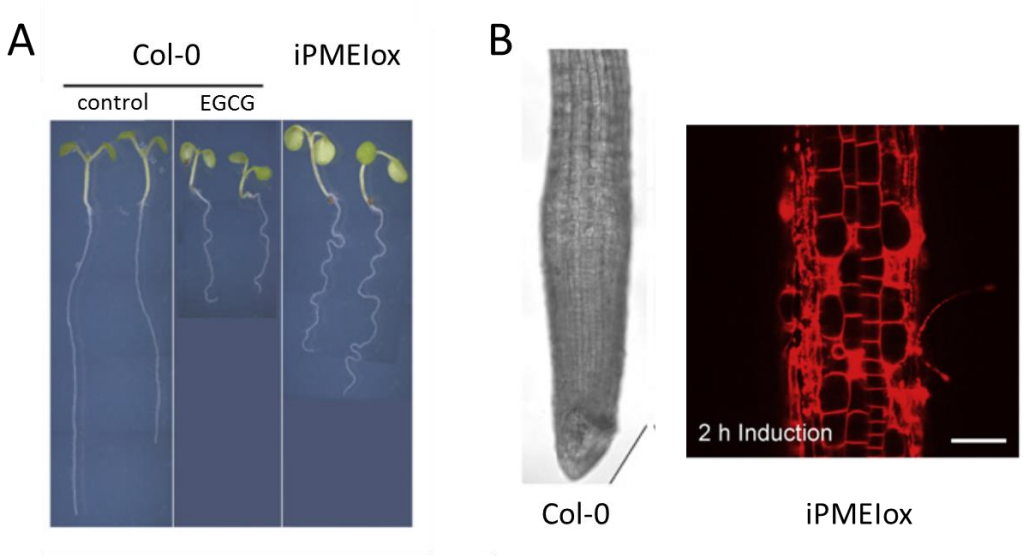

Figure 4.1. Effect of pectin methylesterases inhibition on *Arabidopsis* root. (A) Wild-type seedlings grown on medium supplemented with EGCG respond with a root waving phenotype which is similar to the phenotype of seedlings overexpressing PMEI5 (iPMEIox). (B) Col-0 root tip reacts with mild cell swelling after 24 h EGCG treatment and 2 h induction of iPMEIox lines with β-estradiol results in cell swelling in the root transition zone. Adapted from Wolf et al., 2012.

The chemical approach is one of the methods to examine the influence of PME inhibition on plant development. A complementary approach has been used by overexpressing a PME inhibitor protein, PMEI5 (At2g31430; iPMEIox) in transgenic plants (Wolf et al., 2012). Microspectroscopy revealed that hypocotyls of iPMEIox seedlings had a small increase in the abundance of ester bonds believed to correspond to methylesterified pectin. These plants also showed irregular root waving, similar to the EGCG-induced phenotype, with the difference that iPMEIox plants did not have reduced primary root length (**Fig. 4.1 A**). Moreover, strong induction of PMEI expression for 2 hours led to cell swelling in the root transition/elongation zone of iPMEIox plants (**Fig. 4.1 B**; Wolf et al., 2012). iPMEIox aerial parts were affected too with stems growing in waves, twists and loops. These patterns occurred exclusively at branching points, where a side stem carrying a leaf or an

inflorescence failed to separate from the main stem (Müller et al., 2013). The overexpression of PMEI3 leaded to increased pectin methylesterification and the inhibition of organ formation in aerial parts of the plant (Peaucelle et al., 2011a). The apical meristem in PMEI3-overexpressing lines had a functional but disorganized auxin transport system. This could be due to change in cell wall mechanics or a lack of differential growth which may organize PIN1 through tissue stresses (Braybrook and Peaucelle, 2013). The same research demonstrated using Atomic Force Microscopy (AFM) that auxin leads to tissue softening through the demethylesterification of HG and that this modification of the cell wall is required for auxin-induced organ formation.

Within this study the aim is to examine the role of PMEs in root development using a pharmacological approach. It has been reported that the green tea catechin extract (Polyphenon-60; PP60) inhibits citrus and tomato PME activity (Lewis et al., 2008b). It is shown in this chapter that in contrast to the expected effect of PP60 to reduce PME activity, plants grown on media supplemented with PP60 had surprisingly higher PME activity due to PMEs upregulation and reduced root growth compared to control plants. The short primary root phenotype was observed due to reduced meristem size. Media pH changes showed that possibly higher PME activity reduces acidic pH effect on plants and more basic pH together with PP60 does not have an effect on PME activity.

4.2 Results

4.2.1 PP60 enhances PME activity caused by overexpression of some PME genes

4.2.1.1 PP60 treatment changes PMEs activity

It has been shown that PP60 inhibits PME isolated from orange (Lewis et al., 2008b). There is a high degree of PME sequence conservation (see **Chapter 3**) suggesting that a similar effect of PP60 on PME isolated from *Arabidopsis* might be expected. To test this hypothesis, total protein was extracted from roots of 6-days old seedlings and incubated at pH 5.7 and pH 8.0 together with different PP60 conditions for 30 min. The results showed that PP60 inhibited PME activity at both pH conditions having more profound effect in pH 5.7 where PME activity in 30 and 50 µg/mL PP60 was decreased around 60% compared to control (**Fig. 4.2 A**; $F = 329.1$; $P < 0.01$). These results confirm the ability of PP60 to inhibit PME activity *in vitro*.

PP60 is assumed to decrease PME activity based on *in vitro* data. The PME activity from kiwi was measured after the incubation with different concentrations of PP60 and showed dose-dependent activity decrease. Additionally, EGCG and GCG, were shown to have the highest inhibitory effect from all the PP60 catechin mixture (Lewis et al., 2008b). To test whether PP60 inhibitory effect on PME activity *in vitro* holds true *in vivo*, the PME

activity was monitored in *Arabidopsis* roots after PP60 treatment in media at pH 5.7 and 8.0. It has been shown that purified PME3 activity was optimal at pH 7.5 (Sénéchal et al., 2015), therefore it is expected PME activity would be increased at more basic pH. The activity was determined by extracting cytoplasmic and cell wall-bound proteins from homogenized plant samples with extraction buffer containing LiCl at pH 5.0. The PME activity was measured by spectrophotometric measurement of released methanol and additionally by a gel diffusion assay. When the PME activity was measured with the gel diffusion assay, different pattern for pH 8.0 conditions could be observed compared to pH 5.7 (**Fig. 4.2 B**). The PME activity increased after addition of PP60 and had a higher activity at pH 8.0 compared to pH 5.7 ($F = 245.7$; $P < 0.01$). Elevated PME activity was detected after addition of PP60 in optimal pH conditions (pH 5.7) and it was significantly increased after treatment with 50 µg/mL PP60 (**Fig. 4.2 C**; $F = 8.323$; $P < 0.01$). There was no difference in PME activity after PP60 treatment at pH 8.0 ($F = 1.244$; $P = 0.2971$). Optimal pH conditions had the same PME activity pattern in both methods with increase after addition of 50 µg/mL PP60.

In vivo results showing increase of PME activity after PP60 addition in pH 5.7 differed from *in vitro* results where a decrease in PME activity was observed. One explanation for this observation is that PP60 initially inhibits PME activity and that the plant responds to this reduced activity by overexpressing PME genes to maintain homeostasis. To determine the initial PMEs response to PP60 treatment, seedlings were grown in liquid media for 6 days and then transferred to new flasks with different PP60 conditions. PME activity was measured after 3, 6, 9, 12, and 24 hours following the transfer. In control conditions, PME activity increased up until 6 hours after the transfer, then significantly dropped after 9 hours and was maintained at the same level until 24 hours (**Fig. 4.3**; $F = 13.04$; $P < 0.01$). PP60 addition caused inhibition of PME activity after 6 and 9 hours of treatment comparing to untreated seedlings, but after 12 and 24 hours PME activity was increasing comparing to control conditions ($F = 3.985$; $P < 0.01$). The different activities at the 3 and 6 hours' time points might be caused by the change of plants environment (transfer to a fresh media).

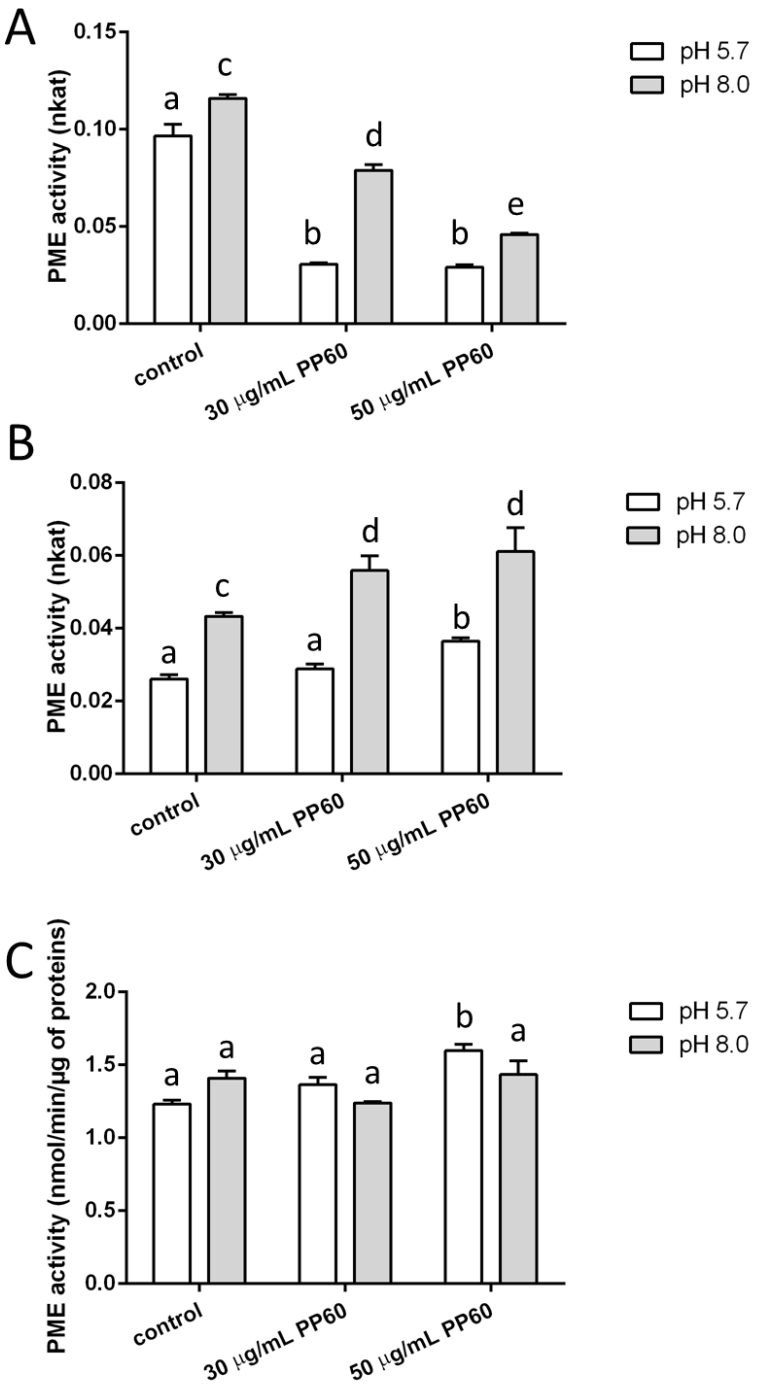

Figure 4.2. *In vitro* and *in vivo* PME activity was differentially altered after PP60 treatment. Total PME activity was determined after PP60 treatment. (A) *In vitro* PME activity assay. PME activity was measured using calorimetric method (B) and gel diffusion assay (C) in *in vivo* experiments. Each assay was repeated in two independent experiments which showed similar trend. Representative data from one experiment is shown. Error bars represent standard error of three technical repeats and lowercase letters indicate significant differences among treatments determined by two-way ANOVA with Sidak's multiple comparisons tests.

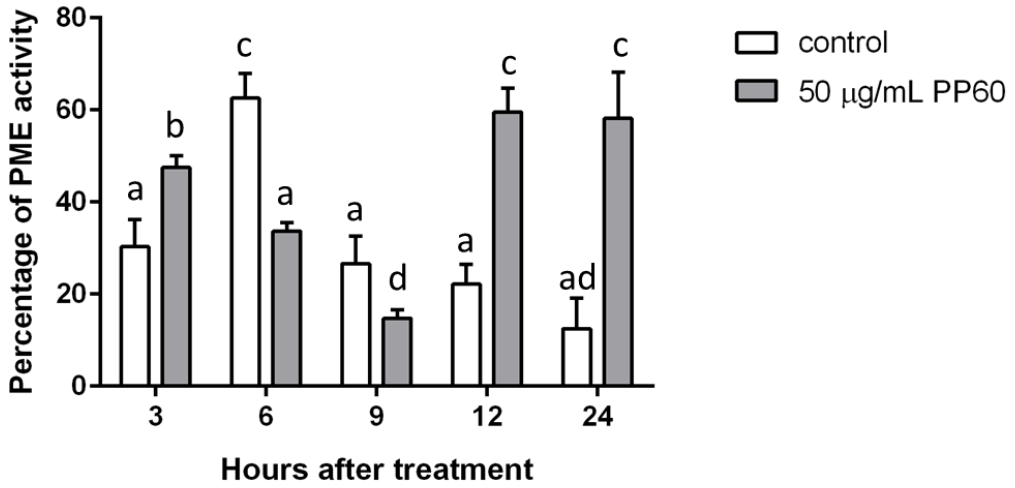

Figure 4.3. *In vivo* PME activity assay in pH 5.7. Total PME activity was determined after PP60 treatment in one independent experiment. Representative data from one experiment is shown. Error bars represent standard error of three biological replicates and lowercase letters indicate significant differences among treatments determined by two-way ANOVA with Sidak's multiple comparisons tests.

4.2.1.2 PP60 causes overexpression of some PME genes

To establish whether increased PME activity and exogenous pH has a general role in the regulation of PMEs transcript abundance, the influence of exogenously supplied PP60 on the *Arabidopsis* PMEs and PMEIs transcriptome in roots was analysed. From predicted 66 pectin methylesterases (PMEs) and 69 pectin methylesterases inhibitors (PMEIs) gene candidates, 14 and 12 showed a change in abundance after PP60 and pH treatment in comparison to roots grew on control media (**Table 4.1**). It was noticed that the pH 8.0 treatment caused overexpression of 7 PME genes (*PME1*, *PME3*, *PME15*, *PME20*, *PME25*, *PME47*, and *PME59*). All the overexpressed genes are transcribed in different root tissues from epidermis to stele (see Chapter 2). After PP60 addition to pH 8.0 conditions the expression of the PME genes was similar to that of the untreated plants with an exception of *PME10* which was overexpressed. In case of PMEI genes the expression had been regulated differentially with *PMEI1*, *At5g62340*, and *At5g62350* being upregulated and *At2g10970*, *At3g17150*, and *At4g02250* being downregulated (**Table 4.1**). In PP60-treated roots at pH 8.0, *At3g17150* and *At4g02250* were overexpressed. Addition of PP60 in normal pH (5.7) conditions caused upregulation of *PME5*, *PME12*, *PME15*, *PME25*, *PME41*, and *PME44*) PME genes. Gene expression seemed to be influenced by basic pH causing PMEs overexpression regardless of PP60 addition.

Table 4.1. List of PMEs and PMEIs transcripts altered more than 2-fold by PP60 treatment. Fold changes are calculated as mean log2IF (treatment/control; n=2) from two independent experiments. "+" in green indicates upregulation and "-" in red downregulation. Significant differences among treatments were determined by t-test (p<0.05).

Identifier	Description	Fold change - PP60 treatment [µg/mL]/pH conditions				
		pH8.0	30/pH8.0	50/pH8.0	30/pH5.7	50/pH5.7
Pectin methylesterases (PMEs)						
At1g53840	PME1	+2.299	0.926	0.710	1.758	1.868
At2g19150	PME10	-0.505	+2.077		1.072	0.701
At2g26440	PME12	1.617	0.992	0.671	+4.239	+3.941
At2g36710	PME15	+3.400	0.585	0.585	+3.763	+2.145
At2g47550	PME20	+2.429	0.872		1.379	1.644
At3g10710	RHS12	1.131	0.888	0.816	-0.486	1.145
At3g10720	PME25	+2.361	0.887	0.617	1.929	+2.143
At3g14310	PME3	+2.467	0.659		1.246	0.879
At4g02330	PME41	0.624	1.360	1.215	+2.672	+2.555
At4g33220	PME44	0.656	0.695		+2.180	+4.306
At5g04970	PME47	+2.008	0.950	0.759	1.336	1.056
At5g47500	PME5	1.100	1.447		+2.250	+2.109
At5g51490	PME59	+2.460	0.798		1.513	1.769
At5g55590	QRT1	-0.496	1.921	1.113	1.214	0.776
Pectin methylesterases inhibitors (PMEIs)						
At1g14890		0.724	+2.336	+2.378	1.141	1.285
At1g48020	PMEI1	+2.401	0.987	0.964	1.092	+2.085
At2g10970		-0.390			1.704	+2.488
At3g17150		-0.267	+4.183	+3.408	-0.445	-0.378
At3g17152		1.058	1.011	-0.402	1.311	1.300
At3g62180		0.532	+2.283	+3.063	1.123	0.581
At3g62820		0.848	0.895	1.030	0.599	-0.366
At4g02250		-0.383	1.789	+2.084	1.180	1.329
At4g03945		1.082		+2.325	1.495	1.020
At4g15750		0.545	1.981	+1.960	0.899	0.780
At5g62340		+2.290	1.264	0.896	0.884	1.310
At5g62350		+1.979	1.044	0.714	0.623	1.402

Molecular analysis of the transcriptome and protein activity following PP60 treatment demonstrated that more basic pH favoured expression of PME genes but had unpredicted responses in PME activity (increase or no change). Addition of PP60 maintained PMEs expression similarly as in the control but enhanced expression of PMEI genes. PP60 at pH 5.7 favoured expression of PMEs and PME activity. This might have been due to PP60 inhibition of specific PME isoforms at the beginning of treatment and compensation of other PME isoforms.

4.2.2 PP60 triggers an increase in activity of polygalacturonases

Higher PME activity produces larger blocks of de-methylesterified homogalacturonan (HG). This might allow hydrolysing enzymes like polygalacturonases (PGs) to act on the HG chain causing degradation of pectin and leading to softening of the cell wall. To determine the PG activity, the extracted proteins from 6-day old *Arabidopsis* seedlings were used and PG activity measured using a calorimetric method. PG activity

increased after 50 µg/mL PP60 treatment by about 30% compared to control conditions at pH 5.7 (**Fig. 4.4**; F = 85.84; P < 0.01). In case of pH 8.0 the PG activity was reduced by nearly 10%. When the PME activity was compared to PG activity between treatments it could be seen that increase in PME activity correlated with a rise in PG activity at pH 5.7 conditions (**Table 4.2**). This data suggests that the PP60-mediated modification of pectin methylesterification status might coordinate the response of other pectin-modifying enzymes.

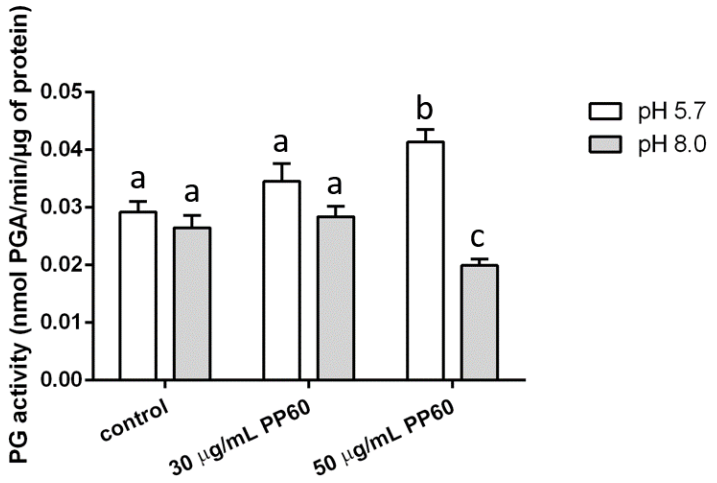

Figure 4.4. Polygalacturonase (PG) activity was altered after PP60 treatment. Total PG activity was determined after PP60 treatment. Root tissue was harvested from 6 days old seedlings. PG activity was measured using calorimetric method in three independent experiments which showed similar trend. Representative data from one experiment is shown. Error bars represent standard error of three technical replicates and lowercase letters indicate significant differences among treatments determined by two-way ANOVA with Sidak's multiple comparisons tests.

Table 4.2. The comparison of PME and PG activity with different pH and PP60 treatments. Asterisks indicate significant difference between PG and PME activities at 50 µg/mL PP60 compared to 30 µg/mL PP60 and control. Significant differences among treatments were determined by two-way ANOVA with Sidak's multiple comparisons tests.

Activity (nmol/min/µg; ± SEM)	pH 5.7	pH 8.0	PP60 treatment
PG	0.029 (±0.002)	0.026 (±0.002)	control
PME	1.229 (±0.026)	1.408 (±0.049)	
PG	0.035 (±0.003)	0.028 (±0.002)	30 µg/mL PP60
PME	1.365 (±0.049)	1.238 (±0.008)	
PG	0.041 (±0.002)**	0.020 (±0.001)	50 µg/mL PP60
PME	1.598 (±0.043)**	1.433 (±0.094)	

4.2.3 PP60-treated *Arabidopsis* seedlings display dwarf phenotype

4.2.3.1 PP60 inhibits primary root elongation

Inhibition of PME activity can influence the state of homogalacturonan (HG) crosslinking thus influencing cell wall rigidity. Differences in cell wall strength influences the ability of cells to elongate and potentially change their shape. Roots are a popular and attractive system to work with as they undergo cell division at the primary root tip, post-

embryonic organogenesis to make lateral roots, cell expansion in the elongation zone of the primary and lateral roots and tip growth elongation in root hairs. The effect of PP60 and EGCG was observed in *Arabidopsis* seedlings grown on either an acidic media (pH 5.7) or a basic one (pH 8.0). Additionally, the effect of catechins ECG and EGC on primary root elongation at pH 5.7 was monitored. It is thought that most of PME isoforms have a basic pI and act in a block-wise fashion, while the ones with an acidic pI act in more random fashion. However, there is not sufficient evidence to confirm this hypothesis and it appears that apoplastic pH rather than pI is the more important determinant for PME activity (Sénéchal et al., 2015a).

PP60 treatment under pH 5.7 conditions caused overexpression of PME genes and increased PME activity. The transcriptomics analysis showed pH 8.0 conditions caused overexpression of some PME genes, whereas addition of PP60 kept PMEs expression at the untreated level. Therefore, it is expected that pH 8.0 would inhibit root elongation and addition of PP60 would rescue the phenotype compared to pH 5.7 conditions. To investigate catechin and pH effect on *Arabidopsis* roots, wild-type Col-0 were treated with PP60 concentrations of 15, 30, 50, and 100 µg/mL. EGCG consists of 34% of total catechins in PP60 thus EGCG concentrations were calculated to 4.4, 9, 15, and 30 µg/mL accordingly. Plants were grown on media pH 8.0 with the same catechin concentrations for 14 days in parallel with the control condition of pH 5.7. The effect of EGCG on primary root elongation was not visible by eye (**Fig. 4.5 A**) and the measurements (**Fig. 4.5 C**) showed no significant differences ($F = 1.015$; $P = 0.4418$). The changes in root length were more prominent when plants were grown with PP60 supplementation. As shown in the **Figure 4.5 B, D** PP60 influence on root elongation on pH 5.7 started from 30 µg/mL PP60, to almost inhibit the primary root development in concentration 100 µg/mL (**Fig. 4.5 D**) compared to control conditions ($F = 8.611$; $P < 0.0001$).

There were no significant changes in root elongation after EGCG treatment at pH 8.0 (**Fig. 4.6 A, C**; $F = 1.015$; $P = 0.4418$). pH 8.0 could effectively reduce the effect of PP60 on acidic media (**Fig. 4.6**). Only high, 100 µg/mL PP60 inhibited root elongation (**Fig. 4.6 B, D**; $F = 14.16$; $P < 0.01$). These results showed the importance of extracellular pH in regulation of PME activity and the primary root elongation.

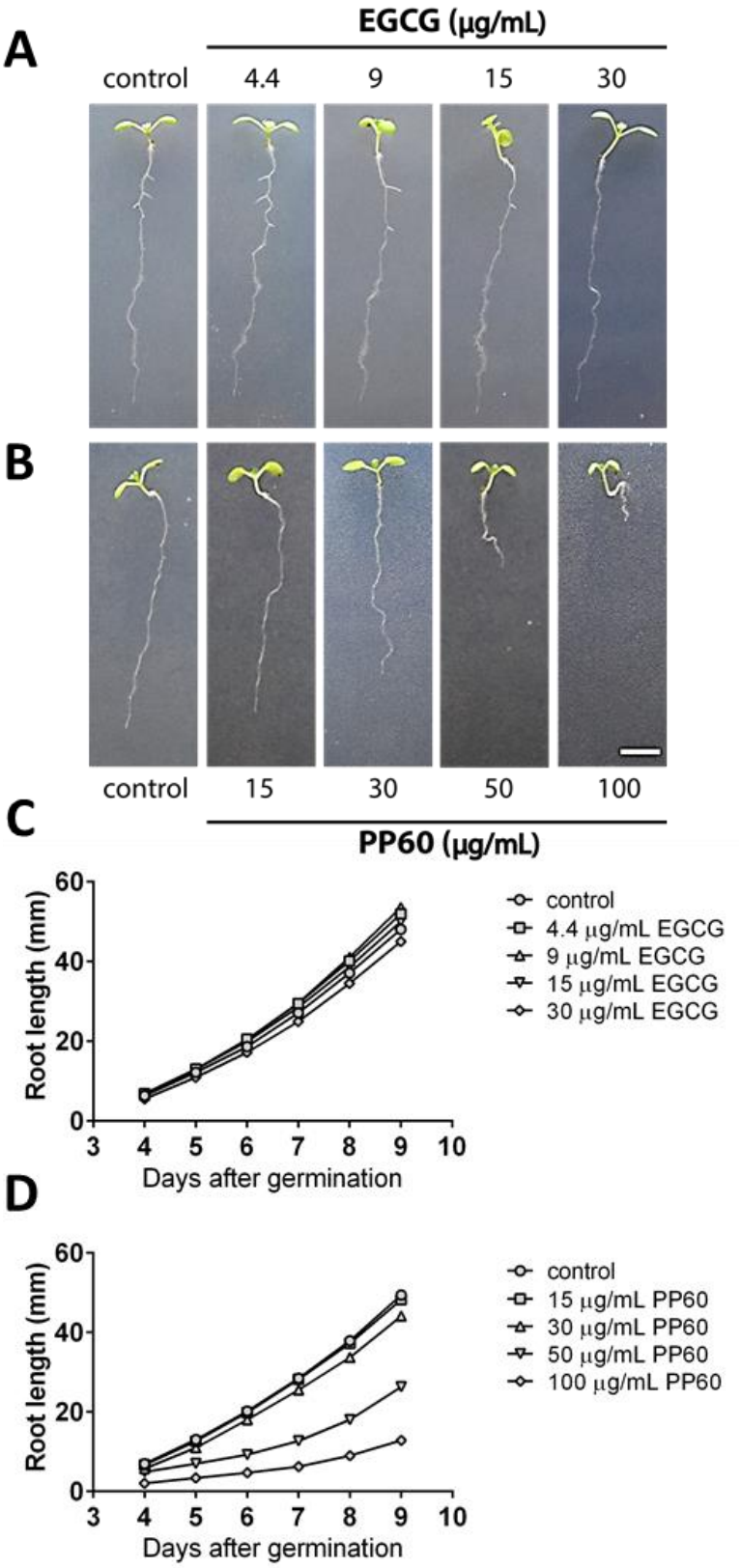

Figure 4.5. Responses of *Arabidopsis* primary root to treatment with polyphenon 60 (PP60) and epigallocatechin-3-gallate (EGCG) at pH 5.7. 7-days old seedlings grown on different EGCG concentration (A) and PP60 concentration (B). Each experiment was repeated three times and showed similar trend. Average root lengths from 4 to 9 days of growing on 0.5 MS media supplemented with different [EGCG] (C) and [PP60] (D) from one representative experiment with three biological replicates (each n>20) are illustrated. Statistical analysis was determined by two-way ANOVA with Tukey's multiple comparisons test. Scale bar 10 mm.

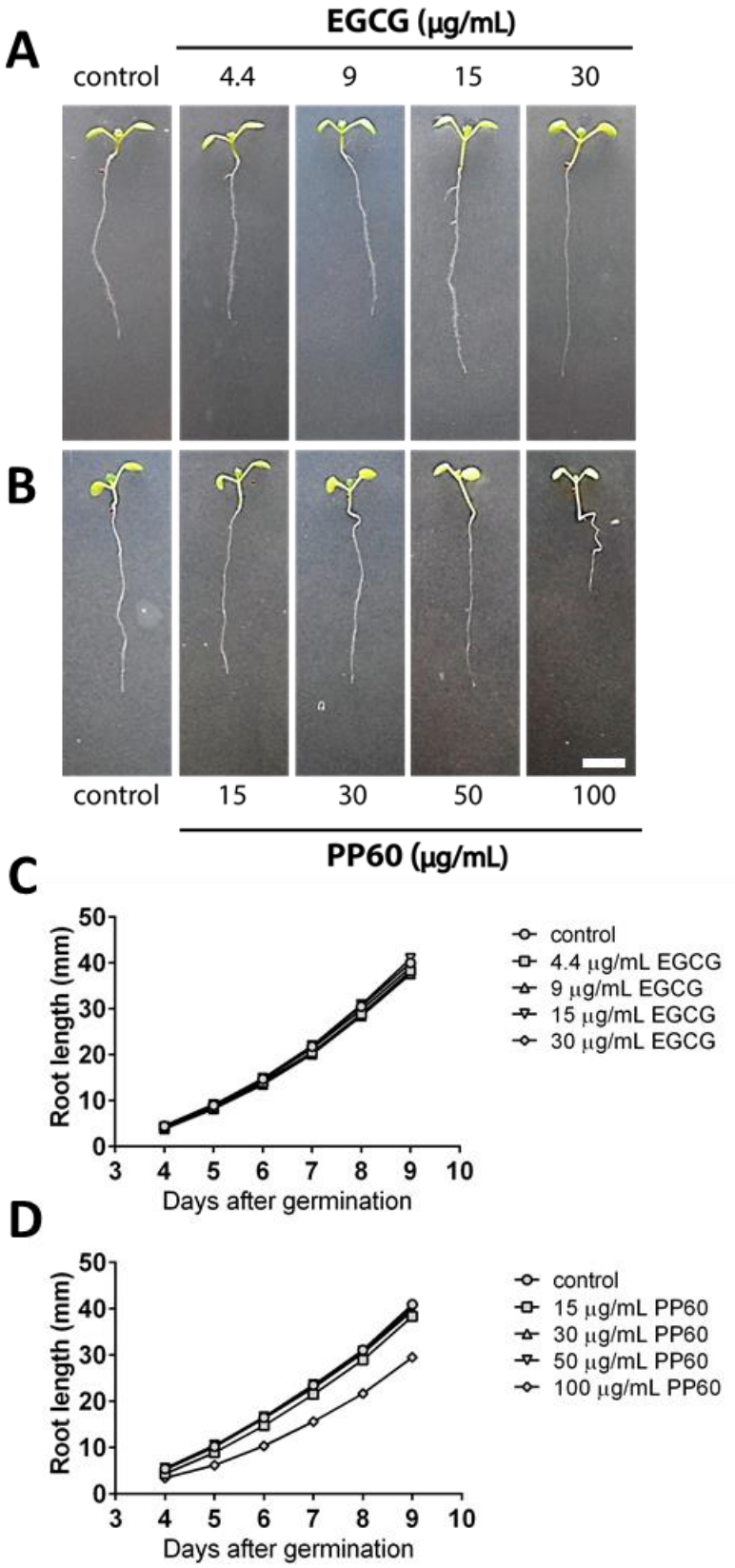

Figure 4.6. Responses of *Arabidopsis* primary root to treatment with polyphenon 60 (PP60) and epigallocatechin-3-gallate (EGCG) at pH 8.0. 7-days old seedlings grown on different EGCG concentration (A) and PP60 concentration (B). Each experiment was repeated three times and showed similar trend. Average root lengths from 4 to 9 days of growing on 0.5 MS media supplemented with different [EGCG] (C) and [PP60] (D) from one representative experiment with three biological replicates (each n>20) are illustrated. Statistical analysis was determined by two-way ANOVA with Tukey's multiple comparisons test. Scale bar 5 mm.

The comparison of EGCG and PP60 treatments between different pHs revealed that low EGCG concentrations (4.4 and 9 µg/mL) promoted root elongation, whereas high EGCG concentration (30 µg/mL) inhibited root growth (**Fig. 4.7 A**; F = 53.59; P < 0.01). Another interesting correlation could be seen between PP60 treatments at different pHs. The primary root elongation at 50 µg/mL PP60 at pH 5.7 was similar to that of 100 µg/mL PP60 at pH 8.0 (**Fig. 4.7 B**) suggesting higher pH might reduce the effect of PP60. There was no primary root growth promotion when grown on PP60 comparing to EGCG treatment.

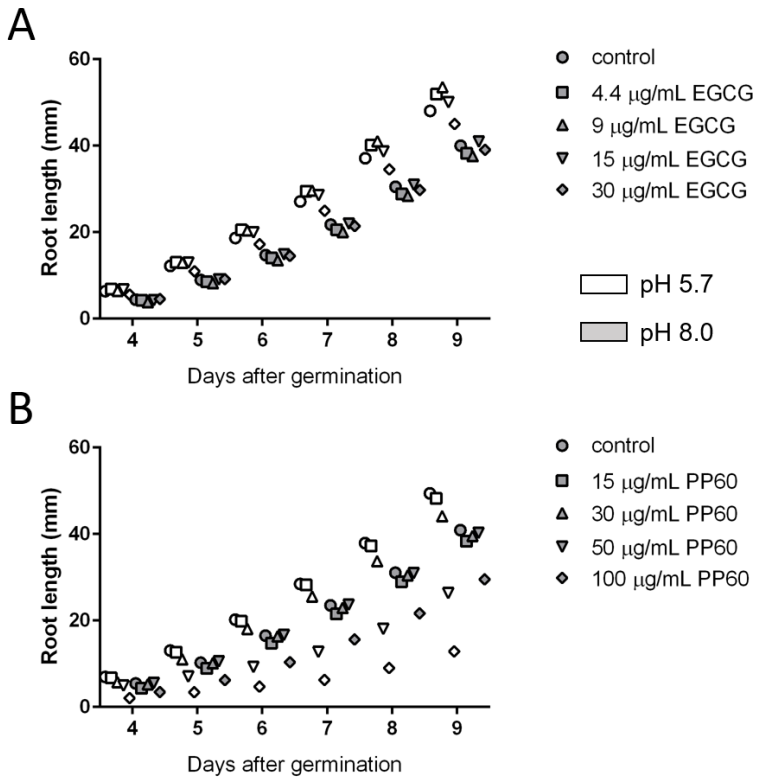

Figure 4.7. The comparison of polyphenon-60 (PP60) and epigallocatechin-3-gallate (EGCG) treatment with pH effect on *Arabidopsis* primary root. Average root lengths from 4 to 9 days of growing on 0.5 MS media supplemented with different [EGCG] (A) and [PP60] on pH 5.7 and pH 8.0 from Fig. 4.6 and Fig. 4.7 are illustrated.

The results showed that EGCG as a component of PP60 had little effect on root growth suggesting that other components of PP60 can have more profound effect on root development. To test this hypothesis, epigallocatechin (EGC) and epicatechin-3-gallate (ECG) being 16.7 and 8.7% of total catechins in PP60 respectively were used. Plants were grown with 20 µg/mL of EGC and 8 µg/mL of ECG on pH 5.7 and 8.0 media. The primary root length was measured as in previous experiment and there was no difference in root development between treatments and pHs (**Fig. 4.8**; F = 0.1055; P = 0.99 and F= 0.4495; P = 0.9196, respectively). The results indicated neither EGC nor ECG inhibited root development meaning only mix of EGCG, ECG, EGC, GCG, EC, and CG (PP60) could strongly influence primary root elongation.

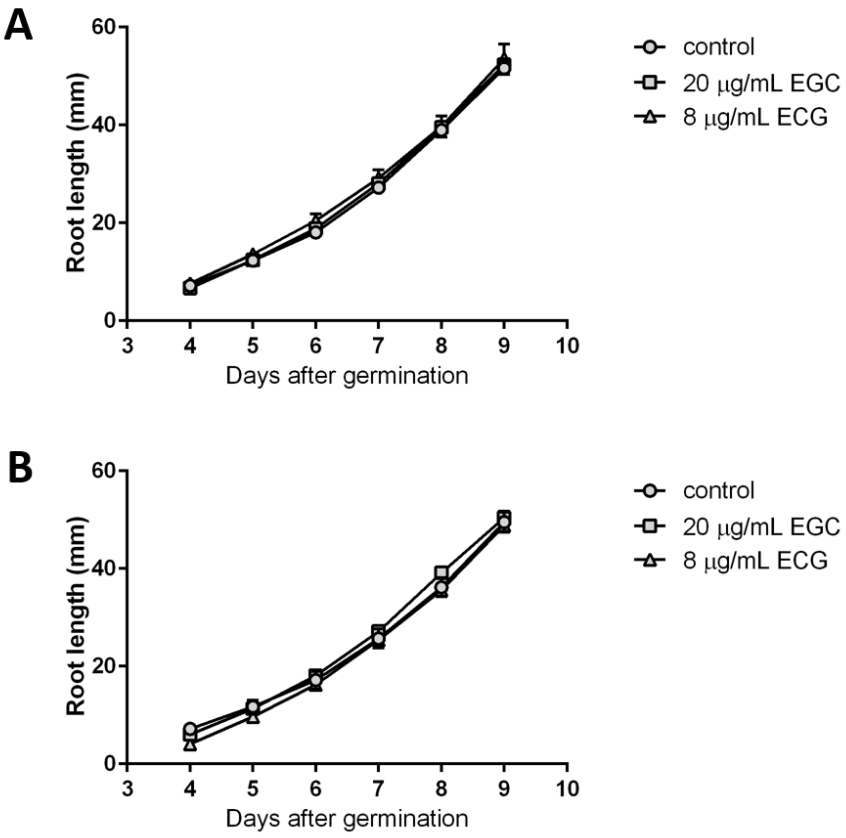

Figure 4.8. Responses of *Arabidopsis* primary root to treatment with epigallocatechin (EGC) and epicatechin-3-gallate (ECG) at different pHs. The experiment was repeated two times with one biological replicate each and showed similar trend. Average root lengths from 4 to 9 days of growing on 0.5 MS media supplemented with different [EGC] and [ECG] on pH 5.7 (A) and pH 8.0 (B) from one representative experiment with one biological replicate (n>20) are illustrated. Statistical analysis was determined by two-way ANOVA with Tukey's multiple comparisons test.

The addition of sucrose to the media can affect plants metabolism and cause stronger responses upon chemical treatment (See **chapter 7**). To test whether PP60 treatment responses might be enhanced upon sucrose supplementation, Col-0 seedlings were grown on media without sucrose together with PP60. The addition of PP60 to the media without sucrose reduced the response of plants to the treatment (**Fig. 4.9 A**). The effect of 50 µg/mL PP60 in media without sucrose on root length was less pronounced compared to plants grown with sucrose (around 10 and 50% root length reduction, respectively; **Fig. 4.5 D**, **Fig. 4.9 B**). These results suggest sucrose may trigger signalling responses which enhance the PP60 effect on root development.

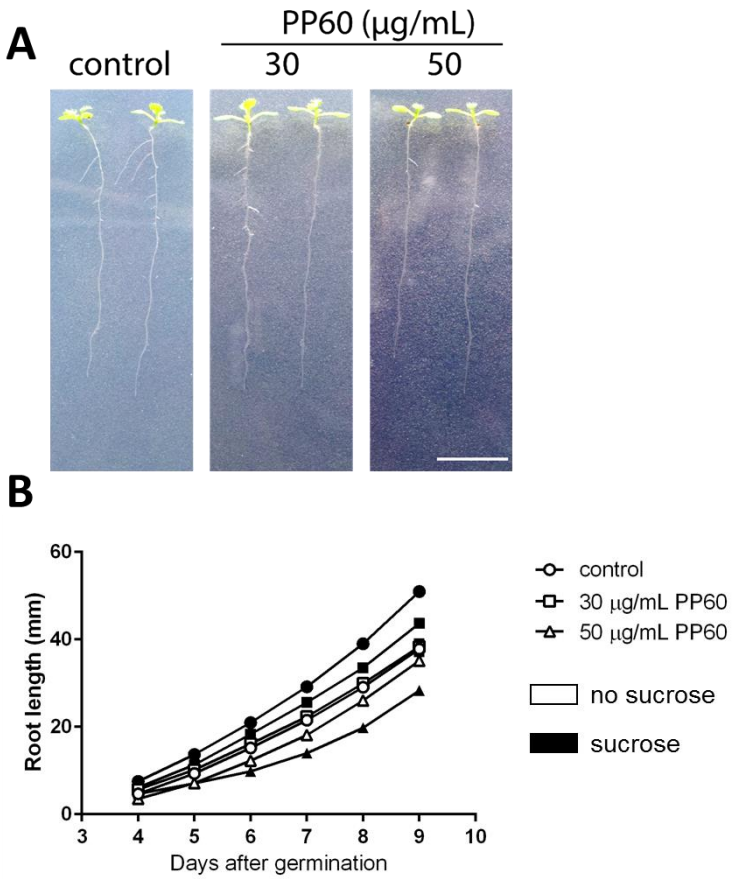

Figure 4.9. Responses of *Arabidopsis* primary root growth to treatment with polyphenon 60 (PP60) at pH 5.7 without sucrose in media. 7-days old seedlings grown on 30 and 50 µg/mL PP60 concentration (A). Average root lengths from 4 to 9 days of growing on 0.5 MS media without sucrose supplemented with different [PP60] (B) from two independent experiments with one biological replicate (n>20) are illustrated. Statistical analysis was determined by two-way ANOVA with Tukey's multiple comparisons test. Scale bar 10 mm.

4.2.3.2 PP60 alters root hairs formation and elongation

The formation of a root hair provides a good model for plant cell development due to the ease of observing cell wall elongation. Root hair formation starts with an initial bulging of the cell wall which coincides with localised cell wall acidification and thinning (Ryan et al., 2001). The localization of Rop proteins at the root hair initiation site causes a drop in pH and activation of expansins. The tip growth requires cell wall loosening to be able to expand and incorporate a new material into the wall. These changes involve activity of cell wall modifying enzymes like expansins. Moreover, PMEs and PMEIs are distributed along the pollen tube with a preferential activity of PMEIs at the tip suggesting that similar distributions also may play role in root hair growth (Röckel et al., 2008). Therefore, the analysis of root hairs formation has been examined.

The results from root hair length analysis (**Fig. 4.10**) showed that plants grown on pH 5.7 had increased length of root hairs and their density after PP60 addition compared to

the control plants. The number of root hairs with lengths between 550-700 µm increased almost 4 times at a concentration of 100 µg/mL PP60 comparing to control plants (159 to 44, respectively; **Fig. 4.10 E**). The root hairs density increased with higher PP60 concentration as well (**Fig. 4.10 B**; F = 14.14; P < 0.01). Contradictory results have been found in plants grown on pH 8.0 where the number of short root hairs increased (from absence in control plants to 381 in 50 µg/mL; **Fig. 4.10 F**) and their density decreased (from 20 per mm to 6; **Fig. 4.10 D**; F = 125.7; P < 0.01) with rising PP60 concentration. The dose of 100 µg/mL totally inhibited the root hairs growth in the basic media. This again confirms the influence of pH on root developmental processes.

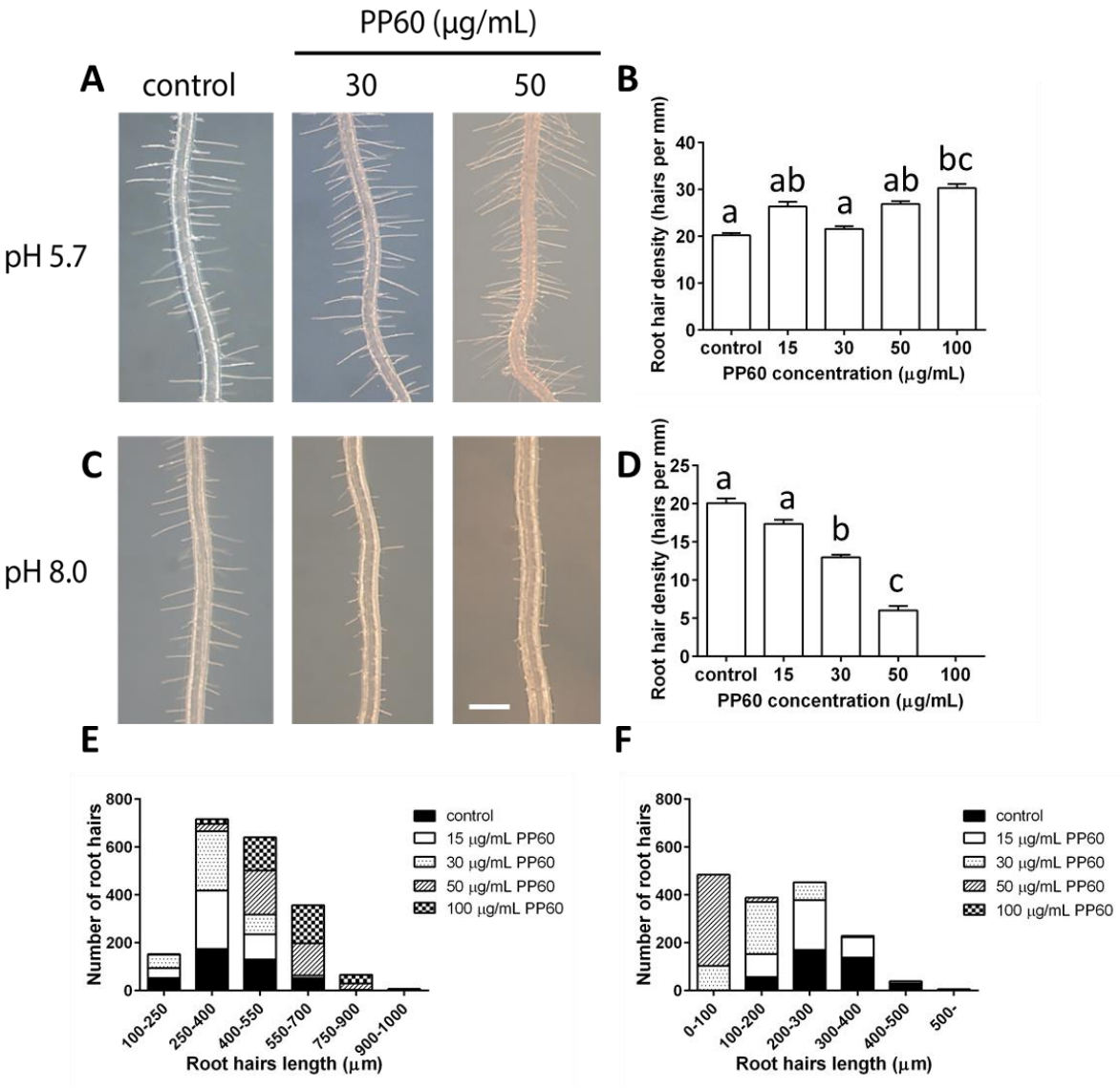

Figure 4.10. PP60 inhibits root hairs formation and elongation. 7-days old seedlings grown on different [PP60] at pH 5.7 (A) and pH 8.0 (C) are shown. The number of root hairs (E, F) and their density (B, D) have changed after PP60 treatment on media with pH 5.7 (A, B, E) and pH 8.0 (C, D, F). The experiment was prepared in three independent repeats with three biological repeats each. Error bars represent standard error of n>20 from one representative experiment and lowercase letters indicate significant differences among treatments determined by one-way ANOVA with Tukey's multiple comparisons test. Scale bar 300 µm.

4.2.3.3 PP60 alters lateral root formation and elongation

Lateral root formation is a good system to study organogenesis as it is a complex process requiring organisation and communication between cells to ensure that the correct cell divisions and expansion take place. The coordination between pectin lyases (PLs) and PMEs activity is required for the lamella degradation to prevent the cell wall loosening of the lateral root primordia (LRP) cells in contact with overlying tissues (Vilches-Barro and Maizel, 2015). The HG in cell walls of LRP is more highly methylesterified than the one of the tissue surrounding it, which could restrict PL activity to these tissues (Laskowski et al., 2006). **Figure 4.11** shows that lateral root formation and density decreased with increasing PP60 concentration, confirming the inhibitory role of the chemical in lateral roots development. The inhibitory effect was much stronger when seedlings were grown on the media at pH 8.0. The number of lateral roots and their density were arrested almost completely by 50 µg/mL and 100 µg/mL (**Fig. 4.11 C, D, F**; $F = 234.67$; $P < 0.01$). In pH 5.7 and 8.0, inhibition of growth and development could be observed from 30 µg/mL concentration. At pH 5.7 the number of lateral roots between 8-12 mm was similar for control and all [PP60]. With the higher [PP60], the number of longer lateral roots decreased and the number of short ones increased (**Fig. 4.11 E**). In both pH conditions the number and density of lateral roots decreased showing that changes in extracellular protonation do not have a significant influence on lateral root development caused by PME activity (**Fig. 4.7 A, B, C, D**).

The previous results on morphological development of *Arabidopsis* after PP60 treatment revealed that the concentrations of 30 and 50 µg/mL PP60 have the most prominent effect on root development. The concentration of 15 µg/mL had little effect on roots and the high concentration of 100 µg/mL caused severe inhibition of root development possibly due to toxic effects (**Fig. 4.12**). Thus, 30 and 50 µg/mL PP60 were selected for further analyses.

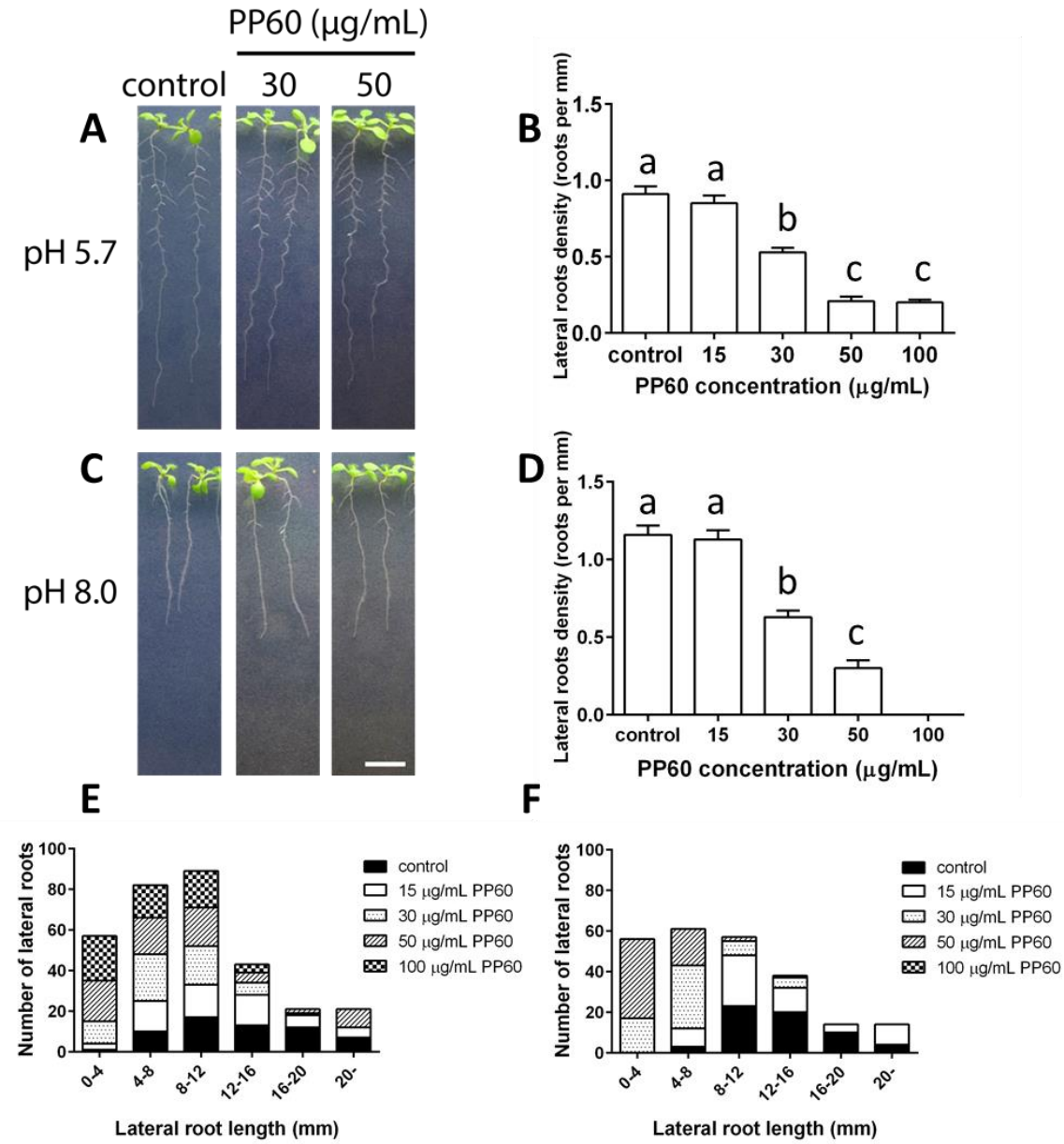

Figure 4.11. PP60 inhibits lateral root formation and elongation. 14-days old seedlings grown on different [PP60] at pH 5.7 (A) and pH 8.0 (C) are shown. The number of lateral roots (E, F) and their density (B, D) have changed after PP60 treatment on media with pH 5.7 (A, B, E) and pH 8.0 (C, D, F). The experiment was prepared in three independent repeats with three biological repeats each. Error bars represent standard error of n>20 from one representative experiment and lowercase letters indicate significant differences among treatments determined by one-way ANOVA with Tukey's multiple comparisons test. Scale bar 10 mm.

.

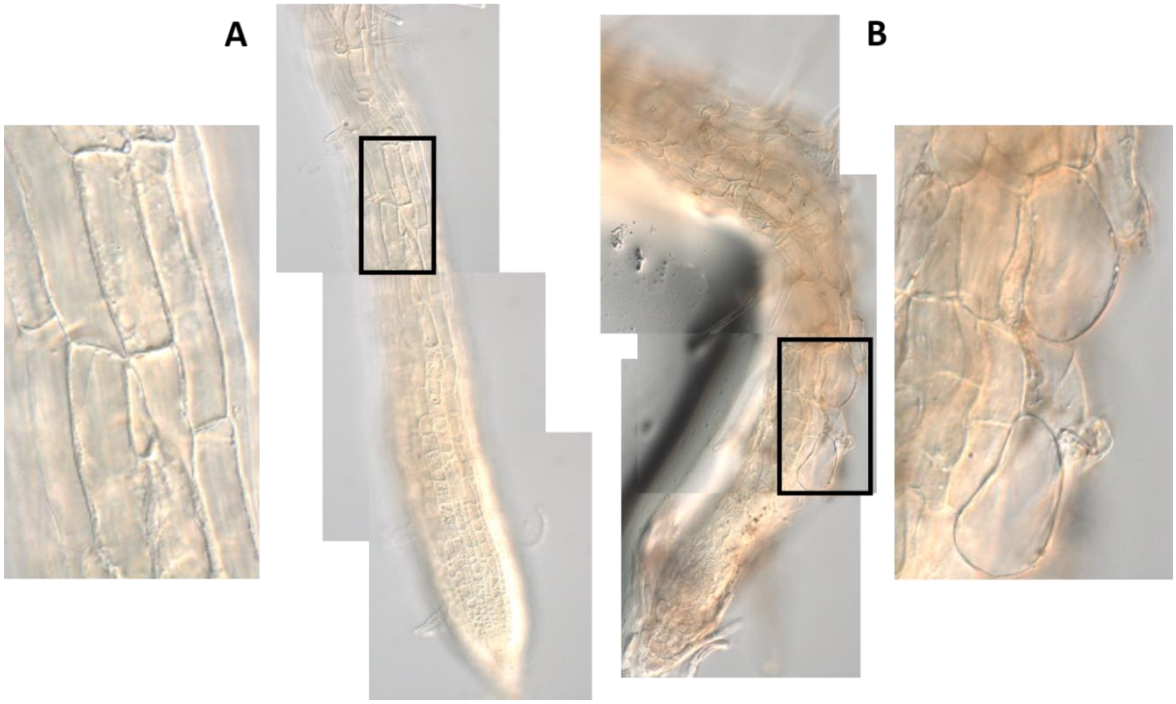

Figure 4.12. High PP60 concentration effect on *Arabidopsis* root cells. (A) A root grown on pH 5.7 media without PP60. As it can be seen on a zoomed part, cells have normal shape (B) A root grown on media supplemented with 100 µg/mL PP60. Cells are radially enlarged and changed in shape.

To see whether lower the lateral roots density caused by PP60 treatment is due to the effects on pericycle cell division, *CYCB1::GUS* plants were examined after PP60 treatment. The *CYCB1::GUS* marker shows actively dividing cells allowing observation of whether pericycle cells are initiated to form a lateral root. There was no significant difference in CYCB1::GUS foci corresponding to lateral root primordia (LRP) number after 5 days of PP60 treatment (**Fig. 4.13 A**; .F = 3.006; P = 0.106). It has been observed that the number of “division centres” was altered after 7 days of PP60 treatment (**Fig. 4.13 A**). The LRP number was two times higher after PP60 treatment compared to control (from 5.6 to 10 for 30 µg/mL PP60 and to 12.4 for 50 µg/mL PP60; F = 9.760; P < 0.01). There were no differences in already growing lateral root formation under PP60 treatment (**Fig. 4.13 B**). Despite this increase in CYCB1::GUS foci, the number of lateral roots was reduced by PP60 indicating that not all primordia progress to form a lateral root

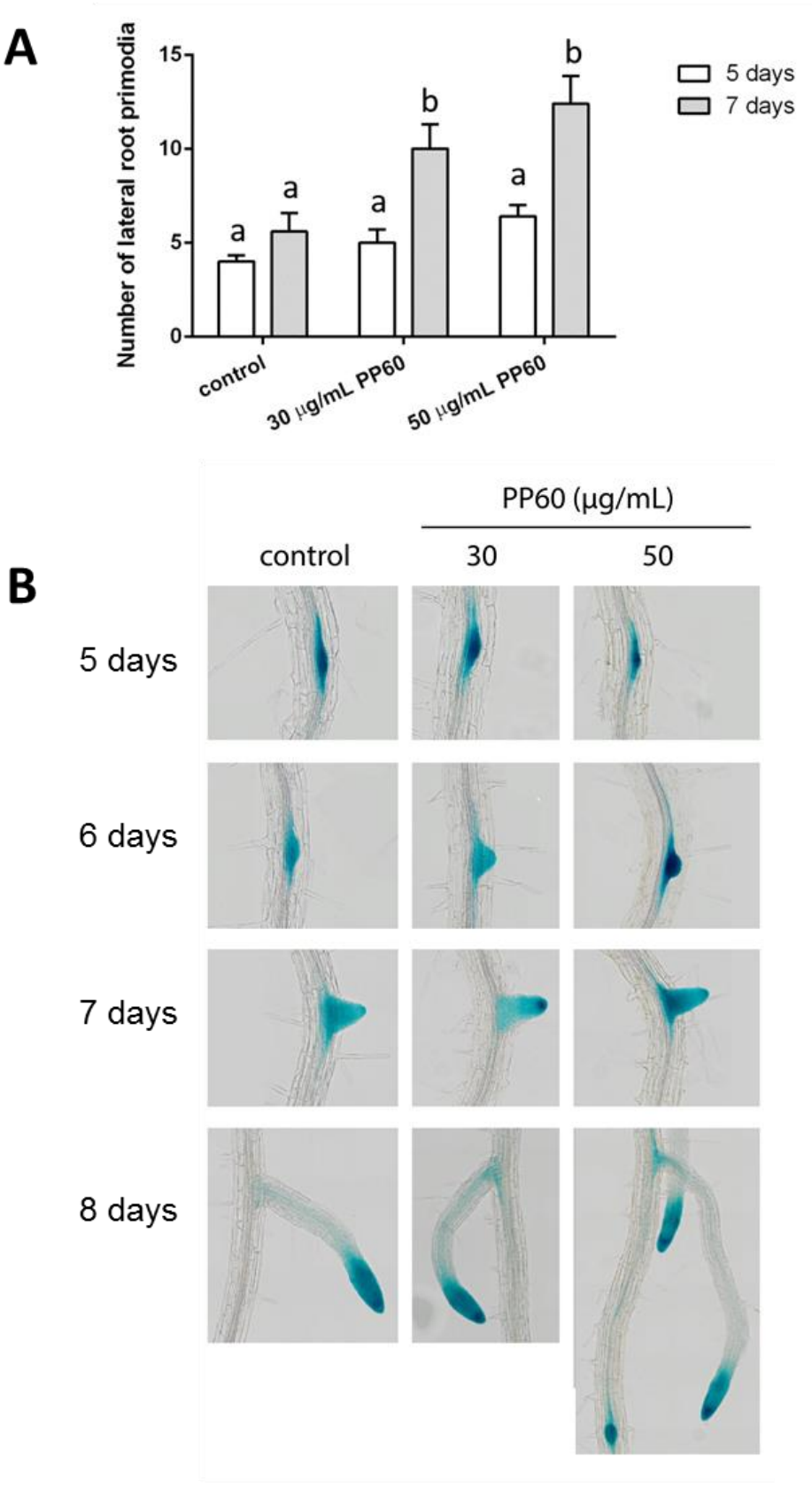

Figure 4.13. PP60 treatment affects number of lateral root primordia but not the development of already growing lateral root. (A) The lateral root primordia were counted at 5 and 7 days after germination. (B) Lateral root primordia development of *CYCB1::GUS* plants growing on 0.5 MS (pH 5.7) with 30 and 50 µg/mL PP60 concentrations at several time points. Roots of 5, 6, 7, and 8 days old *Arabidopsis CYCB1::GUS* seedlings are showed. Error bars represent standard error of n>5 from two biological replicates and lowercase letters indicate significant differences among treatments determined by two-way ANOVA with Sidak's multiple comparisons tests. Scale bar 100 µm.

4.2.4 Short root phenotype caused by PP60 is due to inhibition of cell elongation and division

4.2.4.1 Roots cell length inhibition by PP60

As both the primary root and the lateral root length decreased with higher PP60 concentrations it suggests that the elongation of roots by cell wall loosening is inhibited. Therefore, the increased density of root hairs at pH 5.7 might be due to a reduction in the length of cells. To test this hypothesis, seedlings grown on PP60-supplemented media were observed under a confocal microscope after propidium iodide (PI) staining. PI remains outside of intact cells binding to pectin polysaccharides making the observation of cells shapes very easy. In the elongation zone of Col-0 seedlings, the epidermal cells were long and rectangular. In the PP60-treated plants, however, the elongation zone had regions with nearly square cells (**Fig. 4.14 A**) and the epidermal cells were around 60% shorter with 50 µg/mL of PP60 in the media (**Fig. 4.14 B**).

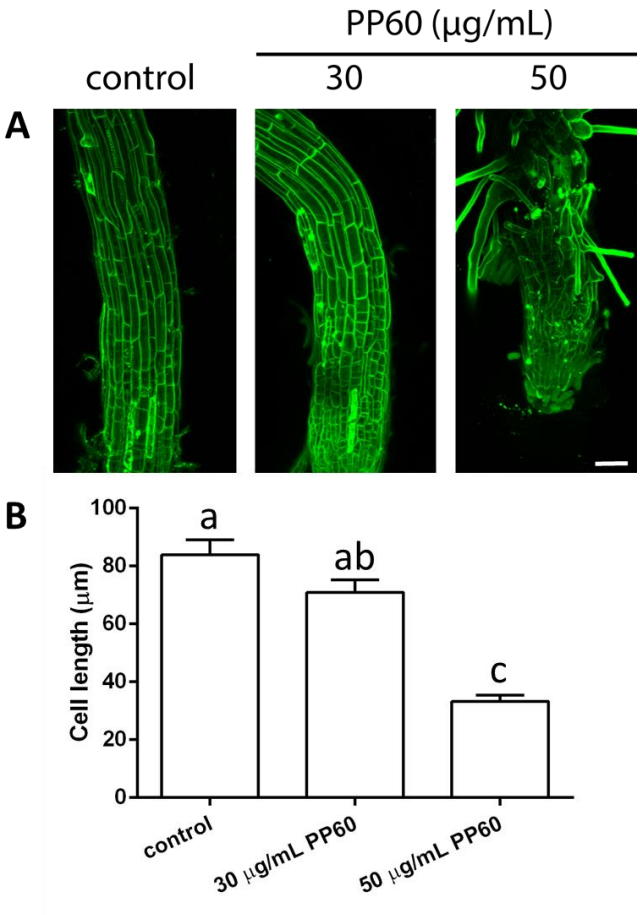

Figure 4.14. Length of root epidermal cells of Col-0 plants growing on 0.5MS (pH 5.7) with 30 and 50 µg/mL PP60 concentrations. (A) Epidermal cells in the elongation zone of Col-0 after PP60 treatment. The roots were stained with propidium iodide (PI) and imaged with a confocal microscope. (B) Root cell length in elongation zones of 7-days old Col-0 after PP60 treatment. Error bars represent standard error of n>5 from two biological replicates and lowercase letters indicate significant differences among treatments determined by one-way ANOVA with Tukey's multiple comparisons tests. Scale bar 50 µm.

The effect of pH on epidermal cell elongation was less at pH 8.0, therefore it was expected the root elongation might be intact. Indeed, in the PP60-treated plants, the elongation zone was identical to that of control plants (**Fig. 4.15 A**) and the epidermal cells were similar in length (**Fig. 4.15 B**) suggesting cell elongation and division is maintained in homeostasis in pH 8.0 regardless of PP60 addition.

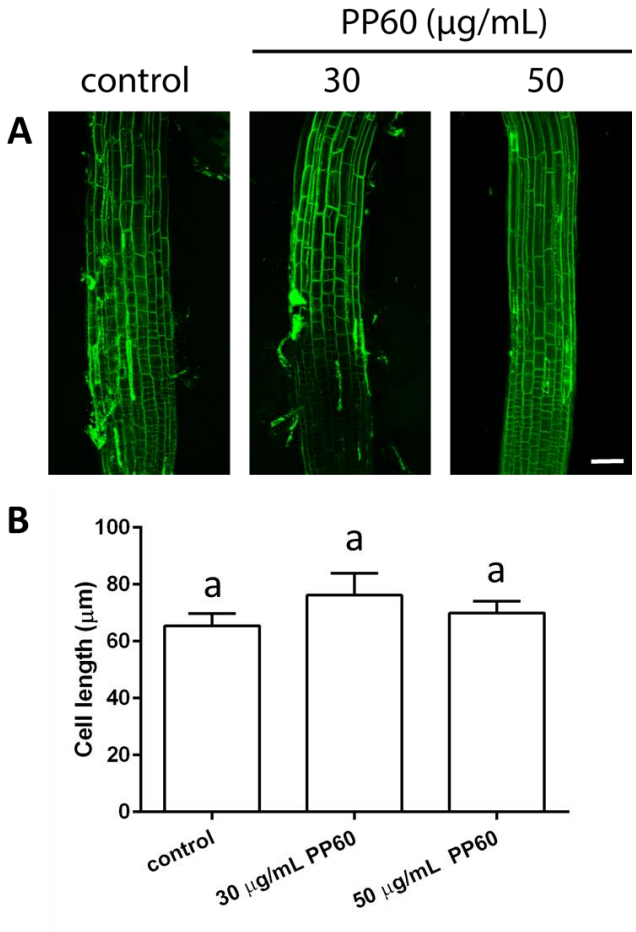

Figure 4.15. Length of root epidermal cells of Col-0 plants growing on 0.5MS (pH 8.0) with 30 and 50 µg/mL PP60 concentrations. (A) Epidermal cells in the elongation zone of Col-0 after PP60 treatment. The roots were stained with propidium iodide (PI) and imaged with a confocal microscope. (B) Root cell length in elongation zones of 7-days old Col-0 after PP60 treatment. Error bars represent standard error of n>5 from two biological replicates and lowercase letters indicate significant differences among treatments determined by one-way ANOVA with Tukey's multiple comparisons tests. Scale bar 50 µm.

4.2.4.2 Cell division in the root meristematic zone is affected by PP60

Root growth is a coordinated process of cell elongation and division. Because cell division activity in roots is reflected by the size of the root meristem, meristem sizes in Col-0 after PP60 treatment were compared by measuring the distance from the quiescent centre (QC) to the first elongated cell. After 4-days, the meristem was much smaller in roots treated with 50 µg/mL than in control plants (**Fig. 4.16 A**). To determine the cause of the low cell

division activity in PP60-treated plants, the Col-0 with the marker gene *CYCB1::GUS* was grown on media with PP60. Expression of the *CYCB1::GUS* marker gene specifically occurs at the transition stage from G_2 to M phase. The expression of *CYCB1::GUS* in meristem cells was lower in PP60-treated plants than in control (**Fig. 4.16 B**). These results indicated that low cell division activity in PP60-treated seedlings was either due to the slower transition of cells from G_2 to M phase or that fewer cells enter the cell cycle instead going into G_0 phase.

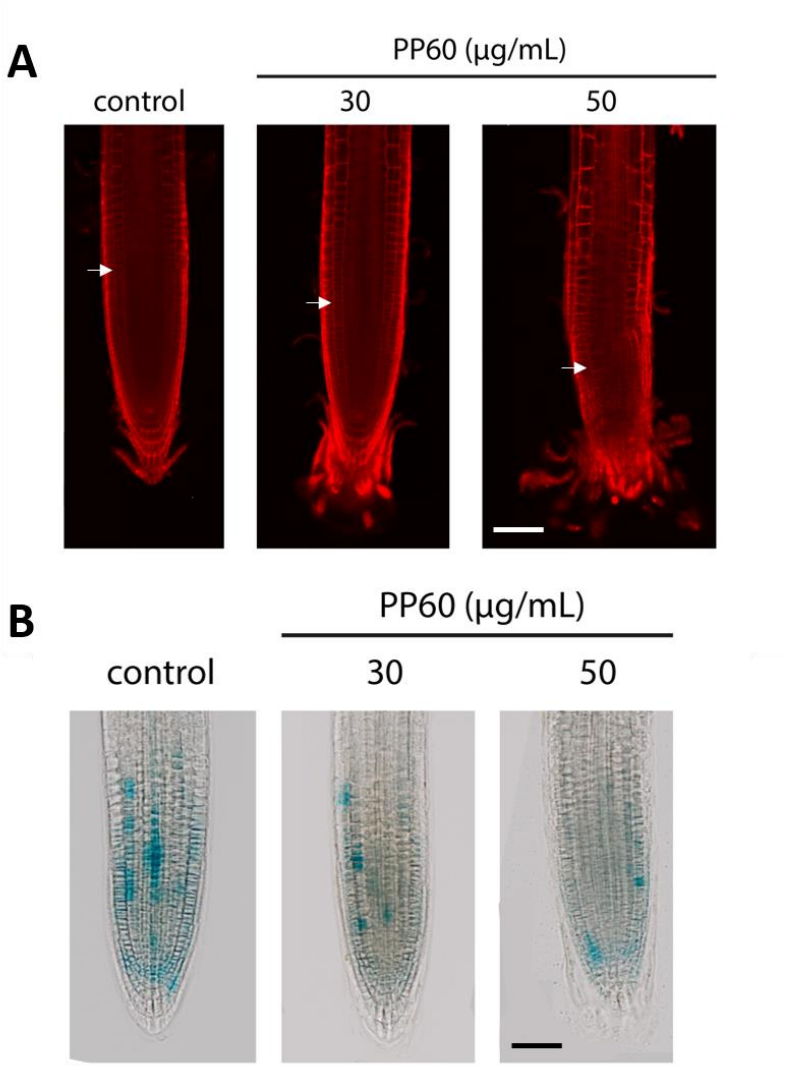

Figure 4.16. Characteristics of root meristematic zone of Col-0 plants growing on 0.5MS (pH 5.7) with 30 and 50 µg/mL PP60 concentrations. (A) Root meristematic zone of 4-days old Col-0 after PP60 treatment. White arrows indicate the boundary between the root meristematic and elongation zones. (B) Expression of *CYCB1::GUS* in the meristematic zones of 4-days old Col-0 after PP60 treatment. Representative pictures from two independent experiments (each n>5). Scale bar 100 µm.

4.2.5 PP60 alters the phenotype of a PMEIs overexpression line

Plants overexpressing PMEI5 (iPMEIox) showed a pronounced irregular root waving phenotype compared to control plants, suggesting that regulated PME activity is important for maintaining the growth rate and direction (Wolf et al., 2012). As shown in the previous subchapter, PP60 enhanced PME activity, thus growing iPMEIox seedlings on PP60 should rescue the root phenotype in these plants. To see whether this is true, iPMEIox plants were grown on pH 5.7 media supplemented with 30 and 50 µg/mL PP60 together with wild-type plants. The root length was monitored for 6 days and root tip position was measured after 7 days of growth. iPMEIox seedlings had significantly reduced root elongation compared to control plants (**Fig. 4.17 A, B**; $F = 85.6$; $P < 0.01$). When grown on 30 µg/mL PP60 iPMEIox roots were longer compared to non-treated ones (**Fig. 4.17 B**; $F = 70.17$; $P < 0.01$) suggesting PP60-mediated PME activity increase overcomes inhibition by exogenous PMEI. Interestingly, 50 µg/mL PP60 addition inhibited iPMEIox root growth compared to control and 30 µg/mL PP60 (**Fig. 4.17 A, B**). This reduction in root elongation could be seen in wild-type plants too, indicating higher PP60 concentration phenotypes may be caused by plant stress responses due to PP60 toxicity and PME activity changes. It could be seen that iPMEIox seedlings grown on PP60 had less wavy phenotype compared to control (**Fig. 4.17 A**). Therefore, root tip measurements were performed and it has been found that indeed PP60 treatment reduced root tip turning by approx. 25% (**Fig. 4.17 C**).

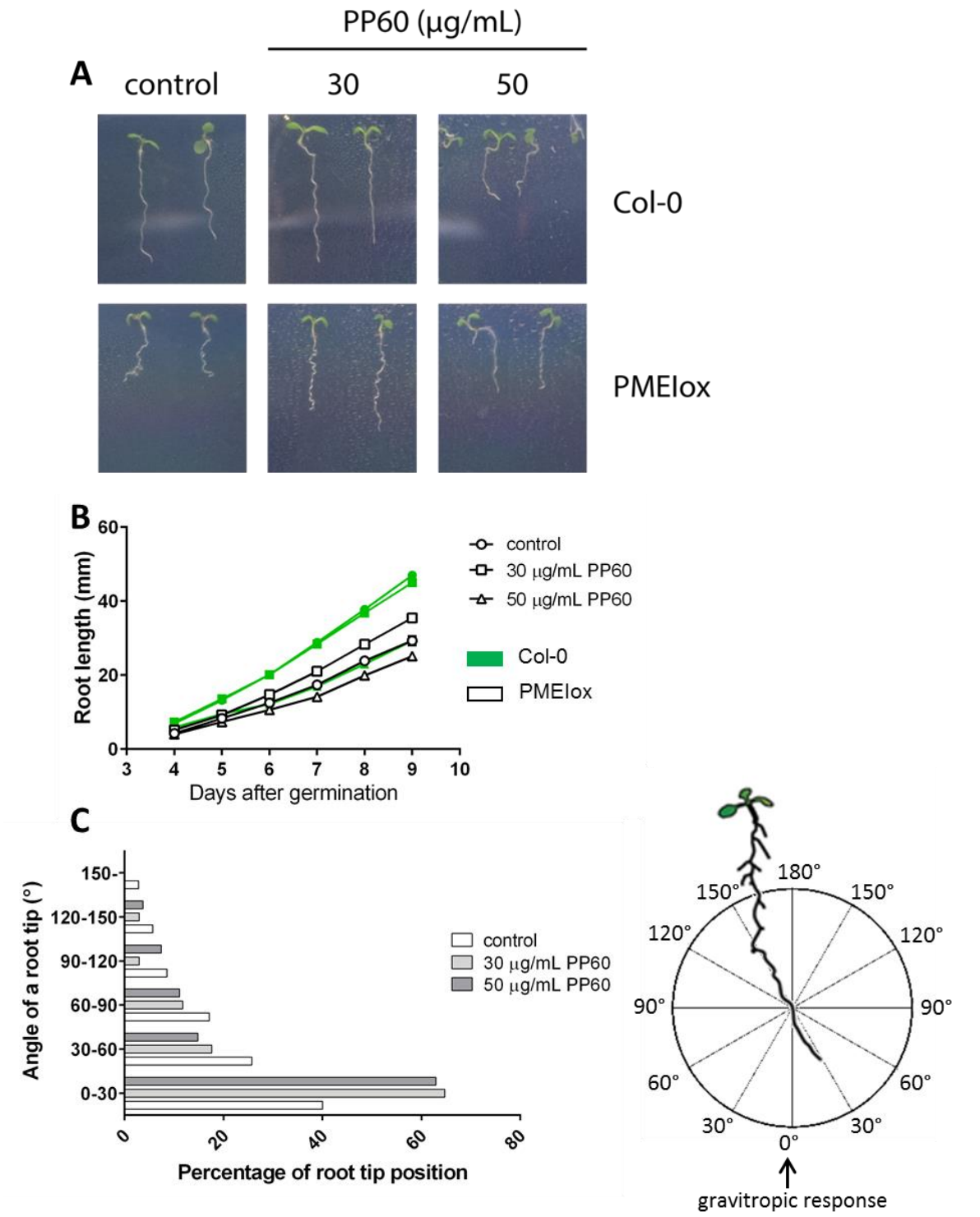

Figure 4.17. Responses of inducible PMEI5 overexpression line (iPMEIox) primary root growth to treatment with polyphenon 60 (PP60) at pH 5.7. 7-days old seedlings grown on 30 and 50 µg/mL PP60 concentration (A). Average root lengths from 4 to 9 days of growing on 0.5 MS media supplemented with different [PP60] (B) from two independent experiments with three biological repeats (each n>20) are illustrated. Root tip position was measured at 7 days for iPMEIox seedlings (C). Statistical analysis was determined by two-way ANOVA with Tukey's multiple comparisons test. Scale bar 10 mm.

4.2.6 Biophysical approach to determine cell wall rigidity

The effects on cell elongation shown above may be due to increased cell wall rigidity or inhibition of loosening of cells caused by the presence of PP60, preventing them from expansion. To investigate the changes in cell wall strength, Atomic Force Microscopy (AFM) was used on living *Arabidopsis* roots after PP60 treatment. AFM was successfully used in studies regarding the relationship between auxin and pectin on shoot apex development in *Arabidopsis* previously (Peaucelle et al., 2011a). To be able to take proper measurements, the tissue must be fixed on a microscope slide. The work on roots seems to be more difficult due to higher sensitivity of cells to mechanical stress thus finding a way to fix them on the microscopic slide is challenging. First, 1% agarose was used as a fixing agent (**Fig. 4.18 A**) and roots were subjected to AFM analysis. The deflection images obtained by this method were disrupted (**Fig. 4.18 B**) and could not be further analysed. The difficulty in this approach was due to the agarose which often covered the examined tissue. A new approach had to be found and a double-sided tape was used (**Fig. 4.18 C**). In this case any disruption on the surface of examined tissue was eliminated. The full deflection images could be obtained (**Fig. 4.18 D**) but there were relatively high differences between measurements. What could be observed under the microscope was that the top part of root was not fixed to the tape and the AFM moving cantilever caused the root to shake. This created disruptions in the deflection maps and inability to read them. To overcome this difficulty, the roots were gently pushed to the slide with a silicon stamp (**Fig. 4.18 E**). Unfortunately, this approach did not fully eliminate the previous problem and additionally, if the stamp was pushed too strongly it caused mechanical damage to cells. The proper deflection maps could not be obtained again (**Fig. 4.18 F**). The biophysical approach to study cell wall rigidity by AFM is very attractive and new methods to overcome the problems should be sought.

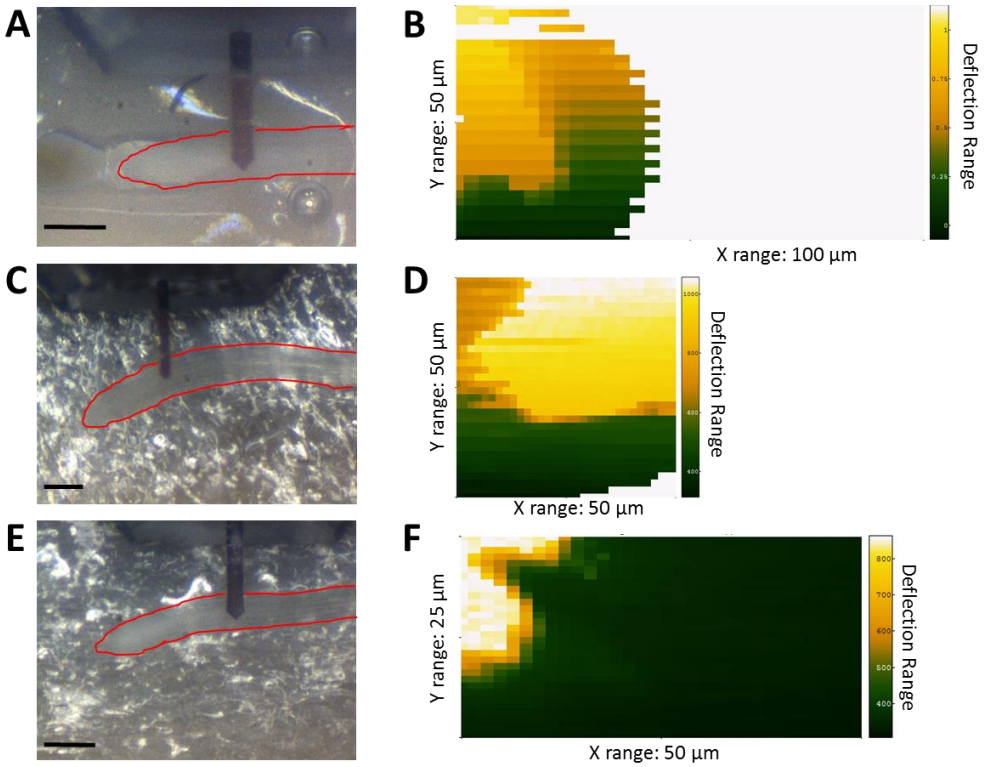

Figure 4.18. Atomic Force Microscopy of PP60-treated roots. AFM was used to determine cell wall rigidity after PP60 treatment. 1% agarose (A), a double-tape (C), and the double-tape with a silicon stamp (E) were used as root glue agents. Red lines indicate root position. (B, D, F) The deflection maps for each glue agent respectively. The brighter colour on the map means higher deflection of the cantilever. Scale bar 200 µm.

4.2.7 Towards understanding the relation between abiotic stress and PME activity

As shown at the beginning of this chapter PP60 seems to have different effects on root development depending on the pH of the media. A summary of genes found to display differential expression in response to transfer of *Arabidopsis* seedlings from a growth media of pH 6.0 to one of pH 4.5 has been created (Lager et al., 2010). Analysis of these genes and quantitative trait locus (QTL) analysis, identified *PME12* as one of the candidate genes for tolerance to acidity. *PME12* had the highest expression of 2.15-fold after 1 hour of exposure to acidity but was downregulated after 8 h (Shavrukov and Hirai, 2016). Moreover, increased PME activity is believed to be induced due to biotic and abiotic stresses to protect plants by strengthening cell walls. To investigate if PME activity increase caused by PP60 might reduce the effect of acidic stress, *Arabidopsis* seedlings were grown on pH 4.5 media together with PP60. As shown in **Figure 4.19 A, B** primary root elongation was reduced in a dose-dependent manner (similarly as in pH 5.7 conditions), where 30 µg/mL PP60 decreased the elongation by nearly 40% and 50 µg/mL PP60 by 80% compared to control conditions after 9 days (**Fig. 4.19 B**). Further, the examination of root hairs showed an increase in root hair length after addition of PP60 (**Fig. 4.19 C**).

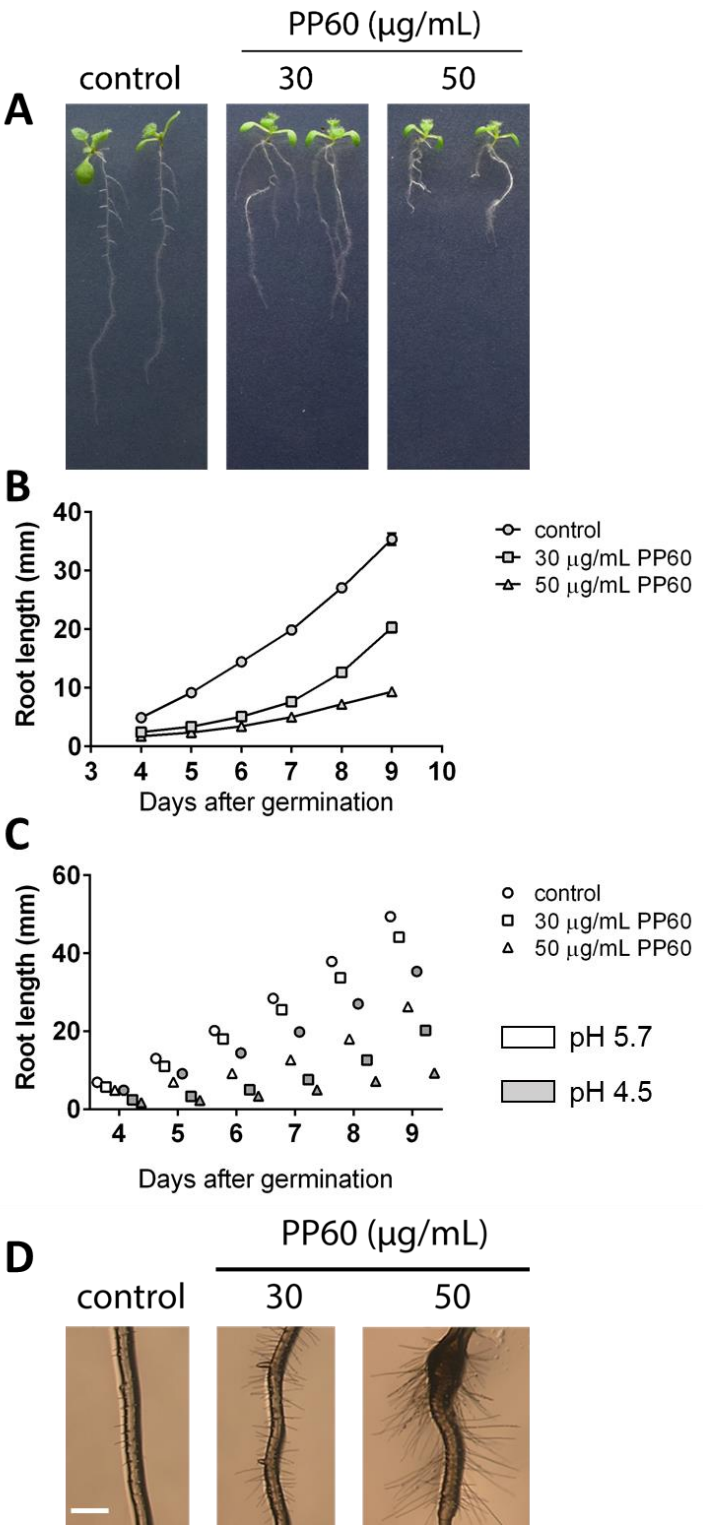

Figure 4.19. *Arabidopsis* root development after treatment with polyphenon 60 (PP60) at pH 4.5. 10-days old seedlings grown on 30 and 50 µg/mL PP60 concentration [PP60] (A) Scale bar 10 mm. Average root lengths from 4 to 9 days of growing on 0.5 MS media supplemented with different [PP60] (B) from one independent experiment with three biological replicates (each n>20) are illustrated. Root hairs phenotype on pH 4.5 media with PP60 (C). Scale bar 300 µm. Statistical analysis was determined by two-way ANOVA with Sidak's multiple comparisons test.

The pattern of pH 4.5 and PP60 effect on root development was similar to observations at pH 5.7. Interestingly, when plants were grown on pH 4.5 together with PP60 for a longer period of time they showed increased resistance to acidic stress. The control

plants grown only on pH 4.5 media presented poor root and rosette development with pale leaves, but when subjected to PP60 treatment, seedlings kept growing without symptoms of stress (**Fig. 4.20 A**). Furthermore, the measurement of total chlorophyll showed high increase in PP60-treated plants suggesting they maintained high level of photosynthesis (**Fig. 4.20 B**).

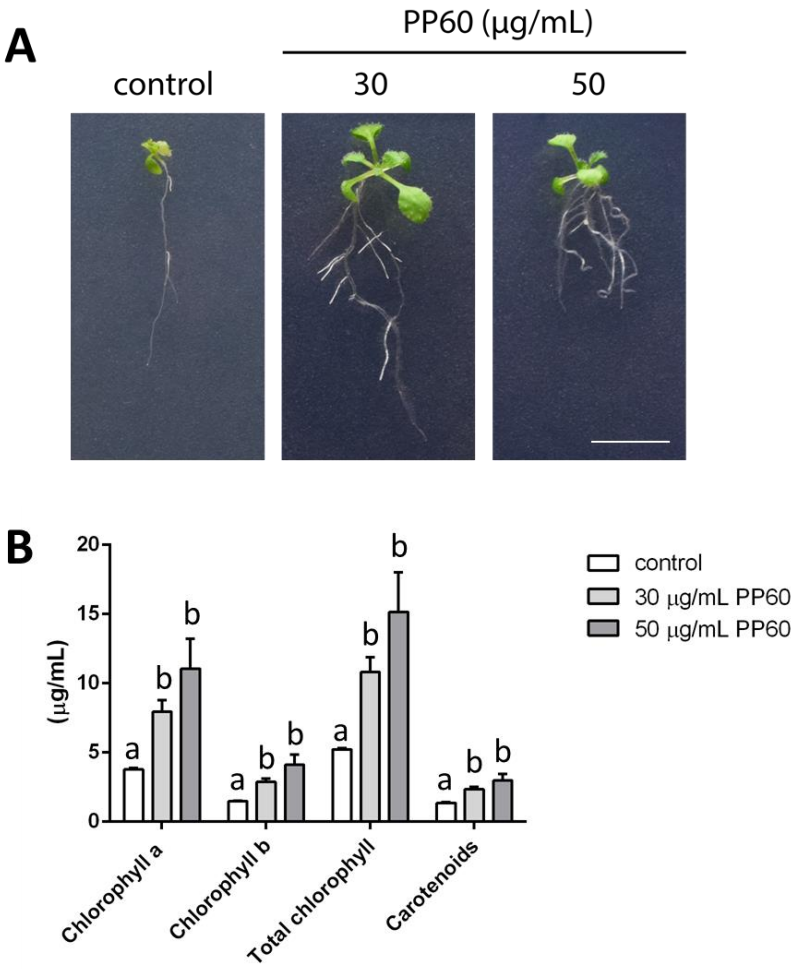

Figure 4.20. 16-days old *Arabidopsis* seedlings after treatment with polyphenon 60 (PP60) at pH 4.5. 16-days old seedlings grown on 30 and 50 µg/mL PP60 concentration [PP60] (A). Scale bar 10 mm. Chlorophyll and carotenoids measurements of 16-days old Arabidopsis rosettes (B) from one independent experiment with three biological replicates (each n=3). Statistical analysis was determined by one-way ANOVA with Tukey's multiple comparisons tests.

4.3 Discussion

Pectin methylesterases (PMEs) and their proteinous inhibitors (PMEIs) are involved in the regulation of many processes in plant development, ranging from tissue growth to fruit ripening. Therefore, the control of PME activity is critical for understanding of plant physiological processes and regulation. It has been shown that the green tea catechin extract, called Polyphenon-60 (PP60) inhibits citrus and tomato PMEs *in vitro* (Lewis et al., 2008b). Recently, it has been observed that PP60 and EGCG catechin are effective inhibitors of *Arabidopsis* PME31 *in vitro* (L'Enfant et al., 2015). The knowledge about PME function and activity in *Arabidopsis* root growth and development is still limited. This chapter provided some advancements in the knowledge of PME involvement in root development and the key results are summarized in **Table 4.3**. More details and discussion is presented below.

PME3 is involved in adventitious roots formation and *PME17* is expressed in primary root and root hairs (Guenin et al., 2011, Sénéchal et al., 2014). The *pme17* knockout line showed upregulation of several genes implicated in HG modification therefore redundancy of other PME isoforms could mask the phenotype (Sénéchal et al., 2014). It has been reported that root PME activity is inhibited by PP60 *in vitro* but interestingly, when the PME activity was measured *in vivo* after PP60 treatment, it slightly increased. Furthermore, the PME genes transcription was altered with same of the isoforms (*PME5*, *PME12*, *PME15*, *PME25*, *PME41*, and *PME44*) being overexpressed during PP60 treatment. PME5 has been shown to be involved in phyllotaxis and meristem primordia formation in elongating *Arabidopsis* stem (Peaucelle et al., 2011b, Peaucelle et al., 2008b). Studies showed that *PME12* was upregulated in response to pathogens and MAMPs. Moreover, the knockout *pme12* line had increased pathogen-induced PME activity (Bethke et al., 2013). The expression of *PME25* and *PME44* has been found to be suppressed by pathogens (Bethke et al., 2013). The *PME41* expression has been shown to be increased after chilling stress in wild type plants and it is believed brassinosteroids (BRs) may modulate total PME activity under chilling stress by regulating *PME41* expression (Qu et al., 2011). Taking together the information about overexpressed PMEs and thus increased PME activity after PP60 treatment suggest PP60 treatment and following PME activity increase might increase resistance of plant roots to pathogen attack and abiotic stress.

The increase in PME activity after PP60 addition could be an effect of initial PME inhibition, and further plant response to increase PME genes expression to overcome this effect. The PME activity time-course experiment showed some fluctuations in activity during the first 9 hours of treatment. This could be caused by the transfer of plants to the fresh media with PP60 and adaptation to a new environment. A similar effect was observed in

seedlings treated with the isoxaben cellulose biosynthesis inhibitor where an initial increase in sucrose content was observed at the start of the treatment (Wormit et al., 2012). Therefore, it is probable that PME activity is initially inhibited by PP60 and then the seedlings response is to increase PMEs expression and activity to overcome the inhibitory effect. The time-course experiment needs more independent repeats to confirm this hypothesis.

Table 4.3 The summary of the key results presented in chapter 4.

	Treatment		
	PP60	**pH 8.0**	**pH 8.0 + PP60**
PME activity	*in vitro* – decrease *in vivo* – increase	*in vitro* – increase *in vivo* - increase	*in vitro* – decrease *in vivo* – variable
PME genes expression	6 PME genes upregulated 2 PMEI genes upregulated, 2 downregulated	7 PME genes upregulated 3 PMEI genes upregulated, 3 downregulated	1 PME gene upregulated 3 PMEI genes upregulated
PG activity	increase	no difference	decrease
Primary root length	decrease	decrease	decrease with high concentrations
Root hairs development	density – increase length – increase with high concentrations	density – no difference length – decrease	density – decrease length – decrease with high concentrations
Lateral root development	density – decrease length – decrease number of lateral root primordia - increase	density – increase length – decrease	density – decrease length – decrease
Cell elongation and division	decrease cell division - lower	decrease	no difference

The PME activity optimal environment is at pH 7.5. It has been shown that PME35 isolated from inflorescence stem had the highest activity at pH 8.0 (Hongo et al., 2012). *In vitro* analysis showed a gradual PME activity decrease after PP60 addition at pH 8.0 but it was still higher when compared to pH 5.7. It has been observed that plants grown on pH 8.0 overexpressed 7 PME isoforms. When the media was supplemented with PP60 there were no PMEs expression changes compared to untreated conditions but instead some of PMEI isoforms were overexpressed. The PME activity measurements showed either upregulation or no changes in four experimental repeats. It is speculated that PME activity was higher at pH 8.0 compared to pH 5.7 as shown in *in vitro* and two *in vivo* PME activity experiments. The variation in PME activity could be caused by influence of PP60-induced overexpression of some PMEI isoforms at pH 8.0. It is possible that different PMEIs have different PME binding specificities. When the medium was alkalinized to pH 8.0 root hair growth was inhibited and this restriction was further enhanced by addition of PP60. This effect could be caused by (1) increase in PME activity and stiffness of cell wall and (2) inhibition of acidic growth by high apoplastic pH.

PGs are enzymes that hydrolyse deesterified HG backbones which mean they depend on PME activity. In *Arabidopsis*, the mutations in QUARTET1 (QRT1), a PME, and QUARTET3 (QRT3), a polygalacturonase (PG) resulted in the failure of tetraspore

separation (Francis et al., 2006). This implies that both PME and PG activity are necessary to separate the tetrads: PME removes the methyl groups from HG backbone and PG breaks down the pectin. This correlation was observed in extracts from roots with PP60 treatment. The higher PME activity correlated with the higher PG activity. The increased PG activity produces short oligogalacturonides (OGAs) which act as signalling molecules in pathogen response. Therefore, increased expression of PME isoforms involved in pathogen response results in increased PME activity and PG activity which further activates proteins involved in plant immunity.

Removal of methylesters from a HG chain by PME creates negatively charged regions of the backbone. Blockwise demethylesterification favours crosslinking of chains via calcium ions. The increase in PME activity resulting from PP60 treatment caused a reduction in growth and development of the root system in a concentration-dependent manner. The shorter roots of PP60-treated seedlings were due to shorter epidermal cells, meristem size and the arrest of cell division. It has been previously shown that expression of PME1 from *Aspergillus aculeatus* in *Arabidopsis* caused higher demethylesterification of HG in hypocotyls which reduced their growth (Derbyshire et al., 2007). It was speculated the *PME1* expression might have resulted in random demethylesterification and affected wall loosening properties more through a reduction in pore space, possibly caused by repulsion of negative charges, leading to swelling of the pectin network and filling of the available spaces with cellulose-xyloglucan substrates (MacDougall et al., 2001). Similarly, inhibition of root elongation in PP60-treated seedlings may be due to increase in PME activity subsequently causing crosslinking of the pectin network and stiffening of walls. Moreover, reduced porosity may limit accessibility of wall loosening proteins to their substrates. Transformation of *Arabidopsis* plants with *Aspergillus* PME1 under the control of a constitutive promoter yielded no transformants and therefore is probably lethal (Derbyshire et al., 2007). Thus high levels of PME are likely to be lethal and the growth arrest of PP60 high concentration-treated seedlings might be the result of it.

It has been shown that EGCG has an inhibitory effect on root PMEs *in vitro* and EGCG-treated plants showed reduced root elongation and a root waving phenotype (Lewis et al., 2008b, Wolf et al., 2012). Similarly, plants overexpressing PMEI (iPMEIox) shared the phenotype of EGCG-treated seedlings (Wolf et al., 2012). Here it has been reported that EGCG promotes root growth at low concentrations and slightly inhibits at higher concentrations. To establish if these changes were due to an increase or decrease in PME activity, the PME activity of EGCG-treated roots needs to be measured. Interestingly, it has been shown that the introduction of *Stevia rebaudiana's* UDP-glycosyltransferase gene *UGT74G1* to *Arabidopsis* caused increase in catechin accumulation. This resulted in a considerable increase in shoot and root length and rosette area (Guleria and Yadav, 2014). Therefore, the catechin accumulation in moderate concentrations may have a positive

influence on plant development. When the iPMEIox plants were treated with PP60 their phenotype was reversed to that of untreated plants. It could be explained by a PP60-induced increase in PME activity which overcomes inhibitory effect of PMEI. This suggests that PP60-induced root phenotypes are due to an increase in PME activity.

It is known that elongating and expanding plant cells undergo wall extension in acidic apoplastic conditions. Disruption of the pectin network may be one of the primary targets for protons derived from acidic soil/media. The conformation for this hypothesis lies in the experiments where addition of Ca^{2+}, which crosslinks the HG chains and boron, which crosslinks RGII molecules, ameliorated the effect of low pH damage (Koyama et al., 2001). Therefore, higher PME activity should increase crosslinks between HG chains and reduce the effect of acidic pH. The effect of growth on pH 4.5 was reduced in the presence of PP60. It has been reported that *Arabidopsis* plants grown in MS medium at low pH had increased sugar production in shoots and sugar transport into roots (Ralet et al., 2012). The exposure of plants to strong acidic conditions has an impact on root cell structure and function. The observations of *Arabidopsis* grown on acidic pH showed reduced root elongation, swollen root hairs and cracks between cells in the root meristem (Ralet et al., 2012, Williams and Benen, 2002). A high concentration of protons responsible for strong acidity stress leads to the gradual shutdown of plasma membrane H^+-ATPase activity in root cells resulting in cessation of plant growth and stagnation (Cameron et al., 2008). The results presented here confirmed reduced root development when grown on more acidic pH 4.5 compared to pH 5.7. It has been shown that several pectin methylesterase genes were found responsive to treatment at pH 4.5 in *Arabidopsis*. These genes were rapidly induced after 1 hour, while after 8 hours the picture reversed with the majority of the cell wall modification genes being repressed (Lager et al., 2010). Overall, this indicated an importance of wall-strength maintenance and suggested a separation between the short- and long-term modifications needed for plant roots to acclimate to a decrease in apoplastic pH. Here it has been shown that *Arabidopsis* seedlings grown on pH 4.5 together with PP60 had initially short roots, but when grown for a longer period of time they seemed to overcome acidic stress and grow better than control plants. As PP60 increased expression of PME genes thus enhancing PME activity, it is probable that the long-term response is changed in plants grown on pH 4.5 with PP60. The expression of PME could be maintained at the high level together with their activity causing higher homogalacturonan demethylesterification. It is known that changes in wall pH may also lead to changes in the activity of wall proteins such as expansins, which can loosen cell walls by affecting hydrogen bonding between load-bearing wall polymers. Therefore, the increase in cell wall ability to expand caused by low pH may be balanced by the addition of PP60 and elevated PME activity.

5. Auxin and brassinosteroid regulation of PME activity

5.1 Introduction

5.1.1 Auxin

Plant growth depends on the production and activity of many phytohormones which regulate all aspects of plant growth and development. Auxin regulates much of division, expansion and differentiation in conjunction with other phytohormones. Auxin is synthesized in source tissues from indole through tryptophan-dependent or –independent pathways (Zhao, 2014). It is involved in mechanisms regulating cell wall modifications and development. Auxin influences the expression and activity of cell wall modifying enzymes. Auxin lowers pH in the apoplast by activating plasma membrane proton pumps which then activate expansins causing the cell wall relaxation (McQueen-Mason et al., 1992). Recently, it has been shown that auxin regulates new organs formation by influencing the demethylesterification of HG (Braybrook and Peaucelle, 2013). This study showed that local application of IAA to a shoot apex led to demethylesterification of pectin and tissue softening, which affected organ formation. Additionally, it has been shown that the AUXIN BINDING PROTEIN 1 (ABP1) influences the expression of genes involved in remodelling xyloglucan side chain structure (Paque et al., 2014). The source organs of auxin are distinct from those tissues in which they regulate growth and development, i.e. auxin produced in shoot has been demonstrated to promote lateral root emergence (Casimiro et al., 2001) thus it could be that PP60 affects auxin transport within the root, which influences PME activity.

At the molecular level, auxin regulates transcription of numerous genes. Transcriptional regulation of auxin-regulated genes is dependent on two related families of transcriptional regulators, AUXIN RESPONSE FACTORs (ARFs) and AUXIN/INDOLE-3-ACETIC ACIDs (Aux/IAAs). The ARF proteins are encoded by a large gene family consisting 23 members in *Arabidopsis*. ARFs bind to the auxin responsive elements (AuxREs) in the promoter region of auxin responsive genes and activate or repress their transcription (Guilfoyle and Hagen, 2007). Auxin activates ARFs by triggering degradation of the Aux/IAA family transcriptional repressor proteins (**Fig. 5.1**). The biological function of two ARFs has been well characterized. ARF7 increased the expression of a brassinosteroid (BR) biosynthetic gene, *DWF4* and it was not regulated by auxin treatment (Chung et al., 2011). Additionally, the *arf7* mutant showed up-regulation of *BAS1* (Youn et al., 2016), with

BAS1 inactivating biologically active BRs. This indicated that *BAS1* expression is inhibited by ARF7 and thereby contributes to the increase in the endogenous level of castasterone, a biologically active BR. The *arf7* mutant possessed a low level of endogenous active BR and it showed reduced primary root length compared to wild-type plants. It has been observed that ARF7 and ARF19 are the key components in a developmental pathway regulating lateral root formation (Okushima et al., 2007). *ARF19* is expressed in vascular tissue, the meristematic region, sites of newly forming lateral roots, root hairs and the root cap, whereas the *ARF7* expression is restricted to the vascular tissues and early stages of lateral root primordia. The microarray data identified that auxin-induced gene expression is globally and severely impaired in the *arf7/19* double mutant (Okushima et al., 2005). Among the targets of ARF7 and ARF19 are *LATERAL ORGAN BOUNDARIES-DOMAIN (LBD)/ASYMMETRIC LEAVES2-like (ASL)* genes LBD16/ASL18 and LBD29/ASL16, which encode nuclear proteins that are important for lateral root initiation (Okushima et al., 2007).

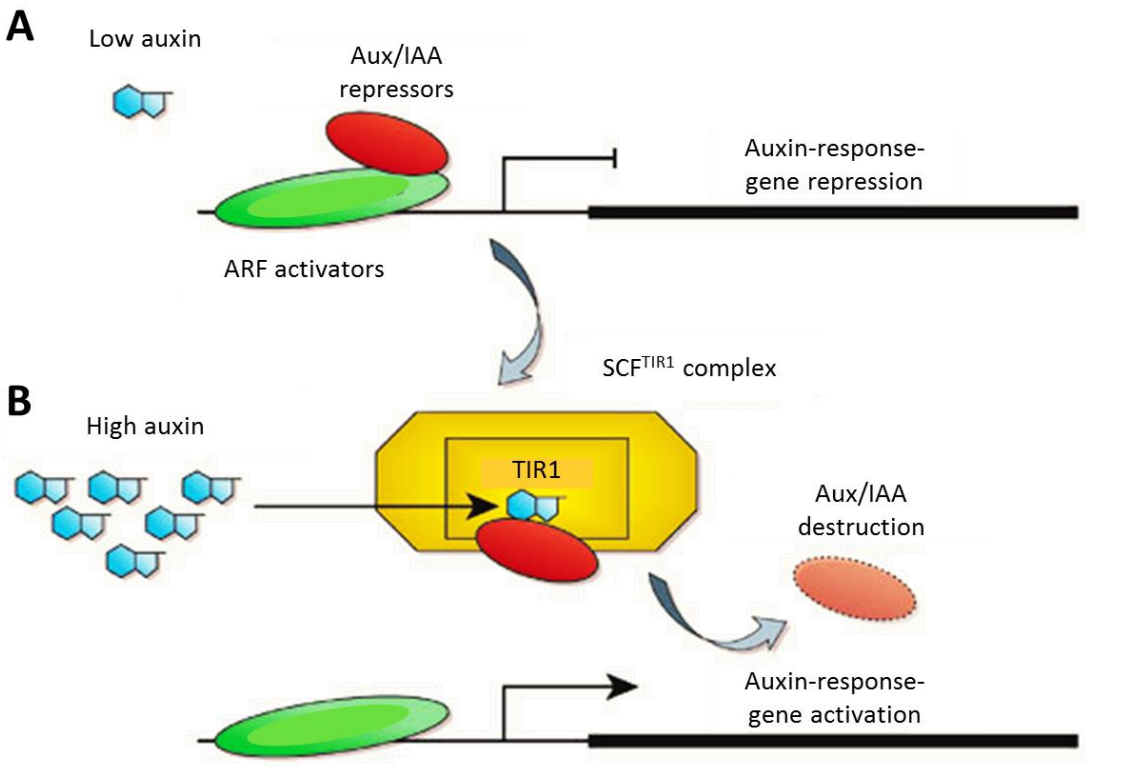

Figure 5.1. ARFs bind to auxin-response elements in promoters of auxin-response genes. (A) When there is a low auxin concentration, Aux/IAA repressors binds to ARF activators and repress the expression of the genes. (B) When there is a high auxin concentration, auxin binds to the transport inhibitor response 1 (TIR1) receptor in the Skp1–Cul1–F-box-protein (SCF^{TIR1}) complex leading to the attachment of the Aux/IAA repressor to the TIR1. Next, the repressor enters a pathway which leads to the Aux/IAA destruction and activation of auxin-response gene. Adapted from Guilfoyle, 2007.

There are other ARFs shown to be involved in root development. ARF5 has been shown to be involved in postembryonic lateral root formation (De Smet et al., 2010a). The

loss of function *arf5* mutant displayed lateral root defects including a severe reduction in emerged lateral root numbers and clustering of primordia. The *arf10/arf16* double mutants produced more lateral roots, whereas the *arf10* or *arf16* single mutants showed no root phenotypes. Moreover, the *arf10/arf16* knockout mutants displayed a root tip defect with uncontrolled cell division and blocked cell differentiation together with loss of gravity-sensing (Wang et al., 2005).

Auxin is involved in another important root developmental process – bending. The low auxin level in the elongation zone allows cell elongation while auxin inhibition of cell elongation mediates gravitropic root bending. The gravitropic response is regulated and coordinated with other tropisms, such as phototropism and hydrotropism to control plant growth and development. The root columella cells are the key sites of gravity sensing, while root bending occurs in the elongation zones. The columella cells contain densely packed starch in an organelle called amyloplast. Amyloplasts settle to the bottom of the cells relative to gravity, which results in a symmetrical distribution of auxin. Upon gravistimulation by reorientation, amyloplasts settle at a new position. This leads to an unequal distribution of auxin where high concentrations of auxin reduce cell growth, resulting in growth-mediated bending of the root in the direction of the new gravity vector. The coordinated and polarized auxin transport by auxin carriers in roots is altered by the columella cells. During normal growth, the columella redirects auxin symmetrically on all sides of the root. After the root is turned on its side, the columella senses the change in the orientation and redirects the flow of auxin asymmetrically to the new lower side of the root (**Fig. 5.2**; Baldwin et al., 2013). The cells on the lower side of the root have to decrease their elongation relative to the cells on the upper side. It is possible that the PME and/or PMEI activity together with regulation by auxin flow differentially regulate cell wall expansion in different regions of the root.

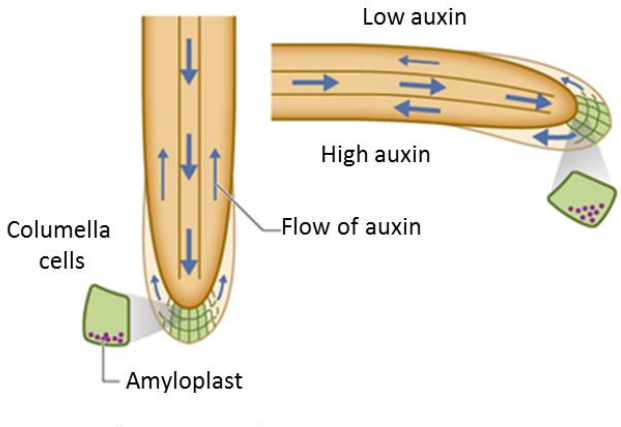

Figure 5.2. The auxin flow regulates root bending.

5.1.2 Brassinosteroids

Brassinosteroids are perceived by BRI1 which activates the transcription factors BZR1 and 2 (also known as BES1) through inhibition of the GSK3-like kinase BIN2. The transcription of BR biosynthesis genes such as *DWF4* or *CPD* is inhibited by BZR1 thus the BR signalling module constitutes a negative feedback loop (**Fig. 5.3**; Zhu et al., 2013).

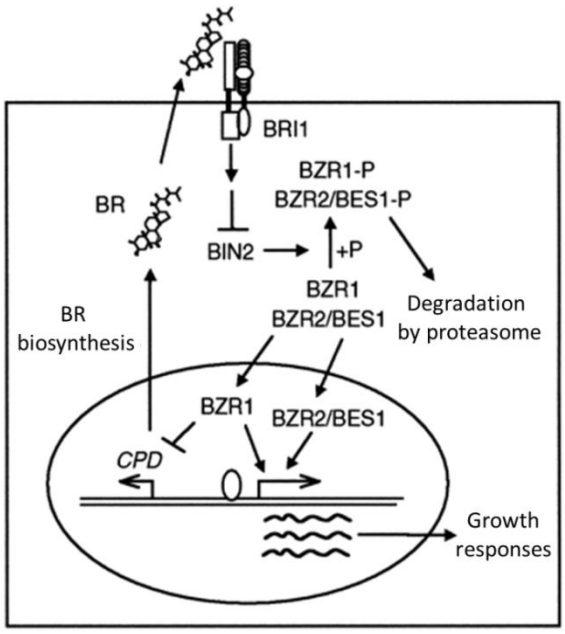

Figure 5.3. The BR signal transduction pathways. In the absence of BR, BRI1 remains inactive, and BIN2 phosphorylates BZR1/2 and targets them for degradation. Binding of BR to the cell-surface receptor BRI1 activates BRI1 kinase and leads to inhibition of the BIN2 allowing the accumulation of BZR1/2 proteins in the nucleus. BZR1 supresses BR biosynthetic genes such as CPD. BZR2 activates BR-induced genes and growth responses. Adapted from He et al., 2002.

The high BRI1 expression in root hair cells drove cell elongation, whereas its higher expression in non-hair cells inhibited root cell elongation (Fridman et al., 2014). This inhibition of cell elongation was due to enhanced sensitivity to the hormone and activation of ethylene biosynthesis genes. Recent studies showed that BR at different concentrations can have opposite effects on root meristem size by promoting both cell-cycle progression and cell differentiation. It has been shown that synthetic brassinosteroid, 2,4-epibrassinolide (eBL), and chilling stress induced significant increases in PME activity in *Arabidopsis*. Furthermore, the results suggested that the regulation of PME activity under chilling stress depended on the BR signalling pathway. The effect of chilling stress on PME activity was impaired in the *pme41* mutant and it has been shown that expression of *PME41* was induced by chilling stress in wild type plants but not in *bri1-116*, a BR insensitive null allele of the BR receptor BRI1 (Qu et al., 2011). Inhibition of PME activity triggers upregulation of at least two PME genes: *At3g49220* and *At3g14310* in the growing zone of the root through a BRI1-dependent feedback loop (Wolf et al., 2012). Furthermore, it was shown that there was an elevated PME activity after treatment with eBL and reduced PME activity in a *bri1*

mutant. To explain the results, they proposed a model in which interfering with PME activity either through PMEI overexpression or EGCG treatment would lead to a reduction in the cell wall pectate causing the activation of the BRI1 receptor and the upregulation of wall remodelling proteins including PMEs (**Fig. 5.4**).

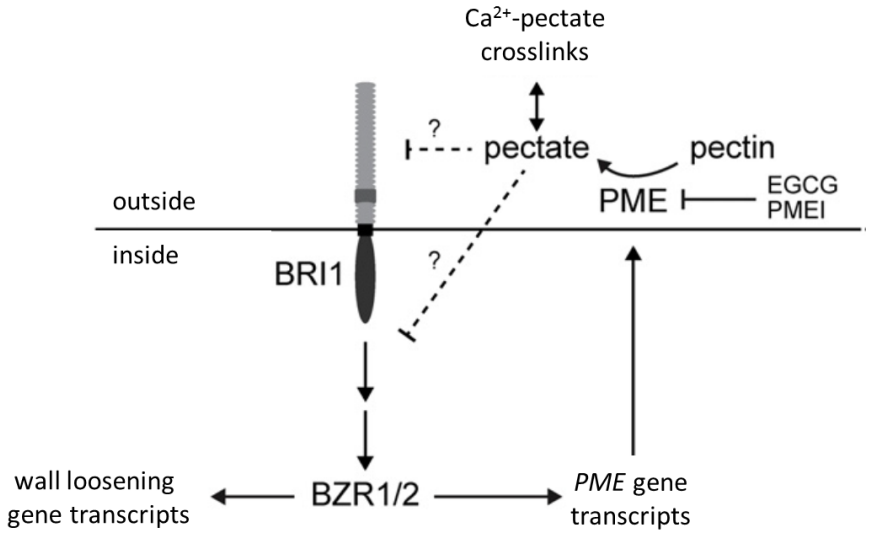

Figure 5.4. Brassinosteroid feedback signalling in plant cell wall homeostasis. Methylesterified pectin in the wall is demethylesterified by wall-bound pectin methylesterases (PMEs), which can be inhibited by endogenous pectin methylesterase inhibitors (PMEIs). The inhibition of PME activity by EGCG or PMEI overexpression causes the activation of the BRI1 receptor and/or a BR signalling component. This in turn leads to the transcription of cell wall-modifying genes including at least two PME genes. Adapted from Wolf, et al. 2012.

5.1.3 Brassinosteroid and auxin dynamics in roots

A high level of BR in the elongation zone is required to promote cell elongation opposite to the situation in the QC and meristem area where a low level of BR is required to maintain stem cell and meristem size. Therefore, the promotive and inhibitory effects of BR must be controlled to maximize root growth. It has been shown that BR and auxin distribute with opposite gradient and interact antagonistically in controlling gene expression, stem cell maintenance, and cell elongation in root tips (Chaiwanon and Wang, 2015). Treatment with a high concentration of exogenous BR was found to accelerate the transition from meristem cell division to cell elongation which caused an initial increase of root growth rate followed by growth inhibition due to reduction of meristem size. Furthermore, the BZR1 transcription factor, promoted expression of target genes in the elongation zone but repressed target genes in the QC and surrounding cells.

The patterning of BR/BZR1 appears to also involve auxin. It has been shown that the BZR1 pattern is overall opposite to that known for auxin. Auxin treatment increased cytoplasmic localization of BZR1 in the elongation zone and the inhibition of auxin

biosynthesis increased the presence of BZR1 in the root tip region, where the endogenous auxin level is at a maximum (Chaiwanon and Wang, 2015). Moreover, the genes that are oppositely regulated by BR and auxin include three out of four PLETHORA factors (PLT1, PLT2, PLT4) which mediate patterning of the *Arabidopsis* root stem niche and whose expression requires auxin but it is repressed in the presence of BR.

Taken together, it seems that PME expression and activity might be regulated by direct or indirect influence of auxin and brassinosteroid. To dissect probable role of auxin on pectin remodelling through PME activity, Col-0 and *arf7/19* double mutant primary root growth was analysed after treatment with 1-Naphthaleneacetic acid (1-NAA) together with PP60. 1-NAA is highly lipophilic therefore enters a cell mainly by diffusion. This characteristic of 1-NAA allows to bypass probable auxin transport disruption in the *arf7/19* mutant. The evidence of brassionosteroid signalling feedback loop in controlling plant cell wall homeostasis highlights its role in regulating PME activity. To study brassionosteroid influence on root development via pectin remodelling, Col-0 and arf7/19 plants were grown on media supplemented with propicozanole (Pcz) – inhibitor of brassenosteroid synthesis – together with PP60. Finally, the dynamics of auxin and brassionosteroid and its probable role in the PME activity modulation was examined using the combination of 1-NAA, Pcz and PP60 on Col-0 and *arf7/19*.

5.2 Results

5.2.1 PP60 treatment rescues the auxin inhibitory effect on root elongation

It has been demonstrated that auxin induces a reduction in cell wall rigidity through demethylesterification of pectin HG (Braybrook and Peaucelle, 2013). It is still unknown if auxin directly influences any of the PME or PMEI isoforms. Interestingly, *PME25* expression is repressed in the *arf7/19* double mutant (Okushima et al., 2005). Here, it has been shown that *PME25* is expressed in roots and is overexpressed after PP60 treatment (**Table 3.1**; **Table 4.1**). As the methylesterification state of HG is regulated by the activity of PMEs/PMEIs enzymes and possibly auxin signalling, the influence of PP60 on primary root development in *arf7/19* double mutant has been examined. Auxin signalling is impaired in the *arf7/19* double mutant causing partial agravitropism (**Fig. 5.5**) possibly due to reduced PME and/or PMEIs activity. The results showed that after PP60 addition the root length of *arf7/19* was reduced similarly to that of Col-0 (**Fig. 5.5**).

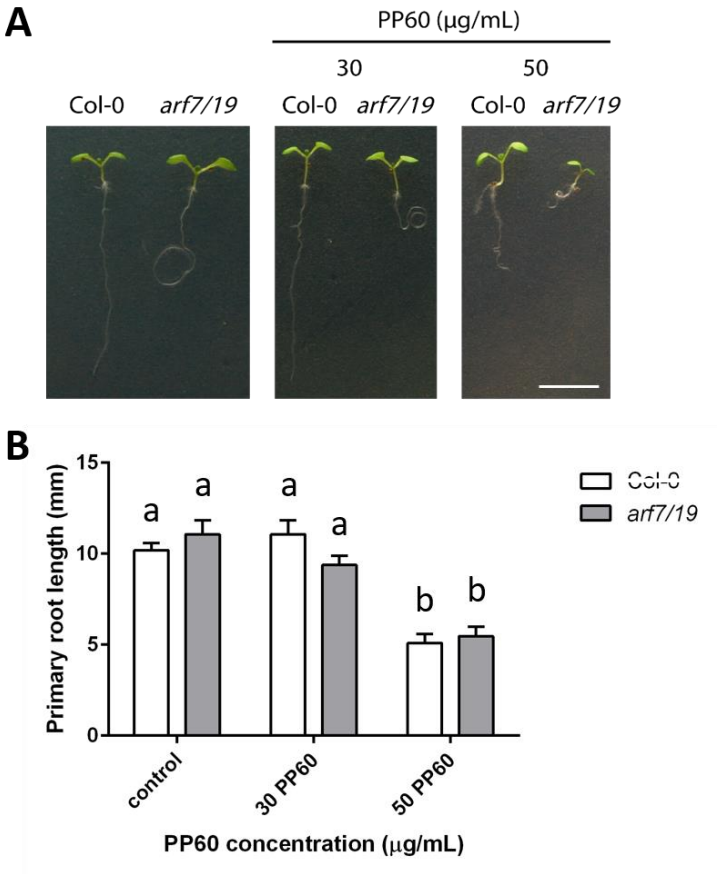

Figure 5.5. Responses of *arf7/19* seedlings to polyphenon-60 treatments. (A) The picture of 7 days old seedlings grown on 0.5MS media without and with 30 and 50 µg/mL of PP60. Scale bar 5 mm. (B) Primary root length of 5 days old seedlings grown on 0.5MS and supplemented with PP60 from two independent experiments with three biological repeats (each n>20). Statistical analysis was determined by one-way ANOVA with Tukey's multiple comparisons tests.

To study possible PME activity alteration caused by auxin, *Arabidopsis* wild type Col-0 and *arf7/19* plants were treated with low 1-NAA concentration of $3x10^{-8}$ M (called here L 1-NAA) and PP60 concentrations of 30 and 50 µg/mL for 9 days. Primary roots showed a slight reduction in growth at 8 and 9th days after germination with the L 1-NAA treatment comparing to a mock control in wild type plants (**Fig. 5.6 A, C**). Additionally, L 1-NAA caused an increase in lateral root density (**Fig. 5.6 A**). In the case of the *arf7/19* mutant, the reduction in root length was higher than in control plants; however, root growth was almost restored to that of control plants at the later days (**Fig. 5.6 B, D**). Evaluation of the PP60 effect together with L 1-NAA on primary root length showed a PP60-dose-dependent reduction of primary root growth in Col-0 (**Fig. 5.6 A, C**) compared to treatment with PP60 only (see results in **chapter 4.3.3.1**). Addition of L 1-NAA and 50 µg/mL PP60 caused reduction in agravitropic response in *arf7/19* mutant but had no influence on root length (**Fig. 5.6 B, D**). In conclusion, the L 1-NAA addition had no additional effect to that of PP60 in Col-0 plants, but changed root phenotype in *arf7/19* after 50 µg/mL PP60 treatment.

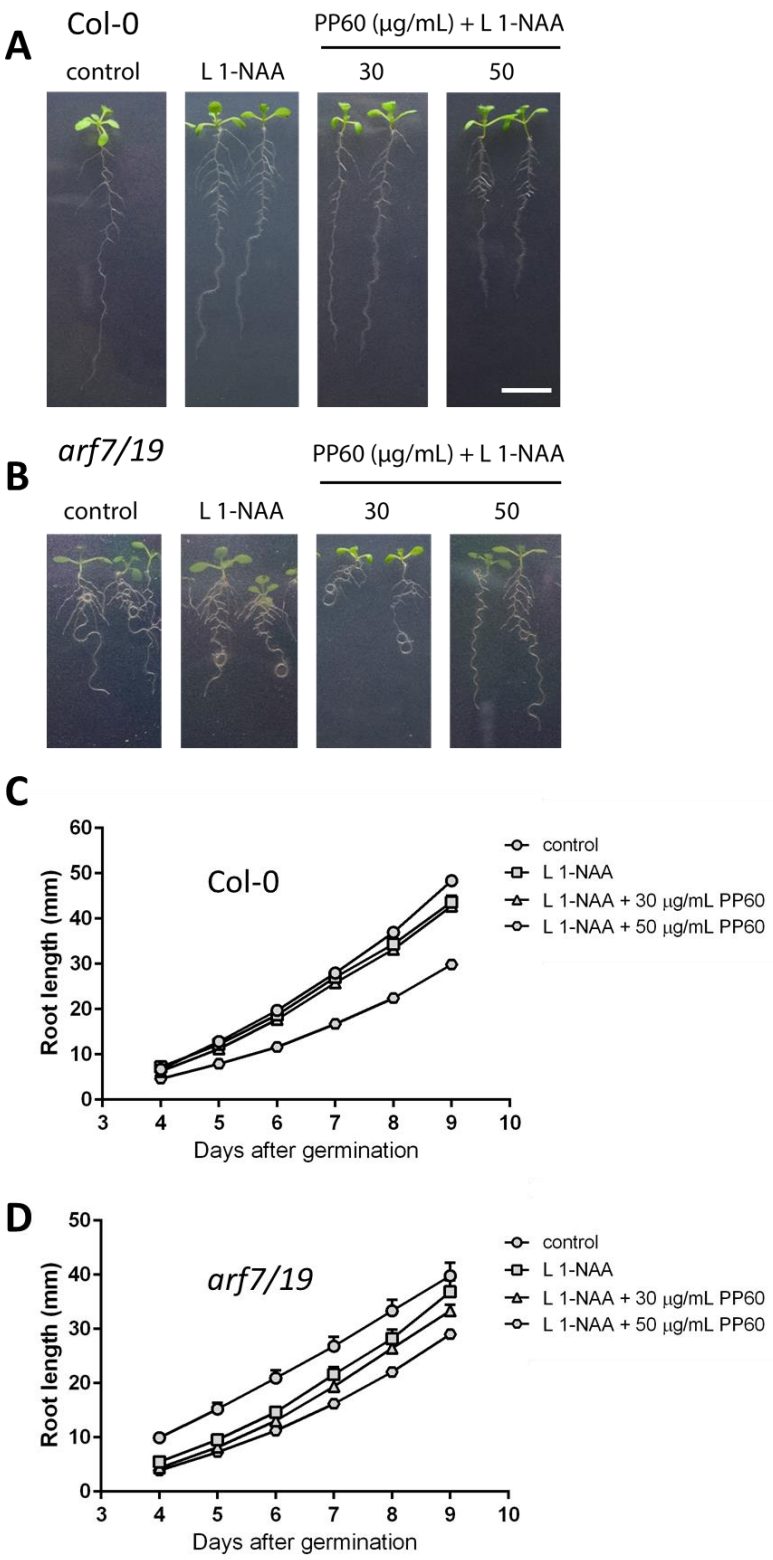

Figure 5.6. Responses of *Arabidopsis* Col-0 and *arf7/19* primary root to treatment with polyphenon 60 (PP60) and 1-naphthaleneacetic acid concentration (L 1-NAA). 10-days old Col-0 (A) and *arf7/19* (B) seedlings grown on $3x10^{-8}$ M 1-NAA (L 1-NAA) together with different PP60 concentrations. Average root lengths from 4 to 9 days of Col-0 (C) and *arf7/19* (D) growing on 0.5 MS media supplemented with L 1-NAA and PP60 from two independent experiments with one biological repeat are illustrated (n>30). Statistical analysis was determined by two-way ANOVA with Tukey's multiple comparisons test. Scale bar 10 mm.

To see whether exogenous auxin could affect PME and PMEI expression and therefore chemical properties of pectin in roots, PME and PG activities were measured from Col-0 plants grown on media with L 1-NAA. Both, gel diffusion and calorimetric assays of PME activity showed no difference between L 1-NAA treated plants and mock control (**Fig. 5.7 A, B**). Similarly, PG activity showed no change after L 1-NAA treatment compared to mock control (**Fig. 5.7 C**).

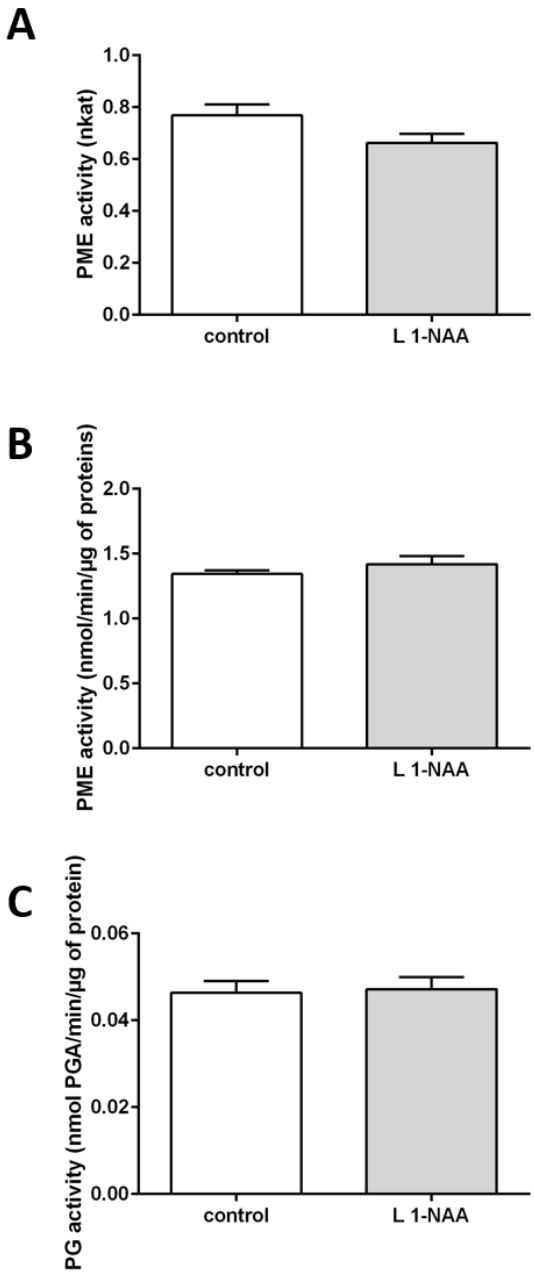

Figure 5.7. PME and PG activity were not affected by L 1-NAA treatment. Total PME and PG activities were determined after L 1-NAA treatment in two independent experiments which showed similar results. Representative results from one experiment are shown. Root tissue was harvested from 6 days old seedlings. PME activity was measured using gel diffusion assay (A) and calorimetric method (B). PG activity was measured using calorimetric method (C). Error bars represent standard error of three technical repeats among treatments. Statistical analysis was determined by one-way ANOVA.

Exogenous auxin at high concentrations has been shown to decrease primary root elongation (Rahman et al., 2007). To test whether root growth inhibition is caused by changes in PME activity, *Arabidopsis* wild type Col-0 and *arf7/19* plants were treated with high 1-NAA concentration of $1.5x10^{-7}$ M (called here H 1-NAA) and PP60 concentrations of 30 and 50 µg/mL for 9 days. Addition of H 1-NAA caused a dramatic reduction in root elongation and increased density of root hairs compared to mock conditions in both Col-0 and *arf7/19* (**Fig. 5.8 C, D**). Additionally, H 1-NAA rescued the agravitropic phenotype of *arf7/19*. Interestingly, after addition of a moderate PP60 concentration (30 µg/mL) primary root length and root hair density was restored to that of the mock control (**Fig. 5.8 A, C**). A similar situation could be seen in *arf7/19* mutant where primary root length recovered to that of the mock control after 9 days (**Fig. 5.8 B, D**). The higher PP60 concentration (50 µg/mL) restored root elongation but with a smaller effect than a moderate concentration of PP60 in Col-0 plants (**Fig. 5.8 A, C**). Similarly, as for L 1-NAA, 50 µg/mL reduced the agravitropic response of *arf7/19* (**Fig. 5.8 B**). These results suggest that modulations in PME activity after PP60 treatment could reduce the effect of exogenous auxin on primary root elongation independently of ARF7/19 presence.

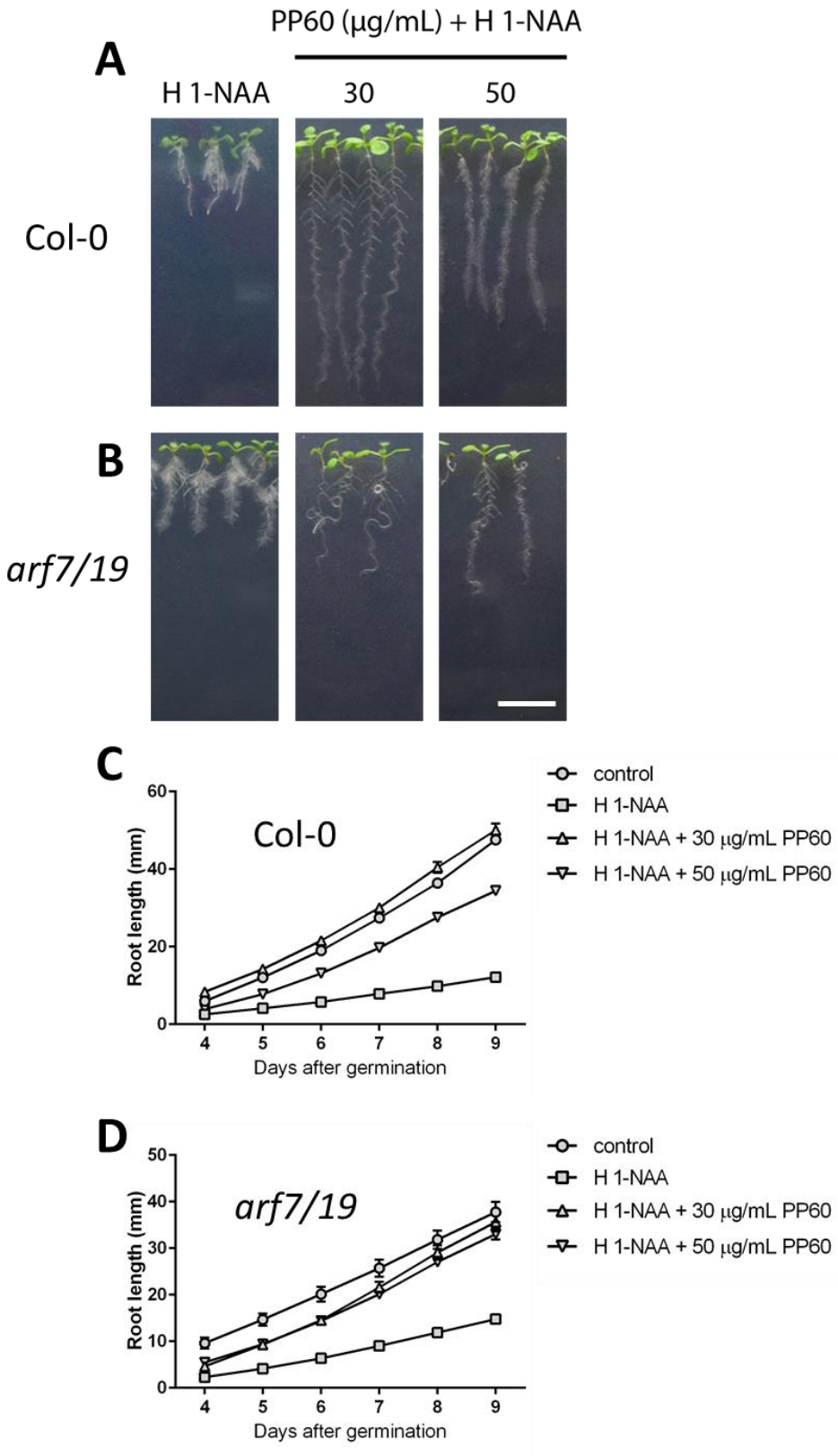

Figure 5.8. Responses of *Arabidopsis* Col-0 and *arf7/19* primary root to treatment with polyphenon 60 (PP60) and higher 1-naphthaleneacetic acid concentration (H 1-NAA). 10-days old Col-0 (A) and *arf7/19* (B) seedlings grown on $1.5x10^{-7}$ M 1-NAA (H 1-NAA) together with different PP60 concentration. Average root lengths from 4 to 9 days of Col-0 (C) and *arf7/19* (D) growing on 0.5 MS media supplemented with H 1-NAA and PP60 from two independent experiments with two biological replicates each are illustrated (n>30). Statistical analysis was determined by two-way ANOVA with Tukey's multiple comparisons test. Scale bar 10 mm.

5.2.2 Brassinosteroids biosynthesis inhibition and its potential influence on PME activity

Propiconazole (Pcz) is a commonly used fungicide that targets lanosterol 14α-demethylase in the ergosterol biosynthesis pathway. Pcz, as a potent inhibitor of BR biosynthesis was first reported after examining its inhibitory effects on cress, showing plant dwarfism that could be rescued considerably by eBL treatment. Furthermore, Hartwig et al., 2012 presented a molecular genetic analysis of Pcz's effects on *Arabidopsis* confirming Pcz as a potent and specific inhibitor of the BR metabolic pathway in plants. As it has been reported, BR influences PME activity and Pcz has been used here to asses root morphological changes in Col-0 and *arf7/19* after Pcz with/without PP60 treatment.

Col-0 and *arf7/19* were treated with Pcz concentrations ranging from 0.1 to 5 µM (similarly as in Hartwig et al., 2012) for 9 days. Plants showed a reduction in size of cotyledons and roots after treatment of Pcz (**Fig. 5.9 A**). The results showed a dose-dependent reduction of primary root growth for both Col-0 and *arf7/19,* where 0.1 µM Pcz decreased the root length by 10% and 5 µM Pcz by 62% in Col-0 compared to mock conditions (**Fig. 5.9 A, B**). Similar results were seen in *arf7/19* mutant, where 0.1 µM Pcz reduced the root growth by 8% and 5 µM Pcz by 56% compared to mock conditions (**Fig. 5.9 C**).

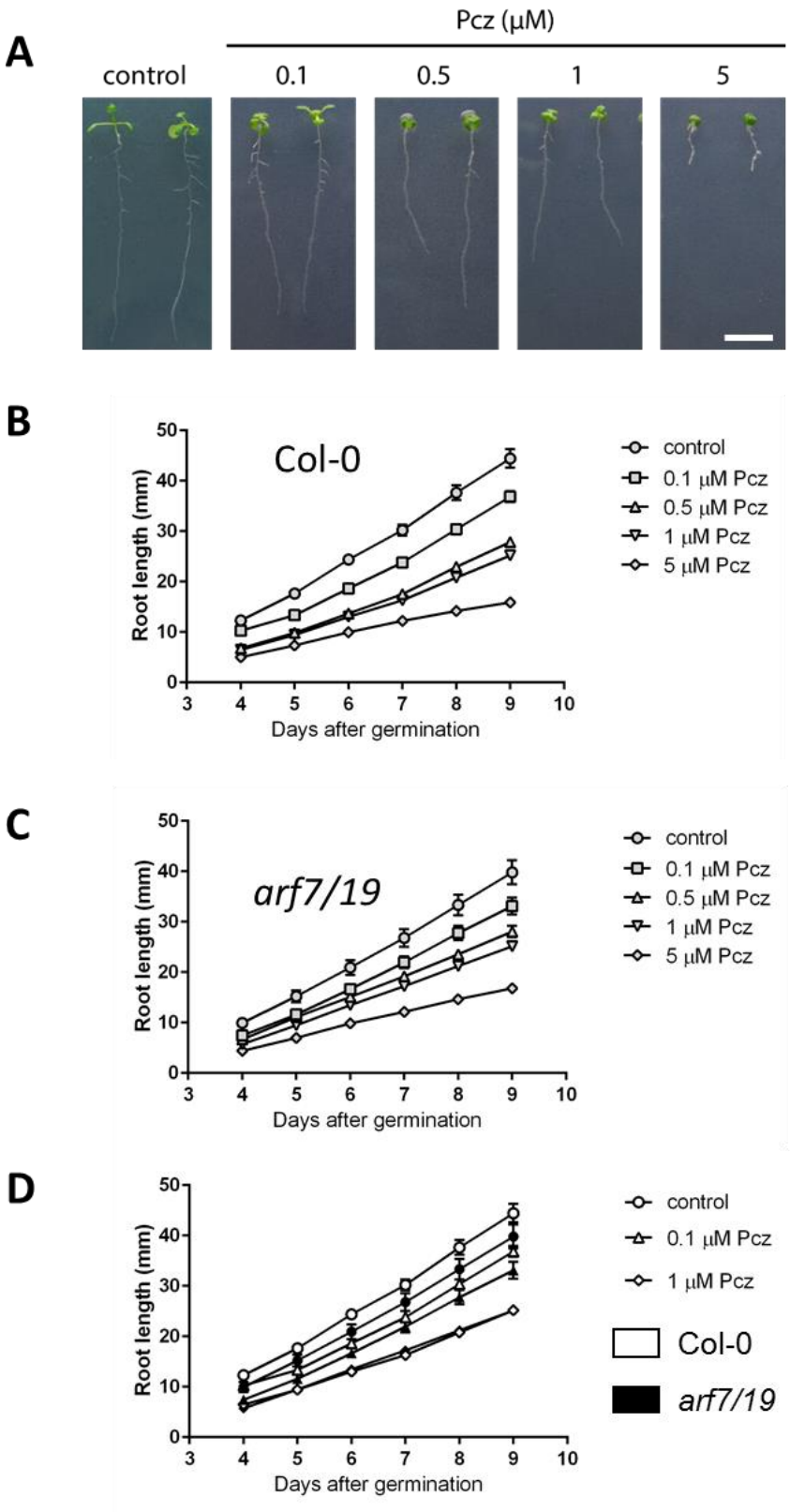

Figure 5.9. Responses of *Arabidopsis* Col-0 and *arf7/19* primary root to treatment with propiconazole (Pcz). 7-days old Col-0 (A) seedlings grown on 0.1, 0.5, 1, and 5 µM Pcz. Average root lengths from 4 to 9 days of Col-0 (B) and *arf7/19* (C) growing on 0.5 MS media supplemented with different Pcz concentrations from two independent experiments with two biological replicates each are illustrated (n>30). (D) The comparison of 0.1 and 1 µM Pcz treatment between Col-0 and *arf7/19*. Statistical analysis was determined by two-way ANOVA with Tukey's multiple comparisons test. Scale bar 10 mm.

To address whether Pcz inhibition of the BR biosynthetic pathway specifically affects PME activity, Col-0 and *arf7/19* plants were grown on media supplemented with Pcz and PP60. For Pcz, moderate 0.5 µM and high 5 µM concentrations were chosen. Col-0 and *arf7/19* were grown on following combinations: 0.5 µM Pcz + 30 µg/mL PP60; 0.5 Pcz + 50 µg/mL PP60; 5 µM Pcz + 30 µg/mL PP60; 5 µM Pcz + 50 µg/mL PP60. Col-0 seedlings co-treated with Pcz and PP60 showed PP60 dose-dependent reduction in primary root length under 0.5 µM Pcz (**Fig. 5.10 A, B**) with root growth being almost restored to that of 0.5 µM Pcz after 0.5 µM Pcz and 30 µg/mL PP60 treatment (**Fig. 5.10 B**). Interestingly, after 5 µM Pcz + 30 µg/mL PP60 root growth was found to be unaffected compared to 5 µM Pcz (**Fig. 5.10 B**). In contrast, the higher PP60 concentration decreased root elongation compared to the Pcz control and 30 µg/mL PP60 treatment. Compared to 0.5 µM Pcz, moderate 30 µg/mL PP60 treatment showed no difference in root elongation in *arf7/19* mutant (**Fig. 5.11 B**). Surprisingly, addition of PP60 to 5 µM Pcz increased root elongation by 28% for 30 µg/mL PP60 and 8% for 50 µg/mL PP60 compared to Pcz condition only (**Fig. 5.11 B**).

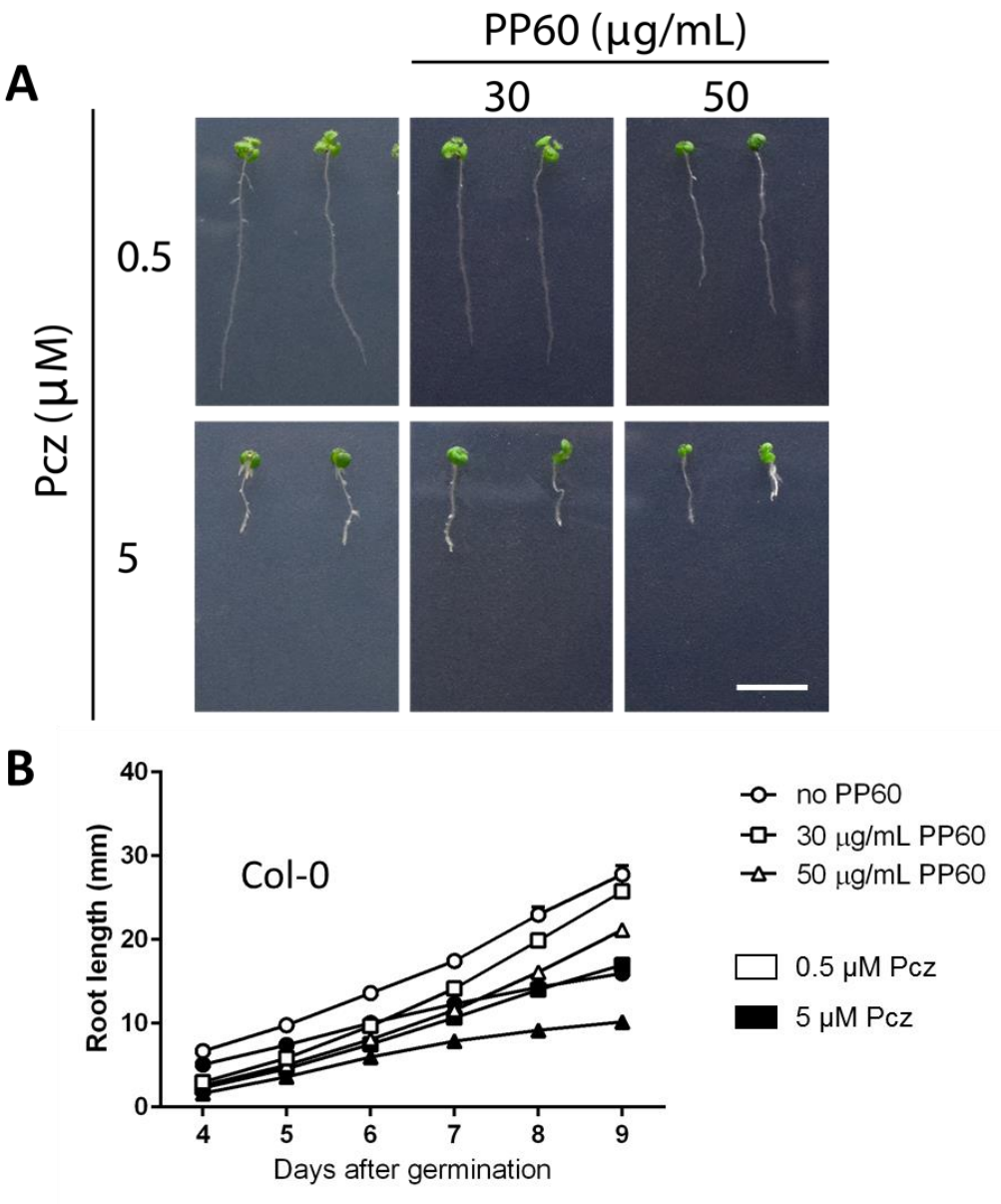

Figure 5.10. Responses of *Arabidopsis* Col-0 primary root to treatment with polyphenon 60 (PP60) and propiconazole (Pcz). 7-days old Col-0 (A) seedlings grown on 0.5 and 5 µM Pcz together with 30 and 50 µg/mL PP60. Average root lengths from 4 to 9 days of Col-0 (B) growing on 0.5 MS media supplemented with Pcz and PP60 from two independent experiments with two biological replicates each are illustrated (n>30). Statistical analysis was determined by two-way ANOVA with Tukey's multiple comparisons test. Scale bar 10 mm.

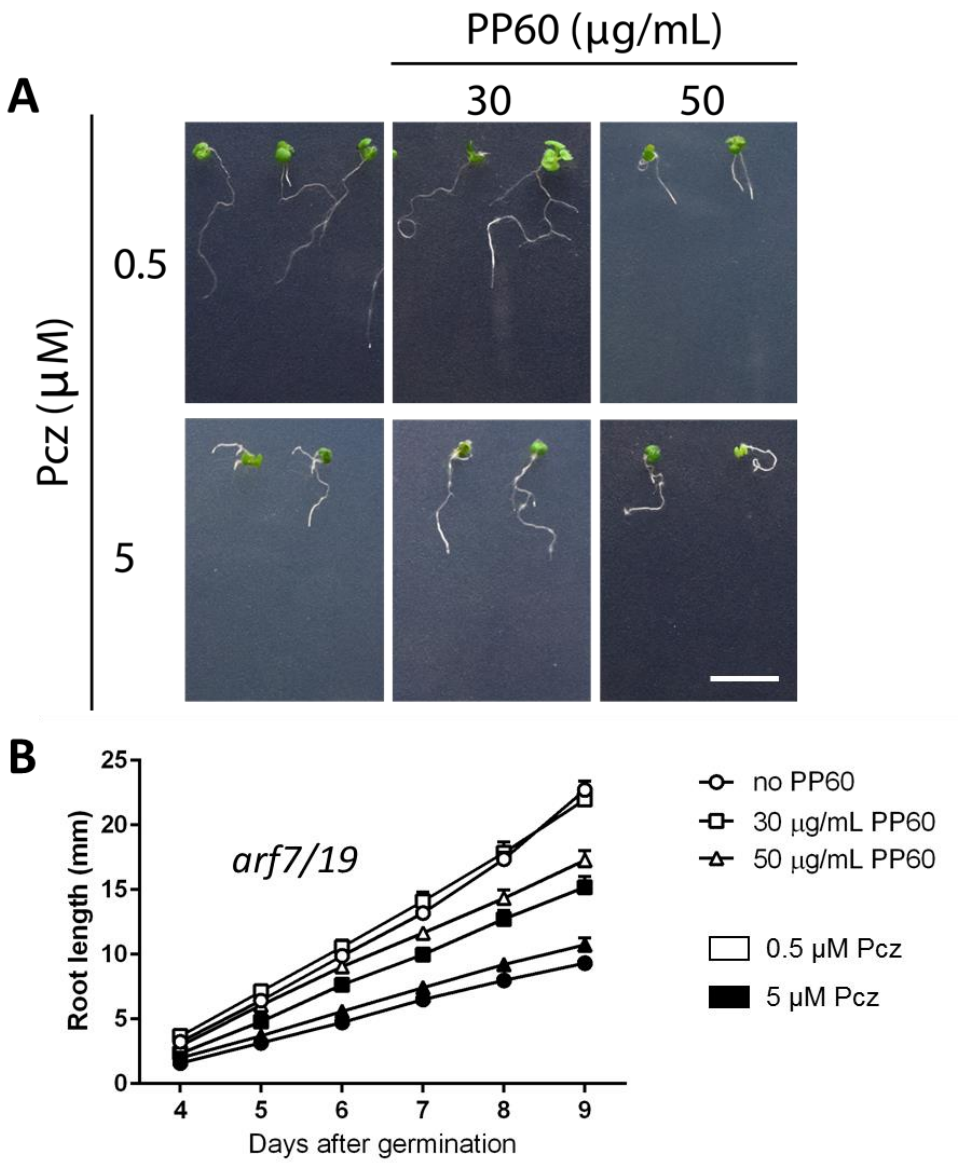

Figure 5.11. Responses of *Arabidopsis arf7/19* primary root to treatment with polyphenon 60 (PP60) and propiconazole (Pcz). 7-days old *arf7/19* (A) seedlings grown on 0.5 and 5 µM Pcz together with 30 and 50 µg/mL PP60. Average root lengths from 4 to 9 days of *arf7/19* (B) growing on 0.5 MS media supplemented with Pcz and PP60 from two independent experiments with one biological replicates each are illustrated (n>30). Statistical analysis was determined by two-way ANOVA with Tukey's multiple comparisons test. Scale bar 10 mm.

5.2.3 Co-treatment of Col-0 and *arf7/19* with auxin and Pcz

To examine if coordination between auxin and BR synthesis influences primary root growth, Col-0 and *arf7/19* plants were grown on media containing range of Pcz concentrations and H 1-NAA. Both, Col-0 and *arf7/19* had primary root growth inhibition after co-treatment with Pcz and H 1-NAA (**Fig. 5.12 A-D**). Addition of 0.5 µM or higher Pcz caused 60% reduction in root length in Col-0 compared to H-1NAA only (**Fig. 5.12 B**). Similarly, *arf7/19* mutant plants showed root elongation inhibition (**Fig. 5.12 C**) and moreover the plant growth was completely arrested with 0.5, 1, and 5 µM Pcz with H 1-NAA (**Fig. 5.12 C, D**).

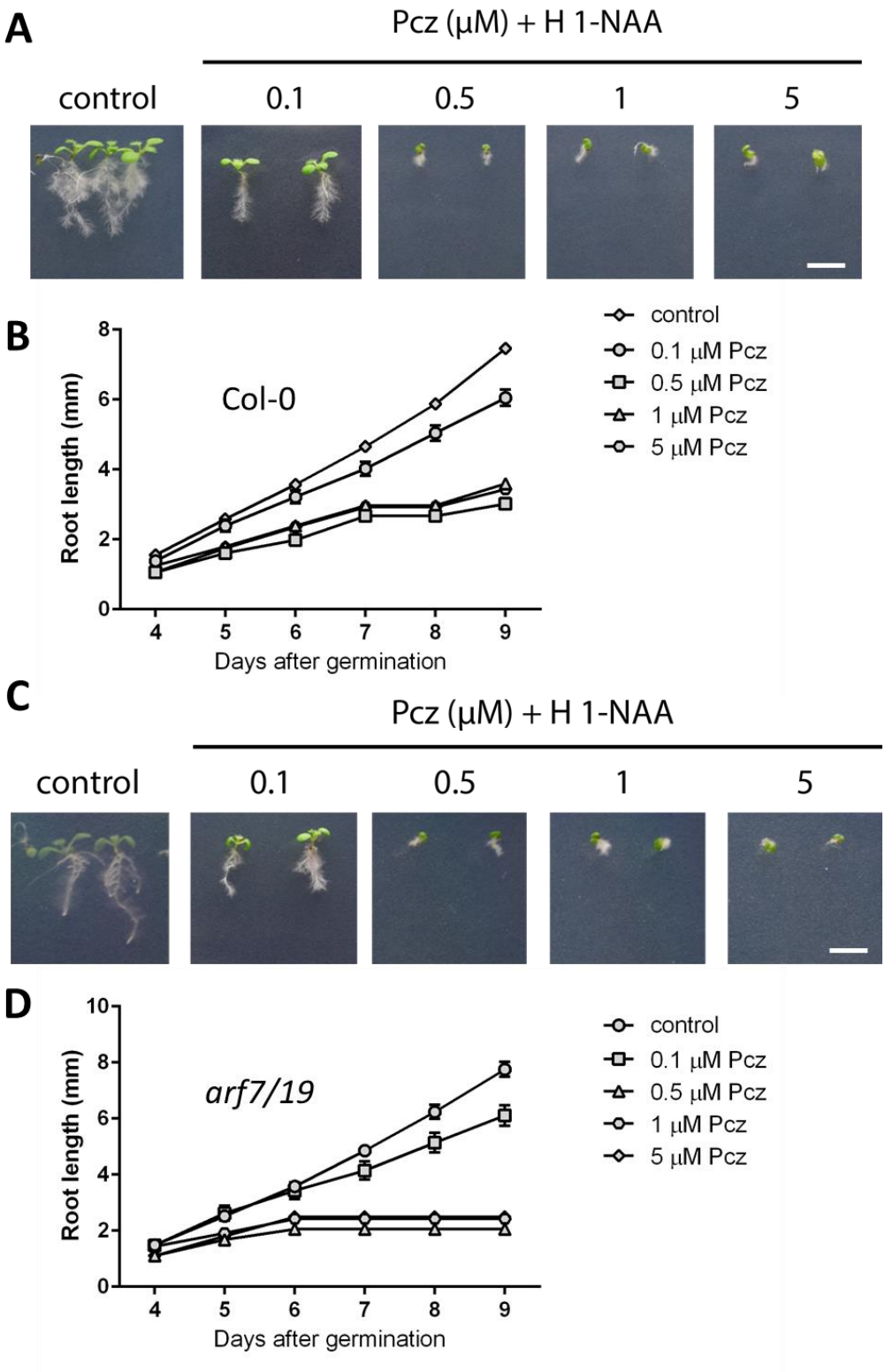

Figure 5.12. Responses of *Arabidopsis* Col-0 and *arf7/19* primary root to treatment with propiconazole (Pcz) and 1-naphthaleneacetic acid (1-NAA). 7-days old Col-0 (A) and *arf7/19* (C) seedlings grown on $1.5x10^{-7}$ M 1-NAA (H 1-NAA) together with different Pcz concentrations. Average root lengths from 4 to 9 days of Col-0 (B) and *arf7/19* (D) growing on 0.5 MS media supplemented with H 1-NAA and Pcz from two independent experiments with one biological replicates each are illustrated (n>30). Statistical analysis was determined by two-way ANOVA with Tukey's multiple comparisons test. Scale bar 10 mm.

5.2.4 Response of Col-0 and *arf7/19* to auxin, Pcz, and PP60 treatment

Finally, the effect of BR biosynthesis inhibition, PME activity increase and exogenous auxin was examined on Col-0 and *arf7/19* plants. Plants were treated with H 1-NAA; 30 and 50 µg/mL PP60; 0.1 and 1 µM Pcz (**Fig. 5.13 A, C**). Lower Pcz concentrations were chosen due to growth cessation caused by high Pcz concentrations together with H 1-NAA treatment. When Col-0 plants were grown on 0.1 µM Pcz with H 1-NAA and 30 µg/mL PP60 primary root length was 28% higher compared to Pcz and H 1-NAA treatment (**Fig. 5.13 B**)**.** Addition of 50 µg/mL PP60 caused root length reduction by 52% compared to Pcz and H 1-NAA treatment. The root growth compared between 1 µM Pcz and H 1-NAA with PP60 addition showed that only higher PP60 concentration (50 µg/mL) increased root elongation by 22% (**Fig. 5.13 B**). 30 µg/mL PP60 caused root growth inhibition by around 10% compared to Pcz and H 1-NAA co-treatment (**Fig. 5.13 B**). *arf7/19* mutant plants were less affected by co-treatment of Pcz, H 1-NAA, and PP60 (**Fig. 5.13 C**). Addition of 30 µg/mL PP60 to 0.1 µM Pcz and H 1-NAA increased root elongation by 31% (**Fig. 5.13 D**). PP60 had no or little effect on the rest of treatments (**Fig. 5.13 D**).

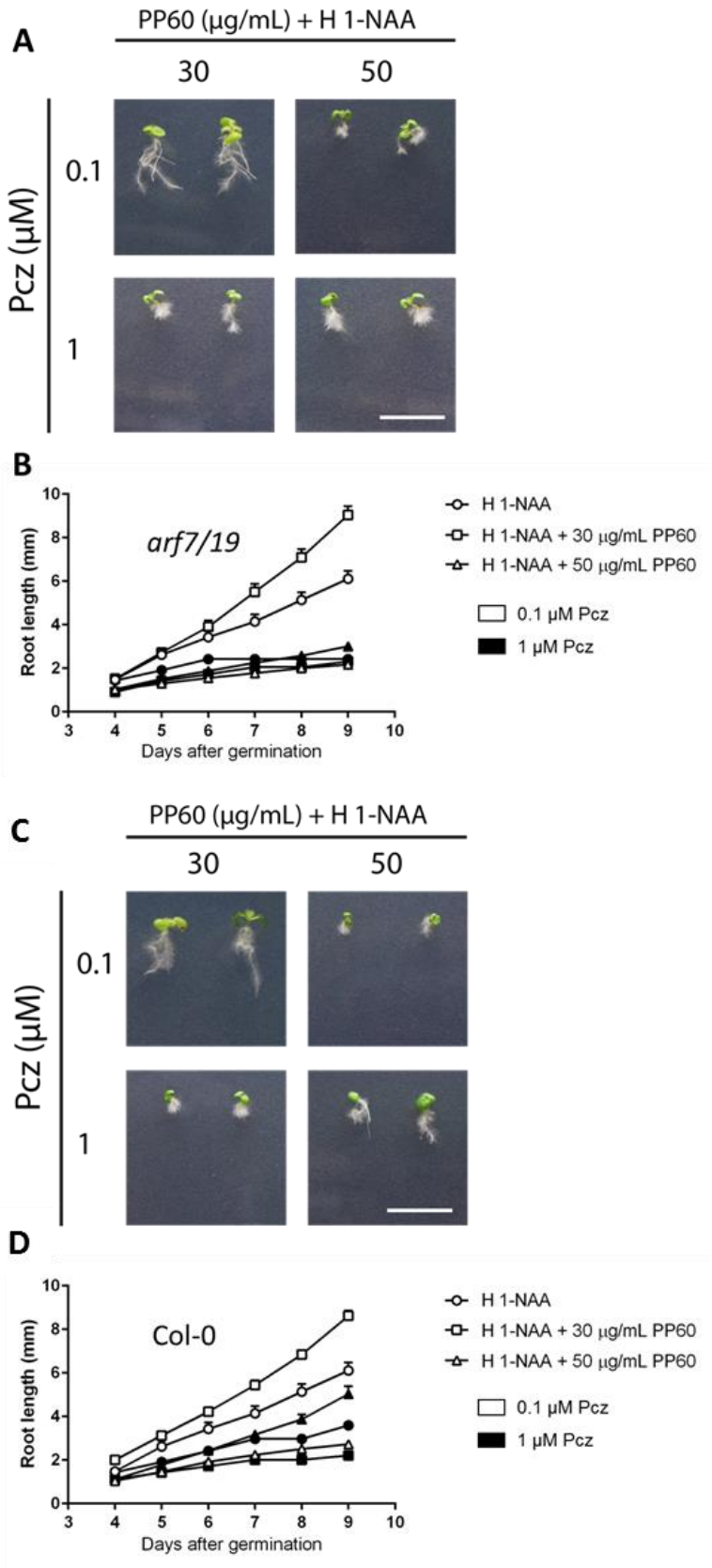

Figure 5.13. Responses of *Arabidopsis* Col-0 and *arf7/19* primary root to treatment with polyphenon 60 (PP60), propiconazole (Pcz), and 1-naphthaleneacetic acid (H 1-NAA). 7-days old Col-0 (A) and **arf7/19** (C) seedlings grown on H 1-NAA together with 0.1 and 1 µM Pcz; 30 and 50 µg/mL PP60. Average root lengths from 4 to 9 days of Col-0 (B) and *arf7/19* (D) growing on 0.5 MS media supplemented with H 1-NAA, Pcz, and PP60 from two independent experiments with one biological replicates each are illustrated (n>30). Statistical analysis was determined by two-way ANOVA with Tukey's multiple comparisons test. Scale bar 10 mm.

5.3 Discussion

Auxin is one of the most important hormones for root development. High levels of auxin maintain cell activities in the stem cell niche to regulate meristem size, partly by activating the transcription factors PLETHORA (Galinha et al., 2007). Low levels of auxin in the elongation zone allows cell elongation and higher levels of auxin inhibit cell elongation mediating gravitropic root bending (Rahman et al., 2007). Auxin activates the auxin response transcription factors (ARFs) by triggering degradation of the Aux/IAA family of transcriptional repressor proteins (Guilfoyle and Hagen, 2007). Here it has been shown that low and high exogenous concentrations of auxin inhibited root growth but when PME activity increased after PP60 treatment, root elongation was restored to that of control conditions (**Fig. 5.14**).

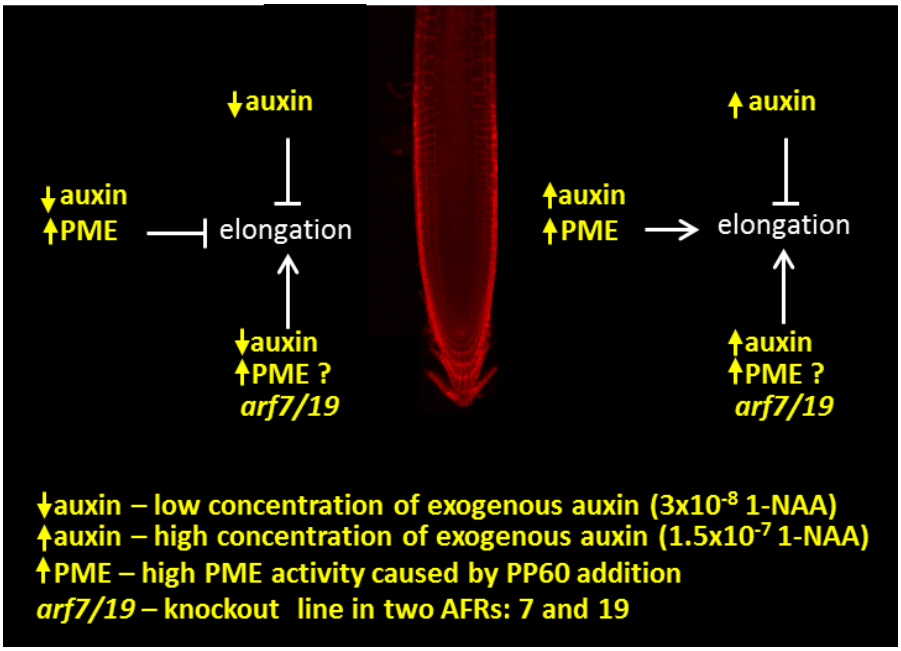

Figure 5.14. Root elongation responses to auxin and PP60 treatment. Low auxin treatment caused a slight inhibition of root elongation; low auxin together with higher PME activity still inhibited root elongation, whereas knockout of two ARFs (7 and 19) reduced the effect of low auxin and higher PME activity. In case of higher auxin treatment, the root elongation was still inhibited but when PME activity increased the primary root length was restored to that of the control. Similarly, as for low auxin, high auxin and high PME activity have not changed root elongation in mutants lacking ARF7/19 compared to wild type plants.

It is possible that exogenous auxin needs low PME activity to be able to inhibit root elongation. High auxin concentration may induce activation of some PME genes through regulation of ARF7/19 transcription factors. Together with the redundancy response after PP60 treatment, the elevated PME activity could increase the content of randomly demethylesterified HG. This could activate PGs which hydrolyse pectin causing the loss of cell wall rigidity and increasing root elongation. OGAs produced due to PG activity could

bind to WAKs and further signal transduction could inhibit the activity of ARFs in a negative feedback loop (**Fig. 5.15 A**). Moreover, the *arf7/19* mutant showed increased root elongation compared to wild type regardless of exogenous auxin concentration. This suggests that transcription factors ARF 7 and 19 could regulate the expression of PMEIs or PMEs and modulate the activity of PME. Future work is needed focusing on PME activity measurements which could be affected in *arf7/19* mutant.

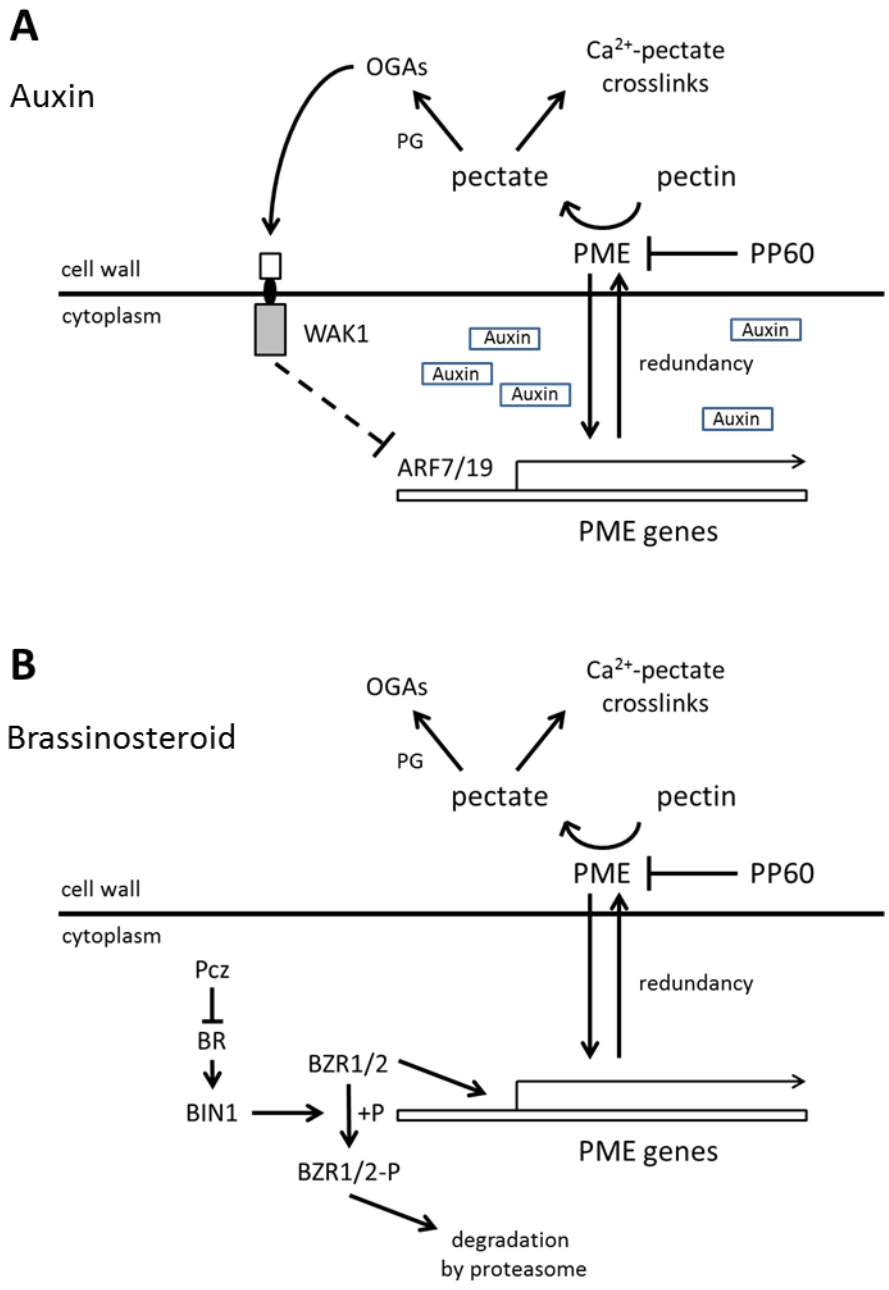

Figure 5.15. Auxin and brassinosteroid feedback signalling in cell wall. (A) Auxin signalling. (B) Brassinosteroid signalling. ARF7/19 – Auxin Response Factor 7 and 19; BR – brassinosteroid; BIN1 – BR INSENSITIVE 1; BZR1/2 – Brassinazole-resistant 1 and 2; OGAs – oligogalacturonides; PG – polygalacturonase; PME – pectin methylesterase; PP60 – polyphenon-60; WAK1 – wall-associated kinase 1.

Another important regulator of root development is brassinosteroid (BR). BR-deficient or BR-insensitive mutants exhibit a wide range of growth effects including short root (Wei and Li, 2015). It has been shown that exogenous BR effects are due to requirement of different BR levels in different developmental zones (Chaiwanon and Wang, 2015). Here, the results showed that disruption of the BR biosynthetic pathway by the chemical inhibitor, propiconazole (Pcz) reduced root growth. This was similar to the results showed before (Hartwig et al., 2012). The root length reduction could be caused by low level of BR, which is required to maintain stem cell and meristem size but inhibits cell elongation in the elongation zone (Chaiwanon and Wang, 2015).

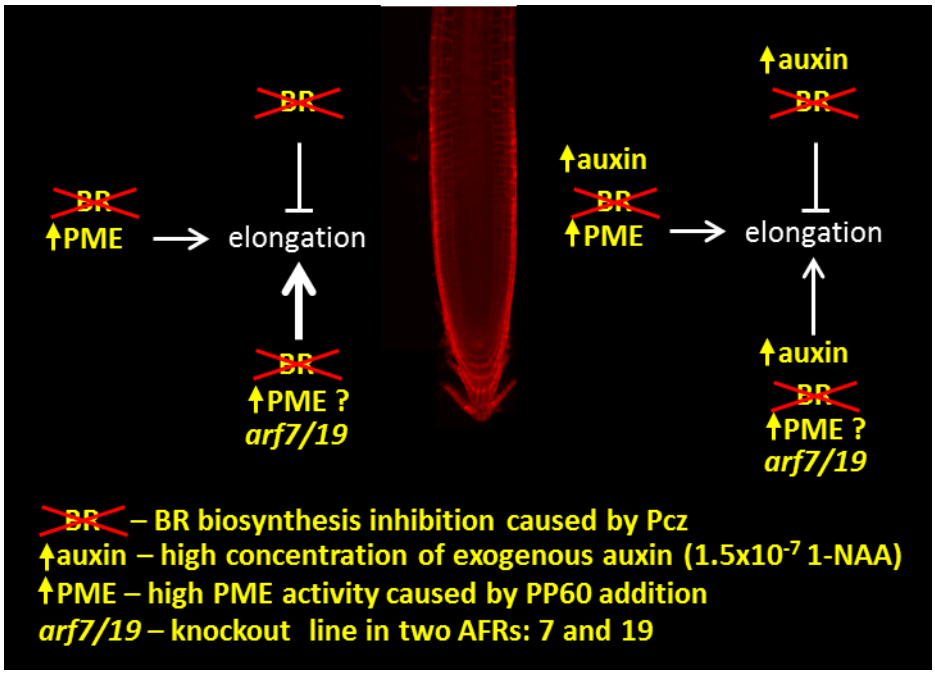

Figure 5.16. Root elongation responses to BR biosynthesis inhibition and PP60 treatment. BR biosynthesis inhibition reduced root elongation but higher PME activity reduced the effect of BR inhibition. Moreover, the *arf7/19* mutant had an additional, positive effect on root elongation following BR biosynthesis inhibition and higher PME activity. High concentration auxin still promoted root elongation but to a lesser effect.

The probable inhibition of PME activity by the chemical inhibitor EGCG or PMEI overexpression caused the activation of the BRI1 receptor and/or downstream BZR1/2 signalling component (Wolf et al., 2012). BR perception by BRI1 activates the transcription factors BZR1/2 which regulate genes involved in cell wall biosynthesis and remodelling. Moreover, BZR1 inhibits the transcription of BR biosynthesis genes creating a negative feedback loop (Sun et al., 2010). Here it has been shown that increase in PME activity caused by PP60 enhanced root growth in plants affected in BR biosynthesis (**Fig. 5.16**). In the presence of BR, BZR1/2 proteins may activate the transcription of subset of PME genes. It is possible that when biosynthesis of BR is inhibited by Pcz, the BIN1 protein phosphorylates BZR1/2 proteins and targets them for degradation. Therefore, the transcription of PMEs which work in a blockwise fashion may be inhibited but the one that

work in non-blockwise fashion are still transcribed. This could lead to pectin hydrolysis by PG and thus weakening of the cell wall and cell elongation (**Fig. 5.15 B**). Moreover, this effect was more profound in plants lacking the ARF7 and ARF19. The ARF7 has been shown to increase the endogenous level of BR through suppression of *BAS1* inactivating active BRs (Youn et al., 2016). Therefore, it is possible that plants with blocked BR biosynthesis and signalling have lower PME activity

.

6. The organisation of border-like cells in the *Arabidopsis* root tip is affected by methylesterification state of homogalacturonan

6.1 Introduction

Plant roots produce a layer of outer cells at the tip which separate from it after contact with water. These cells are defined as border cells (Driouich et al., 2013). Their role is to help root with soil penetration, response to abiotic stresses and pathogen invasion. However, it has been shown that *Arabidopsis* seedlings produce sheets of attached cells which remain joined together after release from root tips and these are referred to as border-like cells (BLCs; Vicré et al., 2005; **Fig. 6.1**). Border cells are defined as individual cells detaching from the root cap, whereas BLCs are released as sheets of cells. In *Arabidopsis* the release of BLCs is age-dependent with cells being released from roots of seedlings grown for more than 5 days.

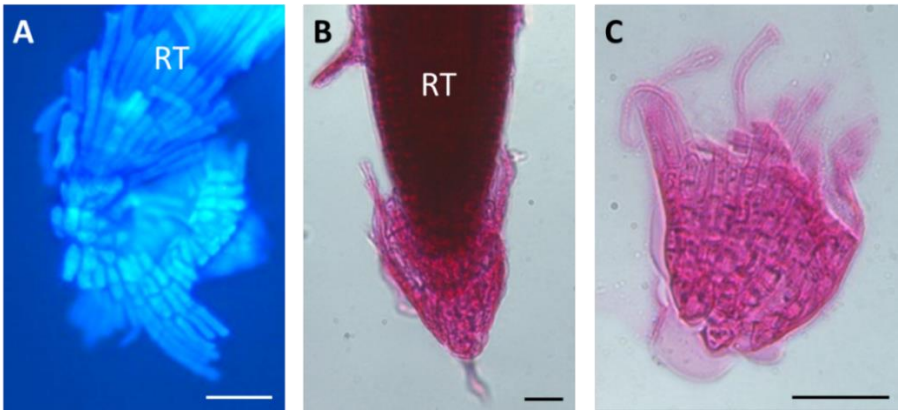

Figure 6.1. *Arabidopsis* border-like cells (BLC). (A) Calcofluor white staining of root tip showing BLC released from the wild type Arabidopsis plants. (B) BLC surrounding root tip. (C) Clustered BLC after release from root tip. Roots were stained with ruthenium red. RT – root tip. Scale bar 50 µm.

The unusual clustering of border-like cells suggests their composition might be different to that of border cells. The cell wall composition of *Arabidopsis* border-like cells has been investigated using an immunofluorescence approach and showed that these cells are rich in the pectic homogalacturonan (HG) and arabinogalactan-proteins (Vicré et al., 2005). Durand et al. characterized mutants affected in biosynthesis of different cell wall polysaccharides including pectin, xyloglucan and cellulose. They showed that only *quasimodo1-1* (*qua1-1*) and *qua2-1*, in which HG biosynthesis is disrupted, have different organization of border-like cells. Analysis of *qua1-1* mutant showed a loss in HG content

combined with mucilage secretion enriched in xylogalacturonan and arabinogalactan-protein epitopes (Durand et al., 2009). The *qua1-1* mutant releases border-like cells which disperse in the surrounding environment, a phenotype similar to that of border cells of pea roots. This observation shows involvement of HG in cell adhesion and attachment. Additionally, separation of border-like cells is accompanied with production and secretion of a mucilaginous matrix not seen in wild type plants. It has been suggested that abundant mucilage resembles a bacteria biofilm which has a role in protecting against harmful substances. Therefore, formation of a border-like cells “biofilm” in *qua1-1* roots is a key factor for their stability and survival (Driouich et al., 2010). Moreover, it prevents border-like cells from moving away from the root tip in the presence of water.

It has been shown that *Arabidopsis* and flax border-like cells are able to respond specifically to microbe-associated molecular patterns (MAMPs) by producing reactive oxygen species (ROS), including superoxide and singlet oxygen, and deposition of callose, a well-known marker of defence. In addition, significant accumulation and alteration of extensin epitopes within the cell wall were also observed upon elicitation (Plancot et al., 2013). Alterations in cell adhesion has been shown to occur during pathogen invasion and involve the activity of pectin hydrolysis enzymes, pectin lyases and methylesterases (Rogers et al., 2000). In pea root caps, the relative expression of PME was measured and showed a six-fold increase during separation of border cells compared to that measured after the process finished (Stephenson and Hawes, 1994). Furthermore, the concentration of soluble demethylesterified pectin increases significantly during the release of border cells from the root cap. Interestingly, when the expression of PME gene was inhibited by antisense mRNA in transgenic pea, border cell segregation was blocked and they accumulated at the root tip as clumps of cells (Wen et al., 1999). Recently, it has been showed that expression levels of PME were low in border cells of *Medicago truncatula*, as determined by both microarray and qRT-PCR data (Watson et al., 2015). Interestingly, a novel transcript for a gene annotated as a PMEI was greatly enhanced in border cells and it was the first time a putative PMEI has been identified in border cells. *Arabidopsis thaliana* is the only species in which significant increase of PME activity at the root cap has not been detected (Stephenson and Hawes, 1994).

Durand, et al. 2009 proposed to use the border-like cell phenotype as an indicator to screen alterations in key developmental processes such as cell attachment and morphology. In this chapter the question whether increased PME activity after PP60 addition influences the phenotype of border-like cells phenotype causing their separation from the root cap is examined using immunolabelling and histochemistry approaches. Observation of border-like cell is fast and easy, promising a good model for detection of changes in cell wall structure and function.

6.2 Results

6.2.1 Organisation of border-like cells after PP60 treatment

It has been shown before that separated border-like cells are released from roots of plants which have the loss of HG content (Vicré et al., 2005). To investigate the involvement of the esterification state of HG in border-like cell (BLC) organization and mucilage secretion, the root cap morphology in Col-0 was examined (**Fig. 6.2**). BLC organization was first examined in plants grown on MS media (pH 5.7) supplemented with a range of PP60 and EGCG concentrations. As illustrated in **Fig. 6.2** PP60 caused separation of border-like cells, which were dispersed individually and in the form of sheets of attached cells in close proximity to the root tip. A very similar phenotype was observed for EGCG. Additionally, these cells were seen to be embedded together in a layer of mucilage, the secretion of which increased with higher concentrations of PP60 and EGCG (**Fig. 6.2**).

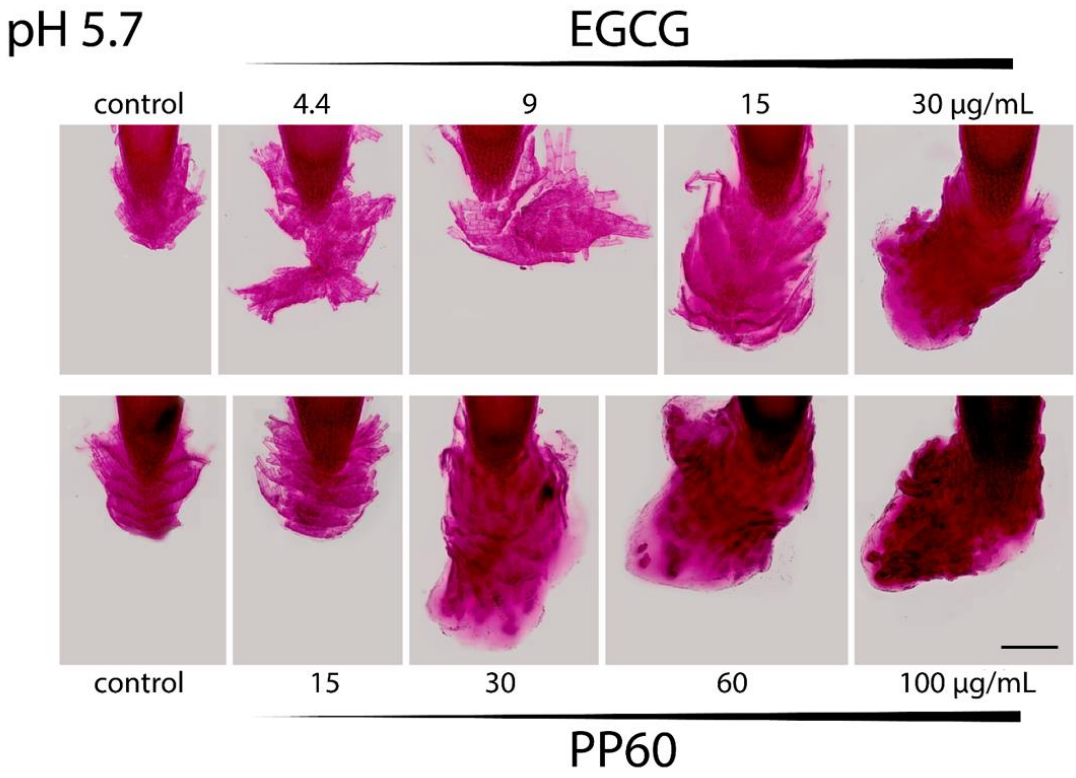

Figure 6.2. Histochemical staining of root tips showing border-like cells (BLC) released from the wild type growing on media supplemented with PP60 and EGCG at pH 5.7. The staining was repeated in two independent experiments (n≥16). 14-days old, representative seedlings grown on 15, 30, 60, and 100 µg/mL of PP60 and 4.4, 9, 15, and 30 µg/mL are illustrated. Roots were stained with ruthenium red. Scale bar 100 µm.

PME activity was not changed after PP60 addition at pH 8.0 (**Fig. 6.3**). Thus it is expected that if BLC release and separation is dependent on PME activity, the BLC phenotype at pH 8.0 should be different to that of pH 5.7. To further investigate the impact of pH, EGCG and PP60 on border-like cell organization, root tips grown on basic pH (8.0) together with EGCG and PP60 treatment were examined. As illustrated in Fig. 4.3, BLC were organized in the files with less mucilage secreted around them for PP0 and EGCG compared to normal conditions. As shown previously, acidic and basic pHs have different influences on PME and possibly polyphenon-60 activity.

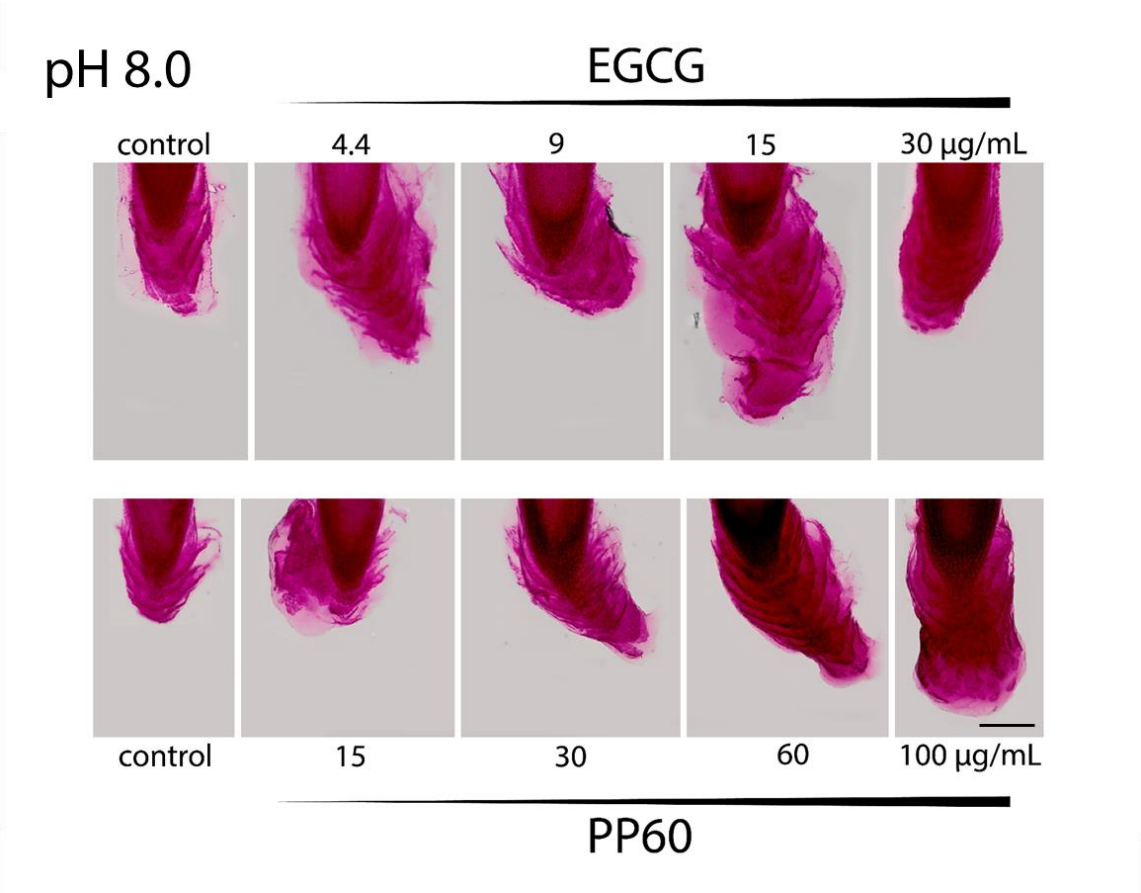

Figure 6.3. Histochemical staining of root tips showing border-like cells (BLC) released from the wild type growing on media supplemented with PP60 and EGCG at pH 8.0. The staining was repeated in two independent experiments (n≥16). 14-days old, representative seedlings grown on 15, 30, 60, and 100 µg/mL of PP60 and 4.4, 9, 15, and 30 µg/mL are illustrated (n≥8). Roots were stained with ruthenium red. Scale bar 100 µm.

As shown in **Figures 6.2** and **6.3** it could be observed that mucilage covered larger areas after PP60 addition. The mucilage area was measured after 30 µg/mL and 50 µg/mL PP60 treatments using ImageJ. There was significantly higher mucilage release after both treatments regardless of media pH ($F = 10.8$; $P < 0.01$; **Fig. 6.4**).

Although ruthenium red staining allows visualisation of the extent of mucilage release, it is difficult to distinguish cells from the red-coloured mucilage. To observe the arrangement of cells within mucilage roots were stained with ruthenium red and calcofluor white. This

method allows visualisation of bright cells and dark mucilage surrounding them under the microscope using UV light. The results confirmed previous statements that BLC were separated and embedded in surrounding mucilage after addition of PP60 at pH 5.7 (**Fig. 6.5**). In case of pH 8.0 cells were more clustered at the root tip with less mucilage around them (**Fig. 6.5**).

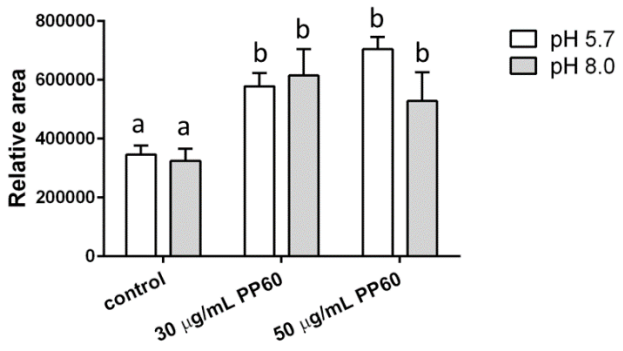

Figure 6.4. Relative mucilage area at the root tip after PP60 treatment at different pH. The mucilage area was measured using ImageJ after 30 µg/mL and 50 µg/mL PP60 treatments at pH 5.7 and pH 8.0. Error bars represent standard error of n≥16 from two independent experiments and lowercase letters indicate significant differences among treatments determined by two-way ANOVA with Sidak's multiple comparisons tests.

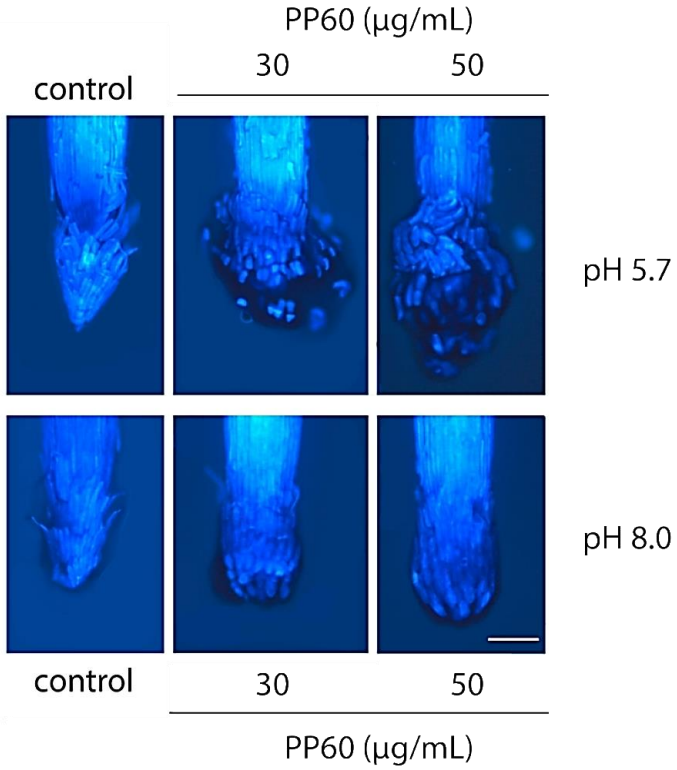

Figure 6.5. Double histochemical staining of root tips showing border-like cells (BLC) released from the wild type growing on media supplemented with PP60 at pH 5.7 and pH 8.0. 14-days old representative seedlings grown on 30 and 50 µg/mL of PP60 from two independent experiments (n≥16) are illustrated. Roots were stained with ruthenium red and calcofluor white. Scale bar 100 µm.

Although EGCG had no influence on primary root development (**Fig. 3.6**), it clearly has an effect on the properties of BLC. To test whether this effect is observed with other catechin components of PP60, ECG and EGC were used to study their impact on BLC. The concentrations of ECG and EGC used in this experiment were the same as for the root development, 8 µg/mL for ECG and 20 µg/mL for EGC. They are equivalent to the amount they compose in 100 µg/mL of the PP60 mixture. EGC showed similar BLC phenotypes to that of EGCG and PP60 in both pHs comparing to a control conditions (**Fig. 6.6**). ECG had no influence on BLC phenotype suggesting epigallocatechins, but not epicatechins, have an effect on BLC separation and mucilage release.

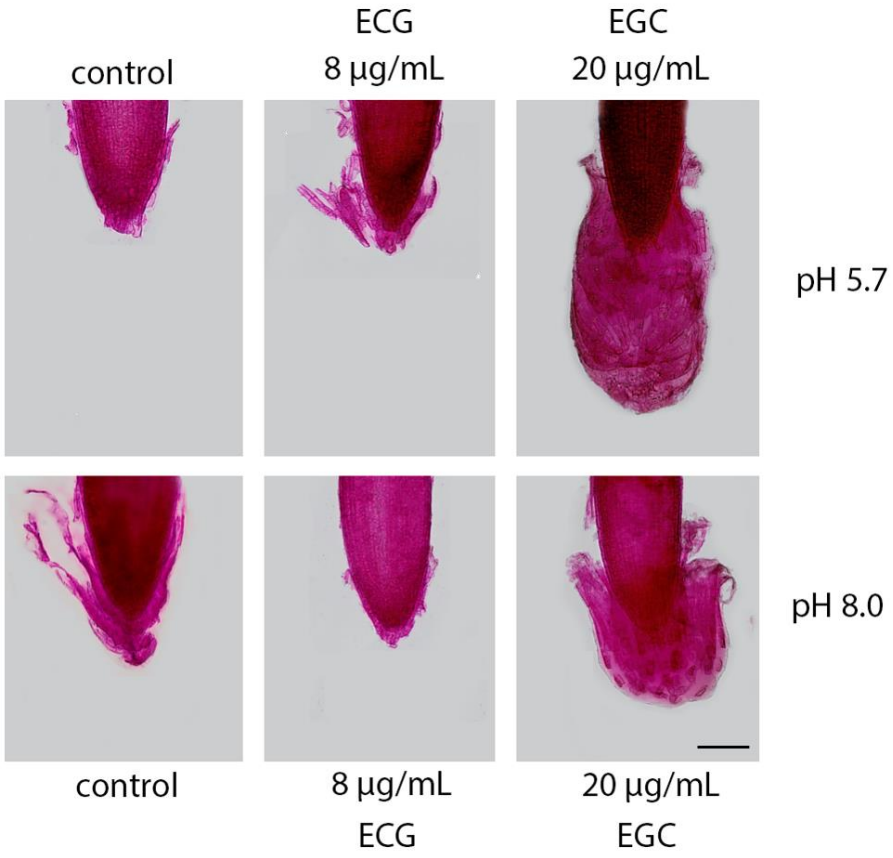

Figure 6.6. Histochemical staining of root tips showing border-like cells (BLC) released from the wild type growing on media supplemented with ECG and EGC at pH 5.7 and pH 8.0. The staining was repeated in two independent experiments (n≥16). 14-days old representative seedlings grown on 8 µg/mL of ECG and 20 µg/mL EGC are illustrated. Roots were stained with ruthenium red. Scale bar 100 µm.

As shown previously PP60 addition to more acidic media (pH 4.5) rescued plants from the inhibitory effect of acidic stress (**Fig. 3.21**). This discovery suggests BLC phenotype may change in pH 4.5 after supplementation with PP60. BLC were observed in acidic conditions and after PP60 addition (**Fig. 6.7**). The BLC phenotype was similar to that of pH 5.7, but with less mucilage and BLC. There was no difference between 30 and 50 µg/mL PP60 treatments at pH 4.5.

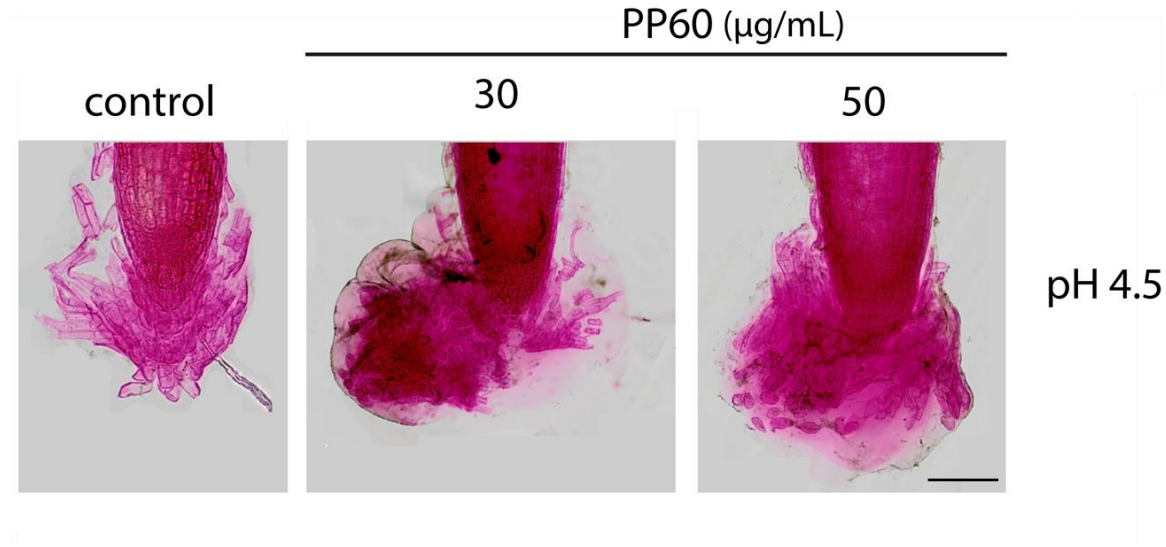

Figure 6.7 Histochemical staining of root tips showing border-like cells (BLC) released from the wild type growing on media supplemented with PP60 at pH 4.5. The staining was repeated in two independent experiments (n≥16). 14-days old representative seedlings grown on 30 and 50 µg/mL PP60 are illustrated. Roots were stained with ruthenium red. Scale bar 100 µm.

It has been shown that border cells separation is significantly increased when roots are incubated with auxin or 1-N-naphthaleneacetic acid (1-NAA). By contrast, roots exposed to the ethylene precursor 1-aminocyclopropane-1-carboxylic acid or treated with the ethylene synthesis inhibitor aminovinylglycine, showed significantly less BC release from the cap (Ponce et al., 2005). Therefore, border cells detachment appears to be regulated by ethylene and by auxin. AUX1 has been identified as putative auxin influx carrier component which performs a dual auxin transport facilitating acropetal and basipetal auxin transport in root apex (Swarup et al., 2001). The *aux1* mutations exhibit an agravitropic root phenotype (Marchant et al., 1999). To investigate the involvement of auxin transport, *AUX1::GUS* plants were used. As shown in **Figure 6.8**, border-like cells separated from the root tip have less or no GUS signal indicating absence of the AUX1 influx transporter after PP60 addition regardless of media pH they were grown on.

The lack of GUS signal in the border-like cells could be due to cell death following release from the root tip. To see whether this is true, the root tips after PP60 treatment were stained with propidium iodide and observed under the confocal microscope. Staining with propidium iodide allows distinguishing viable cells from non-viable ones. The cells with stained cell wall only are considered viable as the dye cannot pass through intact cell membranes, whereas intracellular staining means the cells are non-viable (Rieger et al., 2011). 50 µg/mL PP60-treated plants showed that some of the border-like cells were still viable and some of them were not regardless of the media pH (**Fig. 6.9**).

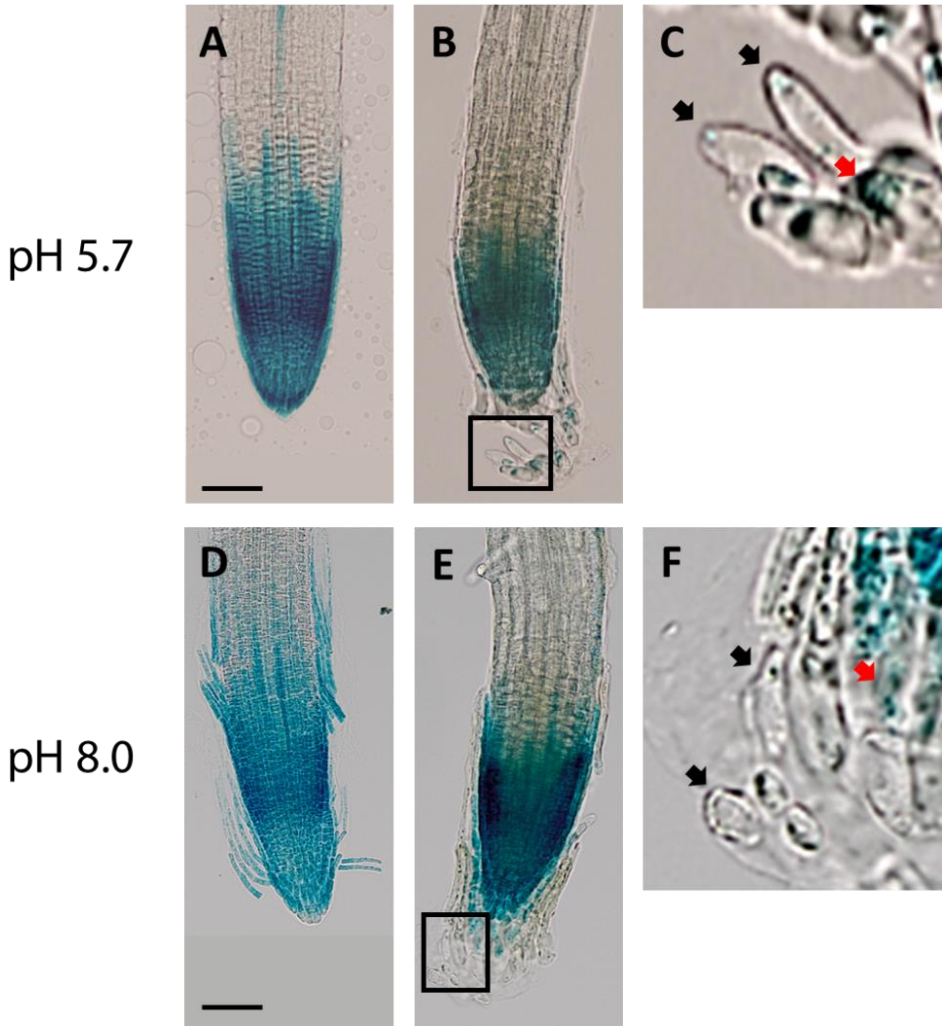

Figure 6.8. Histochemical staining of *AUX1::GUS* root tips showing border-like cells (BLC) released from plants growing on media supplemented with PP60 at pH 5.7 and pH 8.0. 7-days old seedlings grown on pH 5.7 (A, B) and pH 8.0 (D, E) media without PP60 (A, D) and 50 µg/mL of PP60 (B, E) from one independent experiment with two biological replicates each are illustrated (n>10). (C, F) Magnification of marked space from B and E, respectively. Black arrows indicate BLC without marker expression and red ones with *AUX1::GUS* expression. Scale bar 100 µm.

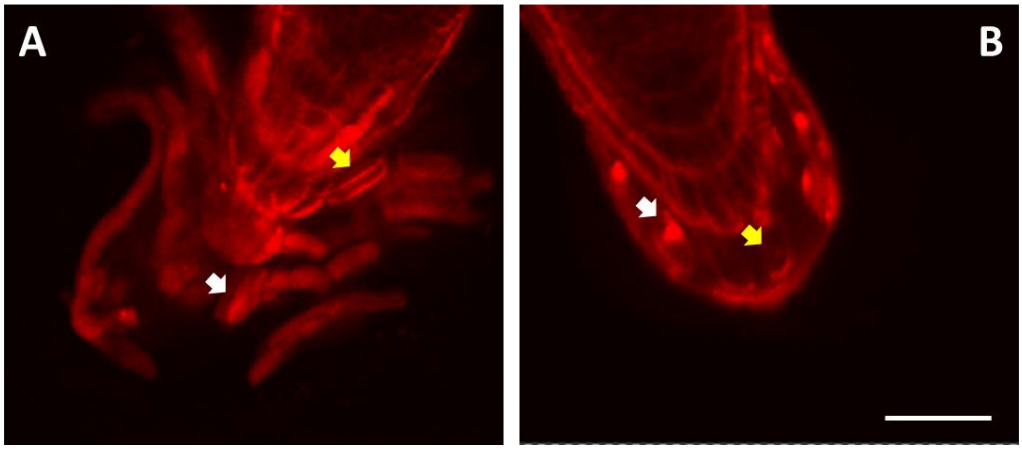

Figure 6.9. Border-like cells viability. *Arabidopsis* roots after 50 µg/mL PP60 treatment at pH 5.7 (A) and pH 8.0 (B) were stained with propidium iodide and the root tips were observed under the confocal microscope (n>5). Yellow arrows indicate viable cells and white arrows indicate non-viable cells. Scale bar 50 µm.

6.2.2 Immunolocalization of polysaccharide epitopes in the cell wall of border-like cells and secreted mucilage after PP60 and pH treatment

Immersion immunofluorescence labelling was used to gain insights into polysaccharide distribution in the cell wall of border-like cells and the released mucilage of the seedlings treated with PP60 and grown under different pH conditions.

6.2.2.1 Pectin immunolabelling

To investigate the occurrence of methylesterified and de-esterified HG, monoclonal antibodies (mAbs), LM19 and LM20 respectively were used. As shown in **Fig. 6.10 A**, antibody LM19 labelled cell walls in the root tip in normal conditions. The proportion of labelling changed after pH 8.0 treatment of roots with more de-esterifed HG at the root tip (**Fig. 6.10 B**). After addition of PP60 cell walls were still stained but the secreted mucilage showed little or no labelling for normal (pH 5.7) and more basic media conditions (**Fig. 6.10 C, D**). Measurements of the relative fluorescence signal in the cell wall showed a slight decrease of the signal after PP60 addition at pH 8.0 (**Fig. 6.10 E**). Fluorescence was significantly decreased in the mucilage after PP60 treatment for both pH conditions ($F = 9.226$; $P < 0.05$; **Fig. 6.10 F**).

In case of methylesterified HG in pH 5.7 condition staining was contrasting that of LM19 with labelling around mucilage (**Fig. 6.11 A**). The pH 8.0 condition showed little or no labelling (**Fig. 6.11 A, B**). PP60 treatment caused less staining for both conditions with only few labelling points (**Fig. 6.11 C, D**). Measurements of fluorescence signal showed significant decrease of LM20 labelling in cell wall and mucilage after PP60 addition at pH 5.7 ($F = 2.779$; $P < 0.05$; **Fig. 6.11 E, F**). There were no significant changes for pH 8.0 where signal was remained low ($F = 2.401$; $P > 0.05$).

Xylogalacturonan epitopes labelled by LM8 were present only in small amounts in the released mucilage in non-PP60 conditions and pH treatment (**Fig. 6.12 A, B**). After PP60 treatment there was weak labelling around the mucilage and root tip (**Fig. 6.12 C**). At pH 8.0 there were no xylogalacturonan epitopes either in the cell wall or the mucilage (**Fig. 6.12 D**).

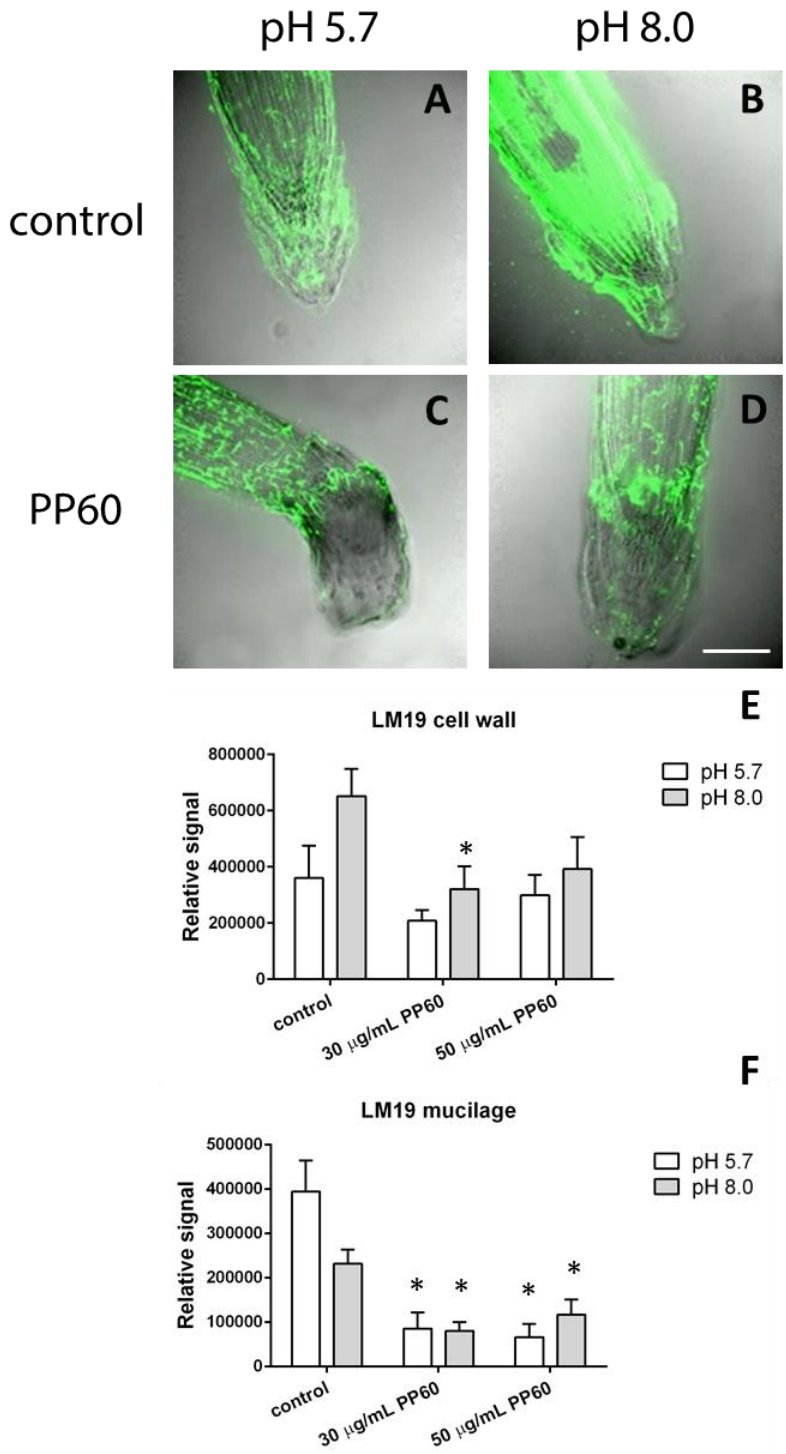

Figure 6.10. Immunofluorescence labelling of border-like cells (BLC) with mAb LM19 after PP60 (50 µg/mL) and pH treatment. Representative micrographs of fixed root tips of wild-type plants stained with LM19 for pH 5.7 control (A), PP60-treated roots (C), plants grown on pH 8.0 (B), PP60-treated at the same pH (D) from two independent experiments (each n>5). Fluorescence intensity was measured for epidermis cell wall (E) and mucilage (F) n≥8. Asterisks (*) indicate significant difference compared to control conditions using two-way ANOVA from both experiments.

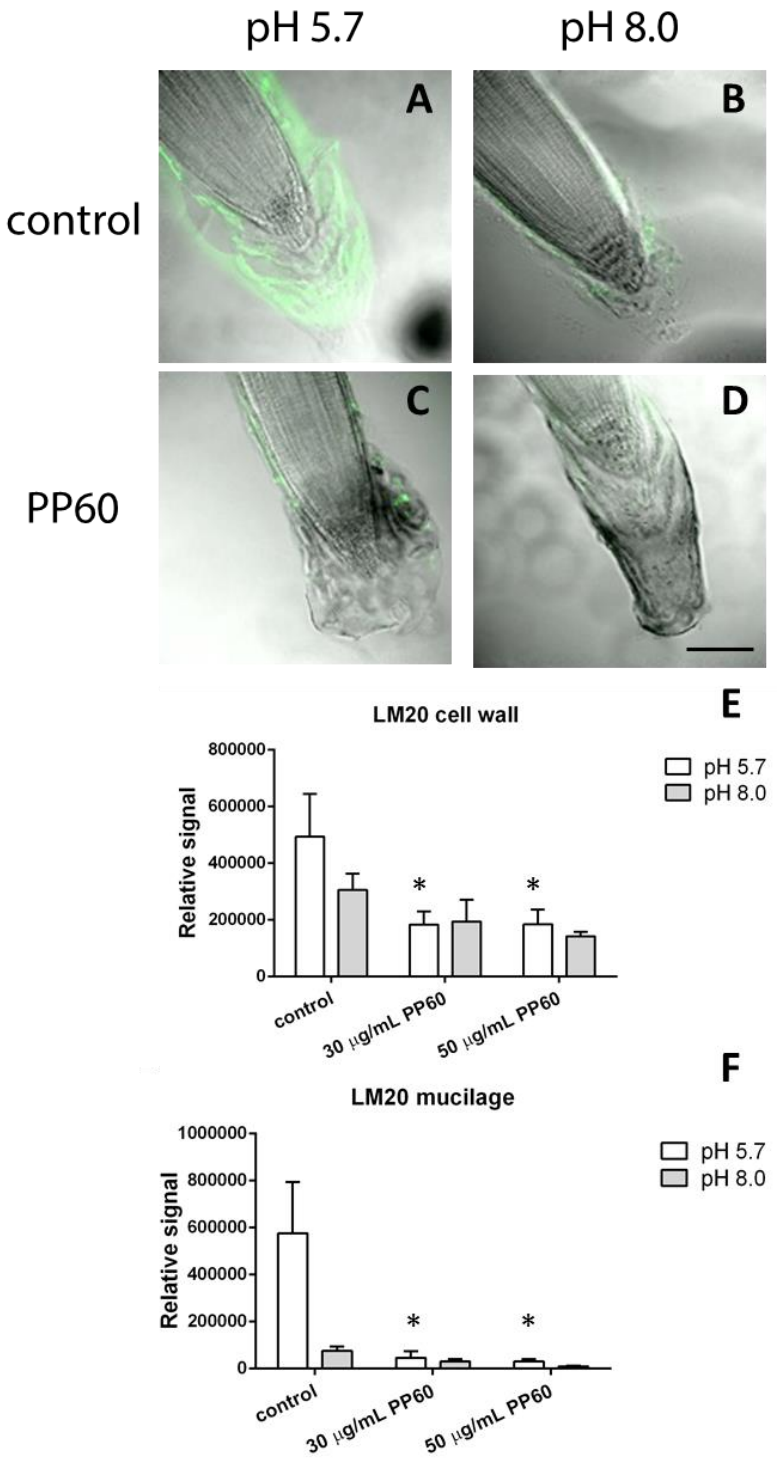

Figure 6.11. Immunofluorescence labelling of border-like cells (BLC) with mAb LM20 after PP60 (50 µg/mL) and pH treatment. Representative micrographs of fixed root tips of wild-type plants stained with LM20 for pH 5.7 control (A), PP60-treated roots (C), plants grown on pH 8.0 (B), PP60-treated at the same pH (D) from two independent experiments (each n>5). Fluorescence intensity was measured for epidermis cell wall (E) and mucilage (F) n≥8. Asterisks (*) indicate significant difference compared to control conditions using two-way ANOVA from both experiments.

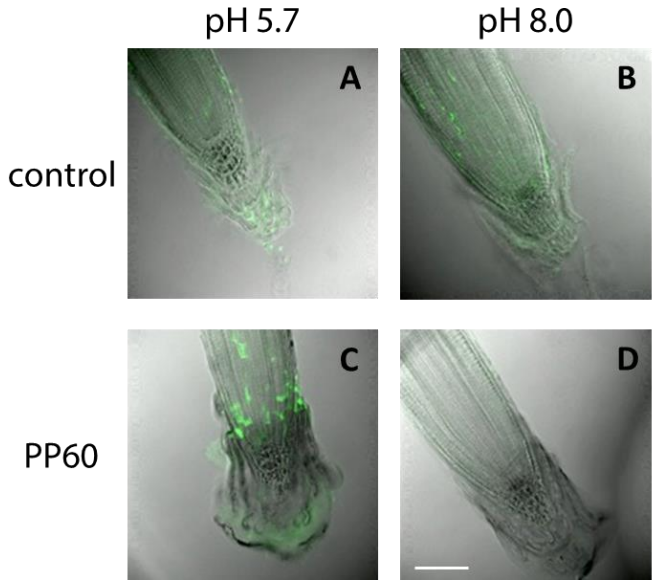

Figure 6.12. Immunofluorescence labelling of border-like cells (BLC) with mAb LM8 after PP60 (50 µg/mL) and pH treatment. Representative micrographs of fixed root tips of wild-type plants stained with LM8 for control (A), PP60-treated roots (C), plants grown on pH 8.0 (B), PP60-treated at the same pH (D) from two independent experiments (each n>5).

6.2.2.2 Arabinogalactan proteins immunolabelling

Arabinogalactan protein epitopes were examined using mAb LM2 and JIM13 in the cell walls and the mucilage of normal and treated *Arabidopsis* seedlings. As shown in the **Fig. 6.13 A, C** staining around mucilage and cell walls has been observed for mAb LM2 regardless of pH conditions on which the plants were grown. After the PP60 addition, labelling was very similar to normal conditions with a lack of staining at the very tip of the mucilage (**Fig. 6.13 E, G**). These observations were different to the ones with mAb JIM13 staining Arabinogalactan Protein 2 (AGP2). There was only little staining around cell walls and mucilage in normal (**Fig. 6.13 B**) and pH 8.0 (**Fig. 6.13 D**) conditions. PP60-treated roots have not shown any staining (**Fig. 6.13 F, H**).

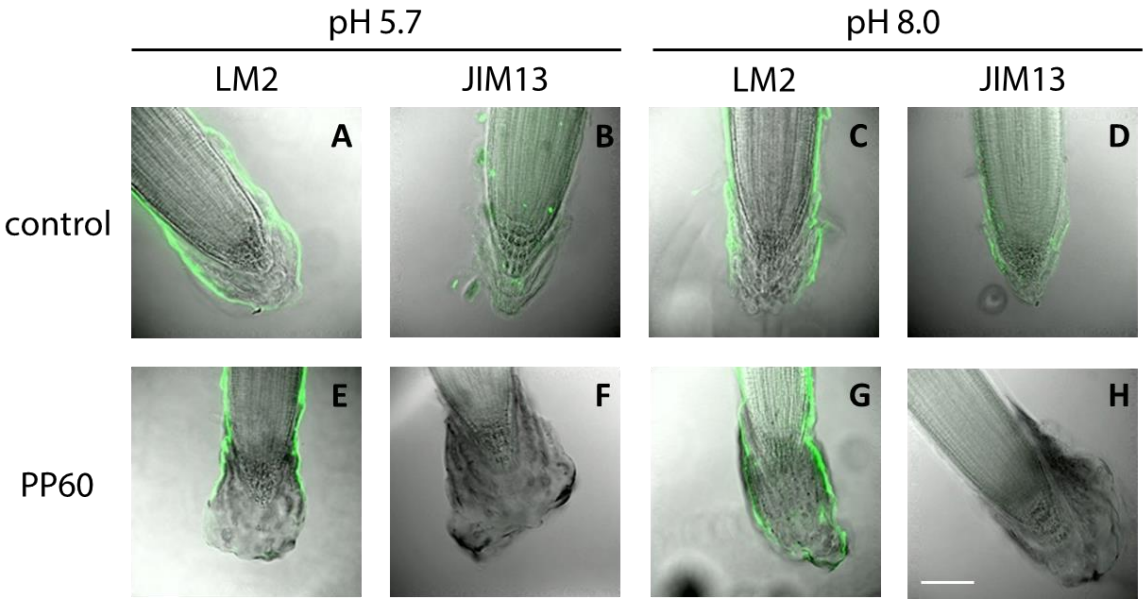

Figure 6.13. Immunofluorescence labelling of border-like cells (BLC) with mAb LM2 and JIM13 after PP60 (50 µg/mL) and pH treatment. Representative micrographs of fixed root tips of wild-type plants stained with LM2 (A, E, C, G) for control (A), PP60-treated roots (E), plants grown on pH 8.0 (C), PP60-treated at the same pH (G), and stained with JIM13 (B, F, D, H) for control (B), PP60-treated roots (F), plants grown on pH 8.0 (D), PP60-treated at the same pH (H) from two independent experiments (each n>5).

6.2.2.3 Extensin immunolabelling

Labelling with mAb LM1 specific for extensin occurred around cell walls and mucilage of plants grown in normal conditions (**Fig. 6.14 A**). The staining intensity was higher under more basic pH conditions (**Fig. 6.14 B**). After PP60 treatment there was no change in labelling for both conditions (**Fig. 6.14 C, D**).

Together, the immunolabelling findings demonstrate that border-like cells and mucilage from plants grown on more basic pH have more de-esterified and fewer methylesterified HG epitopes. Additionally, they have more extensin epitopes. Addition of PP60 caused the occurrence of less methyl- and de-esterified HG epitopes in both pH conditions and disappearance of AGP2 epitopes under pH 8.0 conditions.

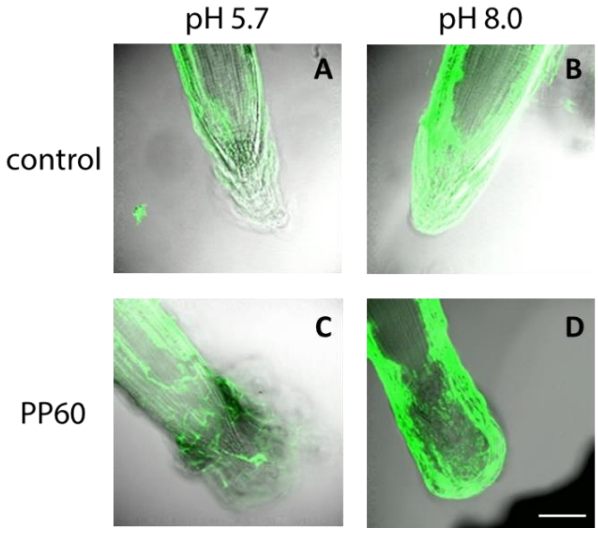

Figure 6.14. Immunofluorescence labelling of border-like cells (BLC) with mAb LM1 after PP60 (50 µg/mL) and pH treatment. Representative micrographs of fixed root tips of wild-type plants stained with LM1 for control (A), PP60-treated roots (C), plants grown on pH 8.0 (B), PP60-treated at the same pH (D) from two independent experiments (each n>5).

6.3 Discussion

It has been shown that loss of adhesion causing release of single border-like cells was due to reduced amounts of homogalaturonan (HG) (Durand et al., 2009). The cell walls of *qua1-1* and *qua2-1* had a 25% and 50% reduction, respectively, in HG content (Mouille et al., 2007). The results shown in this section clearly demonstrate a similar phenotype to that of the *qua1-1* mutant. PP60 acting as the PME activity enhancer indirectly influences the HG composition. PMEs show two different modes of action: blockwise and non-blockwise (Wolf and Greiner, 2012). Blockwise fashion creates long blocks of demethylesterified HG which then can be cleaved by degrading enzymes like polygalacturonases (PG). PG activity leads to formation of short chains of HG, oligogalacturonides (OGAs) which are suggested to play important roles in signalling pathways (Aziz et al., 2004). The activity of PGs allows the hydrolysis of polygalacturonic acid and it is detected several hours before border cell dissociation from the root in pea plants (Stephenson and Hawes, 1994). The activity is localized in the root cap but not in the border cells already released from it. These findings implicate PG activity in border cell separation and suggest that enzyme synthesis and activity are regulated during border cell differentiation. Border-like cell separation together with PG activity increases observed after PP60 addition suggest the involvement of this enzyme in border-like cell detachment from the root cap. Increased PME activity leaves HG more vulnerable to PG activity thus allowing it to degrade the gel matrix which tightens cell wall components. As a result, cells separate from each other as in the observed phenotype. It has been shown that *Arabidopsis* BLCs

remain clustered together and may not be programmed to separate from each other (Vicré et al., 2005). The decrease of PG activity showed before (Stephenson and Hawes, 1994) and no *AUX1* expression and the existence of non-viable border-cells shown here, suggest that BLCs may undergo programmed cell death (PCD) after release and separation from each other following PP60 treatment. In the future BLCs could be marked with fluorescein diacetate (FDA) which allows a distinction to be made between cells that have died necrotically without activating PCD or those that have undergone PCD (Reape et al., 2008). The degradation of HG by PGs seems to be one of the explanations for cell separation and mucilage production. However, PME might also indirectly activate other cell wall-degrading enzymes that function at low pH, such as galactosidases and arabinosidases.

An increase in pH in combination with PP60 addition may inhibit different sets of PMEs and those acting in blockwise fashion seem to be still active and overexpressed. Moreover, demethylation may occur without the activity of enzymes, in alkaline conditions (Renard and Thibault, 1996). It has been shown that pH 7.5 conditions produce longer demethylated blocks than in pH 4.5 conditions (Cameron et al., 2008). The presented results from pH 8.0 showed that border-like cells are more clustered together. The linear mode of action creates free carbohydrate groups which, in the presence of Ca^{2+} bind two adjacent HG chains making the cell wall stiffer and stronger. It seems that PME activity and different pH environments have distinct influences on the organization of border-like cells and production of mucilage.

Although the precise role of xylogalacturonan has not been established yet, it is suggested that it could be involved in the resistance to pathogen attack (Jensen et al., 2008, Willats et al., 2003). This assumption was based on the fact that substitution of galacturonan with xylose makes xylogalacturonan more resistant to the activity of endopolygalacturonases. During pathogen invasion, secretion of enzymes like endopolygalacturonases by the pathogen helps to degrade the plant cell wall. The presence of xylogalacturonan in mucilage of *qua* mutants suggests its possible role in resisting pathogens and providing protection for the roots. Interestingly only a low level of xylogalacturonan epitopes were detected in PP60 treated plants suggesting that the root response to PP60 may not be related to the pathogen response. It has been shown that alteration of biosynthesis and incorporation of arabinogalactan proteins to the cell wall induces a significant reduction in the binding of rhizobacteria to border-like cells and the root cap (Vicré et al., 2005). Additionally, incubation of *Arabidopsis* roots with β-glucosyl Yariv, an agent known to bind arabinogalactan proteins, inhibits attachment and transformation by *Agrobacterium tumefaciens* (Nam et al., 1999, Gaspar et al., 2004). Therefore, it is suggested that arabinogalactan proteins may function in binding and possibly recognition of microorganisms. The absence or low level of arabinogalactan

proteins in the mucilage of PP60 treated roots supports the statement that secretion and detachment of border-like cells is not caused by activation of the plant pathogen response. Durand, et al., 2009 suggested that the *qua1-1* border-like cells phenotype could be caused by an increase in the *de novo* synthesis of xylogalacturonan and arabinogalactan proteins due to the lack of HG. In the case of PP60-treated plants there is probably no change in HG content, thus xylogalacturonan/arabinogalactan proteins are less abundant in the mucilage. The mucilage released after PP60 addition in which the cells are trapped and kept in the vicinity of the root tip must be further examined to establish their composition. These findings indicate that pectin methylesterases are involved in the maintenance of adhesion between border-like cells in *Arabidopsis* and show that the loss of cell-to-cell contact is not necessarily accompanied by secretion of substantial amounts of arabinogalactan-proteins and xylogalacturonan-containing mucilage.

7. Metabolomics of *Arabidopsis* seedlings in response to cellulose biosynthesis inhibition

7.1 Introduction

The plant cell wall is a complex composite structure that is involved in a number of biological processes, including plant-microbe interactions and the control of cell shape. Different types of cell wall damage (CWD) cause a wide range of responses, including enhanced pathogen resistance, increased production of jasmonic acid (JA) as well as changes in neutral cell wall sugars and carbohydrate metabolism (Hamann, 2015b, Hamann, 2015a, Höfte, 2015). Adaptation of the plant cell to CWD can also consist of ectopic lignin deposition and provides evidence for the existence of a dedicated cell wall integrity (CWI) maintenance mechanism (Denness et al., 2011). CWD probably generates a large number of different chemical signals (ligands), based on the large number of plant cell wall components. Around 50% of the primary cell wall consists of pectic polysaccharides (Zablackis et al., 1995). Some of these polysaccharides, homogalacturonan (HG) and rhamnogalacturonan II (RGII) are connected by calcium bridges between dimethylesterified parts of the molecules or through borate ester linkages (RG-II). HG and RG-II are targeted by pathogen-derived cell wall degrading enzymes (polygalacturonases), which generate oligogalacturonides (OGAs) (Ferrari et al., 2008). These biologically active OGAs are short oligomers of galacturonic acid that can function as signalling molecules activating pathogen defence mechanisms (Hamann, 2012). However, their mode of action is not well understood (see more in **chapter 1.6**).

7.1.1 Isoxaben as a tool for characterization of cellulose biosynthesis inhibition

Cellulose is the main load-bearing element of plant cell walls. The cellulose biosynthesis inhibitor isoxaben is a well-established tool for characterization of cellulose production and is known to cause cell wall damage (CWD) by weakening the plant cell walls thus allowing studies of the plant cell wall integrity (CWI) maintenance mechanism (Hamann, 2012). Previously, DNA microarrays have been used to determine the response of the transcriptome to isoxaben treatment (Hamann et al., 2009). More than half of isoxaben-induced genes are also upregulated by treatment of plants with ozone, wounding,

bacterial elicitors, Yariv reagent, chitin and H_2O_2 (Manfield et al., 2004a). These results suggest that isoxaben treatment also affects transcription of genes involved in biotic and abiotic stress responses and highlight the fact that the cell wall is involved in all these biological processes. Several genes implicated in cell wall reinforcement change their expression levels during isoxaben treatment, such as genes encoding members of the pectin esterase family and a pectin acetylesterase. This indicates that calcium-mediated cross-linking of HG may compensate for the disrupted cellulosic network (Manfield et al., 2004a). One conclusion from the observations is that inhibition of cellulose biosynthesis leads to changes in the activity levels of genes required for modification of other cell wall components. This is further supported by the observation that cellulose biosynthesis inhibition produces increased levels of HG domains within the pectic matrix (Díaz-Cacho et al., 1999).

7.1.2 Isoxaben-resistance mutants

Arabidopsis ixr1 mutants show resistance to isoxaben caused by the amino acid changes in the CESA3 cellulose synthase. Both mutations corresponding to *ixr1-1* and *ixr1-2* cause amino acid substitution in a region near the C-terminus of the protein (Scheible et al., 2001). The *IXR1* gene appears to be expressed more highly in roots than shoots. One of the explanations for the resistance of *ixr1-1* plants to isoxaben is that the regions of amino acid substitution are in or around proposed transmembrane helices which are critical for formation of a pore for glucan chain secretion. The hydrophobic herbicides may bind to this region and disrupt pore formation (Scheible et al., 2001).

IXR2 has been shown to encode cellulose synthase isoform, CESA6 and the *ixr2-1 Arabidopsis* mutant has a substitution of a highly conserved amino acid close to the C-terminus. The substitution removes a positive charge at the end of the last predicted membrane spanning domain. This may cause a change in the membrane topology of the protein due to a conformational change, which may prevent the binding of isoxaben or isoxaben-associated proteins (Desprez et al., 2002). Seedlings homozygous for *ixr2-1* grown in dark with isoxaben showed an increased tolerance to the herbicide as shown by the lack of inhibition of hypocotyl and root growth compared to wild type plants (Desprez et al., 2002).

Both, *ixr1-1* and *ixr2-1* carry mutations close to the C-terminus of the CESA protein suggesting that this region is targeted by the herbicide. In both alleles, the mutated amino acid is far downstream from the catalytic site, which makes it unlikely that the compound

binds to the active site residues. Isoxaben could block the interaction between CESA subunits and in this way destabilize the rosette or each particle that constitutes the rosette.

7.1.3 Metabolomics

Metabolomics is a highly efficient tool that if used together with proteomics and transcriptomics and can reveal novel insights into the mechanisms mediating the response to CWD via pectins and maintenance of CWI. The conventional untargeted metabolomics approach is based on two steps. In the first one data is collected and processed to find features of interest. Next data is re-acquired and collected MS/MS information is used for metabolite identification and manual database searching (Alonso et al., 2015).

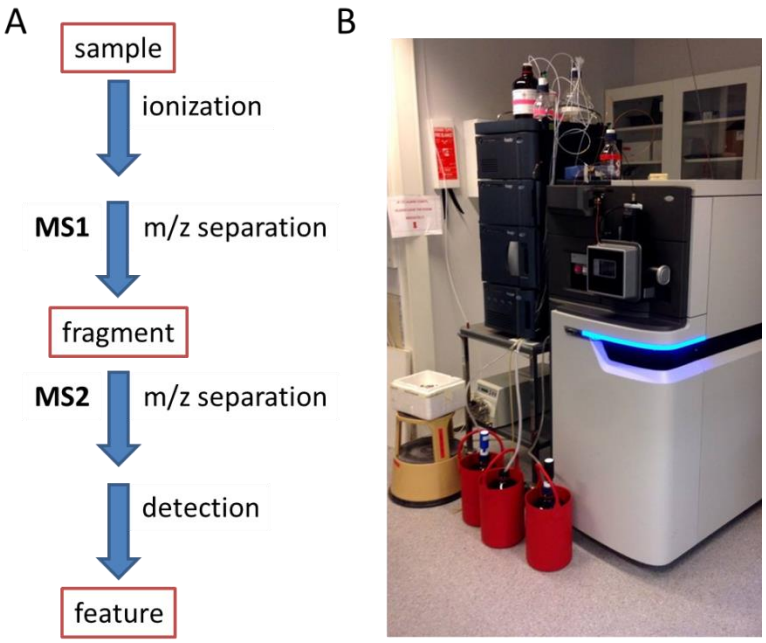

Figure 7.1. Schematic of mass spectrometry workflow used in the experiments. (A) The sample undergoes an ultra-pressure liquid chromatography (UPLC) *en route* to the ionisation source. Once inside the ionisation source, the separated sample molecules are ionised using electrospray ionisation (ESI) for easier manipulation. Traditionally, tandem MS uses two mass spectrometers in tandem. Precursor ions selected by MS1 collide with high pressure helium in the cell and undergo fragmentation. The resulting daughter ions are analysed in MS2. (B) the Waters UPLC-Synapt HDMS machine used in the experiments.

It is not possible for untargeted metabolomics to move onto pathway and network analysis without knowing the identity of metabolites. After ionisation of molecules and scanning in the spectrometer (**Fig. 7.1**), the spectral peaks are extracted, quantified and aligned into a feature table. At this point, each feature is identified by a mass-to-charge ratio (m/z) and retention time in chromatography, but its chemical identity is not known. The tandem mass spectrometry is needed to identify a metabolite from spectral features by the

fragmentation pattern of a specific feature (Honour, 2011). Therefore, considerable effort is required to build a spectral library, which is often of limited size. Databases from different platforms often do not match, thus metabolite identification forms the bottleneck of untargeted metabolomics.

7.1.4 Experimental approach to metabolome analysis after isoxaben treatment

Sugars, similar to hormones, can act as primary messengers and regulate expression of genes involved in carbohydrate metabolism. The *Arabidopsis* mutant, *hsr8* (*high sugar response8*) exhibits increased starch and anthocyanin production and reduced chlorophyll content after glucose treatment. The *HSR8* gene is allelic to *MURUS4* (*MUR4*) which is required for arabinose synthesis. The sugar-hypersensitive phenotype of *hsr8/mur4* is rescued after boric acid treatment, suggesting that alterations in the cell wall (in this case, RGII dimer composition) cause hypersensitive sugar-responsive phenotypes (Li et al., 2007). The Hamann lab has shown that isoxaben induced JA and lignin production is dependent on the presence of hexoses in the media. Non-metabolizable sucrose and glucose can act as signalling molecules or as osmolytes to maintain cell homeostasis (Gupta and Kaur, 2005). Thus, treatment with isoxaben and sucrose may change responses to CWD and partially rescue the cell wall composition.

While induction of stress response mechanisms by isoxaben has been characterized to some degree very little is known about the effects of isoxaben on carbohydrate metabolism. The findings presented above strongly indicate that hexoses and CWD cause changes in cell wall composition/structure, activate stress response mechanisms and induce changes in carbohydrate metabolism. Previously the Hamann lab has performed a transcriptomics based analysis of gene expression changes in *Arabidopsis thaliana* seedlings grown in liquid culture providing basic insights into the response to isoxaben treatment. The liquid culture system allows tight control of environmental conditions and uniform application of the inhibitor. In the experimental design seedlings were grown using the same experimental set up in media +/- sucrose, + starvation and +/- isoxaben (**Fig. 7.2**). In addition to Col-0, *ixr1-1* seedlings will also be grown. This mutation provided an excellent control to ensure specificity of the results generated. Samples were collected during a time course series, at the start of treatment and after 0, 3, 6, 9 and 12 h of isoxaben treatment. This design ensured that the dynamic metabolic changes and complex interactions between metabolic pathways involved in response to CWD could be detected.

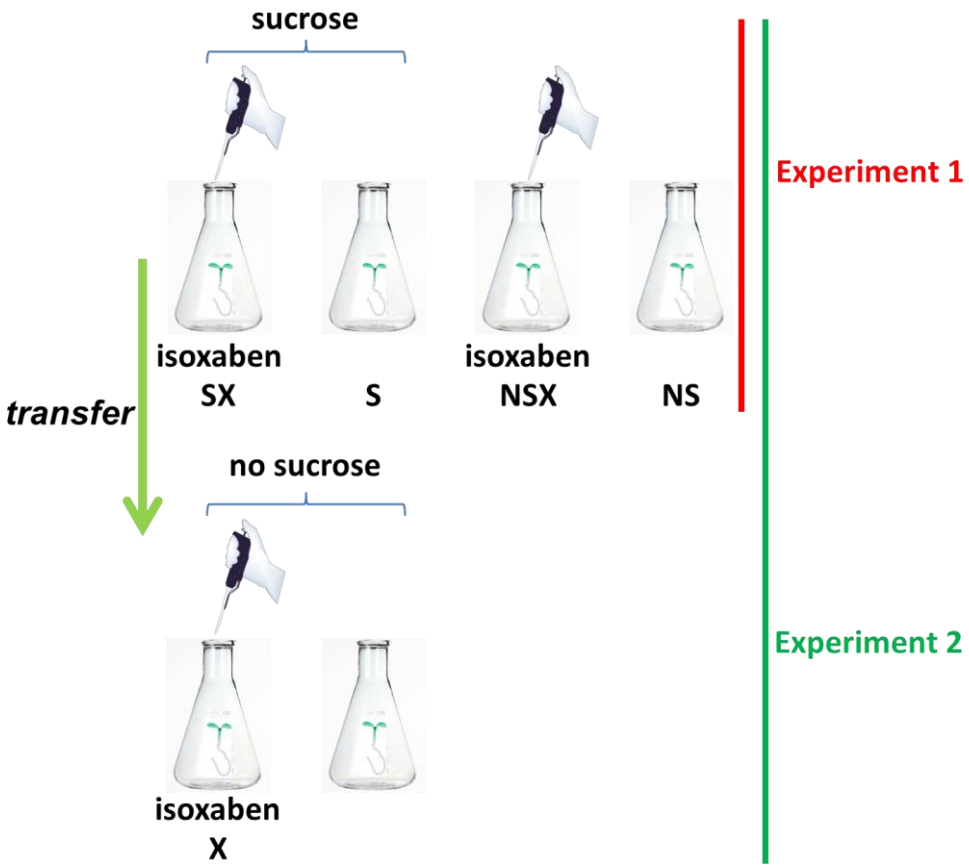

Figure 7.2. Experimental approaches for isoxaben/sucrose/starvation treatments. In the experiment 1 seedlings were grown in media with sucrose (S) and without (NS) plus isoxaben (SX; NSX). In the experiment 2 the seedlings grown in flasks with sucrose (S) and with isoxaben (SX) were transferred after 6 days to media without sucrose and with isoxaben (X). Samples were collected at 0, 3, 6, 9, 12, and 24 hours' time points. Plant materials used in the experiments were seedlings of Arabidopsis thaliana Col-0 (C) and *ixr1-1* (R).

However, it is not known how CWD caused by cellulose biosynthesis inhibition affects metabolites nor do we know how the presence of hexoses modifies these responses. In order to dissect the underlying regulatory mechanisms and to understand the function of hexoses a systematic metabolic profiling was performed (**Fig. 7.3**).

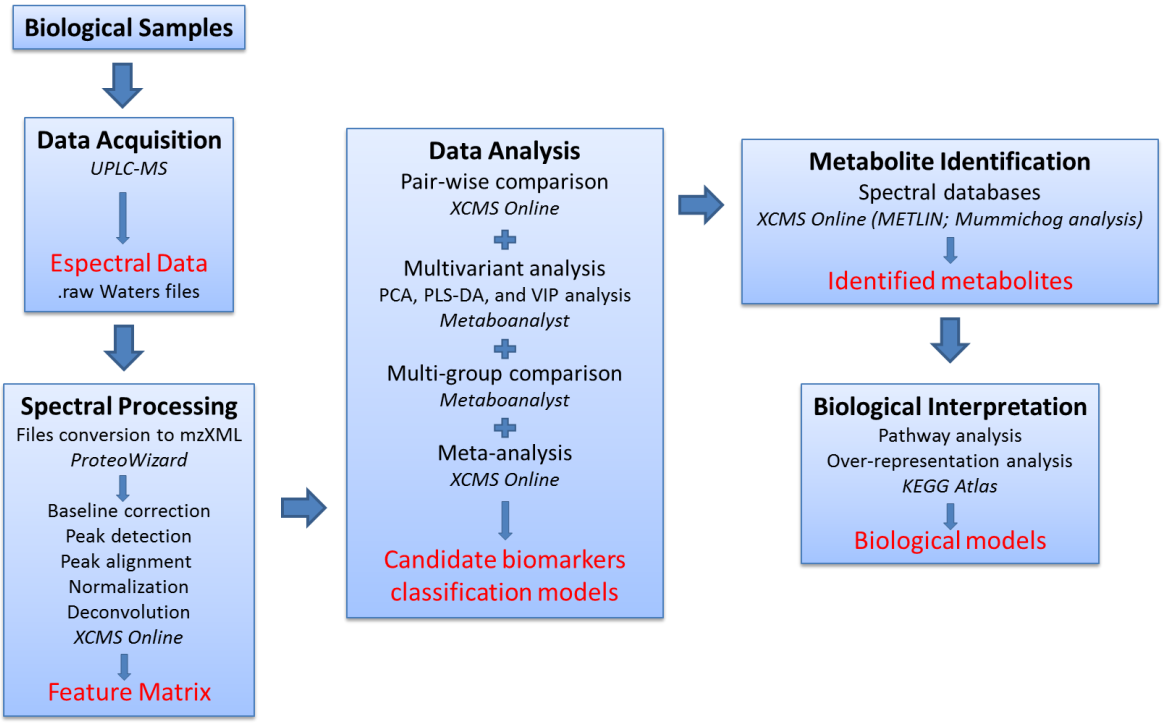

Figure 7.3. Analysis workflow in untargeted metabolomics of *Arabidopsis* seedlings treated with isoxaben. This figure shows the different steps of the metabolomic analysis pipeline.

7.2 Results

7.2.1 Principal component analysis

To investigate and characterise whether changes in cell wall and carbohydrate metabolism after CWD is caused by isoxaben, time course experiments with *Arabidopsis thaliana* seedlings were performed. The seedlings were grown in media with and without sucrose, and mock- and isoxaben-treated in one experiment, and with sucrose and transferred to media without sucrose (starvation stress) plus isoxaben in second experiment, with the samples being analysed by ultra-performance liquid chromatography-mass spectrometry (UPLC-MS). Principal Component Analysis (PCA) and Partial Least Squares Discriminant Analysis (PLS-DA) of the UPLC-MS metabolite data from sucrose, sucrose+isoxaben, and non-sucrose/isoxaben plants showed that their metabolite profiles differed substantially (**Fig. 7.4**). Comparing the sucrose, no sucrose and isoxaben treatment, quantitative non-targeted metabolomics profiling identified distinct differences in Col-0 by PCA and PLS-DA analysis (**Fig. 7.4 A, B**). In both analysis, the principal component 1 accounted for 56% of the differences between sucrose and no sucrose treatment. There was no separation between data points of samples with isoxaben in sucrose and no sucrose suplemented media comparted to those without isoxaben. Compared to the same treatments in mutant *ixr1-1*, metabolomics non-targeted profiling identified similar patterns by PCA and PLS-DA analysis (**Fig. 7.4 C, D**, respectively). Between 50.9 and 51.1% of differences between sucrose and no sucrose accounted for the variability described by principal component 1. Like the analysis of Col-0 compared between isoxaben treatments, there was no difference in treatment with and without isoxaben in each of sugar suplementation. The comparisons of Col-0 to *ixr1-1* in all the conditions were performed to demontrate possible differences between wild type and isoxaben-resistance mutant plants. PCA analysis showed no difference between genotypes in sucrose and no sucrose treatments regardless of isoxaben treatment (**Fig. 7.4 E**). The differences Col-0 and *ixr1-1*, independent of isoxaben treatment, were determined when PLS-DA analysis between Col-0 and *ixr1-1* were combined (**Fig. 7.4 F**). Identified differences in Col-0 and *ixr1-1* were as expected, due to the different genetic background. Each point on graph represented the mean value of three biological replicates from two independent experiments.

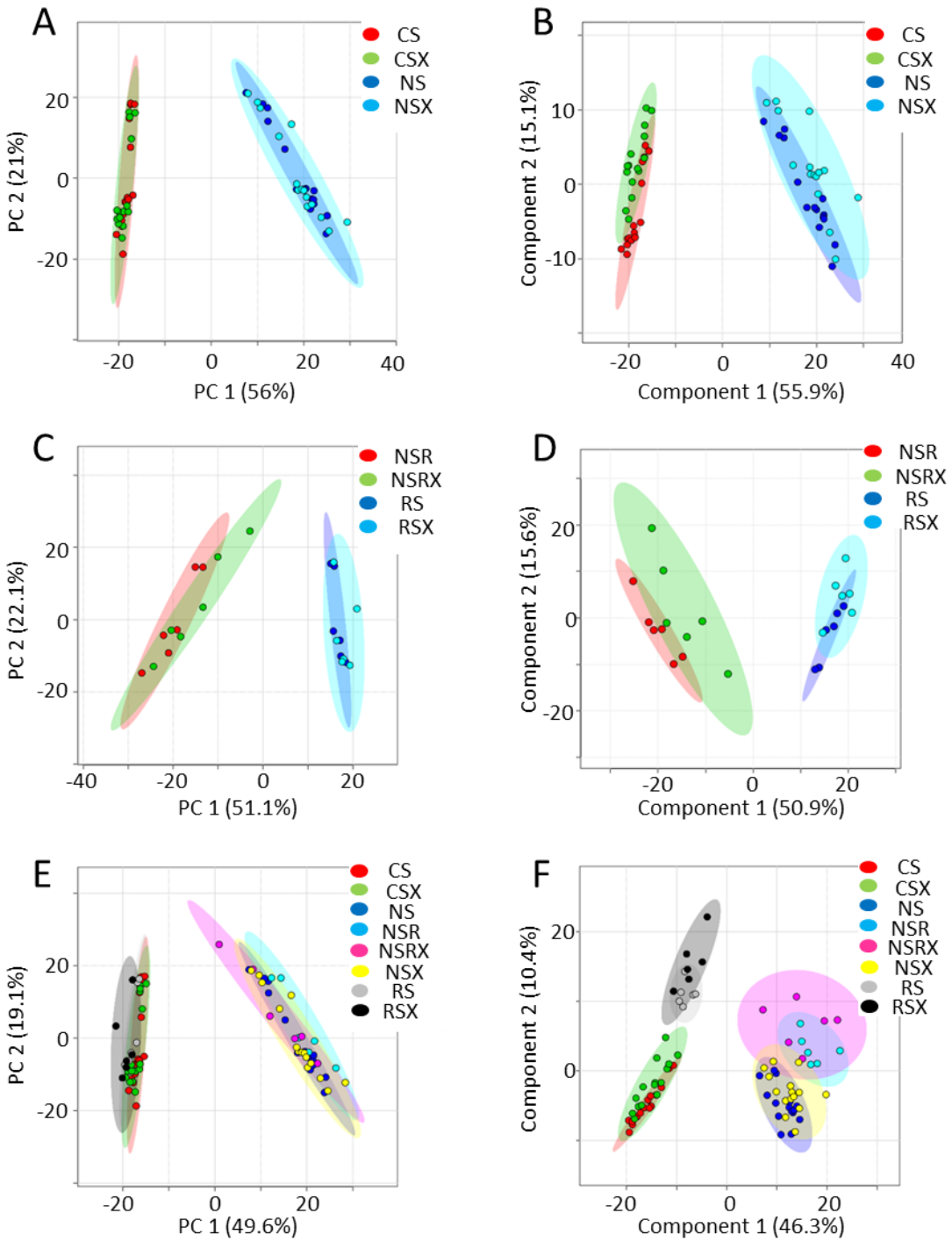

Figure 7.4. The metabolomic profiles of Col-0 and *ixr1-1* are significantly different after sucrose treatment. Principal Component Analysis (PCA) illustrating the unsupervised relationship between sucrose and no sucrose plus isoxaben treatment compared between A Col-0, C *ixr1-1*, and E combined Col-0 and *ixr1-1*. Partial least squares discriminant analysis (PLS-DA) score visualizes supervised clustering of sucrose and no sucrose plus isoxaben treatment compared between B Col-0, D *ixr1-1*, and F combined Col-0 and *ixr1-1*. Data points that are closer together indicate higher degree of similarity than data points that are further apart. Each dot represents the average of three biological replicates for different time points (0, 3, 6, 9, and 12h) and treatment; NS – no sucrose Col-0; NSX – isoxaben Col-0; CS – sucrose Col-0; CSX – sucrose+isoxaben Col-0; NSR – no sucrose *ixr1-1*; NSRX – isoxaben *ixr1-1*; RS – sucrose *ixr1-1*; RSX – sucrose+isoxaben *ixr1-1*.

The analysis was performed for the starvation stress experiment similarly to that of the sucrose and isoxaben treatment. Comparing the sucrose, starvation, and isoxaben treatment, non-targeted metabolomics profiling identified similarities and differences in Col-0 by both PCA and PLS-DA analysis (**Fig. 7.5 A, B**). In both analyses, the principal component 1 accounts for less than 20%, suggesting the differences between sucrose and starvation stress are less prominent compared to the absence of sugar. Compared to the same treatments in *ixr1-1*, metabolomics non-targeted profiling identified similar patterns by PCA and PLS-DA analysis (**Fig. 7.5 C, D**, respectively). Between 13.6 and 23.6% of differences between sucrose, starvation, and isoxaben treatment accounted for the variability described by principal component 1. PCA analysis clearly showed data points accumulated in one region suggesting these points are the time point of 0 where all the samples were subjected to the same treatment (sucrose addition) (**Fig. 7.5 C**). Later data points separated from each other in different directions according to given treatment. The comparisons of Col-0 to *ixr1-1* in all the conditions were performed to demonstrate possible differences between wild type and isoxaben-resistance mutant plants. PCA analysis showed no difference between genotypes in sucrose and no sucrose treatments regardless of isoxaben treatment (**Fig. 7.5 E**). The differences Col-0 and *ixr1-1* have independent of isoxaben treatment were determined when PLS-DA analysis between Col-0 and *ixr1-1* were combined (**Fig. 7.5 F**).

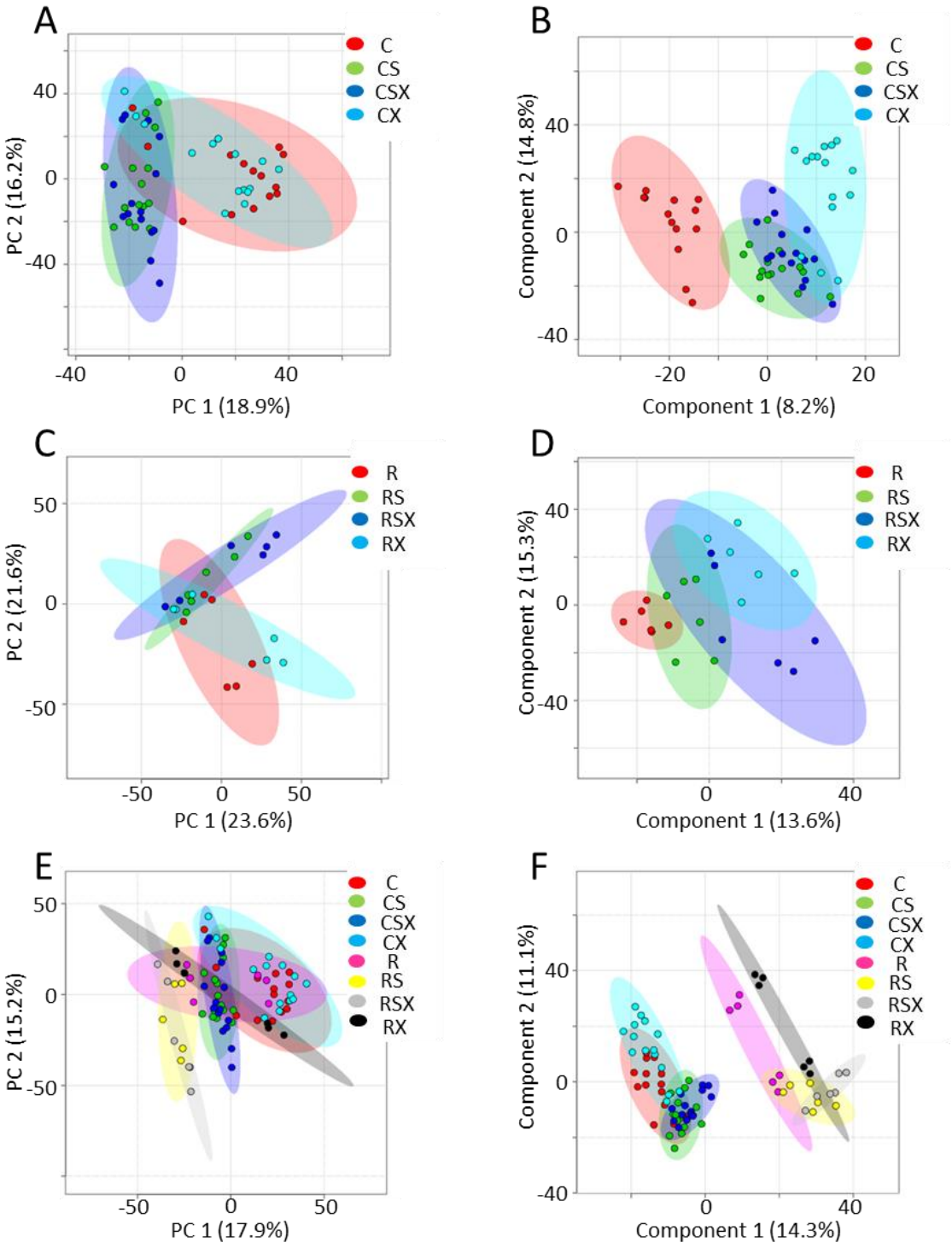

Figure 7.5. The metabolomic profiles of Col-0 and *ixr1-1* are significantly different during starvation stress. Principal Component Analysis (PCA) illustrating the unsupervised relationship between sucrose and starvation plus isoxaben treatment compared between A Col-0, C *ixr1-1*, and E combined Col-0 and *ixr1-1*. Partial least squares discriminant analysis (PLS-DA) score visualizes supervised clustering of sucrose and starvation plus isoxaben treatment compared between B Col-0, D *ixr1-1*, and F combined Col-0 and *ixr1-1*. Data points that are closer together indicate higher degree of similarity than data points that are further apart. Each dot represents the average of three biological replicates for different time points (0, 3, 6, 9, and 12h) and treatment; C – no sucrose Col-0; CX – isoxaben Col-0; CS – sucrose Col-0; CSX – sucrose+isoxaben Col-0; R – no sucrose *ixr1-1*; RX – isoxaben *ixr1-1*; RS – sucrose *ixr1-1*; RSX – sucrose+isoxaben *ixr1-1*.

7.2.2 Comparison of metabolic phenotypes for each treatment and genotype

To identify the metabolites responsible for the separation between the samples, the raw data obtained from MS was analysed using XCMS Online. The number of changing features in *Arabidopsis* seedlings that fulfilled the selection criteria for significant treatment-dependent differences is shown in **Table 7.1**. They clearly demonstrate that there are more significant changes in metabolite profiles in the media additionally supplemented with sucrose or during starvation stress.

Table 7.1 Changes in metabolites after sucrose treatment, starvation stress plus isoxaben treatment in both (p-value ≤ 0.01; fold change ≥ 1.5). The table shows the number of features changing over time after adding isoxaben to the seedlins culture with/without sucrose and starvation stress in Col-0 and *ixr1-1*.

Treatment	Genotype	Total number of features	Number of features (p-value ≤ 0.01; fold change ≥ 1.5)
sucrose	Col-0	19806	695
	ixr1-1	20438	1032
sucrose + isoxaben	Col-0	18365	224
	ixr1-1	18708	213
no sucrose + isoxaben	Col-0	19476	165
	ixr1-1	19913	216
starvation	Col-0	6009	104
	ixr1-1	49760	604
starvation + isoxaben	Col-0	56817	218
	ixr1-1	50980	317

When the filtered metabolic responses were visualized in a mirror plot (**Fig. 7.6**) the isoxaben (**Fig. 7.6 E-J**) and non-isoxaben (**Fig. 7.6 A-D**) samples clearly showed a difference at the retention time around 6.28 minutes in both, Col-0 and *ixr1-1*, but the differences were more prominent in Col-0 (**Fig. 7.6 E, G, I**; blue circle).

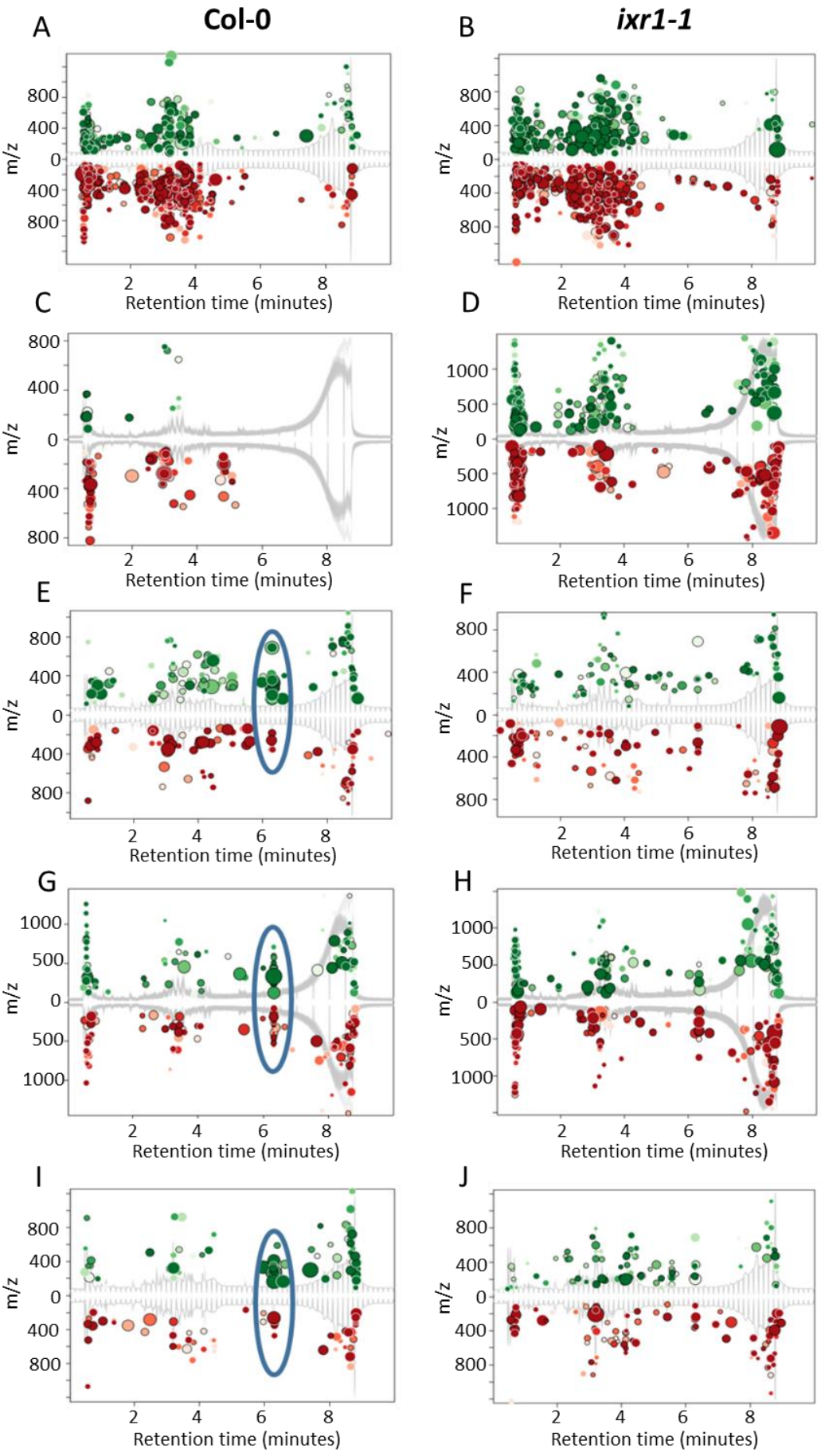
A
Col-0
B
ixr1-1
C
D
E
F
G
H
I
J
m/z
Retention time (minutes)

(previous page) Figure 7.6. Effect of sugar, isoxaben and both together on *Arabidopsis* seedlings. The mirror plot on total ion chromatogram (TIC) displays features whose intensities are altered between sample groups. Natural occurring variations in metabolites levels in Col-0 (A, C, E, G, I) samples are compared to variations in *ixr1-1* (B, D, F, H, J). Each genotype was treated with sucrose (A, B), starvation stress (C, D). Moreover, isoxaben was added to treatment with sucrose (E, F), starvation stress (G, H) and without sucrose (I, J). The higher level of metabolites is shown in green and the lower in red. P-value is represented by how dark or light the colour is. Fold change is represented by the radius of each feature. The main difference between treatments and genotypes is circled blue.

7.2.3 Meta-analysis of isoxaben treatment in samples with and without sucrose

Although the pairwise comparisons of each time point with its respective control resulted in hundreds of altered metabolite features in total, it was suspected that at least some of these molecules may be involved in triggering a specific response to cellulose biosynthesis inhibition. Meta-analysis objective is to identify the shared pattern of metabolic response to stress or treatment. The common pattern of isoxaben response in Col-0 and *ixr1-1* was identified by meta-analysis (**Fig. 7.7**). Simple pairwise comparisons of each genotype under sucrose and no sucrose conditions together with isoxaben treatment resulted in 36 disregulated metabolite features of statistical significance in Col-0 (**Fig. 7.7 A**) and *ixr1-1* (**Fig. 7.7 B**). Comparison of four pair-wise isoxaben-treated jobs between Col-0 and *ixr1-1* resulted in 1137 aligned features. As shown in the Venn diagram, by using meta-analysis the number of unique metabolites which were significantly altered in both genotypes regardless of sugar addition was reduced to four in case of Col-0 and twenty in the *ixr1-1*, when subjected to isoxaben treatment (**Fig. 7.7 C**).

The characteristic metabolites corresponding to a retention time around 6.29 minutes are shown in **Table 7.2**. Only one of the features at m/z of 261.07 was downregulated and the rest upregulated in which features 204.07, 165.06, and 272.09 m/z had more than a 20-fold change (**Table 7.2**).

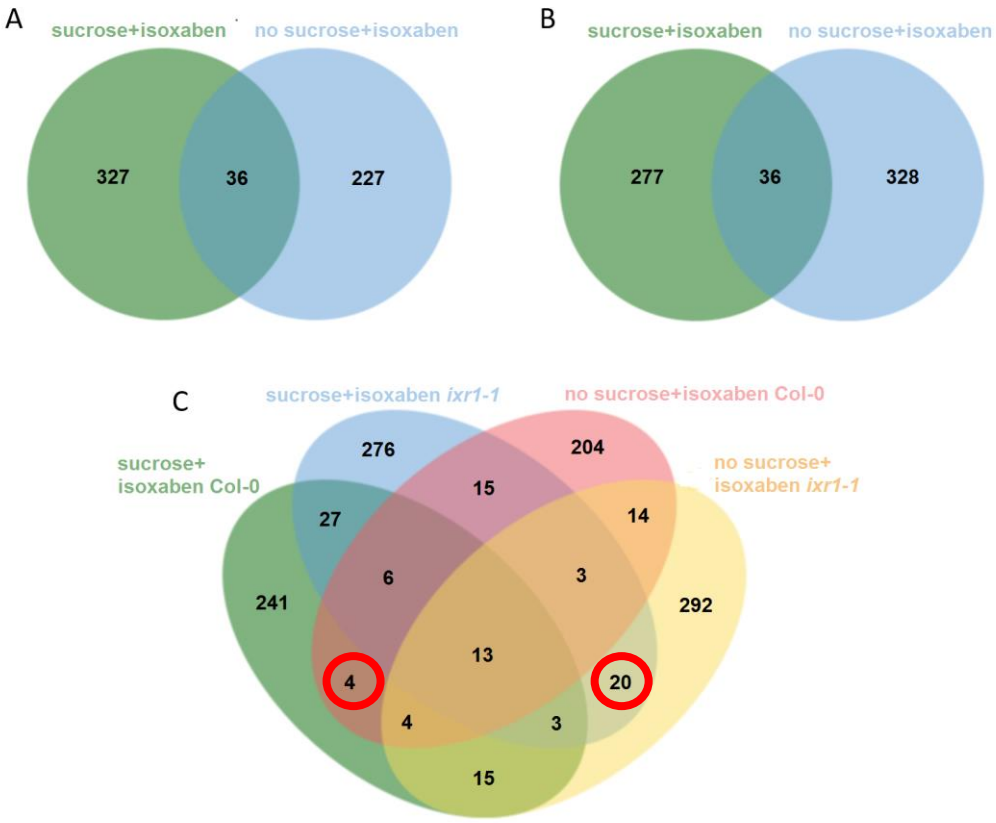

Figure 7.7. Meta-analysis of the isoxaben response across Col-0 and *ixr1-1* with or without sucrose. The results of two-group comparisons between Col-0 (A) and *ixr1-1* (B) showing the same amount of features changing after sugar addition in each genotype. Shared patterns of response of both treatments for each genotype are characterized by significant up-regulation ($p < 0.01$) of four metabolites for Col-0 and twenty for *ixr1-1* displayed in the Venn diagram (red circle).

Table 7.2 Metabolites shared between Col-0 and *ixr1-1* grown with and without sucrose after isoxaben treatment. The metabolite downregulated are shown in red.

m/z	retention time	sucrose		no sucrose	
		Col-0	*ixr1-1*	Col-0	*ixr1-1*
238.05	6.28	2.78037	2.898607	6.703125	3.76628
261.07	6.29	-7.37744	-8.55126	-17.7378	-5.21935
355.56	6.29	2.399779	2.247859	3.316914	2.983582
204.07	6.29	22.0116	35.12039	27.72891	35.00283
250.07	6.27	6.775	4.587419	8.424526	6.992244
205.08	6.29	3.22156	4.171605	5.124784	4.309806
166.07	6.29	2.900078	3.301169	3.416644	4.582199
165.06	6.29	21.24419	26.06012	46.89367	39.74384
342.17	6.00	2.309265	2.549717	2.607262	3.152267
417.01	6.28	6.108984	5.697595	8.452372	2.215975
150.04	6.29	5.168557	4.3544	7.042809	6.84345
317.08	6.29	4.285913	5.577915	8.674106	7.51004
272.09	6.29	15.74336	22.79089	17.7002	9.9491

7.2.4 Identification of sugar and isoxaben treatments biomarkers

Identifying and validating biomarkers from high-throughput metabolomics data is important for understanding the molecular basis underlying biological processes. Typically, candidate biomarkers are identified as features that are differentially expressed between two or more classes of samples. Many feature selection metrics rely on ranking by some measure of differential intensity. Here, the variable importance in projection (VIP) analysis was used. VIP coefficients reflect the relative importance of each metabolite for each treatment in the prediction model. VIP thus represents the importance of each metabolite in fitting both the metabolite and treatment variates. VIP allows classifying the metabolites according to their explanatory power of treatment. Predictions with a VIP larger than 1 are the most relevant for explaining treatments. VIP analysis identified the top 15 metabolites that differed between sucrose supplementation (**Fig. 7.8 A, B**) and starvation stress (**Fig. 7.8 C, D**) in the control groups. Analysis of both Col-0 (**Fig. 7.8 A, C**) and *ixr1-1* (**Fig. 7.8 B, D**) revealed that identified important features for Col-0 were sucrose and 7,8-dihydroneopterin 3'-triphosphate during sucrose starvation stress. Both of them had higher peak intensities after transferring to the media without sucrose. Neither of the metabolites could be identified for *ixr1-1*.

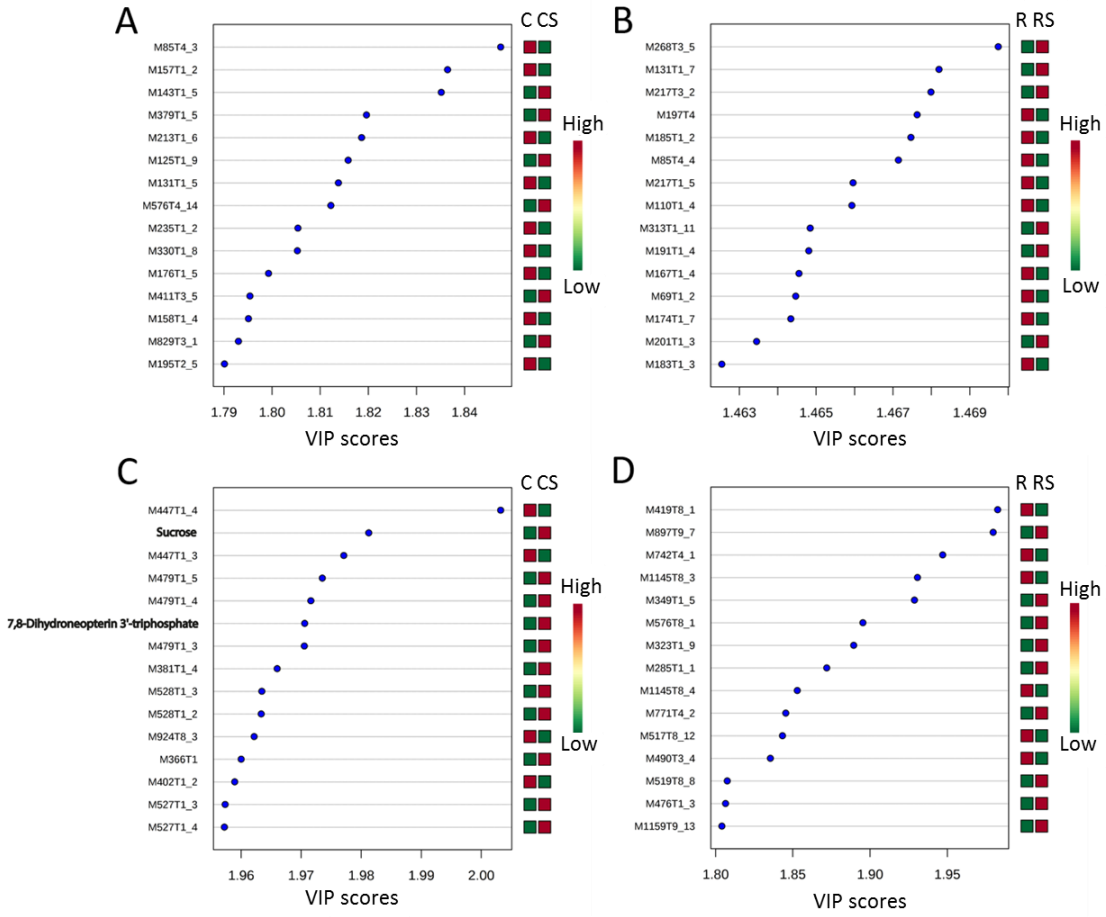

Figure 7.8. Variable importance in projection (VIP) plot of VIP statistical analysis identifying the top 15 metabolites contributing to the differences between Col-0 (A, C) and *ixr1-1* (B, D) together with different sugar availibilities: with sucrose (A, B) and during starvation stress (C, D). Relative concentration is shown to the right of each graph with red color indicating high concentration and green – low concentration. C – Col-0 control; R – *ixr1-1* control; CS – Col-0 sucrose/starvation treatment; RS – *ixr1-1* sucrose/starvation treatment.

Further analysis of the top 15 metabolites using a VIP that differentiated Col-0 grown on media with sucrose from the media with sucrose and isoxaben include biocytin and L-tyrosine (**Fig. 7.9 A**) which had higher peak intensity. During the sucrose starvation stress together with isoxaben treatment, biocytin, N2-succinyl-L-ornithine, and 3-(methylthio)propionic acid were upregulated (**Fig. 7.9 C**). Finally, no sucrose in the media but addition of isoxaben caused higher peak intensity of biocytin and L-tyrosine (**Fig. 7.9 E**). In case of *ixr1-1* mutant, N-(L-arginino)succinate was downregulated during sucrose starvation stress together with isoxaben (**Fig. 7.9 D**), and 6-Hydroxymelatonin downregulated during isoxaben-only treatment (**Fig. 7.9 F**). No identified features were found in sucrose and isoxaben treatment (**Fig. 7.9 B**). Comparison of the top 15 VIP hits between the three Col-0 analyses performed, biocytin was consistently found and represent differences not dependent upon the sugar availability, but specific for isoxaben treatment.

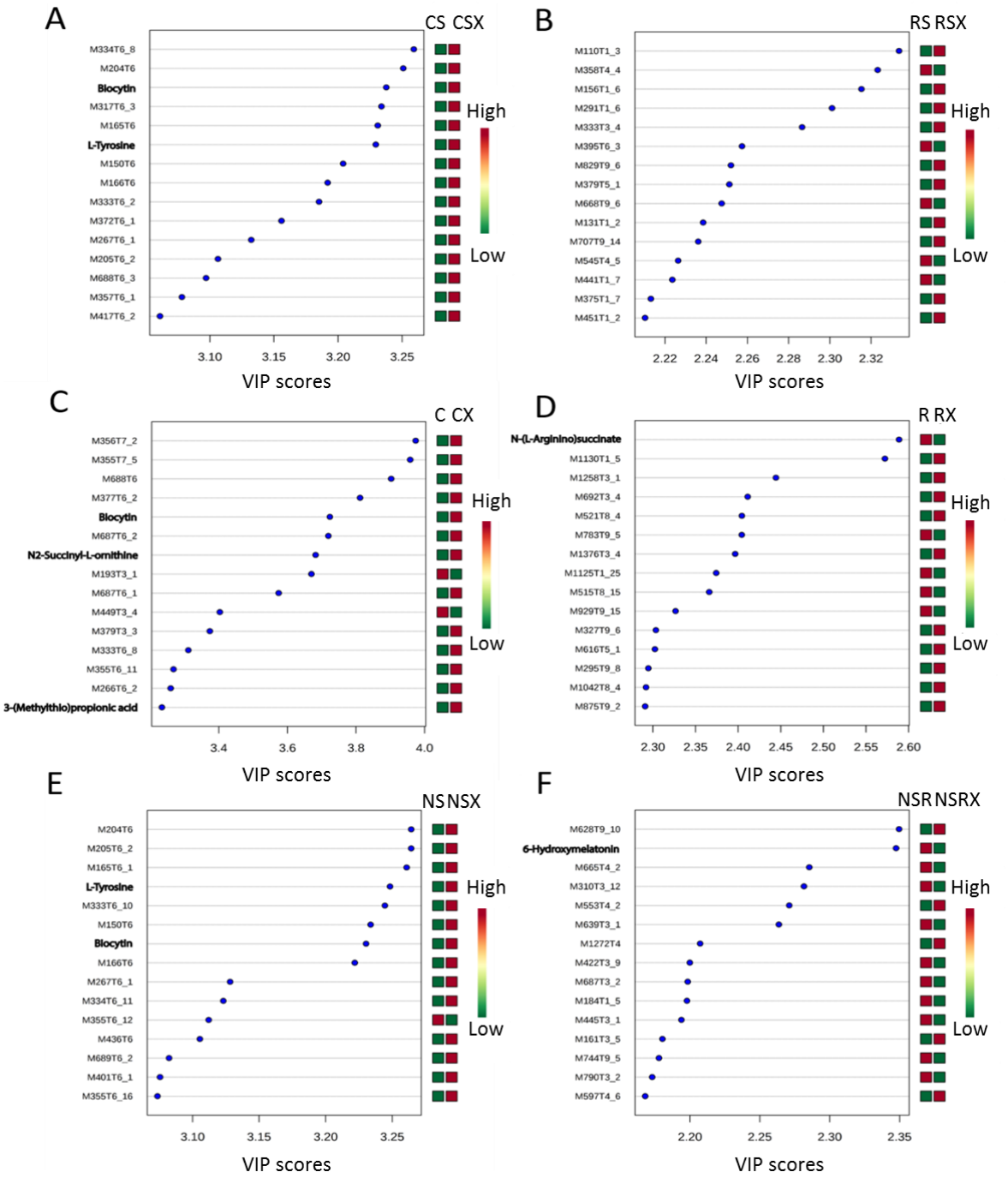

Figure 7.9 Variable importance in projection (VIP) plot of VIP statistical analysis identifying the top 15 metabolites contributing to the differences in isoxaben treatment between Col-0 (A, C, E) and *ixr1-1* (B, D, F) together with different sugar availibilities: with sucrose (A, B), during starvation stress (C, D) and without sucrose (E, F). Relative concentration is shown to the right of each graph with red color indicating high concentration and green – low concentration. CS – Col-0+sucrose; CSX – Col-0+sucrose+isoxaben; RS – *ixr1-1*+sucrose; RSX – *ixr1-1*+sucrose+isoxaben; C – Col-0+starvation; CX – Col-0+starvation+isoxaben; R – *ixr1-1*+starvation; RX – *ixr1-1*+starvation+isoxaben; NS – Col-0; NSX – Col-0+isoxaben; NSR – *ixr1-1*; NSRX – *ixr1-1*+isoxaben.

Biocytin is an intermediate in the metabolism of biotin and L-lysine (Picciocchi et al., 2001). An essential role for biotin is its attachment to the active site of carboxylases such

as acetyl-CoA carboxylase (ACCase), which catalyse carboxylation reactions in crutial metabolic processes such as the synthesis and catabolism of amino acids, fatty acids and isoprenoids (Nikolau et al., 2003). To further examine biocytin as a potential isoxaben treatment biomarker, box-plots (**Fig. 7.10 A, C, E**) with relative peak intensity for each isoxaben condition were created. It showed a clear difference between control and treatment conditions with biocytin being present after 3 hours of treatment and gradually rising in sucrose conditions (**Fig 7.10 A**) and remaining at the same level under sucrose starvation stress and no sucrose treatment (**Fig. 7.10 B, C**). These changes can be seen early on during the treatment showing rapid effect of isoxaben on metabolic pathways in *Arabidopsis*. Looking at the total ion chromatograms from each condition it can be seen that in all of them (**Fig. 7.10 B, D, F**) there was a high visible peak at around 6.3 min. retention time. A comparison of mass spectra from all the conditions revealed a mass peak of 355.172 m/z which resonds to biocytin with M-H_2O+H[1+] adduct (**Fig. 7.10 G**). Analysis of fragmentation patterns have to be conducted to confirm chemical structure of biocytin (**Fig. 7.10 H**).

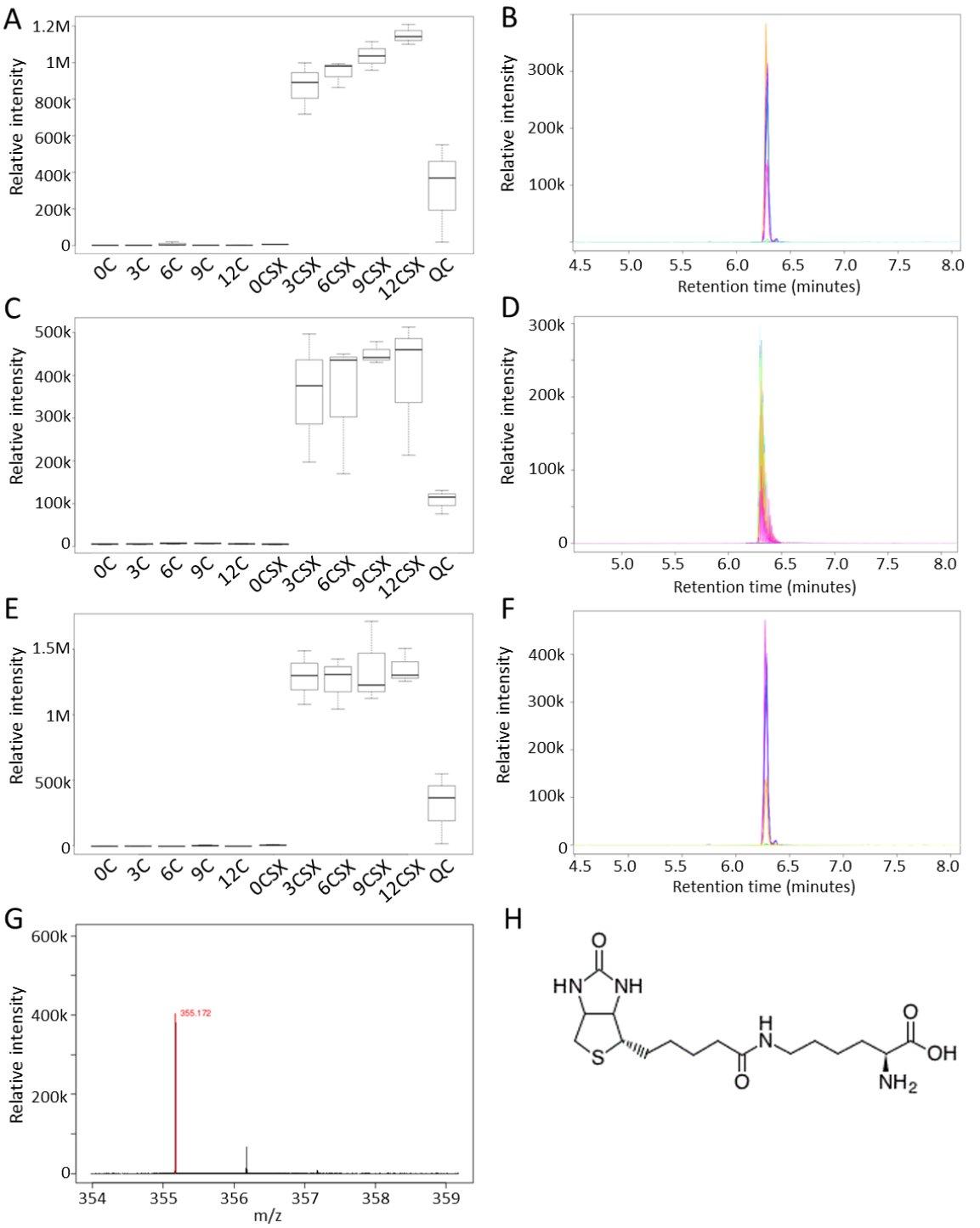

Figure 7.10. Biocytin as one of the isoxaben treatment biomarkers in Col-0. Box-plots (A, C, E) and exctracted ion chromatograms (EICs) (B, D, F) showing appearance of biocytin after isoxaben treatment regardless of sucrose addition (A, B), starvation stress (C, D) or without sucrose (E, F). G MS spectrum; H Chemical structure of biocytin. NS – no sucrose; NSX – isoxaben; CS – sucrose; CSX – sucrose+isoxaben; QC – quality control.

7.2.5 Sugar-dependent changes in metabolome

To investigate differences in the metabolite levels of samples prepared from Col-0 and *ixr1-1* plants grown on different sugar availability, whole seedlings (three biological replicates) were harvested and extracted, and the extract samples processed and analysed using XCMS Online with “mummichog” feature. The samples after 12 hours of treatment were used in this analysis. The differences in the metabolite levels obtained with UPLC-MS in plants grown on media supplemented with sucrose compared to these without sucrose are listed in **Table 7.3**. A total of 8 and 13 metabolites were identified with $p<0.05$ for Col-0 and *ixr1-1*, respectively. In Col-0 all of the features had greater than 2-fold changes, in which 5 were downregulated and 3 upregulated. The main metabolites affected by sugar addition in Col-0 were these involved in metabolism of purines and pyrimidines, vitamins B and C, cysteine and methionine, and CoA biosynthesis (**Table 7.3; Fig. 7.11**). The *ixr1-1* mutant had 3 significantly up- and 3 down-regulated metabolites. Addition of sucrose influenced cysteine and methionine, purine and sugar metabolism in *ixr1-1* mutant. In both Col-0 and *ixr1-1* glutathione metabolism seemed to be the most affected with ascorbate and glutathione, respectively, being highly downregulated.

Table 7.3 Differences in metabolite levels obtained by UPLC-TOF-MS of extracts from Arabidopsis seedlings grown with addition of sucrose compared to those without. Metabolites with fold change > 2 are in bold.

KEGG ID	m/z	retention time	Ionization mode	name	pathway	fold change	up/down	p-value	genotype
C00021	**386.13**	**1.83**	**M(C13)+H[1+]**	**S-Adenosyl-L-homocysteine**	**Cysteine and methionine metabolism**	**18.70**	**DOWN**	**0.001**	**Col-0**
C05512	**254.10**	**3.69**	**M(C13)+H[1+]**	**Deoxyinosine**	**Purine metabolism**	**8.49**	**DOWN**	**0.002**	**Col-0**
C01041	**159.00**	**0.74**	**M-NH3+H[1+]**	**Monodehydroascorbate**	**Ascorbate (Vitamin C) and Aldarate Metabolism**	**5.47**	**DOWN**	**0.003**	**Col-0**
C04352	**425.07**	**2.59**	**M+Na[1+]**	**(R)-4'-Phosphopantothenoyl-L-cysteine**	**Pantothenate and CoA biosynthesis**	**2.72**	**DOWN**	**0.004**	**Col-0**
C00018	**249.03**	**0.66**	**M(C13)+H[1+]**	**Pyridoxal phosphate**	**Vitamin B6 (pyridoxine) metabolism/Thiamine metabolism**	**3.16**	**UP**	**0.004**	**Col-0**
C03090	**231.05**	**4.14**	**M(C13)+H[1+]**	**5-Phosphoribosylamine**	**Purine metabolism**	**2.99**	**DOWN**	**0.016**	**Col-0**
C00239	**330.05**	**1.69**	**M+Na[1+]**	**Deoxycytidine monophosphate (dCMP)**	**Pyrimidine metabolism**	**3.18**	**UP**	**0.023**	**Col-0**
C03838	**287.07**	**0.73**	**M+H[1+]**	**5'-Phosphoribosylglycinamide**	**Purine metabolism/Vitamin B9 (folate) metabolism**	**6.56**	**UP**	**0.043**	**Col-0**
C00072	**199.02**	**0.85**	**M+Na[1+]**	**Ascorbate**	**Ascorbate (Vitamin C) and Aldarate Metabolism/Glutathione metabolism**	**89.50**	**DOWN**	**0.001**	***ixr1-1***
C00019	**382.12**	**0.73**	**M-NH3+H[1+]**	**S-Adenosyl-L-methionine**	**Arginine and Proline Metabolism/Cysteine and methionine metabolism**	**2.61**	**UP**	**0.001**	***ixr1-1***
C00144	**364.06**	**0.70**	**M+H[1+]**	**Guanosine 5'-phosphate(GMP)**	**Purine metabolism**	**5.33**	**UP**	**0.001**	***ixr1-1***
C00159	**219.03**	**0.69**	**M+K[1+]**	**D-Mannose**	**Galactose metabolism/Fructose and mannose metabolism**	**5.03**	**UP**	**0.001**	***ixr1-1***
C00364	324.07	3.24	M(C13)+H[1+]	Thymidine monophosphate (dTMP)	Pyrimidine metabolism	1.59	DOWN	0.002	*ixr1-1*
C00093	195.00	0.89	M+Na[1+]	sn-Glycerol 3-phosphate	Glycerophospholipid metabolism	1.35	DOWN	0.003	*ixr1-1*
C06055	**216.03**	**0.55**	**M+H[1+]**	**O-Phospho-4-hydroxy-L-threonine**	**Vitamin B6 metabolism**	**5.43**	**DOWN**	**0.004**	***ixr1-1***
C01005	208.00	8.94	M+Na[1+]	O-Phospho-L-serine	Biosynthesis of amino acids	1.06	DOWN	0.006	*ixr1-1*
C13747	181.07	0.71	M+H[1+]	1,7-Dimethylxanthine	Caffeine metabolism	1.42	DOWN	0.009	*ixr1-1*
C00062	213.07	0.90	M+K[1+]	L-Arginine	Biosynthesis of amino acids	1.89	DOWN	0.013	*ixr1-1*
C00365	309.05	3.77	M+H[1+]	Deoxyuridine monophosphate (dUMP)	Pyrimidine metabolism	1.81	UP	0.022	*ixr1-1*
C05577	207.01	3.22	M+K[1+]	3,4-Dihydroxymandelaldehyde	Tyrosine metabolism	1.36	UP	0.026	*ixr1-1*
C00051	**309.10**	**2.33**	**M(C13)+H[1+]**	**Glutathione**	**Cysteine and methionine metabolism/Glutathione metabolism**	**10.69**	**DOWN**	**0.035**	***ixr1-1***

The differences in the metabolite levels obtained with UPLC-MS in plants grown on media supplemented with sucrose compared to these transferred from sucrose to media without sucrose are listed in **Table 7.4**. A total number of 9 and 10 identified features changed in Col-0 and *ixr1-1*, respectively. Only myo-Inositol and 5'-Methylthioadenosine had fold changes greater than 2 in Col-0 and were downregulated, while *ixr1-1* had 7 metabolites in which 6 were upregulated. The main changes in metabolic pathways were those of galactose metabolism and cysteine and methionine metabolism in Col-0. Similarly, the same pathways were affected in *ixr1-1* and moreover, purine, caffeine and fatty acid metabolisms were influenced during sucrose starvation together with isoxaben treatment.

Table 7.4 Differences in metabolite levels obtained by UPLC-TOF-MS of extracts from Arabidopsis seedlings grown during sucrose starvation stress compared to those with sucrose. Metabolites with fold change > 2 are in bold.

KEGG ID	m/z	retention time	Ionization mode	name	pathway	fold change	up/down	p-value	genotype
C04734	368.07	0.59	M(C13)+H[1+]	FAICAR	Purine metabolism	1.80	UP	0.001	Col-0
C01081	368.07	0.59	M+Na[1+]	Thiamin monophosphate (TMP)	Vitamin B1 (thiamin) metabolism	1.80	UP	0.001	Col-0
C00137	**203.05**	**0.72**	**M+Na[1+]**	**myo-Inositol**	**Phosphatidylinositol signaling system/Galactose metabolism**	**4.22**	**DOWN**	**0.006**	**Col-0**
C05577	191.03	2.93	M+Na[1+]	3,4-Dihydroxymandelaldehyde	Tyrosine metabolism	1.60	DOWN	0.008	Col-0
C00325	628.04	0.69	M+K[1+]	GDP-L-fucose	Fructose and mannose metabolism/Amino sugar and nucleotide sugar metabolism	1.39	DOWN	0.013	Col-0
C00360	332.08	0.62	M+H[1+]	Deoxyadenosine monophosphate (dAMP)	Purine metabolism	1.27	DOWN	0.014	Col-0
C00170	**320.08**	**4.01**	**M+Na[1+]**	**5'-Methylthioadenosine (MTA)**	**Methionine and cysteine metabolism/Zeatin biosynthesis**	**2.74**	**DOWN**	**0.023**	**Col-0**
C00624	212.05	0.87	M+Na[1+]	N-Acetyl-L-glutamate	Amino group metabolism	1.74	UP	0.023	Col-0
C00064	130.05	0.63	M-NH3+H[1+]	L-Glutamine	Purine metabolism/Pyrimidine metabolism/Arginine and Proline Metabolism/Tyrosine metabolism/Alanine and Aspartate Metabolism	1.24	DOWN	0.047	Col-0
C13747	**163.06**	**2.60**	**M-H2O+H[1+]**	**1,7-Dimethylxanthine**	**Caffeine metabolism**	**3.74**	**UP**	**0.000**	***ixr1-1***
C04734	**368.07**	**0.61**	**M(C13)+H[1+]**	**FAICAR**	**Purine metabolism**	**3.09**	**UP**	**0.000**	***ixr1-1***
C05270	**866.19**	**3.39**	**M+H[1+]**	**Hexanoyl-CoA**	**Fatty acid metabolism**	**2.14**	**UP**	**0.001**	***ixr1-1***
C00052	**550.04**	**0.59**	**M-NH3+H[1+]**	**UDP-D-galactose**	**Amino sugar and nucleotide sugar metabolism/Galactose metabolism**	**2.38**	**DOWN**	**0.001**	***ixr1-1***
C00606	**154.02**	**0.80**	**M+H[1+]**	**3-Sulfino-L-alanine**	**Methionine and cysteine metabolism**	**3.23**	**UP**	**0.001**	***ixr1-1***
C04751	**322.04**	**0.71**	**M-H2O+H[1+]**	**1-(5-Phospho-D-ribosyl)-5-amino-4-imidazolecarboxylate**	**Purine metabolism**	**3.12**	**UP**	**0.001**	***ixr1-1***
C00096	628.06	0.73	M+Na[1+]	GDP-mannose	N-Glycan biosynthesis/Fructose and mannose metabolism	1.96	DOWN	0.001	*ixr1-1*
C05275	942.22	3.41	M+Na[1+]	trans-Dec-2-enoyl-CoA	Fatty acid metabolism	1.56	UP	0.002	*ixr1-1*
C03373	**318.05**	**3.41**	**M+Na[1+]**	**Aminoimidazole ribotide**	**Purine metabolism**	**2.80**	**UP**	**0.002**	***ixr1-1***
C04677	340.07	0.63	M(C13)+H[1+]	1-(5'-Phosphoribosyl)-5-amino-4-imidazolecarboxamide	Purine metabolism	1.71	UP	0.049	*ixr1-1*

In summary, metabolic profiling revealed distinct metabolic phenotypes for each genotype and sugar availability. The metabolic phenotype included metabolites from at least 19 different metabolic pathways. **Figure 7.11** represents some of the metabolic differences observed in Col-0 and in *ixr1-1* samples. The most affected pathways in both genotypes were: purine, cysteine and methionine metabolism, and galactose metabolism.

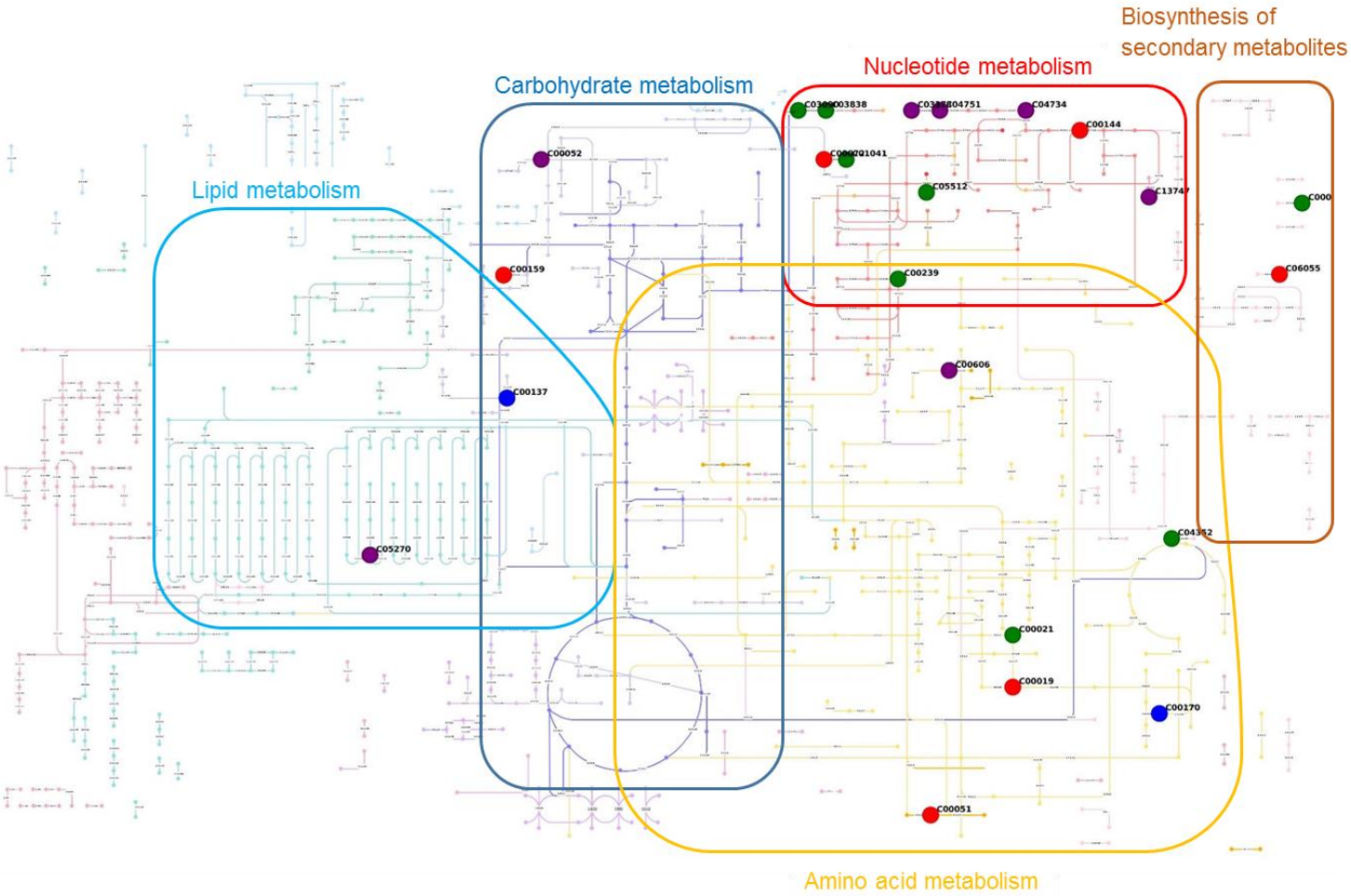

Figure 7.11. Summary of metabolic differences detected in Col-0 and *ixr1-1* during sucrose media supplementation and sucrose starvation. The figure shows the metabolites present in KEGG atlas with its KEGG ID (ID and metabolites names can be found in Tables 7.3 and 7.4). Positioning of metabolites on the metabolic map was made using Pathway Projector Kono et al., 2009. Green and red circles indicate metabolites that were significantly ($p < 0.05$) changed in Col-0 and *ixr1-1*, respectively after addition of sucrose,while blue and purple circles indicate metabolites that were significantly ($p < 0.05$) changed in Col-0 and *ixr1-1*, respectively during sucrose starvation.

7.2.6 Isoxaben-dependent changes in metabolome

To investigate differences in the metabolite levels of samples prepared from Col-0 and *ixr1-1* plants grown on different sugar availability together with isoxaben treatment, whole seedlings (three biological replicates) were harvested and extracted, and the extract samples processed and analysed using XCMS Online with “mummichog” feature. The differences in the metabolite levels obtained with UPLC-MS in plants grown on media supplemented with sucrose after isoxaben treatment are listed in **Table 7.5**. A total of 9 and 20 metabolites were identified with $p<0.05$ for Col-0 and *ixr1-1*, respectively. In Col-0, 5 metabolites had a greater than 2-fold change, in which 2 were downregulated and 3 upregulated. The main metabolites affected by isoxaben addition in Col-0 were these involved in purine and pyrimidine metabolism (**Table 7.5**; **Fig. 7.12**). The main affected metabolites were: deoxycytidine monophosphate (dCMP), 2'-deoxyuridine 5'-diphosphate (dUDP), 2'-deoxyguanosine 5'-diphosphate (dGDP), and deoxythymidine monophosphate (dTMP). The *ixr1-1* mutant had 6 significantly up- and 7 down-regulated metabolites. Isoxaben treatment influenced cysteine and methionine, purine, phosphatidylinositol phosphate, and tyrosine metabolism in *ixr1-1* mutant. In both Col-0 and *ixr1-1* purine metabolism seemed to be the most affected (**Fig. 7.12**).

Table 7.5 Differences in metabolite levels obtained by UPLC-TOF-MS of extracts from *Arabidopsis* seedlings grown after sucrose and isoxaben treatment compared to those with sucrose only. Metabolites with fold change > 2 are in bold.

KEGG ID	m/z	retention time	Ionization mode	name	pathway	fold change	up/down	p-value	genotype
C00906	**151.05**	**4.91**	**M+Na[1+]**	**5,6-Dihydrothymine**	**Pyrimidine metabolism**	**11.47**	**DOWN**	**0.000**	**Col-0**
C00144	346.06	0.69	M-H2O+H[1+]	Guanosine 5'-phosphate(GMP)	Purine metabolism	1.99	UP	0.001	Col-0
C00239	**309.06**	**5.50**	**M(C13)+H[1+]**	**Deoxycytidine monophosphate (dCMP)**	**Pyrimidine metabolism**	**6.26**	**DOWN**	**0.001**	**Col-0**
C00447	408.97	3.20	M+K[1+]	D-Sedoheptulose 1,7-bisphosphate	Carbon metabolism	1.67	UP	0.002	Col-0
C04376	315.06	1.71	M+H[1+]	5'-Phosphoribosyl-N-Formylglycinamide	Purine metabolism	1.62	UP	0.019	Col-0
C00279	183.01	3.38	M-H2O+H[1+]	D-Erythrose 4-phosphate	Carbon metabolism	1.53	UP	0.028	Col-0
C01346	**389.02**	**5.03**	**M+H[1+]**	**2'-Deoxyuridine 5'-diphosphate (dUDP)**	**Pyrimidine metabolism**	**3.37**	**UP**	**0.041**	**Col-0**
C00361	**450.01**	**3.43**	**M+Na[1+]**	**2'-Deoxyguanosine 5'-diphosphate (dGDP)**	**Purine metabolism**	**3.33**	**UP**	**0.045**	**Col-0**
C00364	**345.05**	**5.05**	**M+Na[1+]**	**Deoxythymidine monophosphate (dTMP)**	**Pyrimidine metabolism**	**3.12**	**UP**	**0.047**	**Col-0**
C00360	**332.08**	**0.60**	**M+H[1+]**	**Deoxyadenosine monophosphate (dAMP)**	**Purine metabolism**	**7.76**	**DOWN**	**0.000**	***ixr1-1***
C00021	**368.11**	**3.02**	**M-NH3+H[1+]**	**S-Adenosyl-L-homocysteine**	**Cysteine and methionine metabolism**	**3.36**	**DOWN**	**0.000**	***ixr1-1***
C00191	**217.03**	**0.54**	**M+Na[1+]**	**D-Glucuronate**	**Phosphatidylinositol phosphate metabolism**	**5.47**	**DOWN**	**0.001**	***ixr1-1***
C05378	**342.00**	**5.41**	**M(C13)+H[1+]**	**beta-D-Fructose 1,6-bisphosphate**	**Starch and sucrose metabolism/Amino sugar and nucleotide sugar metabolism**	**3.58**	**DOWN**	**0.001**	***ixr1-1***
C00051	**308.09**	**3.26**	**M+H[1+]**	**Glutathione**	**Cysteine and methionine metabolism/Glutathione metabolism**	**5.70**	**UP**	**0.002**	***ixr1-1***
C00144	**346.05**	**5.06**	**M-H2O+H[1+]**	**Guanosine 5'-phosphate(GMP)**	**Purine metabolism**	**3.13**	**UP**	**0.006**	***ixr1-1***
C00116	**76.03**	**1.96**	**M-NH3+H[1+]**	**Glycerol**	**Phosphatidylinositol phosphate metabolism/Galactose metabolism**	**10.48**	**DOWN**	**0.007**	***ixr1-1***
C00398	**143.10**	**4.14**	**M-H2O+H[1+]**	**Tryptamine**	**Tryptophan metabolism**	**3.08**	**UP**	**0.007**	***ixr1-1***
C00170	320.08	5.03	M+Na[1+]	5'-Methylthioadenosine (MTA)	Methionine and cysteine metabolism/Zeatin biosynthesis	1.85	UP	0.009	*ixr1-1*
C03406	313.11	2.55	M+Na[1+]	N-(L-Arginino)succinate	Biosynthesis of amino acids	1.49	UP	0.009	*ixr1-1*
C00365	309.05	3.77	M+H[1+]	Deoxyuridine monophosphate (dUMP)	Pyrimidine metabolism	1.53	DOWN	0.011	*ixr1-1*
C00101	**447.19**	**0.74**	**M(C13)+H[1+]**	**Tetrahydrofolate**	**Carbon metabolism**	**2.05**	**UP**	**0.026**	***ixr1-1***
C05576	**171.07**	**3.19**	**M+H[1+]**	**3,4-Dihydroxyphenylethyleneglycol**	**Tyrosine metabolism**	**2.53**	**DOWN**	**0.026**	***ixr1-1***

KEGG ID	m/z	retention time	Ionization mode	name	pathway	fold change	up/down	p-value	genotype
C00447	393.00	0.60	M+Na[1+]	D-Sedoheptulose 1,7-bisphosphate	Carbon metabolism	1.50	UP	0.030	*ixr1-1*
C04640	336.06	3.38	M+Na[1+]	2-(Formamido)-N1-(5'-phosphoribosyl)acetamidine	Purine metabolism	1.12	UP	0.031	*ixr1-1*
C00473	**287.24**	**3.54**	**M+H[1+]**	**Retinol**	**Vitamin A (retinol) metabolism**	**2.17**	**UP**	**0.038**	***ixr1-1***
C03373	**297.07**	**1.35**	**M(C13)+H[1+]**	**Aminoimidazole ribotide**	**Purine metabolism**	**2.64**	**UP**	**0.038**	***ixr1-1***
C04043	175.04	0.74	M+Na[1+]	3,4-Dihydroxyphenylacetaldehyde	Tyrosine metabolism	1.39	UP	0.038	*ixr1-1*
C00355	**236.03**	**0.69**	**M+K[1+]**	**3,4-Dihydroxy-L-phenylalanine**	**Tyrosine metabolism**	**2.06**	**DOWN**	**0.044**	***ixr1-1***
C13747	181.07	0.72	M+H[1+]	1,7-Dimethylxanthine	Caffeine metabolism	1.73	UP	0.048	*ixr1-1*

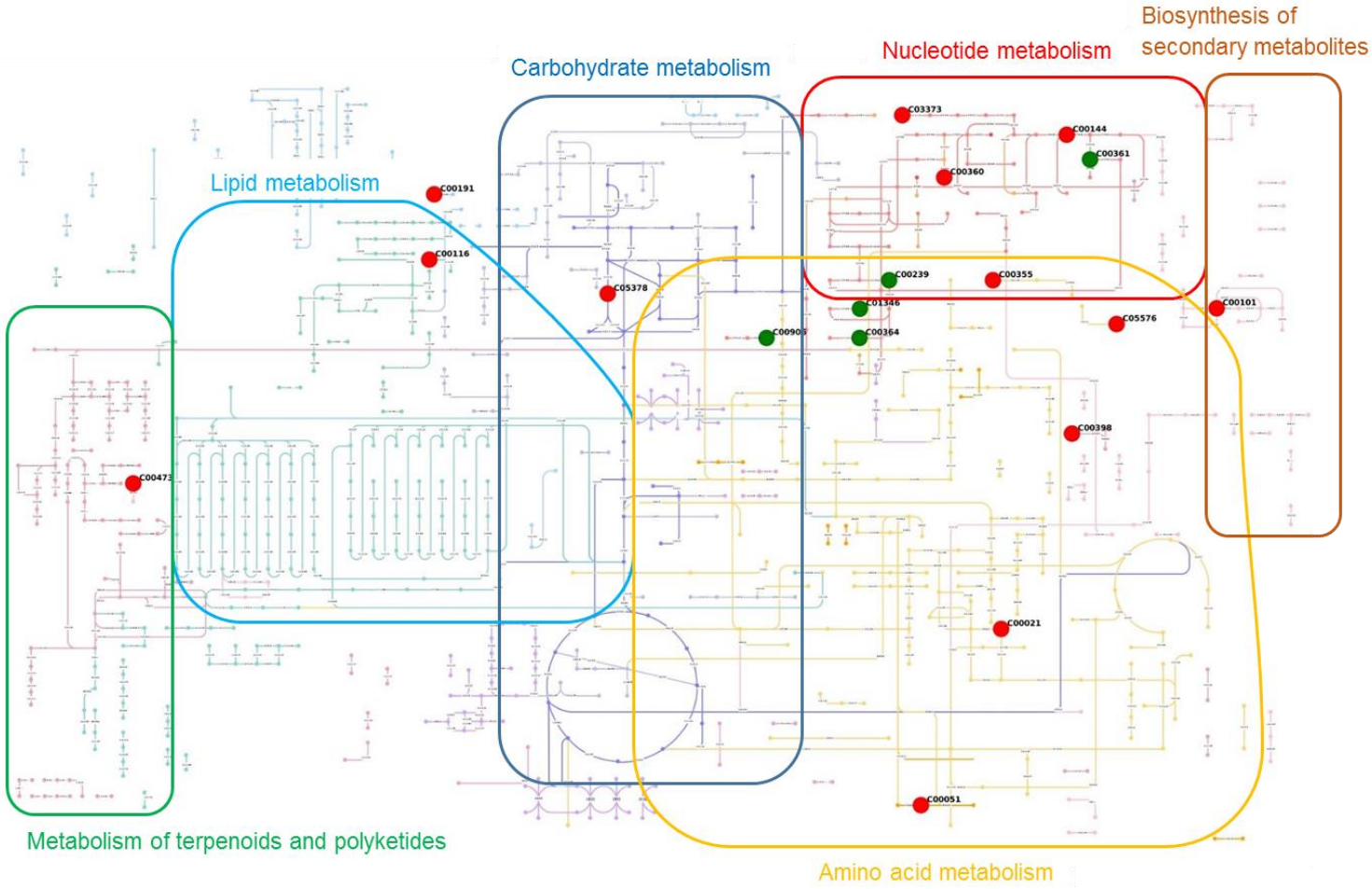

Figure 7.12. Summary of metabolic differences detected in Col-0 and *ixr1-1* grown on media supplemented with sucrose after isoxaben treatment. The figure shows the metabolites present in KEGG atlas with its KEGG ID (ID and metabolites names can be found in Table 7.5). Positioning of metabolites on the metabolic map was made using Pathway Projector Kono et al., 2009. Green circles indicate metabolites that were significantly ($p < 0.05$) changed in Col-0, while red circles indicate metabolites that were significantly ($p < 0.05$) changed in *ixr1-1*.

The differences in the metabolite levels obtained with UPLC-MS in plants grown on media supplemented with sucrose and then transfered to media without sucrose and with isoxaben compared to these grown with sucrose constantly and without isoxaben are listed in **Table 7.6**. A total of 22 and 4 metabolites were identified with $p<0.05$ for Col-0 and *ixr1-1*, respectively. In Col-0, 11 features had a greater than 2-fold change, in which 5 were downregulated and 6 upregulated. The main metabolites affected by sucrose starvation stress together with isoxaben treatment in Col-0 were these involved in purine and pyrimidine, vitamins, and fatty acids metabolism (**Table 7.6**; **Fig. 7.13**). The *ixr1-1* mutant had all features with a greater than 2-fold change in which 2 were significantly up- and 2 down-regulated. Affected pathways included mainly amino acids metabolism in *ixr1-1* mutant. L-lysine and N-acetylornithine involved in biosynthesis of amino acids were upregulated whereas 3-methyl-2-oxobutanoic acid, secondary metabolite of amino acids degradation was downregulated. In both Col-0 and *ixr1-1* pirimidine metabolism seemed to be downregulated with 2'-deoxycytidine diphosphate (dCDP) and uridine 5'-triphosphate (UTP), respectively.

Table 7.6 Differences in metabolite levels obtained by UPLC-TOF-MS of extracts from *Arabidopsis* seedlings grown after sucrose starvation stress and isoxaben treatment compared to those with sucrose only. Metabolites with fold change > 2 are in bold.

KEGG ID	m/z	retention time	Ionization mode	name	pathway	fold change	up/down	p-value	genotype
C04823	**455.08**	**6.32**	**M+H[1+]**	**1-(5'-Phosphoribosyl)-5-amino-4-(N-succinocarboxamide)-imidazole**	**Purine metabolism**	**2.27**	**DOWN**	**0.001**	**Col-0**
C00341	**297.06**	**3.43**	**M-H2O+H[1+]**	**Geranyl diphosphate**	**Terpenoid backbone biosynthesis**	**3.38**	**DOWN**	**0.001**	**Col-0**
C00473	**309.22**	**4.08**	**M+Na[1+]**	**Retinol**	**Vitamin A (retinol) metabolism**	**3.58**	**DOWN**	**0.001**	**Col-0**
C00239	308.06	2.34	M+H[1+]	Deoxycytidine monophosphate (dCMP)	Pyrimidine metabolism	1.94	UP	0.002	Col-0
C00242	174.04	2.30	M+Na[1+]	Guanine	Purine metabolism	1.86	DOWN	0.003	Col-0
C00647	**231.05**	**2.40**	**M-H2O+H[1+]**	**Pyridoxamine phosphate**	**Vitamin B6 (pyridoxine) metabolism**	**2.76**	**UP**	**0.003**	**Col-0**
C00655	**365.05**	**5.28**	**M+H[1+]**	**Xanthosine 5'-phosphate**	**Purine metabolism**	**44.43**	**UP**	**0.003**	**Col-0**
C00129	248.02	6.33	M(C13)+H[1+]	Isopentenyl diphosphate	Terpenoid backbone biosynthesis	1.41	UP	0.004	Col-0
C05527	152.98	0.84	M+H[1+]	3-Sulfinylpyruvate	Methionine and cysteine metabolism	1.72	DOWN	0.006	Col-0
C01143	310.02	0.64	M(C13)+H[1+]	(R)-5-Diphosphomevalonate	Terpenoid backbone biosynthesis	1.45	UP	0.007	Col-0
C00361	**450.02**	**1.36**	**M+Na[1+]**	**dGDP**	**Purine metabolism**	**2.12**	**DOWN**	**0.017**	**Col-0**
C00559	234.10	2.98	M-H2O+H[1+]	Deoxyadenosine	Purine metabolism	1.63	UP	0.018	Col-0
C00250	190.05	6.32	M+Na[1+]	Pyridoxal	Vitamin B6 (pyridoxine) metabolism	1.52	UP	0.021	Col-0
C01137	**356.16**	**5.79**	**M+H[1+]**	**S-Adenosylmethioninamine**	**Methionine and cysteine metabolism**	**2.23**	**UP**	**0.027**	**Col-0**
C05266	**893.20**	**3.23**	**M-NH3+H[1+]**	**(S)-Hydroxyoctanoyl-CoA**	**Fatty acid metabolism**	**3.97**	**UP**	**0.031**	**Col-0**
C00705	**425.99**	**0.76**	**M+K[1+]**	**2'-Deoxycytidine diphosphate (dCDP)**	**Pyrimidine metabolism**	**5.28**	**DOWN**	**0.033**	**Col-0**
C01103	406.99	0.84	M+K[1+]	Orotidine 5'-phosphate	Pyrimidine metabolism	1.60	DOWN	0.034	Col-0
C00627	**288.00**	**2.96**	**M+K[1+]**	**Pyridoxine phosphate**	**Vitamin B6 (pyridoxine) metabolism**	**3.36**	**UP**	**0.037**	**Col-0**
C05265	919.21	0.58	M-NH3+H[1+]	3-Oxodecanoyl-CoA	Fatty acid metabolism	1.73	DOWN	0.041	Col-0
C03221	949.28	2.96	M(C13)+H[1+]	2-trans-Dodecenoyl-CoA	Fatty acid metabolism	1.34	DOWN	0.043	Col-0
C05262	1004.23	0.58	M+K[1+]	(S)-3-Hydroxydodecanoyl-CoA	Fatty acid metabolism	1.36	DOWN	0.047	Col-0
C05275	**921.24**	**3.42**	**M(C13)+H[1+]**	**trans-Dec-2-enoyl-CoA**	**Fatty acid metabolism**	**2.25**	**UP**	**0.048**	**Col-0**
C00047	**147.11**	**3.55**	**M+H[1+]**	**L-Lysine**	**Biosynthesis of amino acids**	**7.32**	**UP**	**0.000**	***ixr1-1***
C00141	**99.04**	**0.67**	**M-H2O+H[1+]**	**3-Methyl-2-oxobutanoic acid**	**Valine, leucine and isoleucine degradation**	**8.10**	**DOWN**	**0.000**	***ixr1-1***
C00437	**197.09**	**0.67**	**M+Na[1+]**	**N-Acetylornithine**	**Arginine biosynthesis**	**4.22**	**UP**	**0.001**	***ixr1-1***
C00075	**484.97**	**0.70**	**M+H[1+]**	**Uridine 5'-triphosphate (UTP)**	**Pyrimidine metabolism**	**2.86**	**DOWN**	**0.001**	***ixr1-1***

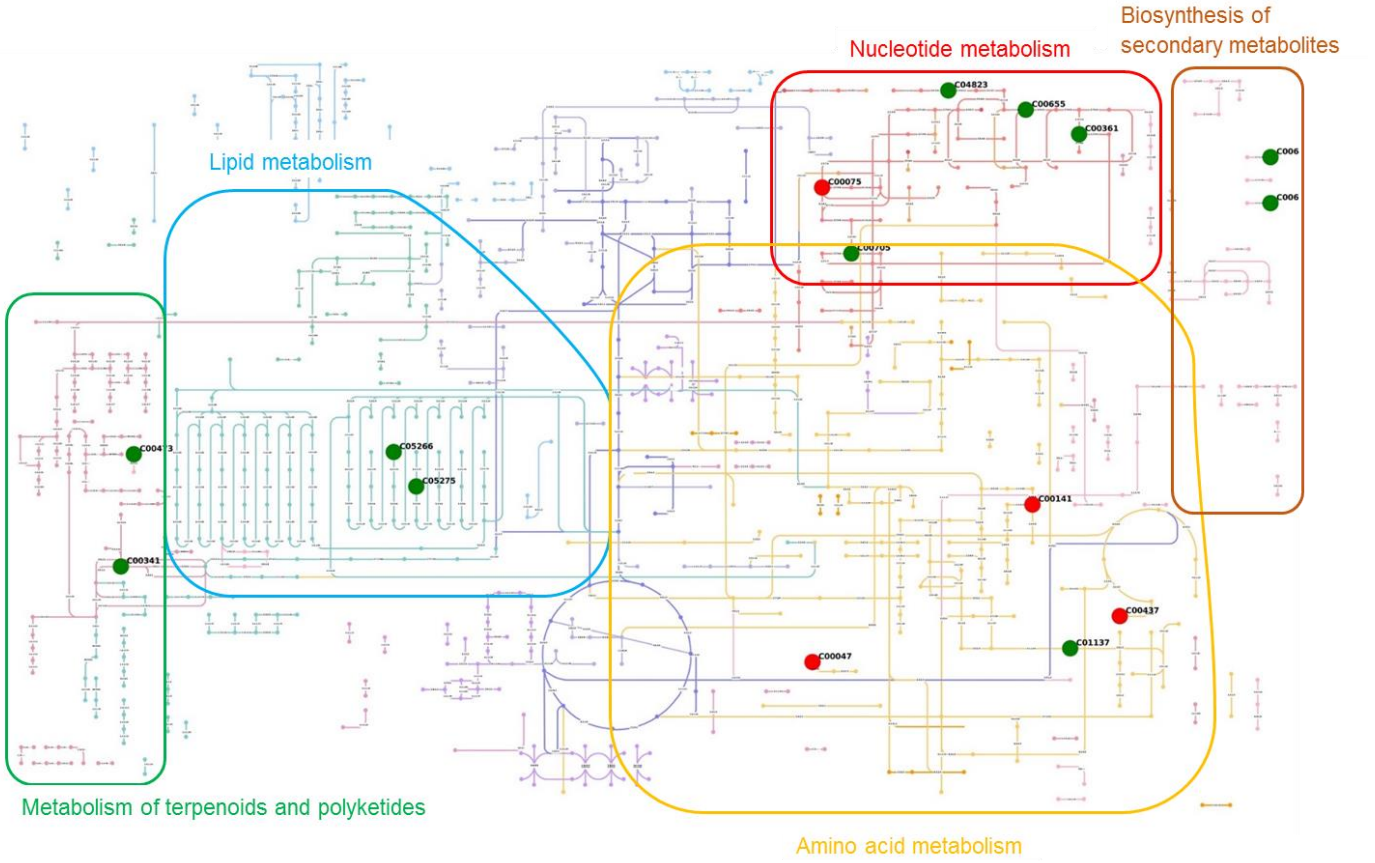

Figure 7.13. Summary of metabolic differences detected in Col-0 and *ixr1-1* grown with sucrose starvation stress and after isoxaben treatment. The figure shows the metabolites present in KEGG atlas with its KEGG ID (ID and metabolites names can be found in Table 7.6). Positioning of metabolites on the metabolic map was made using Pathway Projector Kono et al., 2009. Green circles indicate metabolites that were significantly ($p < 0.05$) changed in Col-0, while red circles indicate metabolites that were significantly ($p < 0.05$) changed in *ixr1-1*.

The differences in the metabolite levels obtained with UPLC-MS in plants grown on media without sucrose and with isoxaben compared to these without sucrose only are listed in **Table 7.7**. A total number of 5 and 13 identified features changed in Col-0 and *ixr1-1*, respectively. Main changes in metabolic pathways regarded those of glycosphingolipid, cysteine and methionine metabolism in Col-0 (**Fig. 7.14**). L-tyrosine was over 13 times higher suggesting biosynthesis of amino acids was greatly affected. Only 3 out of 13 identified metabolites in *ixr1-1* had fold change higher than 2. All of them were upregulated and affected pathways involved in cysteine and methionine, galactose, and pyrimidine metabolism.

In summary, Col-0 metabolism was mostly affected in purine and pyrimidine metabolism after addition of isoxaben to the media supplemented with sucrose. In case of *ixr1-1* purine, amino acids, and galactose/phosphatidylinositol phosphate metabolism. When plants were subjected to sucrose starvation stress together with isoxaben, purine and pyrimidine metabolism and vitamins metabolism were disrupted in Col-0 and amino acids and pyrimidine metabolism in *ixr1-1*. Finally, media without sucrose but with isoxaben influenced biosynthesis of amino acids and glycosphingolipids metabolism in Col-0 and pyrimidine, cysteine, methionine, and galactose metabolism in *ixr1-1*.

.

KEGG ID	m/z	retention time	Ionization mode	name	pathway	fold change	up/down	p-value	genotype
C01190	**644.50**	**7.81**	**M+H[1+]**	**Glucosylceramide**	**Glycosphingolipid metabolism**	**5.38**	**DOWN**	**0.000**	**Col-0**
C00082	**220.04**	**6.29**	**M+K[1+]**	**L-Tyrosine**	**Biosynthesis of amino acid**	**13.81**	**UP**	**0.005**	**Col-0**
C01005	168.00	1.36	M-H2O+H[1+]	O-Phospho-L-serine	Biosynthesis of amino acids	1.29	DOWN	0.014	Col-0
C00021	**386.13**	**1.84**	**M(C13)+H[1+]**	**S-Adenosyl-L-homocysteine**	**Cysteine and methionine metabolism**	**2.17**	**DOWN**	**0.019**	**Col-0**
C05439	368.32	8.80	M-NH3+H[1+]	5alpha-Cholesta-7,24-dien-3beta-ol	Steroid biosynthesis	1.55	UP	0.041	Col-0
C00096	606.08	4.14	M+H[1+]	GDP-mannose	N-Glycan biosynthesis/Fructose and mannose metabolism	1.87	DOWN	0.001	*ixr1-1*
C00021	**368.10**	**4.18**	**M-NH3+H[1+]**	**S-Adenosyl-L-homocysteine**	**Cysteine and methionine metabolism**	**2.19**	**UP**	**0.002**	***ixr1-1***
C00705	371.00	0.57	M-NH3+H[1+]	2'-Deoxycytidine diphosphate (dCDP)	Pyrimidine metabolism	1.39	UP	0.012	*ixr1-1*
C01246	489.22	4.17	M+Na[1+]	Dolichyl beta-D-glucosyl phosphate	N-Glycan biosynthesis	1.62	UP	0.014	*ixr1-1*
C00105	347.03	0.74	M+Na[1+]	Uridine monophosphate (UMP)	Pyrimidine metabolism	1.66	UP	0.015	*ixr1-1*
C00018	248.03	3.22	M+H[1+]	Pyridoxal phosphate	Vitamin B6 (pyridoxine) metabolism/Thiamine metabolism	1.38	DOWN	0.018	*ixr1-1*
C02336	**182.07**	**2.89**	**M(C13)+H[1+]**	**beta-D-Fructose**	**Galactose metabolism**	**2.47**	**UP**	**0.023**	***ixr1-1***
C00299	245.08	1.10	M+H[1+]	Uridine	Pyrimidine metabolism	1.64	DOWN	0.027	*ixr1-1*
C00988	194.95	8.95	M+K[1+]	2-Phosphoglycolate	Carbon metabolism	1.29	UP	0.029	*ixr1-1*
C03722	190.01	7.63	M+Na[1+]	Quinolinate	Vitamin B3 (nicotinate and nicotinamide) metabolism/Tryptophan metabolism	1.40	DOWN	0.034	*ixr1-1*
C05951	535.22	2.02	M+K[1+]	Leukotriene D4	Arachidonic acid metabolism	1.45	UP	0.038	*ixr1-1*
C00214	**244.10**	**5.57**	**M(C13)+H[1+]**	**Thymidine**	**Pyrimidine metabolism**	**2.27**	**UP**	**0.038**	***ixr1-1***
C00364	324.07	5.56	M(C13)+H[1+]	Thymidine monophosphate (dTMP)	Pyrimidine metabolism	1.60	UP	0.039	*ixr1-1*

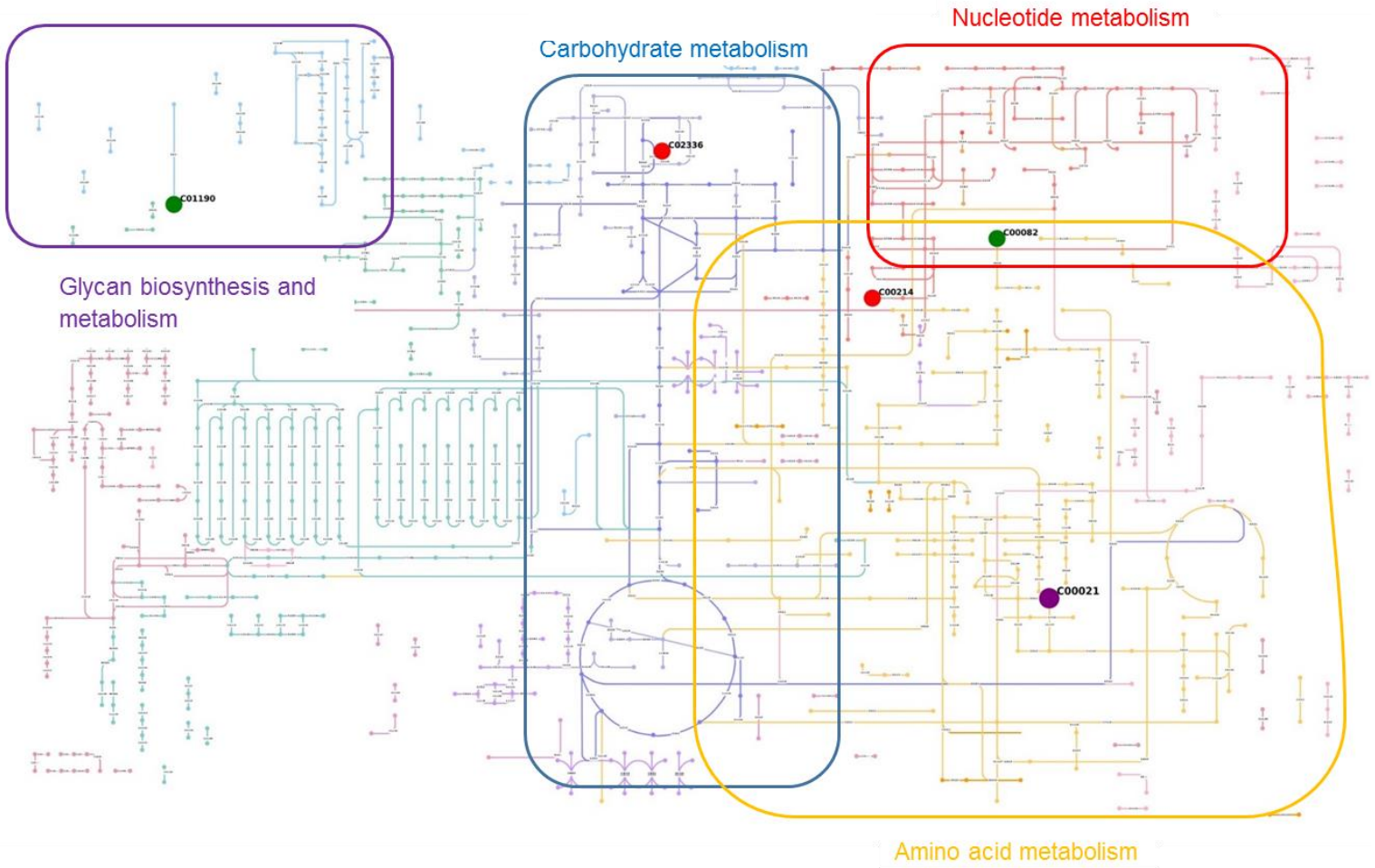

Figure 7.14. Summary of metabolic differences detected in Col-0 and *ixr1-1* grown without sucrose and after isoxaben treatment. The figure shows the metabolites present in KEGG atlas with its KEGG ID (ID and metabolites names can be found in Table 7.7). Positioning of metabolites on the metabolic map was made using Pathway Projector Kono et al., 2009. Green circles indicate metabolites that were significantly ($p < 0.05$) changed in Col-0, while red circles indicate metabolites that were significantly ($p < 0.05$) changed in *ixr1-1*. A purple circle indicates metabolite C00021 - S-Adenosyl-L-homocysteine, which changed in both Col-0 and *ixr1-1*.

7.3 Discussion

Global profiling of direct and indirect gene products (proteins, metabolites) can generate a huge amount of information regarding processes like the cell wall integrity maintenance mechanism, that are crucial for the establishment, growth, and development of plants. This study provides the first quantification of gross metabolic changes in *Arabidopsis* seedlings after cellulose biosynthesis disruption caused by isoxaben. Here, observed patterns of changes in metabolite composition are used to explore major, isoxaben-dependent metabolic shifts.

Strong patterns were observed in the metabolite patterns of the plants grown in the different sucrose conditions as shown by PCA and PLS-DA analyses. Levels of several metabolites directly or indirectly connected to cysteine and methionine metabolism were affected in Col-0 and *ixr1-1* plants regardless of media conditions (addition of sucrose, isoxaben or both). Levels of metabolites involved in purine and pyrimidine metabolism were highly affected in both genotypes and across growing conditions. Addition of sucrose caused lower levels of metabolites involved in purine metabolism in Col-0 compared to *ixr1-1* where it was higher. Purine and pyrimidine nucleotides participate in many biochemical processes in plants. They are building blocks for nucleic acid synthesis, an energy source, precursors for the synthesis of primary products, such as sucrose, polysaccharides, phospholipids, as well as secondary products. Cell wall polysaccharides are often incorporated into the cell wall in nucleotide substituted form. Characterization of the *ixr1-2* mutant showed lower cellulose microfibril crystallinity thus making it more sensitive to enzymatic hydrolysis (Harris et al., 2012). Presumably, one of the explanations for this difference is that as the *ixr1-1* mutant has lower microfibril crystallinity, it may compensate for this by higher production of other cell wall polysaccharides and their nucleotide forms to strengthen cell wall. Moreover, higher level of D-mannose required in mannose, galactose and fructose metabolism may support this hypothesis. These changes are not surprising as sugars, similar to hormones, can act as primary messengers and regulate expression of genes involved in carbohydrate metabolism. Additionally, low and high sucrose contents activate expression of transcription factors responsive to auxin, ethylene and gibberellin (Papini-Terzi et al., 2009).

Many metabolites can act in defence mechanisms against pests such as insects, pathogenic fungi, and bacteria. These metabolites are generally derived from secondary metabolism, such as the phenylpropanoid, isoprenoid, alkaloid, or fatty acid/polyketide pathways. However, precursors of these defence compounds emanate from primary

metabolism. For example, branched-chain amino acids (isoleucine, leucine, and valine) serve as precursors for cyanogenic glycosides (Binder, 2010). Aromatic amino acids (tryptophan, phenylalanine, and tyrosine) serve as precursors for indole glucosinolates, phytoalexins, alkaloids, lignins, flavonoids, isoflavonoids, and hydroxycinnamic acids (Tzin and Galili, 2010). Therefore, it is reasonable that one purpose for branched-chain amino acid accumulation is to support increased production of secondary metabolites as part of a defence response. Such a response could constitute a pre-emptive defence against opportunistic attack by a pathogen on a cell wall-weakened host.

Future work will focus on data analysis of time-course designs over short-term intervals to provide successive snapshots of metabolism status. Such methodology is useful in investigating the complex interacting mechanisms of cellular metabolic pathways in response to perturbations, such as cell wall damage.

The studies presented here have limitations that should be acknowledged. While UPLC-MS method applied here allows global definitions of metabolism, it is not expected that all of the possible metabolites present would be identified. Identification of metabolites is also limited to molecules with precise chemical annotation in established metabolite libraries. The exploratory nature of non-targeted metabolomics methodologies has the limitation of being partly quantitative based on their retention times and mass fragmentation patterns. Computational prediction of metabolite identity, based on m/z alone, is deemed inadequate as a single m/z feature can match multiple metabolites even with high instrumental accuracy. Although automated MS/MS (tandem mass spectrometry) search in databases is improving the efficiency of metabolite identification, this requires additional targeted experiments and relies on extensive databases, where data from different platforms often do not match. The use of non-targeted metabolomics in the present study was to determine the underlying metabolic changes, to allow insight into the global level changes. However, specific mechanisms identified need further validation to make specific conclusions.

8. General discussion

8.1 Summary

Chapter 1 introduces the main components of the primary cell wall: cellulose, hemicellulose and pectin together with details about their synthesis. The growth of the primary cell wall cannot happen without chemical modifications of each component. The main focus of this chapter was put on the backbone of pectin, homogalacturonan (HG) and its modification by pectin methylesterases (PMEs). The activity of PMEs can be inhibited by their proteinaceous inhibitors (PMEIs). PMEs potential function is discussed but little is known about their involvement in root development. The root system provides a good system to study cell elongation, cell division, cell differentiation and organogenesis. Creating knockout mutants in PMEs can be challenging due to potential redundancy caused by other PME isoforms. Therefore, the approach presented here was based on a pharmacological treatment with a green tea catechin extract called polyphenon-60 (PP60) which has been showed to inhibit PME activity *in vitro*. Moreover, the activity of PME could be regulated by plant hormones. Little is known about the involvement of auxin and brassinosteroids in root development and regulation of cell wall extensibility. Finally, border-like cells and mucilage surrounding the root cap have a high content of HG and their potential role is to protect the root cap. There is not much known about the involvement of PMEs in the release of border-like cells and the production of mucilage. The pharmacological approach to study PMEs function in root development is explored in **Chapters 4-6**.

To investigate developmental importance of PME and PMEI genes in roots, **Chapter 3** characterizes the expression and co-expression patterns of PMEs and PMEIs in *Arabidopsis* using available online databases. Potential PME and PMEI pairs were shown to appear in root tissues suggesting that they may act together to regulate the methylesterification status of HG. The phylogenetic tree for PME and PMEI proteins has placed each into four groups. Comparing both, expression and phylogenetic analyses, group 1 and a subset of group 4 PMEs and group 2 PMEIs were shown to be expressed in the *Arabidopsis* root. Moreover, the analysis of chromosomal distribution of PME genes has suggested that duplicated genes may have not been segmentally duplicated and may have adapted their function to environmental changes.

The high amount of PME isoforms present in the root makes it difficult to examine it by traditional knockout methods due to potential redundancy. In **Chapter 4** a pharmacological approach was used as an alternative method to examine a function of PMEs in root development. It has been shown before that EGCG, a component of green tea catechin extract, has an inhibitory effect on PMEs *in vitro* in *Arabidopsis* (Wolf et al., 2012; L'Enfant et al., 2015). Here, PP60 was shown to enhance PME activity *in vivo* probably due to induced overexpression of some PME isoforms. The redundancy effect may be caused by initial inhibition of PME activity by PP60 to which plants respond by overexpressing some of the PME isoforms. Moreover, it could be possible that PP60 acts only on a subset of PMEs partially inhibiting the total PME activity and causing the redundancy effect. Therefore, conclusions from previous studies based on *in vitro* PME activity analysis alone may not be sufficient to explain plant growth and developmental processes. An optimal condition in which PME has the highest activity is more basic pH. Indeed, when plants were grown on media with pH 8.0 they showed higher PME activity compared to pH 5.7 control conditions. When plants were grown on more acidic pH 4.5 together with PP60 they seemed to overcome an environmental stress and grow better than control plants. Elevated PME activity could possibly balance the changes in other enzymes, like expansins caused by low pH and therefore maintain cell wall homeostasis. PME activity produces HG backbones without methyl groups which is then vulnerable to hydrolysis by PGs. Therefore, PG activity depends on that of PMEs. It has been shown that PG activity increased after PP60 treatment and this might have influenced the production of OGAs involved in pathogen response as signalling molecules. Modulations in PME and PG activity caused reduction in primary root development due to shorter epidermal cells, meristem size and the arrest of cell division. The inhibition of cell expansion may be caused by an increase in PME activity, crosslinking of the pectin network and stiffening of walls.

Plant phytohormones regulate all the growth and developmental processes. Auxin is one of the most important hormones involved in root development and bending. **Chapter 5** describes preliminary efforts to characterize hormonal regulation of PME activity in *Arabidopsis* roots using pharmacological and hormonal treatments. Seedlings were grown on media supplemented with PP60, synthetic auxin (1-NAA) and the brassinosteroid synthesis inhibitor (Propiconazole; Pcz). Many genes involved in plant developmental processes are responsive to auxin and they are potentially regulated by the auxin response transcription factors (ARFs; Li et al., 2016). The mutant *arf7/19* in two ARFs was imposed to the same treatments as wild type plants. Exogenously applied auxin inhibited root elongation but the root growth could be restored after addition of PP60. These results suggested that auxin may require low PME activity to be able to inhibit root elongation. The *arf7/19* seedlings showed increased root elongation regardless of exogenous auxin when

compared to wild type. It is possible that ARF7 and ARF19 could regulate the expression of PMEs and PMEIs in roots to modulate the activity of PME. Another hormone involved in root development is brassinosteroid (BR). BR perception by BRI1 activates the transcription factors BZR1/2 which could regulate genes involved in cell wall remodelling. Therefore, it is believed BR could possibly regulate the transcription of PME and/or PMEI genes. Using the BR biosynthesis inhibitor, Pcz it was shown that plants affected in BR biosynthesis and with increased PME activity had longer roots compared to those with BR biosynthesis inhibition only. Therefore, it is possible that BR regulates the activity of PME and lower BR levels are required for cell elongation.

The loss of cell adhesion is caused by the hydrolysis of pectin in the middle lamella and is required for developmental processes like root emergence from germinating seeds or leaf expansion (Jeremy A. Roberts et al., 2002). It is also required for release of single border-like cells (BLCs) which may be required for root cap protection from abiotic and biotic stresses. **Chapter 6** presents approaches used to investigate PMEs involvement in HG composition and BLCs phenotype. Using biochemical staining and immunolabelling root tips were observed after application of PP60 to the media. PP60 treatment caused release of BLCs and production of mucilage in which they were trapped. It is suggested that the PME and PG activity increase after PP60 addition may affect the BLCs separation from the root cap. Additionally, the low level of arabinogalactan proteins which are found in high levels in mucilage and are required in plant pathogen response may suggest that the detachment of BLCs is not caused by the plant pathogen response. Results from this chapter indicated that a low level of PME activity is required for the maintenance of adhesion between BLCs in *Arabidopsis*.

Finally, **Chapter 7** reports the characterization of the metabolome after cellulose biosynthesis inhibition. Cell wall damage caused by the cellulose biosynthesis inhibitor, isoxaben trigger responses required for maintenance of the cell wall integrity. One of these responses includes higher production of pectin to compensate for the reduced level of functional cellulose. Using isoxaben as a tool, untargeted metabolic profiling was performed on wild type and *isoxaben resistant 1-1* (*ixr1-1*) plants. Overall, both genotypes showed changes in metabolism of purine and pyrimidine nucleotides and branched-chain amino acids. It is possible to speculate that a higher nucleotide level is required for the production of activated nucleotide sugars required for synthesis of new cell wall components. Whereas accumulation of branched-chain amino acids may support the production of secondary metabolites required for defence responses in cell wall-weakened plants. Future work regarding the data analysis of time-course experiment will provide insights into a metabolism status over short term intervals.

Taken together, these results confirm the importance of pectin in plant developmental processes. Contrary to previous suggestions that catechins inhibit PME activity based on an *in vitro* experiment, it has been shown that the addition of PP60 caused a PME activity increase *in vivo*. *In vitro* results can be obtained quickly without the use of plant material. They can have better control of the environment knowing that there are no other molecules present which would interfere with a studying enzyme. However, it can be a disadvantage at the same time. *In vitro* experiments do not create special conditions which some enzymes may require and which can be provided only in the cell/organism. Therefore, *in vivo* studies provide a better understanding of organismal response to changes caused by the addition of inhibitor. As the *Arabidopsis* genome contains 66 isoforms of PME it is possible that: (1) inhibitor could work only on some of the isoforms, whereas other are still active. The *in vitro* results confirmed inhibition of an orange PME and one of the *Arabidopsis* isoforms (Lewis et al., 2008b; L'Enfant et al., 2015). Besides the highly conserved amino acid sequence between isoforms, the affinity of inhibitor to the active site could be influenced even by a single amino acid substitution as it has been shown in case of isoxaben resistance mutants (Scheible et al., 2001); (2) plant activates the redundancy mechanism to counter the inhibitory effect as shown by transcriptomics and time-course activity experiments. This confirms existence of a compensatory mechanism, which as well may change the activity of other cell wall modifying enzymes like PGs and/or expansins.

Chemical properties of pectin can influence cell wall properties and therefore the ability of cells to expand and divide. These processes greatly influence plant growth and development. It has been proposed that there is a mechano-chemical regulatory loop underlying organ formation in plants which includes pectin and auxin coordination. Local auxin accumulation, driven by coordinated PIN1 polarity could lead to HG demethylesterification. Demethylesterifed HG could be hydrolysed by PGs causing tissue softening, which then allows for tissue outgrowth (Braybrook and Peaucelle, 2013). Therefore, modulation of PME activity is required and regulated by hormones as shown in previous studies and here. It can be speculated that auxin and brassinosteroids (BR) could modulate specific PME isoforms either working in a blockwise or non-blockwise mode of action. As BR is required in the elongation zone of the root, a high level of BR could possibly activate PMEs with a non-blockwise mode of action. Partially demethylesterifed pectin could be then hydrolysed by PG making the cell wall more extensible. It therefore seems that coordination between hormones and PME activity may be required for proper shoot and root development.

The response of plants to cell wall integrity disturbance seems to be very complex and it is not well understood. Cellulose biosynthesis inhibition by isoxaben has been shown

to cause ectopic lignin deposition and increased levels of HG domains of the pectic matrix (Hamann et al., 2009, Manfield et al., 2004b). It is thought that calcium-mediated cross linking of HG may compensate to some extent for the diminished load-bearing capacity of the disrupted cellulosic network. Both the degree and pattern of methyl and acetyl esterification is known to profoundly influence the structural properties of HG domains. The differential production of a large number of purine and pyrimidine nucleotides may indicate that modulation and production of HG is an aspect of the habituation process.

Arabidopsis seedlings are raised *in vitro* on artificial media, which supplies the nutrients necessary for growth and development. Sugars are required in synthetic pathway of many compounds, acting as building blocks of cell wall polysaccharides and may control expression of genes involved in several developmental processes in the cell (Lei and Liu, 2011). Sucrose is often assumed to be the sugar of choice in the media due to its cheap and easy availability. Sucrose is partially hydrolysed into fructose and glucose during autoclaving making the sugars even more accessible for metabolomic processes. Sucrose has been shown to regulate the osmotic pressure in the cytosol, photosynthesis, and respiration (Lei and Liu, 2011). Moreover, it can act as a signalling molecule in the control of translation of basic leucine zipper transcription factors (bZIP) and it has been shown to repress the translation of *Arabidopsis* bZIP11 (Hanson et al., 2008). A previous study showed that sucrose promoted root growth in *Brassica napus* probably because the sucrose was absorbed and used as carbon source by the roots, which improved growth of roots by counteracting negative regulating of sucrose signalling. Transcript profiles indicated that sucrose depressed the gluconeogenesis but increased sugar catabolism (Feng et al., 2010). Here it has been shown that addition of sucrose to the media increased responses caused by pharmacological treatments. In the case of PP60 addition, roots showed a less severe phenotype when compared to sucrose treatment. This could be caused by enhanced signalling and changes in cell wall polysaccharide production, which in turn could affect the activity of cell wall modifying enzymes and cell extensibility. It also has been reported here that addition of sucrose significantly changes plant metabolism including changes in nucleotides, amino acids and secondary metabolites production. Therefore, it has to be noted that addition of sucrose to the growing media may change plant responses to particular treatments.

The results presented here reveal the possibility of cross talk between the synthetic mechanisms of wall polymers and the ability of plants to perceive alterations in cell wall structure. The ability of plants to compensate with other polymers when cellulose synthesis or PME activity are modulated may be necessary for the high degree of functional specialization within CESA and PME family. Future analysis of cell wall composition and

transcriptomics of PP60-treated seedlings may be useful for identifying plant response and candidate components of signalling pathways that mediate the sensing and control of cell wall quality and composition when pectin structure is altered.

8.2 Impact of the presented research

Pectins are polysaccharides that control cell wall porosity. Some studies demonstrated that the porosity of the substrate walls is the main limiting factor in the enzymatic hydrolysis of lignocellulosic biomass (Chandra et al., 2007). The general idea of cell wall degradation for biofuels is that the process starts with cell separation that probably involves the action of endopolygalacturonases on the pectins of the middle lamella. This might be involved with the release of calcium that could be responsible for the signalling related to programmed cell death. This seems to occur in parallel with cell expansion and subsequent production and release of glycosyl hydrolases that would attack hemicelluloses and cellulose.

There could be two possible ways to use the information about effects of PME modulation on cell wall properties for biotechnology purposes: (1) using them for production of transformed plants or (2) express the genes heterologously in order to use them as additions to enzyme cocktails already in use in industry. In the first option, it should be possible to use the modern tools of synthetic biology in order to induce cell separation and expansion. In this case plants would produce biomass with the properties expected to be analogous to a pre-treated biomass material. As for the both options, the enzymes should be studied regarding their specificity. Thus, the knowledge about the effects of PME modulation on cell wall properties could be a way to improve the biomass hydrolysis to bioethanol.

In fruit systems, the most studied degradation process is the activity of endopolygalacturonases, PMEs and β-galactosidases on pectic matrix of the walls. It has been demonstrated that pectinases are associated with ripening and softening through pectin degradation by endopolygalacturonases present in the middle lamella. The action of these enzymes is thought to lead to cell separation, a phenomenon that is linked to the subsequent softening of the fruits and change in their texture and taste. Therefore, changes in PME and PG activity caused by PP60 may influence fruits softening and ripening.

References:

ABBOTT, D. W. & BORASTON, A. B. 2007. The structural basis for exopolygalacturonase activity in a family 28 glycoside hydrolase. *J Mol Biol,* 368**,** 1215-22.

ADACHI, T., ANDO, S. & WATANABE, J. 2002. Characterization of synthetic adsorbents with fine particle sizes for preparative-scale chromatographic separation. *Journal of Chromatography A,* 944**,** 41-59.

ALONSO, A., MARSAL, S. & JULIÀ, A. 2015. Analytical methods in untargeted metabolomics: state of the art in 2015. *Frontiers in Bioengineering and Biotechnology,* 3**,** 23.

ANTHON, G. E. & BARRETT, D. M. 2004. Comparison of three colorimetric reagents in the determination of methanol with alcohol oxidase. Application to the assay of pectin methylesterase. *J Agric Food Chem,* 52**,** 3749-53.

AQUILANO, K., BALDELLI, S., ROTILIO, G. & CIRIOLO, M. R. 2008. Role of nitric oxide synthases in Parkinson's disease: a review on the antioxidant and anti-inflammatory activity of polyphenols. *Neurochem Res,* 33**,** 2416-26.

ARIOLI, T. 1998. Molecular analysis of cellulose biosynthesis in *Arabidopsis*. *Science,* 279**,** 717-720.

AZIZ, A., HEYRAUD, A. & LAMBERT, B. 2004. Oligogalacturonide signal transduction, induction of defense-related responses and protection of grapevine against *Botrytis cinerea*. *Planta,* 218**,** 767-774.

AZPEITIA, E., WEINSTEIN, N., BENÍTEZ, M., MENDOZA, L. & ALVAREZ-BUYLLA, E. R. 2013. Finding missing interactions of the *Arabidopsis thaliana* root stem cell niche gene regulatory network. *Frontiers in Plant Science,* 4.

BABU, Y., MUSIELAK, T., HENSCHEN, A. & BAYER, M. 2013. Suspensor length determines developmental progression of the embryo in *Arabidopsis*. *Plant Physiol,* 162**,** 1448-58.

BAETZ, U. & MARTINOIA, E. 2014. Root exudates: the hidden part of plant defense. *Trends Plant Sci,* 19**,** 90-8.

BALCEROWICZ, D., SCHOENAERS, S. & VISSENBERG, K. 2015. From diffuse growth to planar polarity in *Arabidopsis* root epidermal cells. *Frontiers in Plant Science,* 6.

BALDWIN, K. L., STROHM, A. K. & MASSON, P. H. 2013. Gravity sensing and signal transduction in vascular plant primary roots. *American Journal of Botany,* 100**,** 126-142.

BALESTRIERI, C., CASTALDO, D., GIOVANE, A., QUAGLIUOLO, L. & SERVILLO, L. 1990. A glycoprotein inhibitor of pectin methylesterase in kiwi fruit (*Actinidia chinensis*). *European Journal of Biochemistry,* 193**,** 183-187.

BALUŠKA, F., SALAJ, J., MATHUR, J., BRAUN, M., JASPER, F., ŠAMAJ, J., CHUA, N.-H., BARLOW, P. W. & VOLKMANN, D. 2000. Root hair formation: F-actin-dependent tip growth is initiated by local assembly of profilin-supported F-actin

meshworks accumulated within expansin-enriched bulges. *Developmental Biology,* 227**,** 618-632.

BAND, L. R., WELLS, D. M., LARRIEU, A., SUN, J., MIDDLETON, A. M., FRENCH, A. P., BRUNOUD, G., SATO, E. M., WILSON, M. H., PÉRET, B., OLIVA, M., SWARUP, R., SAIRANEN, I., PARRY, G., LJUNG, K., BEECKMAN, T., GARIBALDI, J. M., ESTELLE, M., OWEN, M. R., VISSENBERG, K., HODGMAN, T. C., PRIDMORE, T. P., KING, J. R., VERNOUX, T. & BENNETT, M. J. 2012. Root gravitropism is regulated by a transient lateral auxin gradient controlled by a tipping-point mechanism. *Proceedings of the National Academy of Sciences,* 109**,** 4668-4673.

BAR-PELED, M., URBANOWICZ, B. R. & O'NEILL, M. A. 2012. The synthesis and origin of the pectic polysaccharide rhamnogalacturonan II - insights from nucleotide sugar formation and diversity. *Front Plant Sci,* 3**,** 92.

BARLOW, P. 2002. The root cap: cell dynamics, cell differentiation and cap function. *Journal of Plant Growth Regulation,* 21**,** 261-286.

BAUM, S. F., DUBROVSKY, J. G. & ROST, T. L. 2002. Apical organization and maturation of the cortex and vascular cylinder in *Arabidopsis thaliana* (*Brassicaceae*) roots. *American Journal of Botany,* 89**,** 908-920.

BENEDETTI, M., PONTIGGIA, D., RAGGI, S., CHENG, Z., SCALONI, F., FERRARI, S., AUSUBEL, F. M., CERVONE, F. & DE LORENZO, G. 2015. Plant immunity triggered by engineered in vivo release of oligogalacturonides, damage-associated molecular patterns. *Proceedings of the National Academy of Sciences,* 112**,** 5533-5538.

BETHKE, G., GRUNDMAN, R. E., SREEKANTA, S., TRUMAN, W., KATAGIRI, F. & GLAZEBROOK, J. 2013. *Arabidopsis* PECTIN METHYLESTERASES contribute to immunity against *Pseudomonas syringae*. *Plant Physiology*, 164(2), 1093-107.

BIBIKOVA, T. N., BLANCAFLOR, E. B. & GILROY, S. 1999. Microtubules regulate tip growth and orientation in root hairs of *Arabidopsis thaliana*. *The Plant Journal,* 17**,** 657-665.

BIBIKOVA, T. N., JACOB, T., DAHSE, I. & GILROY, S. 1998. Localized changes in apoplastic and cytoplasmic pH are associated with root hair development in *Arabidopsis thaliana*. *Development,* 125**,** 2925-2934.

BINDER, S. 2010. Branched-chain amino acid metabolism in *Arabidopsis thaliana*. *The Arabidopsis Book / American Society of Plant Biologists,* 8**,** e0137.

BLANC, G., BARAKAT, A., GUYOT, R., COOKE, R. & DELSENY, M. 2000. Extensive duplication and reshuffling in the *Arabidopsis* genome. *The Plant Cell,* 12**,** 1093-1101.

BLANC, G. & WOLFE, K. H. 2004. Widespread paleopolyploidy in model plant species inferred from age distributions of duplicate genes. *The Plant Cell,* 16**,** 1667-1678.

BLANCAFLOR, E. B., FASANO, J. M. & GILROY, S. 1998. Mapping the functional roles of cap cells in the response of *Arabidopsis* primary roots to gravity. *Plant Physiology,* 116**,** 213-222.

BONKE, M., THITAMADEE, S., MAHONEN, A. P., HAUSER, M.-T. & HELARIUTTA, Y. 2003. APL regulates vascular tissue identity in *Arabidopsis*. *Nature,* 426**,** 181-186.

BOSCH, M., CHEUNG, A. Y. & HEPLER, P. K. 2005. Pectin methylesterase, a regulator of pollen tube growth. *Plant Physiol,* 138**,** 1334-46.

BRAYBROOK, S. A. & PEAUCELLE, A. 2013. Mechano-chemical aspects of organ formation in *Arabidopsis thaliana*: the relationship between auxin and pectin. *PLoS ONE,* 8**,** e57813.

BRUEX, A., KAINKARYAM, R. M., WIECKOWSKI, Y., KANG, Y. H., BERNHARDT, C., XIA, Y., ZHENG, X., WANG, J. Y., LEE, M. M., BENFEY, P., WOOLF, P. J. & SCHIEFELBEIN, J. 2012. A gene regulatory network for root epidermis cell differentiation in *Arabidopsis*. *PLoS Genet,* 8**,** e1002446.

BRUTUS, A., SICILIA, F., MACONE, A., CERVONE, F. & DE LORENZO, G. 2010. A domain swap approach reveals a role of the plant wall-associated kinase 1 (WAK1) as a receptor of oligogalacturonides. *Proc Natl Acad Sci U S A,* 107**,** 9452-7.

CABRERA, J. C., BOLAND, A., MESSIAEN, J., CAMBIER, P. & VAN CUTSEM, P. 2008. Egg box conformation of oligogalacturonides: the time-dependent stabilization of the elicitor-active conformation increases its biological activity. *Glycobiology,* 18**,** 473-82.

CAFFALL, K. H. & MOHNEN, D. 2009. The structure, function, and biosynthesis of plant cell wall pectic polysaccharides. *Carbohydr Res,* 344**,** 1879-900.

CAMARDELLA, L., CARRATORE, V., CIARDIELLO, M. A., SERVILLO, L., BALESTRIERI, C. & GIOVANE, A. 2000. Kiwi protein inhibitor of pectin methylesterase amino-acid sequence and structural importance of two disulfide bridges. *Eur J Biochem,* 267**,** 4561-5.

CAMERON, R. G., LUZIO, G. A., GOODNER, K. & WILLIAMS, M. A. K. 2008. Demethylation of a model homogalacturonan with a salt-independent pectin methylesterase from citrus: I. Effect of pH on demethylated block size, block number and enzyme mode of action. *Carbohydrate Polymers,* 71**,** 287-299.

CANET, W., ALVAREZ, M. A. D., LUNA, P., FERNANDEZ, C. & TORTOSA, M. A. E. 2004. Blanching effects on chemistry, quality and structure of green beans (cv. *Moncayo*). *European Food Research and Technology,* 220**,** 421-430.

CANNESAN, M. A., GANGNEUX, C., LANOUE, A., GIRON, D., LAVAL, K., HAWES, M., DRIOUICH, A. & VICRÉ-GIBOUIN, M. 2011. Association between border cell responses and localized root infection by pathogenic *Aphanomyces euteiches*. *Annals of Botany,* 108**,** 459-469.

CAO, J. 2012. The pectin lyases in *Arabidopsis thaliana*: evolution, selection and expression profiles. *PLoS ONE,* 7**,** e46944.

CARPITA, N. C. & GIBEAUT, D. M. 1993. Structural models of primary cell walls in flowering plants: consistency of molecular structure with the physical properties of the walls during growth. *The Plant Journal,* 3**,** 1-30.

CASIMIRO, I., BEECKMAN, T., GRAHAM, N., BHALERAO, R., ZHANG, H., CASERO, P., SANDBERG, G. & BENNETT, M. J. 2003. Dissecting *Arabidopsis* lateral root development. *Trends in Plant Science,* 8**,** 165-171.

CHAIWANON, J. & WANG, Z. Y. 2015. Spatiotemporal brassinosteroid signaling and antagonism with auxin pattern stem cell dynamics in *Arabidopsis* roots. *Curr Biol,* 25**,** 1031-42.

CHANDRA, R. P., BURA, R., MABEE, W. E., BERLIN, A., PAN, X. & SADDLER, J. N. 2007. Substrate pretreatment: the key to effective enzymatic hydrolysis of lignocellulosics? *Adv Biochem Eng Biotechnol,* 108**,** 67-93.

CHASSOT, C., BUCHALA, A., SCHOONBEEK, H. J., METRAUX, J. P. & LAMOTTE, O. 2008. Wounding of *Arabidopsis* leaves causes a powerful but transient protection against *Botrytis* infection. *Plant J,* 55**,** 555-67.

CHOE, S., SCHMITZ, R. J., FUJIOKA, S., TAKATSUTO, S., LEE, M. O., YOSHIDA, S., FELDMANN, K. A. & TAX, F. E. 2002. *Arabidopsis* brassinosteroid-insensitive *dwarf12* mutants are semidominant and defective in a glycogen synthase kinase 3β-like kinase. *Plant Physiol,* 130**,** 1506-15.

CHORMOVA, D., MESSENGER, D. J. & FRY, S. C. 2014. Rhamnogalacturonan-II cross-linking of plant pectins via boron bridges occurs during polysaccharide synthesis and/or secretion. *Plant Signaling & Behavior,* 9**,** e28169.

CHUNG, Y., MAHARJAN, P. M., LEE, O., FUJIOKA, S., JANG, S., KIM, B., TAKATSUTO, S., TSUJIMOTO, M., KIM, H., CHO, S., PARK, T., CHO, H., HWANG, I. & CHOE, S. 2011. Auxin stimulates *DWARF4* expression and brassinosteroid biosynthesis in *Arabidopsis*. *The Plant Journal,* 66**,** 564-578.

COIMBRA, S., COSTA, M., MENDES, M. A., PEREIRA, A. M., PINTO, J. & PEREIRA, L. G. 2010. Early germination of *Arabidopsis* pollen in a double null mutant for the arabinogalactan protein genes *AGP6* and *AGP11*. *Sex Plant Reprod,* 23**,** 199-205.

COSGROVE, D. 1989. Characterization of long-term extension of isolated cell walls from growing cucumber hypocotyls. *Planta,* 177**,** 121-130.

COSGROVE, D. J. 1997. Relaxation in a high-stress environment: the molecular bases of extensible cell walls and cell enlargement. *Plant Cell,* 9**,** 1031-1041.

COSGROVE, D. J. 2000. Loosening of plant cell walls by expansins. *Nature,* 407**,** 321-326.

COSGROVE, D. J. 2005. Growth of the plant cell wall. *Nat Rev Mol Cell Biol,* 6**,** 850-61.

CUI, H. & BENFEY, P. N. 2009. Cortex proliferation: Simple phenotype, complex regulatory mechanisms. *Plant Signaling & Behavior,* 4**,** 551-553.

DARVILL, A. G., MCNEIL, M. & ALBERSHEIM, P. 1978. Structure of plant cell walls. VIII. A new pectic polysaccharide. *Plant Physiol,* 62**,** 418-422.

DASTIDAR, M. G., JOUANNET, V. & MAIZEL, A. 2012. Root branching: mechanisms, robustness, and plasticity. *Wiley Interdisciplinary Reviews: Developmental Biology,* 1**,** 329-343.

DAVIÈRE, J.-M. & ACHARD, P. 2013. Gibberellin signaling in plants. *Development,* 140**,** 1147-1151.

DAVIS, J., BRANDIZZI, F., LIEPMAN, A. H. & KEEGSTRA, K. 2010. *Arabidopsis* mannan synthase CSLA9 and glucan synthase CSLC4 have opposite orientations in the Golgi membrane. *Plant J,* 64**,** 1028-37.

DE-LA-PEÑA, C., BADRI, D. V., LEI, Z., WATSON, B. S., BRANDÃO, M. M., SILVA-FILHO, M. C., SUMNER, L. W. & VIVANCO, J. M. 2010. Root secretion of defense-related proteins is development-dependent and correlated with flowering time. *Journal of Biological Chemistry,* 285**,** 30654-30665.

DE CASTRO, M., LARGO-GOSENS, A., ALVAREZ, J. M., GARCÍA-ANGULO, P. & ACEBES, J. L. 2014. Early cell-wall modifications of maize cell cultures during habituation to dichlobenil. *Journal of Plant Physiology,* 171**,** 127-135.

DE LORENZO, G., CERVONE, F., HAHN, M. G., DARVILL, A. & ALBERSHEIM, P. 1991. Bacterial endopectate lyase: evidence that plant cell wall pH prevents tissue maceration and increases the half-life of elicitor-active oligogalacturonides. *Physiological and Molecular Plant Pathology,* 39**,** 335-344.

DE SMET, I., LAU, S., VOSS, U., VANNESTE, S., BENJAMINS, R., RADEMACHER, E. H., SCHLERETH, A., DE RYBEL, B., VASSILEVA, V., GRUNEWALD, W., NAUDTS, M., LEVESQUE, M. P., EHRISMANN, J. S., INZE, D., LUSCHNIG, C., BENFEY, P. N., WEIJERS, D., VAN MONTAGU, M. C., BENNETT, M. J., JURGENS, G. & BEECKMAN, T. 2010. Bimodular auxin response controls organogenesis in *Arabidopsis*. *Proc Natl Acad Sci U S A,* 107**,** 2705-10.

DE SMET, I., VASSILEVA, V., DE RYBEL, B., LEVESQUE, M. P., GRUNEWALD, W., VAN DAMME, D., VAN NOORDEN, G., NAUDTS, M., VAN ISTERDAEL, G., DE CLERCQ, R., WANG, J. Y., MEULI, N., VANNESTE, S., FRIML, J., HILSON, P., JÜRGENS, G., INGRAM, G. C., INZÉ, D., BENFEY, P. N. & BEECKMAN, T. 2008. Receptor-like kinase ACR4 restricts formative cell divisions in the *Arabidopsis* root. *Science,* 322**,** 594-597.

DELLO IOIO, R., LINHARES, F. S., SCACCHI, E., CASAMITJANA-MARTINEZ, E., HEIDSTRA, R., COSTANTINO, P. & SABATINI, S. 2007. Cytokinins determine *Arabidopsis* root-meristem size by controlling cell differentiation. *Current Biology,* 17**,** 678-682.

DENNESS, L., MCKENNA, J. F., SEGONZAC, C., WORMIT, A., MADHOU, P., BENNETT, M., MANSFIELD, J., ZIPFEL, C. & HAMANN, T. 2011. Cell wall damage-induced lignin biosynthesis is regulated by a reactive oxygen species- and jasmonic acid-dependent process in *Arabidopsis*. *Plant Physiol,* 156**,** 1364-74.

DERBYSHIRE, P., MCCANN, M. C. & ROBERTS, K. 2007. Restricted cell elongation in *Arabidopsis* hypocotyls is associated with a reduced average pectin esterification level. *BMC Plant Biology,* 7**,** 1-12.

DESPREZ, T., VERNHETTES, S., FAGARD, M., REFRÉGIER, G., DESNOS, T., ALETTI, E., PY, N., PELLETIER, S. & HÖFTE, H. 2002. Resistance against herbicide isoxaben and cellulose deficiency caused by distinct mutations in same cellulose synthase isoform CESA6. *Plant Physiology,* 128**,** 482-490.

DI MATTEO, A., GIOVANE, A., RAIOLA, A., CAMARDELLA, L., BONIVENTO, D., DE LORENZO, G., CERVONE, F., BELLINCAMPI, D. & TSERNOGLOU, D. 2005. Structural basis for the interaction between pectin methylesterase and a specific inhibitor protein. *The Plant Cell,* 17**,** 849-858.

DÍAZ-CACHO, P., MORAL, R., ENCINA, A., LUIS ACEBES, J. & ALVAREZ, J. 1999. Cell wall modifications in bean (*Phaseolus vulgaris*) callus cultures tolerant to isoxaben. *Physiologia Plantarum,* 107**,** 54-59.

DOLAN, L., JANMAAT, K., WILLEMSEN, V., LINSTEAD, P., POETHIG, S., ROBERTS, K. & SCHERES, B. 1993. Cellular organisation of the *Arabidopsis thaliana* root. *Development,* 119**,** 71-84.

DOWNIE, B., DIRK, L. M., HADFIELD, K. A., WILKINS, T. A., BENNETT, A. B. & BRADFORD, K. J. 1998. A gel diffusion assay for quantification of pectin methylesterase activity. *Anal Biochem,* 264**,** 149-57.

DRIOUICH, A., DURAND, C., CANNESAN, M.-A., PERCOCO, G. & VICRÉ-GIBOUIN, M. 2010. Border cells versus border-like cells: are they alike? *Journal of Experimental Botany,* 61**,** 3827-3831.

DRIOUICH, A., DURAND, C. & VICRÉ-GIBOUIN, M. 2007. Formation and separation of root border cells. *Trends in Plant Science,* 12**,** 14-19.

DRIOUICH, A., FOLLET-GUEYE, M.-L., VICRÉ-GIBOUIN, M. & HAWES, M. 2013. Root border cells and secretions as critical elements in plant host defense. *Current Opinion in Plant Biology,* 16**,** 489-495.

DRIOUICH, A., FOLLET-GUEYE, M. L., BERNARD, S., KOUSAR, S., CHEVALIER, L., VICRE-GIBOUIN, M. & LEROUXEL, O. 2012. Golgi-mediated synthesis and secretion of matrix polysaccharides of the primary cell wall of higher plants. *Front Plant Sci,* 3**,** 79.

DU, G.-J., ZHANG, Z., WEN, X.-D., YU, C., CALWAY, T., YUAN, C.-S. & WANG, C.-Z. 2012. Epigallocatechin gallate (EGCG) is the most effective cancer chemopreventive polyphenol in green tea. *Nutrients,* 4**,** 1679-1691.

DUAN, Q., KITA, D., LI, C., CHEUNG, A. Y. & WU, H. M. 2010. FERONIA receptor-like kinase regulates RHO GTPase signaling of root hair development. *Proc Natl Acad Sci U S A,* 107**,** 17821-6.

DUBROVSKY, J. G., GAMBETTA, G. A., HERNÁNDEZ-BARRERA, A., SHISHKOVA, S. & GONZÁLEZ, I. 2006. Lateral root initiation in *Arabidopsis*: developmental window, spatial patterning, density and predictability. *Annals of Botany,* 97**,** 903-915.

DUBROVSKY, J. G., SAUER, M., NAPSUCIALY-MENDIVIL, S., IVANCHENKO, M. G., FRIML, J., SHISHKOVA, S., CELENZA, J. & BENKOVÁ, E. 2008. Auxin acts as a local morphogenetic trigger to specify lateral root founder cells. *Proceedings of the National Academy of Sciences,* 105**,** 8790-8794.

DUCKETT, C. M., GRIERSON, C., LINSTEAD, P., SCHNEIDER, K., LAWSON, E., DEAN, C., POETHIG, S. & ROBERTS, K. 1994. Clonal relationships and cell patterning in the root epidermis of *Arabidopsis*. *Development,* 120**,** 2465-2474.

DURAND, C., VICRÉ-GIBOUIN, M., FOLLET-GUEYE, M. L., DUPONCHEL, L., MOREAU, M., LEROUGE, P. & DRIOUICH, A. 2009. The organization pattern of root border-like cells of *Arabidopsis* is dependent on cell wall homogalacturonan. *Plant Physiology,* 150**,** 1411-1421.

ENDLER, A. & PERSSON, S. 2011. Cellulose synthases and synthesis in *Arabidopsis*. *Mol Plant,* 4**,** 199-211.

ENGELSDORF, T. & HAMANN, T. 2014. An update on receptor-like kinase involvement in the maintenance of plant cell wall integrity. *Ann Bot,* 114**,** 1339-47.

FENG, X., T., X. & WANG, Z. 2010. Effects of sucrose on germination and seedling development of *Brassica napus*. *International Journal of Biology,* 2**,** 150-154.

FERRARI, S., GALLETTI, R., PONTIGGIA, D., MANFREDINI, C., LIONETTI, V., BELLINCAMPI, D., CERVONE, F. & DE LORENZO, G. 2008. Transgenic expression of a fungal endo-polygalacturonase increases plant resistance to pathogens and reduces auxin sensitivity. *Plant Physiology,* 146**,** 669-681.

FERRARI, S., SAVATIN, D. V., SICILIA, F., GRAMEGNA, G., CERVONE, F. & LORENZO, G. D. 2013. Oligogalacturonides: plant damage-associated molecular patterns and regulators of growth and development. *Front Plant Sci,* 4**,** 49.

FORCAT, S., BENNETT, M., MANSFIELD, J. & GRANT, M. 2008. A rapid and robust method for simultaneously measuring changes in the phytohormones ABA, JA and SA in plants following biotic and abiotic stress. *Plant Methods,* 4**,** 16.

FORZANI, C., AICHINGER, E., SORNAY, E., WILLEMSEN, V., LAUX, T., DEWITTE, W. & MURRAY, JAMES A. H. 2014. WOX5 Suppresses *CYCLIN D* activity to establish quiescence at the center of the root stem cell niche. *Current Biology,* 24**,** 1939-1944.

FRANCIS, K. E., LAM, S. Y. & COPENHAVER, G. P. 2006. Separation of *Arabidopsis* pollen tetrads is regulated by QUARTET1, a pectin methylesterase gene. *Plant Physiology,* 142**,** 1004-1013.

FRIDMAN, Y., ELKOUBY, L., HOLLAND, N., VRAGOVIĆ, K., ELBAUM, R. & SAVALDI-GOLDSTEIN, S. 2014. Root growth is modulated by differential hormonal sensitivity in neighboring cells. *Genes & Development,* 28**,** 912-920.

FRIDMAN, Y. & SAVALDI-GOLDSTEIN, S. 2013. Brassinosteroids in growth control: how, when and where. *Plant Sci,* 209**,** 24-31.

FRIML, J., VIETEN, A., SAUER, M., WEIJERS, D., SCHWARZ, H., HAMANN, T., OFFRINGA, R. & JURGENS, G. 2003. Efflux-dependent auxin gradients establish the apical-basal axis of *Arabidopsis*. *Nature,* 426**,** 147-153.

FRY, S. C., SMITH, R. C., RENWICK, K. F., MARTIN, D. J., HODGE, S. K. & MATTHEWS, K. J. 1992. Xyloglucan endotransglycosylase, a new wall-loosening enzyme activity from plants. *Biochem J,* 282**,** 821-828.

FRY, S. C., YORK, W. S., ALBERSHEIM, P., DARVILL, A., HAYASHI, T., JOSELEAU, J.-P., KATO, Y., LORENCES, E. P., MACLACHLAN, G. A., MCNEIL, M., MORT, A. J., GRANT REID, J. S., SEITZ, H. U., SELVENDRAN, R. R., VORAGEN, A. G. J. & WHITE, A. R. 1993. An unambiguous nomenclature for xyloglucan-derived oligosaccharides. *Physiol Plantarium,* 89**,** 1-3.

FUKAKI, H., OKUSHIMA, Y. & TASAKA, M. 2007. Auxin-mediated lateral root formation in higher plants. *Int Rev Cytol,* 256**,** 111-37.

GALINHA, C., HOFHUIS, H., LUIJTEN, M., WILLEMSEN, V., BLILOU, I., HEIDSTRA, R. & SCHERES, B. 2007. PLETHORA proteins as dose-dependent master regulators of Arabidopsis root development. *Nature,* 449**,** 1053-1057.

GALLETTI, R., DENOUX, C., GAMBETTA, S., DEWDNEY, J., AUSUBEL, F. M., DE LORENZO, G. & FERRARI, S. 2008. The AtrbohD-mediated oxidative burst elicited by oligogalacturonides in *Arabidopsis* is dispensable for the activation of defense responses effective against *Botrytis cinerea*. *Plant Physiol,* 148**,** 1695-706.

GALLETTI, R., FERRARI, S. & DE LORENZO, G. 2011. *Arabidopsis* MPK3 and MPK6 play different roles in basal and oligogalacturonide- or flagellin-induced resistance against *Botrytis cinerea*. *Plant Physiol,* 157**,** 804-14.

GALWAY, M. E., MASUCCI, J. D., LLOYD, A. M., WALBOT, V., DAVIS, R. W. & SCHIEFELBEIN, J. W. 1994. The *TTG* gene is required to specify epidermal cell

fate and cell patterning in the *Arabidopsis* root. *Developmental Biology,* 166**,** 740-754.

GASPAR, Y. M., NAM, J., SCHULTZ, C. J., LEE, L. Y., GILSON, P. R., GELVIN, S. B. & BACIC, A. 2004. Characterization of the *Arabidopsis* lysine-rich arabinogalactan-protein AtAGP17 mutant (*rat1*) that results in a decreased efficiency of agrobacterium transformation. *Plant Physiol,* 135**,** 2162-71.

GESHI, N., JORGENSEN, B. & ULVSKOV, P. 2004. Subcellular localization and topology of β(1-->4)galactosyltransferase that elongates β(1-->4)galactan side chains in rhamnogalacturonan I in potato. *Planta,* 218**,** 862-8.

GIBSON, L. J. 2012. The hierarchical structure and mechanics of plant materials. *J R Soc Interface,* 9**,** 2749-66.

GOMEZ-CADENAS, A., VIVES, V., ZANDALINAS, S. I., MANZI, M., SANCHEZ-PEREZ, A. M., PEREZ-CLEMENTE, R. M. & ARBONA, V. 2015. Abscisic acid: a versatile phytohormone in plant signaling and beyond. *Curr Protein Pept Sci,* 16**,** 413-34.

GONZÁLEZ-CARRANZA, Z. H., ELLIOTT, K. A. & ROBERTS, J. A. 2007. Expression of polygalacturonases and evidence to support their role during cell separation processes in *Arabidopsis thaliana*. *Journal of Experimental Botany,* 58**,** 3719-3730.

GOUBET, F., MISRAHI, A., PARK, S. K., ZHANG, Z., TWELL, D. & DUPREE, P. 2003. AtCSLA7, a cellulose synthase-like putative glycosyltransferase, is important for pollen tube growth and embryogenesis in *Arabidopsis*. *Plant Physiol,* 131**,** 547-57.

GRIERSON, C., NIELSEN, E., KETELAARC, T. & SCHIEFELBEIN, J. 2014. Root hairs. *The Arabidopsis Book / American Society of Plant Biologists,* 12**,** e0172.

GUENIN, S., MARECK, A., RAYON, C., LAMOUR, R., ASSOUMOU NDONG, Y., DOMON, J. M., SENECHAL, F., FOURNET, F., JAMET, E., CANUT, H., PERCOCO, G., MOUILLE, G., ROLLAND, A., RUSTERUCCI, C., GUERINEAU, F., VAN WUYTSWINKEL, O., GILLET, F., DRIOUICH, A., LEROUGE, P., GUTIERREZ, L. & PELLOUX, J. 2011. Identification of pectin methylesterase 3 as a basic pectin methylesterase isoform involved in adventitious rooting in *Arabidopsis thaliana*. *New Phytol,* 192**,** 114-26.

GUERRIERO, G., FUGELSTAD, J. & BULONE, V. 2010. What do we really know about cellulose biosynthesis in higher plants? *J Integr Plant Biol,* 52**,** 161-75.

GUILFOYLE, T. 2007. Plant biology: Sticking with auxin. *Nature,* 446**,** 621-622.

GUILFOYLE, T. J. & HAGEN, G. 2007. Auxin response factors. *Current Opinion in Plant Biology,* 10**,** 453-460.

GULERIA, P. & YADAV, S. K. 2014. Overexpression of a glycosyltransferase gene *SrUGT74G1* from *Stevia* improved growth and yield of transgenic *Arabidopsis* by catechin accumulation. *Molecular Biology Reports,* 41**,** 1741-1752.

GUNAWARDENA, U. & HAWES, M. C. 2002. Tissue specific localization of root infection by fungal pathogens: role of root border cells. *Molecular Plant-Microbe Interactions,* 15**,** 1128-1136.

GUPTA, A. K. & KAUR, N. 2005. Sugar signalling and gene expression in relation to carbohydrate metabolism under abiotic stresses in plants. *J Biosci,* 30**,** 761-76.

HADFI, K., SPETH, V. & NEUHAUS, G. 1998. Auxin-induced developmental patterns in *Brassica juncea* embryos. *Development,* 125**,** 879-887.

HADFIELD, K. A. & BENNETT, A. B. 1998. Polygalacturonases: many genes in search of a function. *Plant Physiology,* 117**,** 337-343.

HAECKER, A., GROß-HARDT, R., GEIGES, B., SARKAR, A., BREUNINGER, H., HERRMANN, M. & LAUX, T. 2004. Expression dynamics of *WOX* genes mark cell fate decisions during early embryonic patterning in *Arabidopsis thaliana*. *Development,* 131**,** 657-668.

HAMANN, T. 2012. Plant cell wall integrity maintenance as an essential component of biotic stress response mechanisms. *Front Plant Sci,* 3**,** 77.

HAMANN, T. 2015a. The Plant Cell Wall Integrity Maintenance Mechanism—Concepts for Organization and Mode of Action. *Plant and Cell Physiology,* 56**,** 215-223.

HAMANN, T. 2015b. The plant cell wall integrity maintenance mechanism – A case study of a cell wall plasma membrane signaling network. *Phytochemistry,* 112**,** 100-109.

HAMANN, T., BENNETT, M., MANSFIELD, J. & SOMERVILLE, C. 2009. Identification of cell-wall stress as a hexose-dependent and osmosensitive regulator of plant responses. *Plant J,* 57**,** 1015-26.

HANSON, J., HANSSEN, M., WIESE, A., HENDRIKS, M. M. & SMEEKENS, S. 2008. The sucrose regulated transcription factor bZIP11 affects amino acid metabolism by regulating the expression of ASPARAGINE SYNTHETASE1 and PROLINE DEHYDROGENASE2. *Plant J,* 53**,** 935-49.

HARDTKE, C. S. & BERLETH, T. 1998. The Arabidopsis gene *MONOPTEROS* encodes a transcription factor mediating embryo axis formation and vascular development. *The EMBO Journal,* 17**,** 1405-1411.

HARHOLT, J., JENSEN, J. K., VERHERTBRUGGEN, Y., SOGAARD, C., BERNARD, S., NAFISI, M., POULSEN, C. P., GESHI, N., SAKURAGI, Y., DRIOUICH, A., KNOX, J. P. & SCHELLER, H. V. 2012. ARAD proteins associated with pectic arabinan biosynthesis form complexes when transiently overexpressed *in planta*. *Planta,* 236**,** 115-28.

HARHOLT, J., SUTTANGKAKUL, A. & VIBE SCHELLER, H. 2010. Biosynthesis of pectin. *Plant Physiol,* 153**,** 384-95.

HARRIS, D. M., CORBIN, K., WANG, T., GUTIERREZ, R., BERTOLO, A. L., PETTI, C., SMILGIES, D.-M., ESTEVEZ, J. M., BONETTA, D., URBANOWICZ, B. R., EHRHARDT, D. W., SOMERVILLE, C. R., ROSE, J. K. C., HONG, M. & DEBOLT, S. 2012. Cellulose microfibril crystallinity is reduced by mutating C-terminal transmembrane region residues CESA1A903V and CESA3T942I of cellulose synthase. *Proceedings of the National Academy of Sciences,* 109**,** 4098-4103.

HARTWIG, T., CORVALAN, C., BEST, N. B., BUDKA, J. S., ZHU, J.-Y., CHOE, S. & SCHULZ, B. 2012. Propiconazole is a specific and accessible brassinosteroid (BR) biosynthesis inhibitor for *Arabidopsis* and maize. *PLoS ONE,* 7**,** e36625.

HARUTA, M., SABAT, G., STECKER, K., MINKOFF, B. B. & SUSSMAN, M. R. 2014. A peptide hormone and its receptor protein kinase regulate plant cell expansion. *Science,* 343**,** 408-11.

HAUBRICK, L. L. & ASSMANN, S. M. 2006. Brassinosteroids and plant function: some clues, more puzzles. *Plant Cell Environ,* 29**,** 446-57.

HAWES, M., BENGOUGH, G., CASSAB, G. & PONCE, G. 2002. Root aaps and rhizosphere. *Journal of Plant Growth Regulation,* 21**,** 352-367.

HE, J.-X., GENDRON, J. M., YANG, Y., LI, J. & WANG, Z.-Y. 2002. The GSK3-like kinase BIN2 phosphorylates and destabilizes BZR1, a positive regulator of the brassinosteroid signaling pathway in *Arabidopsis*. *Proceedings of the National Academy of Sciences,* 99**,** 10185-10190.

HEIM, D. R., SKOMP, J. R., TSCHABOLD, E. E. & LARRINUA, I. M. 1990. Isoxaben inhibits the synthesis of acid insoluble cell wall materials in *Arabidopsis thaliana*. *Plant Physiology,* 93**,** 695-700.

HOFHUIS, H., LASKOWSKI, M., DU, Y., PRASAD, K., GRIGG, S., PINON, V. & SCHERES, B. 2013. Phyllotaxis and rhizotaxis in *Arabidopsis* are modified by three PLETHORA transcription factors. *Current Biology,* 23**,** 956-962.

HÖFTE, H. 2015. The Yin and Yang of cell wall integrity control: brassinosteroid and FERONIA signaling. *Plant and Cell Physiology,* 56**,** 224-231.

HONGO, S., SATO, K., YOKOYAMA, R. & NISHITANI, K. 2012. Demethylesterification of the primary wall by PECTIN METHYLESTERASE35 provides mechanical support to the *Arabidopsis* stem. *Plant Cell,* 24**,** 2624-34.

HONOUR, J. W. 2011. Development and validation of a quantitative assay based on tandem mass spectrometry. *Annals of Clinical Biochemistry,* 48**,** 97-111.

IKEDA, I., TSUDA, K., SUZUKI, Y., KOBAYASHI, M., UNNO, T., TOMOYORI, H., GOTO, H., KAWATA, Y., IMAIZUMI, K., NOZAWA, A. & KAKUDA, T. 2005. Tea catechins with a galloyl moiety suppress postprandial hypertriacylglycerolemia by delaying lymphatic transport of dietary fat in rats. *J Nutr,* 135**,** 155-9.

IVEN, T., KÖNIG, S., SINGH, S., BRAUS-STROMEYER, S. A., BISCHOFF, M., TIETZE, L. F., BRAUS, G. H., LIPKA, V., FEUSSNER, I. & DRÖGE-LASER, W. 2012. Transcriptional activation and production of tryptophan-derived secondary metabolites in *Arabidopsis* roots contributes to the defense against the fungal vascular pathogen *Verticillium longisporum*. *Molecular Plant,* 5**,** 1389-1402.

IWAI, H., MASAOKA, N., ISHII, T. & SATOH, S. 2002. A pectin glucuronyltransferase gene is essential for intercellular attachment in the plant meristem. *Proc Natl Acad Sci U S A,* 99**,** 16319-24.

JAMET, E., ALBENNE, C., BOUDART, G., IRSHAD, M., CANUT, H. & PONT-LEZICA, R. 2008. Recent advances in plant cell wall proteomics. *PROTEOMICS,* 8**,** 893-908.

JENSEN, J. K., SCHULTINK, A., KEEGSTRA, K., WILKERSON, C. G. & PAULY, M. 2012. RNA-Seq analysis of developing nasturtium seeds (*Tropaeolum majus*): identification and characterization of an additional galactosyltransferase involved in xyloglucan biosynthesis. *Mol Plant,* 5**,** 984-92.

JENSEN, J. K., SØRENSEN, S. O., HARHOLT, J., GESHI, N., SAKURAGI, Y., MØLLER, I., ZANDLEVEN, J., BERNAL, A. J., JENSEN, N. B., SØRENSEN, C., PAULY, M., BELDMAN, G., WILLATS, W. G. T. & SCHELLER, H. V. 2008. Identification of a xylogalacturonan xylosyltransferase involved in pectin biosynthesis in *Arabidopsis*. *The Plant Cell,* 20**,** 1289-1302.

JEREMY A. ROBERTS, KATHERINE A. ELLIOTT, A. & GONZALEZ-CARRANZA, Z. H. 2002. Abscission, dehiscence, and other cell separation processes. *Annual Review of Plant Biology,* 53**,** 131-158.

JOLIE, R. P., DUVETTER, T., VAN LOEY, A. M. & HENDRICKX, M. E. 2010. Pectin methylesterase and its proteinaceous inhibitor: a review. *Carbohydr Res,* 345**,** 2583-95.

JONES, J. D. G. & DANGL, J. L. 2006. The plant immune system. *Nature,* 444**,** 323-329.

JONES, M. A., RAYMOND, M. J., YANG, Z. & SMIRNOFF, N. 2007. NADPH oxidase-dependent reactive oxygen species formation required for root hair growth depends on ROP GTPase. *Journal of Experimental Botany,* 58**,** 1261-1270.

KALUNKE, R. M., TUNDO, S., BENEDETTI, M., CERVONE, F., DE LORENZO, G. & D'OVIDIO, R. 2015. An update on polygalacturonase-inhibiting protein (PGIP), a leucine-rich repeat protein that protects crop plants against pathogens. *Frontiers in Plant Science,* 6**,** 146.

KESHISHIAN, E. A. & RASHOTTE, A. M. 2015. Plant cytokinin signalling. *Essays Biochem,* 58**,** 13-27.

KETELAAR, T., FAIVRE-MOSKALENKO, C., ESSELING, J. J., DE RUIJTER, N. C. A., GRIERSON, C. S., DOGTEROM, M. & EMONS, A. M. C. 2002. Positioning of nuclei in *Arabidopsis* root hairs: an actin-regulated process of tip growth. *The Plant Cell,* 14**,** 2941-2955.

KIELISZEWSKI, M. J., O'NEILL, M., LEYKAM, J. & ORLANDO, R. 1995. Tandem mass spectrometry and structural elucidation of glycopeptides from a hydroxyproline-rich plant cell wall glycoprotein indicate that contiguous hydroxyproline residues are the major sites of hydroxyproline O-arabinosylation. *Journal of Biological Chemistry,* 270**,** 2541-2549.

KIRCHER, S. & SCHOPFER, P. 2016. Priming and positioning of lateral roots in *Arabidopsis*. An approach for an integrating concept. *Journal of Experimental Botany,* 67**,** 1411-1420.

KONO, N., ARAKAWA, K., OGAWA, R., KIDO, N., OSHITA, K., IKEGAMI, K., TAMAKI, S. & TOMITA, M. 2009. Pathway Projector: web-based zoomable pathway browser using KEGG Atlas and Google Maps API. *PLoS ONE,* 4**,** e7710.

KOYAMA, H., TODA, T. & HARA, T. 2001. Brief exposure to low-pH stress causes irreversible damage to the growing root in *Arabidopsis thaliana*: pectin–Ca interaction may play an important role in proton rhizotoxicity. *Journal of Experimental Botany,* 52**,** 361-368.

KUMAR, M. & TURNER, S. 2015. Plant cellulose synthesis: CESA proteins crossing kingdoms. *Phytochemistry,* 112**,** 91-99.

KURIYAMA, S., SHIMAZU, T., OHMORI, K., KIKUCHI, N., NAKAYA, N., NISHINO, Y., TSUBONO, Y. & TSUJI, I. 2006. Green tea consumption and mortality due to cardiovascular disease, cancer, and all causes in Japan: the Ohsaki study. *JAMA,* 296**,** 1255-65.

L'ENFANT, M., DOMON, J.-M., RAYON, C., DESNOS, T., RALET, M.-C., BONNIN, E., PELLOUX, J. & PAU-ROBLOT, C. 2015. Substrate specificity of plant and fungi pectin methylesterases: Identification of novel inhibitors of PMEs. *International Journal of Biological Macromolecules,* 81**,** 681-691.

LAGER, I., ANDREASSON, O., DUNBAR, T. L., ANDREASSON, E., ESCOBAR, M. A. & RASMUSSON, A. G. 2010. Changes in external pH rapidly alter plant gene expression and modulate auxin and elicitor responses. *Plant Cell Environ,* 33**,** 1513-28.

LASKOWSKI, M. 2013. Lateral root initiation is a probabilistic event whose frequency is set by fluctuating levels of auxin response. *Journal of Experimental Botany,* 64**,** 2609-2617.

LASKOWSKI, M., BILLER, S., STANLEY, K., KAJSTURA, T. & PRUSTY, R. 2006. Expression profiling of auxin-treated *Arabidopsis* roots: toward a molecular analysis of lateral root emergence. *Plant Cell Physiol,* 47**,** 788-92.

LAVENUS, J., GOH, T., ROBERTS, I., GUYOMARC'H, S., LUCAS, M., DE SMET, I., FUKAKI, H., BEECKMAN, T., BENNETT, M. & LAPLAZE, L. 2013. Lateral root development in *Arabidopsis*: fifty shades of auxin. *Trends in Plant Science,* 18**,** 450-458.

LECLERE, L., CUTSEM, P. V. & MICHIELS, C. 2013. Anti-cancer activities of pH- or heat-modified pectin. *Front Pharmacol,* 4**,** 128.

LEI, M. & LIU, D. 2011. Sucrose regulates plant responses to deficiencies in multiple nutrients. *Plant Signaling & Behavior,* 6**,** 1247-1249.

LEROUX, C., BOUTON, S., KIEFER-MEYER, M. C., FABRICE, T. N., MARECK, A., GUENIN, S., FOURNET, F., RINGLI, C., PELLOUX, J., DRIOUICH, A., LEROUGE, P., LEHNER, A. & MOLLET, J. C. 2015. PECTIN METHYLESTERASE48 is involved in *Arabidopsis* pollen grain germination. *Plant Physiol,* 167**,** 367-80.

LEVESQUE-TREMBLAY, G., MULLER, K., MANSFIELD, S. D. & HAUGHN, G. W. 2015. HIGHLY METHYL ESTERIFIED SEEDS is a pectin methyl esterase involved in embryo development. *Plant Physiol,* 167**,** 725-37.

LEVIN, D. E. 2011. Regulation of cell wall biogenesis in *Saccharomyces cerevisiae*: the cell wall integrity signaling pathway. *Genetics,* 189**,** 1145-75.

LEWIS, K. C., SELZER, T., SHAHAR, C., UDI, Y., TWOROWSKI, D. & SAGI, I. 2008. Inhibition of pectin methyl esterase activity by green tea catechins. *Phytochemistry,* 69**,** 2586-92.

LI, L., XU, J., XU, Z.-H. & XUE, H.-W. 2005. Brassinosteroids stimulate plant tropisms through modulation of polar auxin transport in *Brassica* and *Arabidopsis*. *The Plant Cell,* 17**,** 2738-2753.

LI, S.-B., XIE, Z.-Z., HU, C.-G. & ZHANG, J.-Z. 2016. A review of auxin response factors (ARFs) in plants. *Frontiers in Plant Science,* 7**,** 47.

LI, Y., SMITH, C., CORKE, F., ZHENG, L., MERALI, Z., RYDEN, P., DERBYSHIRE, P., WALDRON, K. & BEVAN, M. W. 2007. Signaling from an altered cell wall to the nucleus mediates sugar-responsive growth and development in *Arabidopsis thaliana*. *Plant Cell,* 19**,** 2500-15.

LIAO, C., HOCHHOLDINGER, F. & LI, C. 2012. Comparative analyses of three legume species reveals conserved and unique root extracellular proteins. *PROTEOMICS,* 12**,** 3219-3228.

LIM, H. J., SHIM, S. B., JEE, S. W., LEE, S. H., LIM, C. J., HONG, J. T., SHEEN, Y. Y. & HWANG, D. Y. 2013. Green tea catechin leads to global improvement among Alzheimer's disease-related phenotypes in NSE/hAPP-C105 Tg mice. *The Journal of Nutritional Biochemistry,* 24**,** 1302-1313.

LINK, B. M. & COSGROVE, D. J. 1998. Acid-growth response and β-expansins in suspension cultures of bright yellow 2 tobacco. *Plant Physiol,* 118**,** 907-916.

LIONETTI, V., CERVONE, F. & DE LORENZO, G. A lower content of de-methylesterified homogalacturonan improves enzymatic cell separation and isolation of mesophyll protoplasts in *Arabidopsis*. *Phytochemistry*, 112, 188-94.

LISZKAY, A., KENK, B. & SCHOPFER, P. 2003. Evidence for the involvement of cell wall peroxidase in the generation of hydroxyl radicals mediating extension growth. *Planta,* 217**,** 658-67.

LIWANAG, A. J., EBERT, B., VERHERTBRUGGEN, Y., RENNIE, E. A., RAUTENGARTEN, C., OIKAWA, A., ANDERSEN, M. C., CLAUSEN, M. H. & SCHELLER, H. V. 2012. Pectin biosynthesis: GALS1 in *Arabidopsis thaliana* is a β-1,4-galactan β-1,4-galactosyltransferase. *Plant Cell,* 24**,** 5024-36.

LOUVET, R., CAVEL, E., GUTIERREZ, L., GUÉNIN, S., ROGER, D., GILLET, F., GUERINEAU, F. & PELLOUX, J. 2006. Comprehensive expression profiling of the pectin methylesterase gene family during silique development in *Arabidopsis thaliana*. *Planta,* 224**,** 782-791.

MACDOUGALL, A. J., RIGBY, N. M., RYDEN, P., TIBBITS, C. W. & RING, S. G. 2001. Swelling behavior of the tomato cell wall network. *Biomacromolecules,* 2**,** 450-5.

MADSON, M. 2003. The *MUR3* gene of *Arabidopsis* encodes a xyloglucan galactosyltransferase that is evolutionarily related to animal exostosins. *The Plant Cell Online,* 15**,** 1662-1670.

MALAMY, J. E. & BENFEY, P. N. 1997. Organization and cell differentiation in lateral roots of *Arabidopsis thaliana*. *Development,* 124**,** 33-44.

MANFIELD, I. W., ORFILA, C., MCCARTNEY, L., HARHOLT, J., BERNAL, A. J., SCHELLER, H. V., GILMARTIN, P. M., MIKKELSEN, J. D., PAUL KNOX, J. & WILLATS, W. G. 2004. Novel cell wall architecture of isoxaben-habituated *Arabidopsis* suspension-cultured cells: global transcript profiling and cellular analysis. *Plant J,* 40**,** 260-75.

MANSFIELD, S. G. & BRIARTY, L. G. 1991. Early embryogenesis in *Arabidopsis thaliana*. II. The developing embryo. *Canadian Journal of Botany,* 69**,** 461-476.

MARCHANT, A., KARGUL, J., MAY, S. T., MULLER, P., DELBARRE, A., PERROT-RECHENMANN, C. & BENNETT, M. J. 1999. AUX1 regulates root gravitropism in *Arabidopsis* by facilitating auxin uptake within root apical tissues. *EMBO J,* 18**,** 2066-2073.

MARÍN-RODRÍGUEZ, M. C., ORCHARD, J. & SEYMOUR, G. B. 2002. Pectate lyases, cell wall degradation and fruit softening. *Journal of Experimental Botany,* 53**,** 2115-2119.

MARKOVIČ, O. & JANEČEK, Š. 2004. Pectin methylesterases: sequence-structural features and phylogenetic relationships. *Carbohydrate Research,* 339**,** 2281-2295.

MAURO, M. L., DE LORENZO, G., COSTANTINO, P. & BELLINCAMPI, D. 2002. Oligogalacturonides inhibit the induction of late but not of early auxin-responsive genes in tobacco. *Planta,* 215**,** 494-501.

MCCARTHY, T. W., DER, J. P., HONAAS, L. A., DEPAMPHILIS, C. W. & ANDERSON, C. T. 2014. Phylogenetic analysis of pectin-related gene families in *Physcomitrella patensand* nine other plant species yields evolutionary insights into cell walls. *BMC Plant Biology,* 14**,** 1-14.

MCFARLANE, H. E., DÖRING, A. & PERSSON, S. 2014. The cell biology of cellulose synthesis. *Annual Review of Plant Biology,* 65**,** 69-94.

MCQUEEN-MASON, S., DURACHKO, D. M. & COSGROVE, D. J. 1992. Two endogenous proteins that induce cell wall extension in plants. *The Plant Cell Online,* 4**,** 1425-33.

MICHELI, F. 2001. Pectin methylesterases: cell wall enzymes with important roles in plant physiology. *Trends Plant Sci,* 6**,** 414-419.

MILANI, P., BRAYBROOK, S. A. & BOUDAOUD, A. 2013. Shrinking the hammer: micromechanical approaches to morphogenesis. *J Exp Bot,* 64**,** 4651-62.

MIYASAKA, S. C. & HAWES, M. C. 2001. Possible role of root border cells in detection and avoidance of aluminum toxicity. *Plant Physiology,* 125**,** 1978-1987.

MIYASHIMA, S. & NAKAJIMA, K. 2011. The root endodermis: A hub of developmental signals and nutrient flow. *Plant Signaling & Behavior,* 6**,** 1954-1958.

MOHNEN, D. 2008. Pectin structure and biosynthesis. *Curr Opin Plant Biol,* 11**,** 266-77.

MOLENDIJK, A. J., BISCHOFF, F., RAJENDRAKUMAR, C. S. V., FRIML, J., BRAUN, M., GILROY, S. & PALME, K. 2001. *Arabidopsis thaliana* Rop GTPases are localized to tips of root hairs and control polar growth. *The EMBO Journal,* 20**,** 2779-2788.

MOSTAFAVI, S., RAY, D., WARDE-FARLEY, D., GROUIOS, C. & MORRIS, Q. 2008. GeneMANIA: a real-time multiple association network integration algorithm for predicting gene function. *Genome Biology,* 9**,** S4.

MOUILLE, G., RALET, M.-C., CAVELIER, C., ELAND, C., EFFROY, D., HÉMATY, K., MCCARTNEY, L., TRUONG, H. N., GAUDON, V., THIBAULT, J.-F., MARCHANT, A. & HÖFTE, H. 2007. Homogalacturonan synthesis in *Arabidopsis thaliana* requires a Golgi-localized protein with a putative methyltransferase domain. *The Plant Journal,* 50**,** 605-614.

MULLER, B. & SHEEN, J. 2008. Cytokinin and auxin interaction in root stem-cell specification during early embryogenesis. *Nature,* 453**,** 1094-1097.

MÜLLER, K., LEVESQUE-TREMBLAY, G., FERNANDES, A., WORMIT, A., BARTELS, S., USADEL, B. & KERMODE, A. 2013. Overexpression of a pectin methylesterase inhibitor in *Arabidopsis thaliana* leads to altered growth morphology of the stem and defective organ separation. *Plant Signaling & Behavior,* 8**,** e26464.

MÜLLER, K., LINKIES, A., VREEBURG, R. A. M., FRY, S. C., KRIEGER-LISZKAY, A. & LEUBNER-METZGER, G. 2009. *In vivo* cell wall loosening by hydroxyl radicals during cress seed germination and elongation growth. *Plant Physiology,* 150**,** 1855-1865.

MUTWIL, M., DEBOLT, S. & PERSSON, S. 2008. Cellulose synthesis: a complex complex. *Curr Opin Plant Biol,* 11**,** 252-7.

NAKAGAWA, H., HASUMI, K., WOO, J. T., NAGAI, K. & WACHI, M. 2004. Generation of hydrogen peroxide primarily contributes to the induction of Fe(II)-dependent apoptosis in *Jurkat* cells by (-)-epigallocatechin gallate. *Carcinogenesis,* 25**,** 1567-74.

NAM, J., MYSORE, K. S., ZHENG, C., KNUE, M. K., MATTHYSSE, A. G. & GELVIN, S. B. 1999. Identification of T-DNA tagged *Arabidopsis* mutants that are resistant to transformation by *Agrobacterium*. *Mol Gen Genet,* 261**,** 429-38.

NGUEMA-ONA, E., COIMBRA, S., VICRE-GIBOUIN, M., MOLLET, J. C. & DRIOUICH, A. 2012. Arabinogalactan proteins in root and pollen-tube cells: distribution and functional aspects. *Ann Bot,* 110**,** 383-404.

NI, L., LIN, D. & BARRETT, D. M. 2005. Pectin methylesterase catalyzed firming effects on low temperature blanched vegetables. *Journal of Food Engineering,* 70**,** 546-556.

NIKOLAU, B. J., OHLROGGE, J. B. & WURTELE, E. S. 2003. Plant biotin-containing carboxylases. *Arch Biochem Biophys,* 414**,** 211-22.

NUNAN, K. J. & SCHELLER, H. V. 2003. Solubilization of an arabinan arabinosyltransferase activity from mung bean hypocotyls. *Plant Physiol,* 132**,** 331-42.

O'BRIEN, J. A. & BENKOVA, E. 2013. Cytokinin cross-talking during biotic and abiotic stress responses. *Frontiers in Plant Science,* 4.

O'NEILL, M. A., EBERHARD, S., ALBERSHEIM, P. & DARVILL, A. G. 2001. Requirement of borate cross-linking of cell wall rhamnogalacturonan II for *Arabidopsis* growth. *Science,* 294**,** 846-9.

O'NEILL, M. A., ISHII, T., ALBERSHEIM, P. & DARVILL, A. G. 2004. Rhamnogalacturonan II: structure and function of a borate cross-linked cell wall pectic polysaccharide. *Annu Rev Plant Biol,* 55**,** 109-39.

OGAWA, M., KAY, P., WILSON, S. & SWAIN, S. M. 2009. ARABIDOPSIS DEHISCENCE ZONE POLYGALACTURONASE1 (ADPG1), ADPG2, and QUARTET2 are polygalacturonases required for cell separation during reproductive development in *Arabidopsis*. *The Plant Cell,* 21**,** 216-233.

OKUSHIMA, Y., FUKAKI, H., ONODA, M., THEOLOGIS, A. & TASAKA, M. 2007. ARF7 and ARF19 regulate lateral root formation via direct activation of *LBD/ASL* genes in *Arabidopsis*. *The Plant Cell Online,* 19**,** 118-130.

OKUSHIMA, Y., OVERVOORDE, P. J., ARIMA, K., ALONSO, J. M., CHAN, A., CHANG, C., ECKER, J. R., HUGHES, B., LUI, A., NGUYEN, D., ONODERA, C., QUACH, H., SMITH, A., YU, G. & THEOLOGIS, A. 2005. Functional genomic analysis of the AUXIN RESPONSE FACTOR gene family members in *Arabidopsis thaliana*: unique and overlapping functions of ARF7 and ARF19. *The Plant Cell Online,* 17**,** 444-463.

OVERVOORDE, P., FUKAKI, H. & BEECKMAN, T. 2010. Auxin control of root development. *Cold Spring Harbor Perspectives in Biology,* 2**,** a001537.

PALUSA, S. G., GOLOVKIN, M., SHIN, S.-B., RICHARDSON, D. N. & REDDY, A. S. N. 2007. Organ-specific, developmental, hormonal and stress regulation of expression of putative pectate lyase genes in *Arabidopsis*. *New Phytologist,* 174**,** 537-550.

PANDEY, K. B. & RIZVI, S. I. 2009. Plant polyphenols as dietary antioxidants in human health and disease. *Oxidative Medicine and Cellular Longevity,* 2**,** 270-278.

PAPINI-TERZI, F., ROCHA, F., VENCIO, R., FELIX, J., BRANCO, D., WACLAWOVSKY, A., DEL BEM, L., LEMBKE, C., COSTA, M., NISHIYAMA, M., VICENTINI, R., VINCENTZ, M., ULIAN, E., MENOSSI, M. & SOUZA, G. 2009. Sugarcane genes associated with sucrose content. *BMC Genomics,* 10**,** 120.

PAQUE, S., MOUILLE, G., GRANDONT, L., ALABADI, D., GAERTNER, C., GOYALLON, A., MULLER, P., PRIMARD-BRISSET, C., SORMANI, R., BLAZQUEZ, M. A. & PERROT-RECHENMANN, C. 2014. AUXIN BINDING PROTEIN1 links cell wall remodeling, auxin signaling, and cell expansion in *Arabidopsis*. *Plant Cell,* 26**,** 280-95.

PAREDEZ, A. R., SOMERVILLE, C. R. & EHRHARDT, D. W. 2006. Visualization of cellulose synthase demonstrates functional association with microtubules. *Science,* 312**,** 1491-5.

PEAUCELLE, A., BRAYBROOK, S. A., LE GUILLOU, L., BRON, E., KUHLEMEIER, C. & HOFTE, H. 2011a. Pectin-induced changes in cell wall mechanics underlie organ initiation in *Arabidopsis*. *Curr Biol,* 21**,** 1720-6.

PEAUCELLE, A., LOUVET, R., JOHANSEN, J. N., HOFTE, H., LAUFS, P., PELLOUX, J. & MOUILLE, G. 2008. *Arabidopsis* phyllotaxis is controlled by the methyl-esterification status of cell-wall pectins. *Curr Biol,* 18**,** 1943-8.

PEAUCELLE, A., LOUVET, R., JOHANSEN, J. N., SALSAC, F., MORIN, H., FOURNET, F., BELCRAM, K., GILLET, F., HOFTE, H., LAUFS, P., MOUILLE, G. & PELLOUX, J. 2011b. The transcription factor BELLRINGER modulates phyllotaxis by regulating the expression of a pectin methylesterase in *Arabidopsis*. *Development,* 138**,** 4733-41.

PEI, W., DU, F., ZHANG, Y., HE, T. & REN, H. 2012. Control of the actin cytoskeleton in root hair development. *Plant Science,* 187**,** 10-18.

PELLOUX, J., RUSTÉRUCCI, C. & MELLEROWICZ, E. J. 2007. New insights into pectin methylesterase structure and function. *Trends in Plant Science,* 12**,** 267-277.

PENA, M. J., KONG, Y., YORK, W. S. & O'NEILL, M. A. 2012. A galacturonic acid-containing xyloglucan is involved in *Arabidopsis* root hair tip growth. *Plant Cell,* 24**,** 4511-24.

PERET, B., DE RYBEL, B., CASIMIRO, I., BENKOVA, E., SWARUP, R., LAPLAZE, L., BEECKMAN, T. & BENNETT, M. J. 2009. *Arabidopsis* lateral root development: an emerging story. *Trends Plant Sci,* 14**,** 399-408.

PÉRET, B., LI, G., ZHAO, J., BAND, L. R., VOß, U., POSTAIRE, O., LUU, D.-T., DA INES, O., CASIMIRO, I., LUCAS, M., WELLS, D. M., LAZZERINI, L., NACRY, P., KING, J. R., JENSEN, O. E., SCHÄFFNER, A. R., MAUREL, C. & BENNETT, M. J. 2012. Auxin regulates aquaporin function to facilitate lateral root emergence. *Nat Cell Biol,* 14**,** 991-998.

PÉREZ, S., RODRÍGUEZ-CARVAJAL, M. A. & DOCO, T. 2003. A complex plant cell wall polysaccharide: rhamnogalacturonan II. A structure in quest of a function. *Biochimie,* 85**,** 109-121.

PERRIN, R. M. 1999. Xyloglucan fucosyltransferase, an enzyme involved in plant cell wall biosynthesis. *Science,* 284**,** 1976-1979.

PETERSSON, S. V., JOHANSSON, A. I., KOWALCZYK, M., MAKOVEYCHUK, A., WANG, J. Y., MORITZ, T., GREBE, M., BENFEY, P. N., SANDBERG, G. & LJUNG, K. 2009. An auxin gradient and maximum in the *Arabidopsis* root apex shown by high-resolution cell-specific analysis of IAA distribution and synthesis. *Plant Cell,* 21**,** 1659-68.

PETRICKA, J. J., WINTER, C. M. & BENFEY, P. N. 2012. Control of *Arabidopsis* root development. *Annual Review of Plant Biology,* 63**,** 563-590.

PICCIOCCHI, A., DOUCE, R. & ALBAN, C. 2001. Biochemical characterization of the *Arabidopsis* biotin synthase reaction. The importance of mitochondria in biotin synthesis. *Plant Physiology,* 127**,** 1224-1233.

PLANCOT, B., SANTAELLA, C., JABER, R., KIEFER-MEYER, M. C., FOLLET-GUEYE, M.-L., LEPRINCE, J., GATTIN, I., SOUC, C., DRIOUICH, A. & VICRÉ-GIBOUIN, M. 2013. Deciphering the responses of root border-like cells of *Arabidopsis* and flax to pathogen-derived elicitors. *Plant Physiology,* 163**,** 1584-1597.

PONCE, G., BARLOW, P. W., FELDMAN, L. J. & CASSAB, G. I. 2005. Auxin and ethylene interactions control mitotic activity of the quiescent centre, root cap size, and pattern of cap cell differentiation in maize. *Plant, Cell & Environment,* 28**,** 719-732.

PROTSENKO, M. A., BUZA, N. L., KRINITSYNA, A. A., BULANTSEVA, E. A. & KORABLEVA, N. P. 2008. Polygalacturonase-inhibiting protein is a structural component of plant cell wall. *Biochemistry (Moscow),* 73**,** 1053-1062.

QU, T., LIU, R., WANG, W., AN, L., CHEN, T., LIU, G. & ZHAO, Z. 2011. Brassinosteroids regulate pectin methylesterase activity and *AtPME41* expression in *Arabidopsis* under chilling stress. *Cryobiology,* 63**,** 111-7.

QUIDEAU, S., DEFFIEUX, D., DOUAT-CASASSUS, C. & POUYSÉGU, L. 2011. Plant polyphenols: chemical properties, biological activities, and synthesis. *Angewandte Chemie International Edition,* 50**,** 586-621.

RAHMAN, A., BANNIGAN, A., SULAMAN, W., PECHTER, P., BLANCAFLOR, E. B. & BASKIN, T. I. 2007. Auxin, actin and growth of the *Arabidopsis thaliana* primary root. *Plant J,* 50**,** 514-28.

RAHMAN, A., HOSOKAWA, S., OONO, Y., AMAKAWA, T., GOTO, N. & TSURUMI, S. 2002. Auxin and ethylene response interactions during *Arabidopsis* root hair development dissected by auxin influx modulators. *Plant Physiology,* 130**,** 1908-1917.

RALET, M. C., WILLIAMS, M. A., TANHATAN-NASSERI, A., ROPARTZ, D., QUEMENER, B. & BONNIN, E. 2012. Innovative enzymatic approach to resolve homogalacturonans based on their methylesterification pattern. *Biomacromolecules,* 13**,** 1615-24.

RAPOPORT, T. A. 2007. Protein translocation across the eukaryotic endoplasmic reticulum and bacterial plasma membranes. *Nature,* 450**,** 663-9.

REAPE, T. J., MOLONY, E. M. & MCCABE, P. F. 2008. Programmed cell death in plants: distinguishing between different modes. *Journal of Experimental Botany,* 59**,** 435-444.

REINHARDT, H., HACHEZ, C., BIENERT, M. D., BEEBO, A., SWARUP, K., VOß, U., BOUHIDEL, K., FRIGERIO, L., SCHJOERRING, J. K., BENNETT, M. J. & CHAUMONT, F. 2016. Tonoplast aquaporins facilitate lateral root emergence. *Plant Physiology,* 170**,** 1640-1654.

RENARD, C. M. G. C. & THIBAULT, J.-F. 1996. Degradation of pectins in alkaline conditions: kinetics of demethylation. *Carbohydrate Research,* 286**,** 139-150.

RIDLEY, B. L., O'NEILL, M. A. & MOHNEN, D. 2001. Pectins: structure, biosynthesis, and oligogalacturonide-related signaling. *Phytochemistry,* 57**,** 929-967.

RIEGER, A. M., NELSON, K. L., KONOWALCHUK, J. D. & BARREDA, D. R. 2011. Modified annexin V/propidium iodide apoptosis assay for accurate assessment of cell death. *Journal of Visualized Experiments : JoVE***,** 2597.

RÖCKEL, N., WOLF, S., KOST, B., RAUSCH, T. & GREINER, S. 2008. Elaborate spatial patterning of cell-wall PME and PMEI at the pollen tube tip involves PMEI endocytosis, and reflects the distribution of esterified and de-esterified pectins. *The Plant Journal,* 53**,** 133-143.

RODRIGUEZ, S. K., GUO, W., LIU, L., BAND, M. A., PAULSON, E. K. & MEYDANI, M. 2006. Green tea catechin, epigallocatechin-3-gallate, inhibits vascular endothelial growth factor angiogenic signaling by disrupting the formation of a receptor complex. *Int J Cancer,* 118**,** 1635-44.

ROGERS, L. M., KIM, Y.-K., GUO, W., GONZÁLEZ-CANDELAS, L., LI, D. & KOLATTUKUDY, P. E. 2000. Requirement for either a host- or pectin-induced pectate lyase for infection of Pisum sativum by *Nectria hematococca*. *Proceedings of the National Academy of Sciences,* 97**,** 9813-9818.

ROSE, J. K., BRAAM, J., FRY, S. C. & NISHITANI, K. 2002. The XTH family of enzymes involved in xyloglucan endotransglucosylation and endohydrolysis: current perspectives and a new unifying nomenclature. *Plant Cell Physiol,* 43**,** 1421-35.

ROSE, J. K. & LEE, S. J. 2010. Straying off the highway: trafficking of secreted plant proteins and complexity in the plant cell wall proteome. *Plant Physiol,* 153**,** 433-6.

RYAN, E., STEER, M. & DOLAN, L. 2001. Cell biology and genetics of root hair formation in *Arabidopsis thaliana*. *Protoplasma,* 215**,** 140-149.

RYDEN, P., SUGIMOTO-SHIRASU, K., SMITH, A. C., FINDLAY, K., REITER, W. D. & MCCANN, M. C. 2003. Tensile properties of *Arabidopsis* cell walls depend on both a xyloglucan cross-linked microfibrillar network and rhamnogalacturonan II-borate complexes. *Plant Physiol,* 132**,** 1033-40.

SAEZ-AGUAYO, S., RALET, M. C., BERGER, A., BOTRAN, L., ROPARTZ, D., MARION-POLL, A. & NORTH, H. M. 2013. PECTIN METHYLESTERASE INHIBITOR6 promotes *Arabidopsis* mucilage release by limiting methylesterification of homogalacturonan in seed coat epidermal cells. *Plant Cell,* 25**,** 308-23.

SAVATIN, D. V., FERRARI, S., SICILIA, F. & DE LORENZO, G. 2011. Oligogalacturonide-auxin antagonism does not require posttranscriptional gene silencing or stabilization of auxin response repressors in *Arabidopsis*. *Plant Physiol,* 157**,** 1163-74.

SCHALLER, G. E. 2012. Ethylene and the regulation of plant development. *BMC Biology,* 10**,** 1-3.

SCHEIBLE, W.-R., ESHED, R., RICHMOND, T., DELMER, D. & SOMERVILLE, C. 2001. Modifications of cellulose synthase confer resistance to isoxaben and thiazolidinone herbicides in *Arabidopsis ixr1* mutants. *Proceedings of the National Academy of Sciences,* 98**,** 10079-10084.

SCHELLER, H. V. & ULVSKOV, P. 2010. Hemicelluloses. *Annu Rev Plant Biol,* 61**,** 263-89.

SCHLAEPPI, K., ABOU-MANSOUR, E., BUCHALA, A. & MAUCH, F. 2010. Disease resistance of *Arabidopsis* to *Phytophthora brassicae* is established by the sequential action of indole glucosinolates and camalexin. *The Plant Journal,* 62**,** 840-851.

SCOGNAMIGLIO, M. A., CIARDIELLO, M. A., TAMBURRINI, M., CARRATORE, V., RAUSCH, T. & CAMARDELLA, L. 2003. The plant invertase inhibitor shares structural properties and disulfide bridges arrangement with the pectin methylesterase inhibitor. *J Protein Chem,* 22**,** 363-9.

SÉNÉCHAL, F., GRAFF, L., SURCOUF, O., MARCELO, P., RAYON, C., BOUTON, S., MARECK, A., MOUILLE, G., STINTZI, A., HÖFTE, H., LEROUGE, P., SCHALLER, A. & PELLOUX, J. 2014. *Arabidopsis* PECTIN METHYLESTERASE17 is co-expressed with and processed by SBT3.5, a subtilisin-like serine protease. *Annals of Botany*, 114(6), 1161-75.

SÉNÉCHAL, F., L'ENFANT, M., DOMON, J.-M., ROSIAU, E., CRÉPEAU, M.-J., SURCOUF, O., ESQUIVEL-RODRIGUEZ, J., MARCELO, P., MARECK, A., GUÉRINEAU, F., KIM, H.-R., MRAVEC, J., BONNIN, E., JAMET, E., KIHARA, D., LEROUGE, P., RALET, M.-C., PELLOUX, J. & RAYON, C. 2015a. Tuning of pectin methylesterification: PECTIN METHYLESTERASE INHIBITOR 7 modulates the processive activity of co-expressed PECTIN METHYLESTERASE 3 in a pH-dependent manner. *Journal of Biological Chemistry,* 290**,** 23320-23335.

SÉNÉCHAL, F., MARECK, A., MARCELO, P., LEROUGE, P. & PELLOUX, J. 2015b. *Arabidopsis* PME17 Activity can be controlled by pectin methylesterase inhibitor4. *Plant Signaling & Behavior,* 10**,** e983351.

SENECHAL, F., WATTIER, C., RUSTERUCCI, C. & PELLOUX, J. 2014. Homogalacturonan-modifying enzymes: structure, expression, and roles in plants. *J Exp Bot,* 65**,** 5125-60.

SHAVRUKOV, Y. & HIRAI, Y. 2016. Good and bad protons: genetic aspects of acidity stress responses in plants. *Journal of Experimental Botany,* 67**,** 15-30.

SHIGEMATSU, H., IIDA, K., NAKANO, M., CHAUDHURI, P., IIDA, H. & NAGAYAMA, K. 2014. Structural characterization of the mechanosensitive channel candidate MCA2 from *Arabidopsis thaliana*. *PLoS ONE,* 9**,** e87724.

SHOWALTER, A. M. 2001. Arabinogalactan-proteins: structure, expression and function. *Cell Mol Life Sci,* 58**,** 1399-1417.

SILA, D. N., SMOUT, C., VU, S. T., VAN LOEY, A. & HENDRICKX, M. 2005. Influence of pretreatment conditions on the texture and cell wall components of carrots during thermal processing. *J Food Sci,* 70**,** E85-E91.

SILA, D. N., SMOUT, C., VU, T. S. & HENDRICKX, M. E. 2004. Effects of high-pressure pretreatment and calcium soaking on the texture degradation kinetics of carrots during thermal processing. *J Food Sci,* 69**,** E205-E211.

SILLERO, A. & RIBEIRO, J. M. 1989. Isoelectric points of proteins: theoretical determination. *Anal Biochem,* 179**,** 319-25.

SOLBAK, A. I., RICHARDSON, T. H., MCCANN, R. T., KLINE, K. A., BARTNEK, F., TOMLINSON, G., TAN, X., PARRA-GESSERT, L., FREY, G. J., PODAR, M., LUGINBÜHL, P., GRAY, K. A., MATHUR, E. J., ROBERTSON, D. E., BURK, M. J., HAZLEWOOD, G. P., SHORT, J. M. & KEROVUO, J. 2005. Discovery of pectin-degrading enzymes and directed evolution of a novel pectate lyase for processing cotton fabric. *Journal of Biological Chemistry,* 280**,** 9431-9438.

SOMERVILLE, C. 2006. Cellulose synthesis in higher plants. *Annu Rev Cell Dev Biol,* 22**,** 53-78.

SOMOGYI, M. 1952. Notes on sugar determination. *Journal of Biological Chemistry,* 195**,** 19-23.

STAEHELIN, L. A., GIDDINGS, T. H., KISS, J. Z. & SACK, F. D. 1990. Macromolecular differentiation of Golgi stacks in root tips of *Arabidopsis* and *Nicotiana* seedlings as visualized in high pressure frozen and freeze-substituted samples. *Protoplasma,* 157**,** 75-91.

STEPHENSON, M. B. & HAWES, M. C. 1994. Correlation of pectin methylesterase activity in root caps of pea with root border cell separation. *Plant Physiology,* 106**,** 739-745.

STERLING, J. D., ATMODJO, M. A., INWOOD, S. E., KUMAR KOLLI, V. S., QUIGLEY, H. F., HAHN, M. G. & MOHNEN, D. 2006. Functional identification of an *Arabidopsis* pectin biosynthetic homogalacturonan galacturonosyltransferase. *Proc Natl Acad Sci U S A,* 103**,** 5236-41.

SUN, Y., FAN, X.-Y., CAO, D.-M., TANG, W., HE, K., ZHU, J.-Y., HE, J.-X., BAI, M.-Y., ZHU, S., OH, E., PATIL, S., KIM, T.-W., JI, H., WONG, W. H., RHEE, S. Y. & WANG, Z.-Y. 2010. Integration of brassinosteroid signal transduction with the transcription network for plant growth regulation in *Arabidopsis*. *Developmental Cell,* 19**,** 765-777.

SWARUP, R., FRIML, J., MARCHANT, A., LJUNG, K., SANDBERG, G., PALME, K. & BENNETT, M. 2001. Localization of the auxin permease AUX1 suggests two functionally distinct hormone transport pathways operate in the *Arabidopsis* root apex. *Genes & Development,* 15**,** 2648-2653.

TALBOTT, L. D. & RAY, P. M. 1992. Molecular size and separability features of pea cell wall polysaccharides. Implications for models of primary wall structure. *Plant Physiol,* 98**,** 357-368.

TAYLOR, N. G., HOWELLS, R. M., HUTTLY, A. K., VICKERS, K. & TURNER, S. R. 2003. Interactions among three distinct CesA proteins essential for cellulose synthesis. *Proc Natl Acad Sci U S A,* 100**,** 1450-5.

TRIGUI-LAHIANI, H. & GARGOURI, A. 2007. Cloning, genomic organisation and mRNA expression of a pectin lyase gene from a mutant strain of *Penicillium occitanis*. *Gene,* 388**,** 54-60.

TROUVELOT, S., HÉLOIR, M.-C., POINSSOT, B., GAUTHIER, A., PARIS, F., GUILLIER, C., COMBIER, M., TRDÁ, L., DAIRE, X. & ADRIAN, M. 2014. Carbohydrates in plant immunity and plant protection: roles and potential application as foliar sprays. *Frontiers in Plant Science,* 5**,** 592.

TSANG, D. L., EDMOND, C., HARRINGTON, J. L. & NUHSE, T. S. 2011. Cell wall integrity controls root elongation via a general 1-aminocyclopropane-1-carboxylic acid-dependent, ethylene-independent pathway. *Plant Physiol,* 156**,** 596-604.

TURBANT, A., FOURNET, F., LEQUART, M., ZABIJAK, L., PAGEAU, K., BOUTON, S. & VAN WUYTSWINKEL, O. 2016. PME58 plays a role in pectin distribution during seed coat mucilage extrusion through homogalacturonan modification. *Journal of Experimental Botany,* 67**,** 2177-2190.

TZIN, V. & GALILI, G. 2010. The biosynthetic pathways for shikimate and aromatic amino acids in *Arabidopsis thaliana*. *The Arabidopsis Book / American Society of Plant Biologists,* 8**,** e0132.

UBEDA-TOMAS, S., SWARUP, R., COATES, J., SWARUP, K., LAPLAZE, L., BEEMSTER, G. T., HEDDEN, P., BHALERAO, R. & BENNETT, M. J. 2008. Root growth in *Arabidopsis* requires gibberellin/DELLA signalling in the endodermis. *Nat Cell Biol,* 10**,** 625-8.

VAN BUGGENHOUT, S., SILA, D. N., DUVETTER, T., VAN LOEY, A. & HENDRICKX, M. E. 2009. Pectins in processed fruits and vegetables: Part III—texture engineering. *CRFSFS,* 8**,** 105-117.

VAN DEN BERG, C., WILLEMSEN, V., HENDRIKS, G., WEISBEEK, P. & SCHERES, B. 1997. Short-range control of cell differentiation in the *Arabidopsis* root meristem. *Nature,* 390**,** 287-289.

VANETTEN, H. D., MANSFIELD, J. W., BAILEY, J. A. & FARMER, E. E. 1994. Two Classes of plant antibiotics: phytoalexins versus "phytoanticipins". *The Plant Cell,* 6**,** 1191-1192.

VANZIN, G. F., MADSON, M., CARPITA, N. C., RAIKHEL, N. V., KEEGSTRA, K. & REITER, W. D. 2002. The *mur2* mutant of *Arabidopsis thaliana* lacks fucosylated xyloglucan because of a lesion in fucosyltransferase AtFUT1. *Proc Natl Acad Sci U S A,* 99**,** 3340-5.

VAZQUEZ, L. A. B., SANCHEZ, R., HERNANDEZ-BARRERA, A., ZEPEDA-JAZO, I., SÁNCHEZ, F., QUINTO, C. & TORRES, L. C. 2014. Actin polymerization drives polar growth in *Arabidopsis* root hair cells. *Plant Signaling & Behavior,* 9**,** e29401.

VICRÉ, M., SANTAELLA, C., BLANCHET, S., GATEAU, A. & DRIOUICH, A. 2005. Root border-like cells of *Arabidopsis*. Microscopical characterization and role in the interaction with Rhizobacteria. *Plant Physiology,* 138**,** 998-1008.

VILCHES-BARRO, A. & MAIZEL, A. 2015. Talking through walls: mechanisms of lateral root emergence in *Arabidopsis thaliana*. *Current Opinion in Plant Biology,* 23**,** 31-38.

VOGEL, J. P., RAAB, T. K., SCHIFF, C. & SOMERVILLE, S. C. 2002. *PMR6*, a pectate lyase-like gene required for powdery mildew susceptibility in *Arabidopsis*. *Plant Cell,* 14**,** 2095-106.

WANG, J. W., WANG, L. J., MAO, Y. B., CAI, W. J., XUE, H. W. & CHEN, X. Y. 2005. Control of root cap formation by MicroRNA-targeted auxin response factors in *Arabidopsis*. *Plant Cell,* 17**,** 2204-16.

WANG, L. & CHONG, K. 2015. The essential role of cytokinin signaling in root apical meristem formation during somatic embryogenesis. *Frontiers in Plant Science,* 6**,** 1196.

WANG, T. & HONG, M. 2016. Solid-state NMR investigations of cellulose structure and interactions with matrix polysaccharides in plant primary cell walls. *Journal of Experimental Botany,* 67**,** 503-514.

WANG, Y., DINDAS, J., RIENMÜLLER, F., KREBS, M., WAADT, R., SCHUMACHER, K., WU, W.-H., HEDRICH, R. & ROELFSEMA, M. ROB G. 2015. Cytosolic Ca^{2+} signals enhance the vacuolar ion conductivity of bulging *Arabidopsis* root hair cells. *Molecular Plant,* 8**,** 1665-1674.

WATSON, B. S., BEDAIR, M. F., URBANCZYK-WOCHNIAK, E., HUHMAN, D. V., YANG, D. S., ALLEN, S. N., LI, W., TANG, Y. & SUMNER, L. W. 2015. Integrated metabolomics and transcriptomics reveal enhanced specialized metabolism in *Medicago truncatula* root border cells. *Plant Physiology,* 167**,** 1699-1716.

WEI, Z. & LI, J. 2015. Brassinosteroids regulate root growth, development, and symbiosis. *Molecular Plant,* 9**,** 86-100.

WEIJERS, D., SCHLERETH, A., EHRISMANN, J. S., SCHWANK, G., KIENTZ, M. & JÜRGENS, G. 2006. Auxin triggers transient local signaling for cell specification in *Arabidopsis* embryogenesis. *Developmental Cell,* 10**,** 265-270.

WEN, F., VANETTEN, H. D., TSAPRAILIS, G. & HAWES, M. C. 2007. Extracellular proteins in pea root tip and border cell exudates. *Plant Physiology,* 143**,** 773-783.

WEN, F., ZHU, Y. & HAWES, M. C. 1999. Effect of pectin methylesterase gene expression on pea root development. *The Plant Cell Online,* 11**,** 1129-1140.

WENZEL, C. L. & ROST, T. L. 2001. Cell division patterns of the protoderm and root cap in the “closed” root apical meristem of *Arabidopsis thaliana*. *Protoplasma,* 218**,** 203-213.

WHITNEY, S. E. C., GIDLEY, M. J. & MCQUEEN-MASON, S. J. 2000. Probing expansin action using cellulose/hemicellulose composites. *Plant J,* 22.

WILLATS, W. G. T. & KNOX, J. P. 1996. A role for arabinogalactan-proteins in plant cell expansion: evidence from studies on the interaction of β-glucosyl Yariv reagent with seedlings of *Arabidopsis thaliana*. *Plant J,* 9**,** 919-925.

WILLATS, W. G. T., MCCARTNEY, L., STEELE-KING, C. G., MARCUS, S. E., MORT, A., HUISMAN, M., ALEBEEK, G.-J., SCHOLS, H. A., VORAGEN, A. G. J., GOFF, A., BONNIN, E., THIBAULT, J.-F. & KNOX, J. P. 2003. A xylogalacturonan epitope is specifically associated with plant cell detachment. *Planta,* 218**,** 673-681.

WILLIAMS, M. A. & BENEN, J. A. 2002. A novel enzyme activity involving the demethylation of specific partially methylated oligogalacturonides. *Biochem J,* 367**,** 511-5.

WING, R. A., YAMAGUCHI, J., LARABELL, S. K., URSIN, V. M. & MCCORMICK, S. 1990. Molecular and genetic characterization of two pollen-expressed genes that

have sequence similarity to pectate lyases of the plant pathogen *Erwinia*. *Plant Mol Biol,* 14**,** 17-28.

WOLF, S. & GREINER, S. 2012. Growth control by cell wall pectins. *Protoplasma,* 249 Suppl 2**,** S169-75.

WOLF, S., GRSIC-RAUSCH, S., RAUSCH, T. & GREINER, S. 2003. Identification of pollen-expressed pectin methylesterase inhibitors in *Arabidopsis*. *FEBS Letters,* 555**,** 551-555.

WOLF, S., MOUILLE, G. & PELLOUX, J. 2009. Homogalacturonan methyl-esterification and plant development. *Molecular Plant,* 2**,** 851-860.

WOLF, S., MRAVEC, J., GREINER, S., MOUILLE, G. & HOFTE, H. 2012. Plant cell wall homeostasis is mediated by brassinosteroid feedback signaling. *Curr Biol,* 22**,** 1732-7.

WOODWARD, A. W. & BARTEL, B. 2005. Auxin: regulation, action, and interaction. *Ann Bot,* 95**,** 707-35.

WORDEN, N., PARK, E. & DRAKAKAKI, G. 2012. Trans-Golgi network: an intersection of trafficking cell wall components. *J Integr Plant Biol,* 54**,** 875-86.

WORMIT, A., BUTT, S. M., CHAIRAM, I., MCKENNA, J. F., NUNES-NESI, A., KJAER, L., O'DONNELLY, K., FERNIE, A. R., WOSCHOLSKI, R., BARTER, M. C. & HAMANN, T. 2012. Osmosensitive changes of carbohydrate metabolism in response to cellulose biosynthesis inhibition. *Plant Physiol,* 159**,** 105-17.

XI, B., GU, H., BANIASADI, H. & RAFTERY, D. 2014. Statistical analysis and modeling of mass spectrometry-based metabolomics data. *Methods in molecular biology (Clifton, N.J.),* 1198**,** 333-353.

XIA, J., SINELNIKOV, I. V., HAN, B. & WISHART, D. S. 2015. MetaboAnalyst 3.0—making metabolomics more meaningful. *Nucleic Acids Research,* 43**,** W251-W257.

XU, W., JIA, L., SHI, W., LIANG, J., ZHOU, F., LI, Q. & ZHANG, J. 2013. Abscisic acid accumulation modulates auxin transport in the root tip to enhance proton secretion for maintaining root growth under moderate water stress. *New Phytol,* 197**,** 139-50.

YADAV, P. K., SINGH, V. K., YADAV, S., YADAV, K. D. & YADAV, D. 2009. *In silico* analysis of pectin lyase and pectinase sequences. *Biochemistry (Mosc),* 74**,** 1049-55.

YANG, Z. & OHLROGGE, J. B. 2009. Turnover of fatty acids during natural senescence of *Arabidopsis*, *Brachypodium*, and switchgrass and in *Arabidopsis* beta-oxidation mutants. *Plant Physiol,* 150**,** 1981-9.

YARIV, J., LIS, H. & KATCHALSKI, E. 1967. Precipitation of arabic acid and some seed polysaccharides by glycosylphenylazo dyes. *Biochem J,* 105**,** 1c.

YOUN, J. H., KIM, M. K., KIM, E. J., SON, S. H., LEE, J. E., JANG, M. S., KIM, T. W. & KIM, S. K. 2016. ARF7 increases the endogenous contents of castasterone through suppression of BAS1 expression in *Arabidopsis thaliana*. *Phytochemistry,* 122**,** 34-44.

ZABLACKIS, E., HUANG, J., MÜLLERZ, B., DARVILL, A. C. & ALBERSHEIM, P. 1995. Characterization of the cell-wall polysaccharides of *Arabidopsis thaliana* leaves. *Plant Physiol,* 107**,** 1129-1138.

ZABOTINA, O. A., AVCI, U., CAVALIER, D., PATTATHIL, S., CHOU, Y. H., EBERHARD, S., DANHOF, L., KEEGSTRA, K. & HAHN, M. G. 2012. Mutations in multiple *XXT* genes of *Arabidopsis* reveal the complexity of xyloglucan biosynthesis. *Plant Physiol,* 159**,** 1367-84.

ZHANG, G. F. & STAEHELIN, L. A. 1992. Immunocytochemical analysis of high-pressure frozen- and freeze-substituted sycamore maple suspension culture cells. *Plant Physiol,* 99**,** 1070-1083.

ZHAO, Y. 2010. Auxin biosynthesis and its role in plant development. *Annual Review of Plant Biology,* 61**,** 49-64.

ZHAO, Y. 2014. Auxin biosynthesis. *The Arabidopsis Book / American Society of Plant Biologists,* 12**,** e0173.

ZHU, J.-Y., SAE-SEAW, J. & WANG, Z.-Y. 2013. Brassinosteroid signalling. *Development,* 140**,** 1615-1620.

Appendix

Detailed XCMS parameters

Feature Detection:

Method: centWave (Highly sensitive feature detection using a peak density and wavelet based method. Applicable for high resolution LC/MS data in centroid mode)

ppm: 15 (maximal tolerated m/z deviation in consecutive scans, in ppm (parts per million))

minimum peak width: 5 (minimum chromatographic peak width in seconds)

maximum peak width: 20 (maximum chromatographic peak width in seconds)

Signal/Noise threshold: 6

mzdiff: 0.01 (minimum difference in m/z for peaks with overlapping retention times, can be negative to allow overlap)

Integration method: peak limits are found through descent on the mexican hat filtered data.

prefilter peaks: 3 (Prefilter step for the first phase. Mass traces are only retained if they contain at least [prefilter peaks] peaks with intensity >= [prefilter intensity])

prefilter intensity: 100 (Prefilter step for the first phase. Mass traces are only retained if they contain at least [prefilter peaks] peaks with intensity >= [prefilter intensity])

Noise Filter: 0 (optional argument which is useful for data that was centroided without any intensity threshold, centroids with intensity < noise are omitted from ROI detection)

Retention Time Correction:

Method: obiwarp (Retention time correction method based on correlations of the raw data.)

profStep: 1 (step size (in m/z) to use for profile generation from the raw data files)

Alignment:

minfrac: 0.5 (minimum fraction of samples necessary in at least one of the sample groups for it to be a valid group)

bw: 5 (Allowable retention time deviations, in seconds. In more detail: bandwidth (standard deviation or half width at half maximum) of gaussian smoothing kernel to apply to the peak density chromatogram)

mzwid: 0.015 (width of overlapping m/z slices to use for creating peak density chromatograms and grouping peaks across samples)

max: 100 (maximum number of groups to identify in a single m/z slice)

minsamp: 1 (minimum number of samples necessary in at least one of the sample groups for it to be a valid group)

Statistics:

Statistical test: Welch t-test (unequal variances)

fold change threshold (highly significant features): 1.5 (Features with a fold change greater than this threshold are considered highly significant. Some statistical figures (e.g. Mirror plot) are generated using only the dysregulated features according to this threshold.)

p-value threshold (highly significant features): 0.01 (Features with a p-value less than this threshold are considered highly significant. Some statistical figures (e.g. Mirror plot) are generated using only the dysregulated features according to this threshold.)

p-value threshold (significant features): 0.05 (Features with a p-value less than this threshold are not considered significant and are omitted from some calculations to save time and space. EIC's, annotations and database ID's are not generated for features with p-values above this threshold.)

value: into (intensity values to be used for the diffreport. If value="into", integrated peak intensities are used. If value="maxo", maximum peak intensities are used.)

Annotation:

Search for: isotopes + adducts

m/z absolute error: 0.015

ppm error: 5

Identification:

ppm: 10 (tolerance for database search)

adducts: [M+H]+; [M+Na]+; [M+K]+ (adducts to be considered for database search)